	1.0	4.5 5.0 5.6	2.8	2.5
			3.2	2.2
			3.6	
			4.0	2.0
	1.1			
				1.8
	1.25	1.4		1.6

MICROCOPY RESOLUTION TEST CHART
NATIONAL BUREAU OF STANDARDS-1963-A

DOT/FAA/PM-83/39

Program Engineering &
Maintenance Service
Washington. D.C. 20591

AD A138228

Instrument Landing System
Critical Area Studies

R.H. McFarland
J.D. Longworth

Avionics Engineering Center
Department of Electrical Engineering
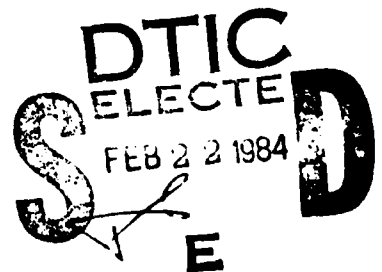Ohio University
Athens, Ohio 45701

November 1983

Final Report

This document is available to the U.S. public
through the National Technical Information
Service, Springfield, Virginia 22161.

DTIC
ELECTE
FEB 2 2 1984
E

US Department of Transportation
Federal Aviation Administration

DTIC FILE COPY

84 02 22 048

NOTICE

This document is disseminated under the sponsorship of
the Department of Transportation in the interest of
information exchange. The United States Government
assumes no liability for the contents or use thereof.

1. Report No.	2. Government Accession No.	3. Recipient's Catalog No.
DOT/FAA/PM-83/39	AD-A138 228	

4. Title and Subtitle	5. Report Date
Instrument Landing System Critical Area Studies	November 1983
	6. Performing Organization Code
	OU/AEC/EER-59-3

7. Author(s)	8. Performing Organization Report No.
R.H. McFarland, J.D. Longworth	

9. Performing Organization Name and Address	10. Work Unit No. (TRAIS)
Avionics Engineering Center	
Department of Electrical and Computer Engineering	11. Contract or Grant No.
Ohio University	DTFA01-82-C-10050
Athens, Ohio 45701	13. Type of Report and Period Covered

12. Sponsoring Agency Name and Address	
Federal Aviation Administration	
Program Engineering and Maintenance Service	Final Report
800 Independence Ave., S.W.	14. Sponsoring Agency Code
Washington, D.C. 20591	APM-410

15. Supplementary Notes

16. Abstract

Theoretical and experimental studies have been performed to determine the perturbational effects on glide slope and localizer course structures. The effects are those produced by aircraft parked in front of the transmitting antennas. Contours are given which indicate the maximum path irregularity for a particular ILS zone given a specific size aircraft, its location and orientation. From these, critical – area designations for particular airdromes can be determined. Special concerns have been given to the effects of the Boeing 747 on the performance of the Cat III, two-frequency localizer and on the 8- and 14- element, single-frequency systems. Also, effects of general aviation type aircraft on the null-reference glide slope have been calculated and measured.

17. Key Words	18. Distribution Statement
Glide slope structure, scattering, aircraft effects on navigation signals, critical areas, CDI contours, theoretical models, glide slope interference effects, diffraction, reflection	Document is available to the public through the National Technical Information Service, Springfield, Virginia 22161.

19. Security Classif. (of this report)	20. Security Classif. (of this page)	21. No. of Pages	22. Price
Unclassified	Unclassified	199	

Form DOT F 1700.7 (8-72)   Reproduction of completed page authorized   1

METRIC CONVERSION FACTORS

Approximate Conversions to Metric Measures

Symbol	When You Know	Multiply by	To Find	Symbol
LENGTH				
in	inches	*2.5	centimeters	cm
ft	feet	30	centimeters	cm
yd	yards	0.9	meters	m
mi	miles	1.6	kilometers	km
AREA				
in²	square inches	6.5	square centimeters	cm²
ft²	square feet	0.09	square meters	m²
yd²	square yards	0.8	square meters	m²
mi²	square miles	2.6	square kilometers	km²
	acres	0.4	hectares	ha
MASS (weight)				
oz	ounces	28	grams	g
lb	pounds	0.45	kilograms	kg
	short tons (2000 lb)	0.9	tonnes	t
VOLUME				
tsp	teaspoons	5	milliliters	ml
Tbsp	tablespoons	15	milliliters	ml
fl oz	fluid ounces	30	milliliters	ml
c	cups	0.24	liters	l
pt	pints	0.47	liters	l
qt	quarts	0.95	liters	l
gal	gallons	3.8	liters	l
ft³	cubic feet	0.03	cubic meters	m³
yd³	cubic yards	0.76	cubic meters	m³
TEMPERATURE (exact)				
°F	Fahrenheit temperature	5/9 (after subtracting 32)	Celsius temperature	°C

*1 in = 2.54 (exactly). For other exact conversions and more detailed tables, see NBS Misc. Publ. 286, Units of Weights and Measures. Price $2.25, SD Catalog No. C13.10 286.

Approximate Conversions from Metric Measures

Symbol	When You Know	Multiply by	To Find	Symbol
LENGTH				
mm	millimeters	0.04	inches	in
cm	centimeters	0.4	inches	in
m	meters	3.3	feet	ft
m	meters	1.1	yards	yd
km	kilometers	0.6	miles	mi
AREA				
cm²	square centimeters	0.16	square inches	in²
m²	square meters	1.2	square yards	yd²
km²	square kilometers	0.4	square miles	mi²
ha	hectares (10,000 m²)	2.5	acres	
MASS (weight)				
g	grams	0.035	ounces	oz
kg	kilograms	2.2	pounds	lb
t	tonnes (1000 kg)	1.1	short tons	
VOLUME				
ml	milliliters	0.03	fluid ounces	fl oz
l	liters	2.1	pints	pt
l	liters	1.06	quarts	qt
l	liters	0.26	gallons	gal
m³	cubic meters	35	cubic feet	ft³
m³	cubic meters	1.3	cubic yards	yd³
TEMPERATURE (exact)				
°C	Celsius temperature	9/5 (then add 32)	Fahrenheit temperature	°F

°F -40   32   98.6   212
     -40 0 32 80 120 160 200
°C -40 -20 0 20 37 40 60 80 100

TABLE OF CONTENTS

Accession For	
NTIS GRA&I	☒
DTIC TAB	☐
Unannounced	☐
Justification____	
By_____	
Distribution/	
Availability Codes	
Dist	Avail and/or Special
A-1	

iii

ABSTRACTS

(Phase I)   A theoretical and experimental investigation of GRN-27 dual
             frequency localizer signal derogation by the Boeing 747
             was performed in order to recommend the Category III minimum
             crtical area required for this type localizer.

(Phase II)   A study to recommend ILS Category-III critical area limits
             for two types of single-frequency localizer arrays has been
             performed. The 8-and 14-element directional localizer arrays
             utilizing log periodic dipole antennas (also O-ring for the
             14-element) have been modeled to calculate the localizer
             signal scattering in the presence of wide-body aircraft.

(Phase III) A theoretical and experimental study has been performed to
             determine the perturbational effects on the glide slope
             structure produced by general aviation type aircraft parked
             in front of the transmitting antennas. Contours are given
             which indicate the maximum path irregularity for a particular
             ILS zone given a specific size aircraft, its location and
             orientation. From these, critical-area designations for
             particular airdromes can be determined. In general, aircraft
             of the size of the Convair 440 and smaller have little or no
             significant effect on Cat I glide slope performance when they
             are located on typical taxiway configurations alongside of
             and in front of the transmitting array.

PHASE I

THEORETICAL AND EXPERIMENTAL INVESTIGATION

OF BOEING 747 DUAL-FREQUENCY LOCALIZER SIGNAL SCATTERING

FOR CAT III CRITICAL AREA DETERMINATION

by

Joe D. Longworth

November 1982
(Revised August 1983)

LIST OF ILLUSTRATIONS (Continued)

LIST OF TABLES

iv

INTRODUCTION

PURPOSE.

A FAA requirement to support the United States contribution to ICAO Instrument Landing System (ILS) subgroup has generated the need for information concerning the critical areas for Category III dual-frequency localizers. Of this effort, a primary consideration is whether or not the critical area can be reduced to 300 feet as proposed for ICAO Annex 14 criteria for aircraft obstructions.

In addition to the specific requirements to support the ICAO contribution the effort also provides valuable information for use in the revision of current U.S. siting criteria. An ancillary effort is to determine the feasibility of using the current far-field monitors to protect the established critical areas.

The critical area as defined in this report is that area in which a parked or taxiing aircraft could cause the ILS flight inspection tolerances to be exceeded. Critical areas are established for various aircraft orientations with respect to the runway centerline.

BACKGROUND.

In 1974 Ohio University performed a theoretical and experimental study to recommend critical areas for ILS localizer and glide slope equipments in use at that time. A single-frequency localizer computer model was established and used to compute contour maps of peak course deviation indicator (CDI) currents for a grid of positions of a Boeing 747 series aircraft located within 600 feet laterally and 10000 feet longitudinally of the localizer (reference 1). In addition, the effects of specific aircraft locations were computed and then experimentally validated using a National Airlines Boeing 747 at the Miami International Airport (reference 2).

The computer model used in this effort was upgraded to a two-frequency model using traveling wave antennas in early 1982 to support an anomaly investigation at the Los Angeles International Airport (reference 3). With this specific background and the availability of the localizer computer models, the earlier work has been extended to the current effort.

DISCUSSION

DISCUSSION OF CONTOUR MAPS.

The contour maps of peak CDI deviations generated in report FAA-RD-74-57 were used as the basis for the work on the two-frequency systems. In the earlier work these maps were used to determine the critical areas for the specific category approach. In the current effort contour maps have again been generated to present essentially the same information as for the single-frequency system. In the previous work the contour maps show the peak CDI deviation from 0 microamperes for all positions along the approach. This approach was deemed valid at the time since maximum

deviations usually occur near the aircraft location. Advances made in the computing capability of the localizer model have made it possible to generate contour maps for each ILS zone. The advantages of this are that the peak deviations can be directly related to the tolerances for the specific zones.

Contour maps of the CDI deviations have been generated for three aircraft orientations. These are with the aircraft parallel to the centerline, with the aircraft perpendicular to the centerline and the nose toward the centerline, and with the aircraft perpendicular to centerline with the tail toward the centerline. The orientations have substantially different effects on the localizer performance. The basic reason for this is that the tail of the aircraft is the major contributor to the reflections and the closer the tail is to the centerline the greater the signal derogation.

The maps generated for the various orientations are shown in figures 1 through 9. On each of the maps the x-axis is aligned along the runway centerline and shows the distance in feet from the localizer array. The y-axis is perpendicular to the runway centerline and shows the distance in feet from the localizer array. The contours are then the peak deviation in CDI generated by the reflecting aircraft located at the specific x, y coordinate. For example in figure 1 if the aircraft is positioned at a y distance of 200 feet and an x distance of 2000 feet, the resultant peak CDI is the value of the intersecting contour of 10 microamperes. Note that the localizer array is located at the origin of these maps. Also note that the reference point on the aircraft is the center of the fuselage. The contour lines represent the peak CDI value only. The solid lines represent the minimum recommended distance to centerline after application of flight inspection tolerances to the localizer structure for each point. Contour maps are included only for those ILS zones in which the peak CDI exceeded 5 microamperes. All computations assume a constant approach speed of 200 ft/sec.

EXPERIMENTAL TEST PLAN.

In the effort of 1974, experimental measurements were made at the Miami International Airport using a National Airlines (presently Pan American) Boeing 747 as the reflector. Eight positions of the aircraft were modeled and subsequently measured for comparison purposes. These measurements were then used to validate the use of the model to construct contour maps and to apply flight inspection criteria to the effects.

Calculated and measured positions similar to the previous work have been performed for the two-frequency system. The Dallas-Ft. Worth Regional Airport was selected for the measurement phase of the study. This was primarily because of the availability of an American Airlines Boeing 747 and the taxiway layout of the airport is very conducive to the measurement activity.

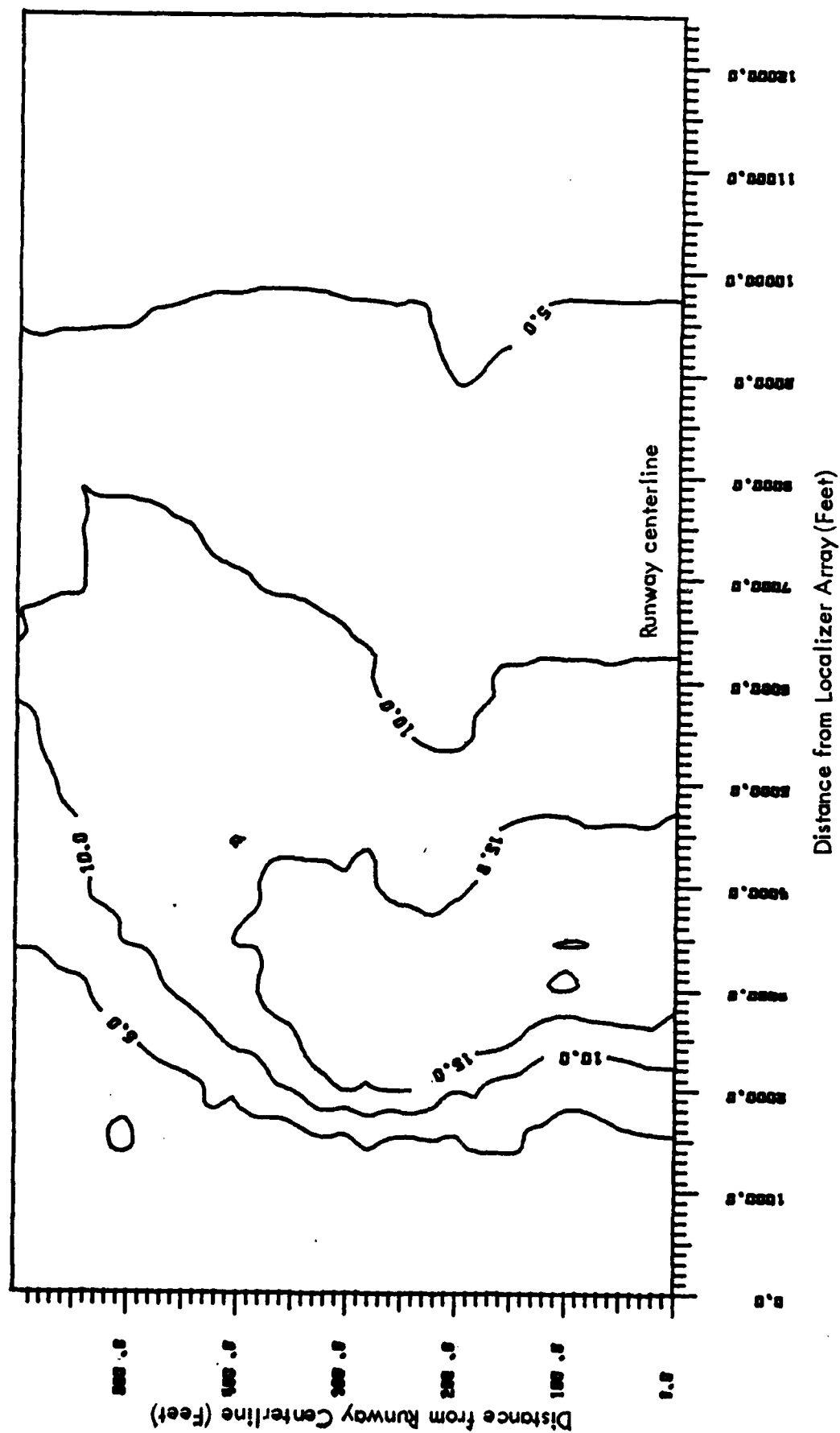Prior to field measurements nine locations were chosen for validation.

Figure 1. B-747 Parallel to the Centerline. Peak CDI Between ILS Points D and E. Simulated approach speed of 200 ft/sec.

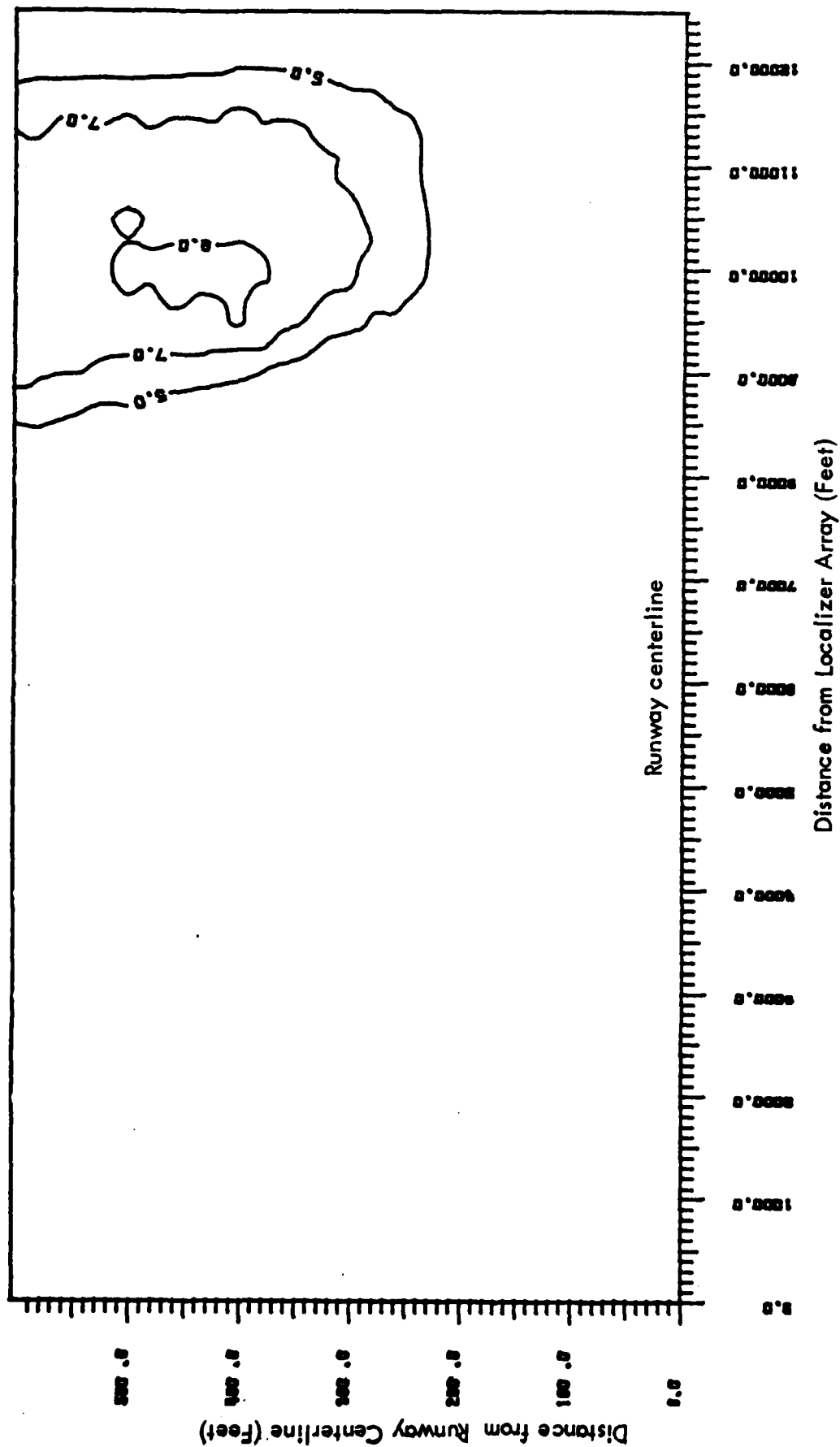Note: Localizer structure "In Tolerance" for all locations.

Figure 2. B-747 Parallel to the Centerline. Peak CDI Between ILS Points C and D. Simulated approach speed of 200 ft/sec.

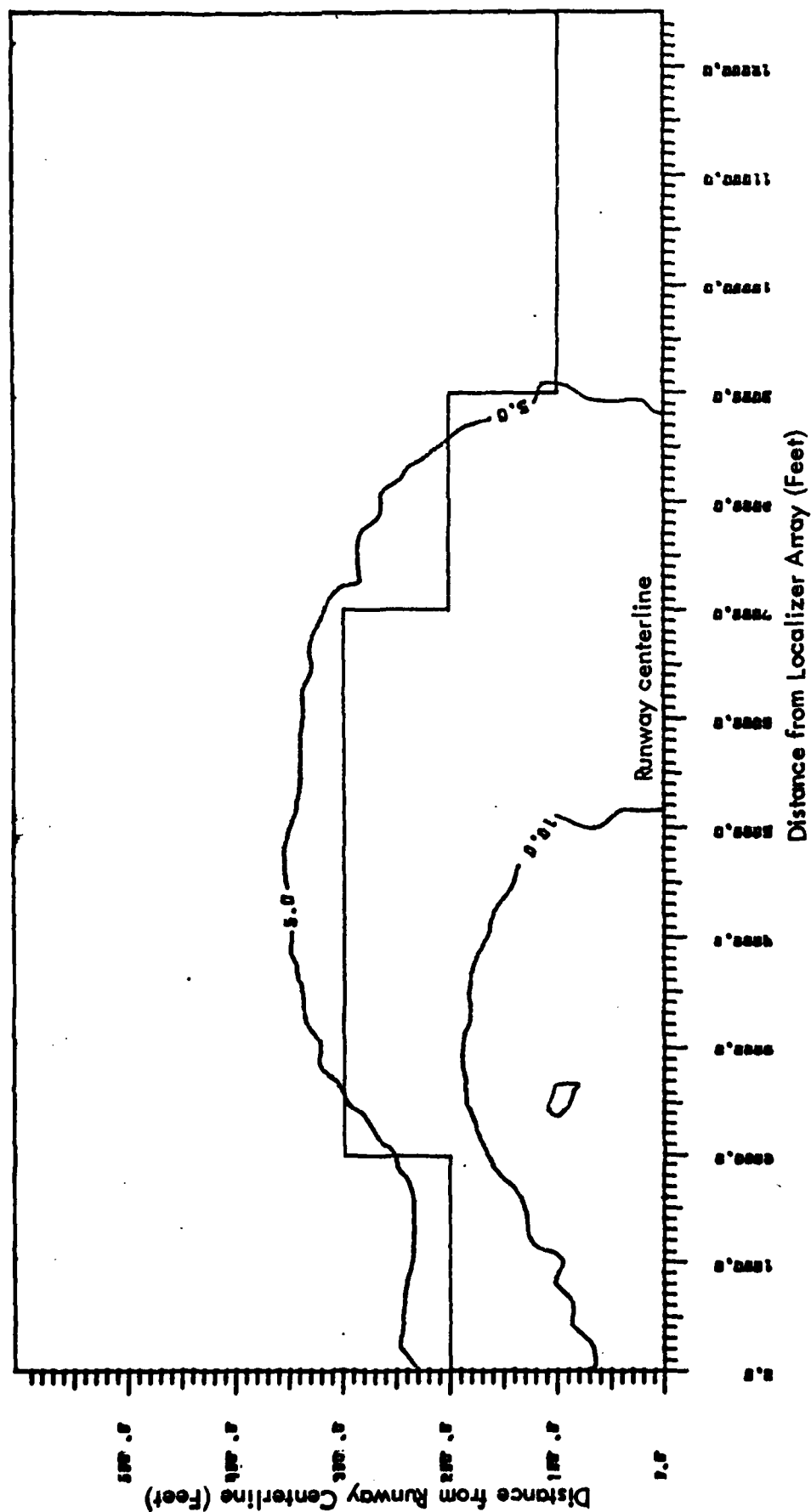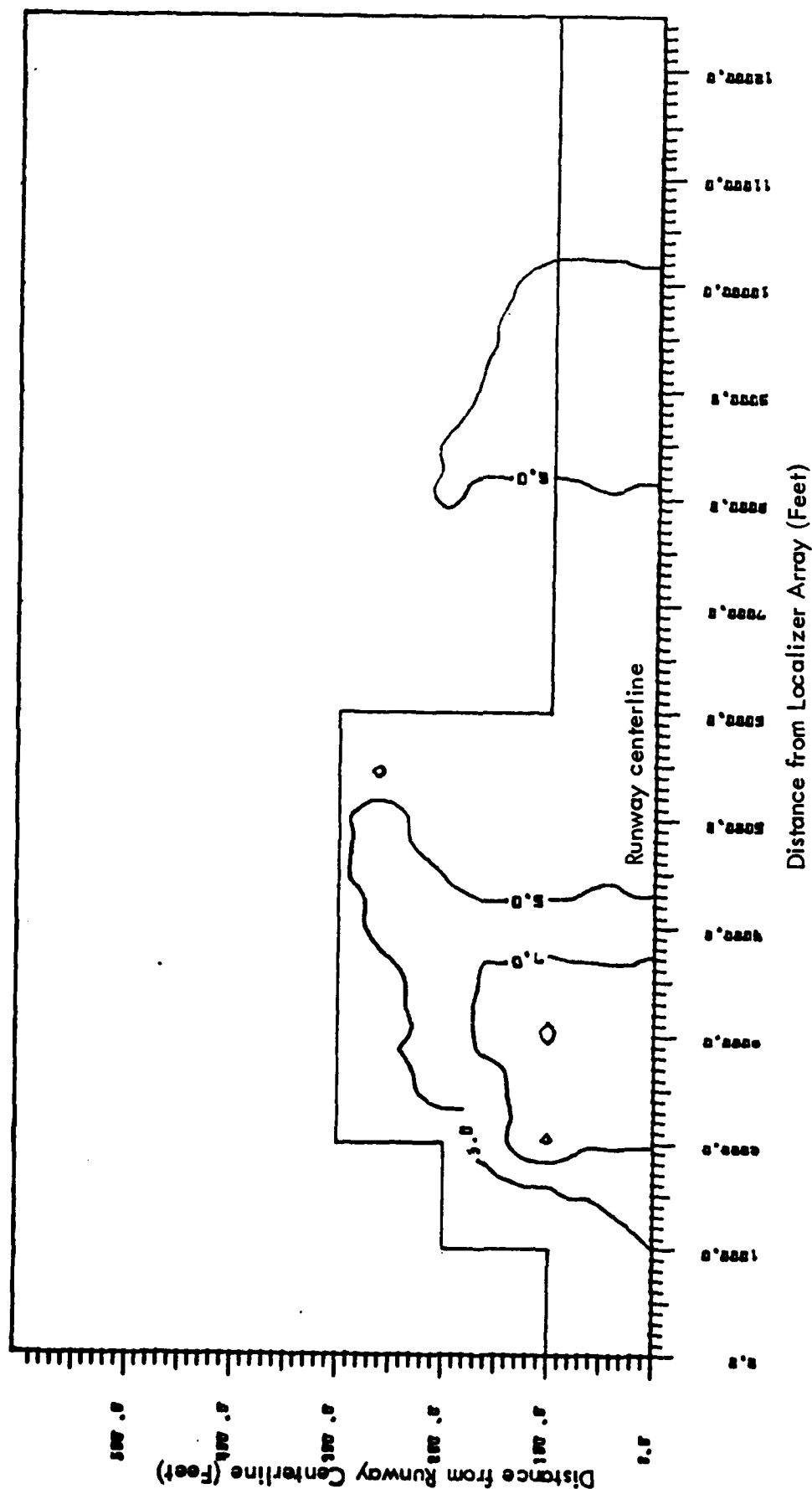Note: Localizer structure "In Tolerance" for all locations.
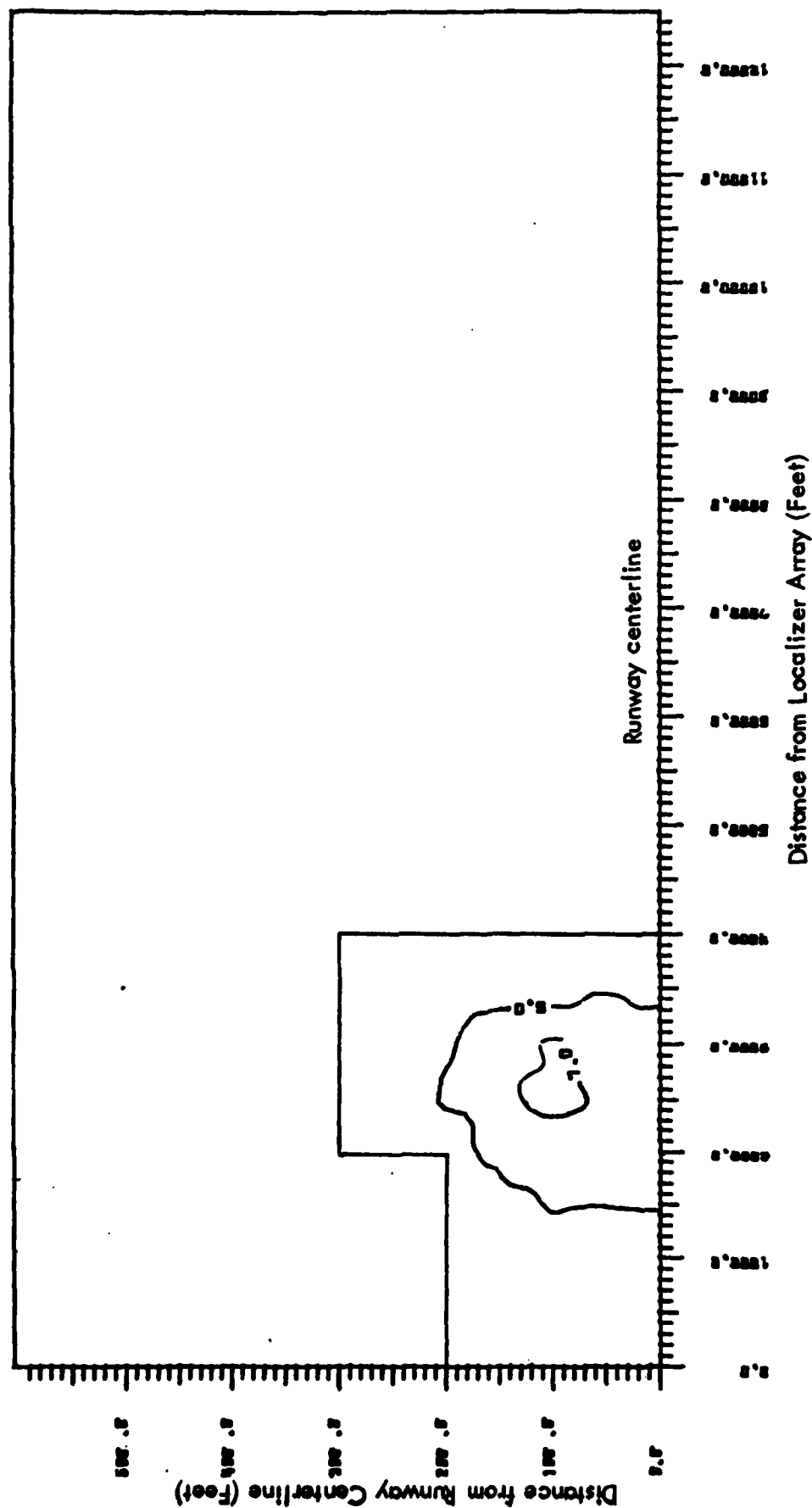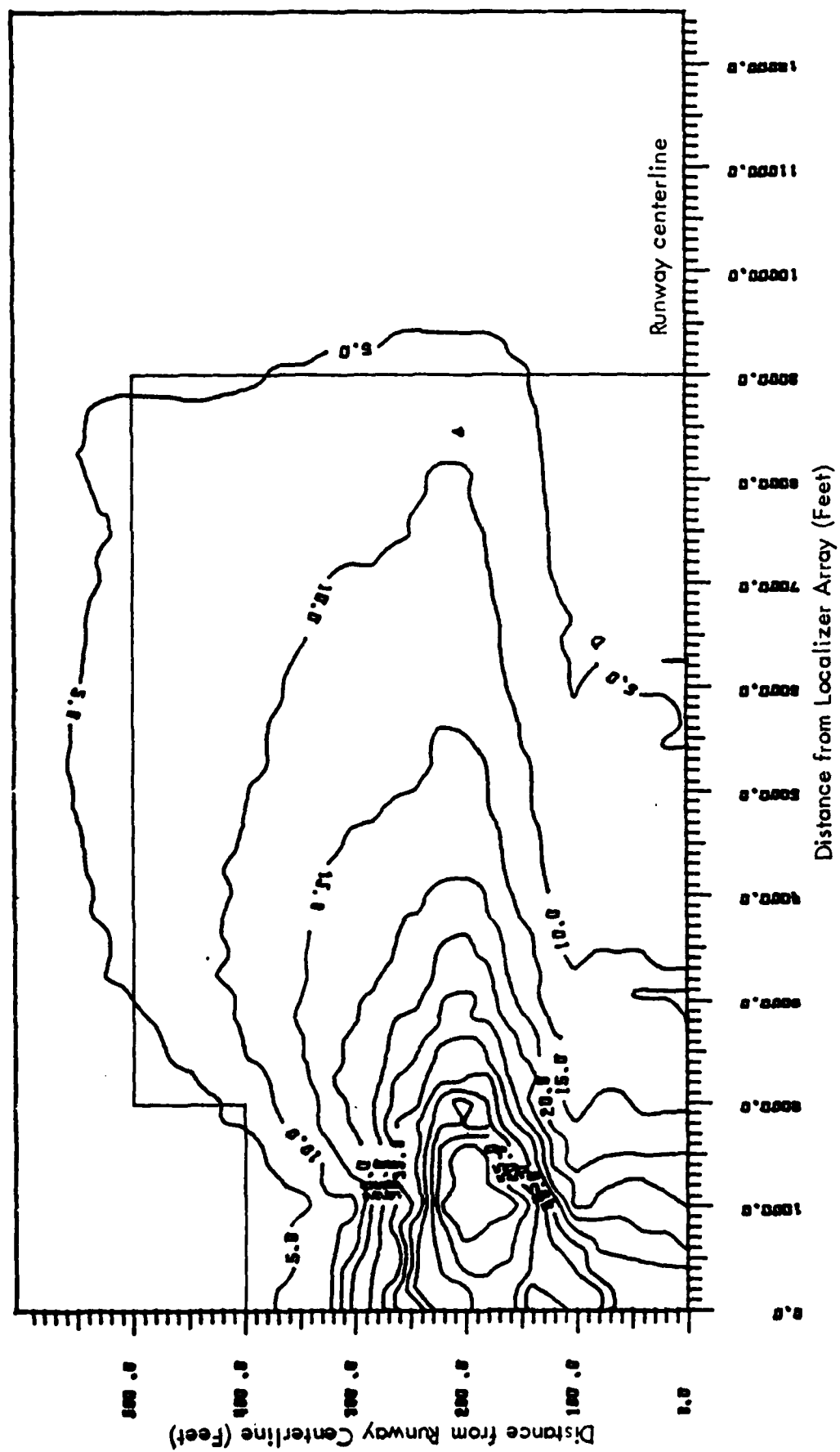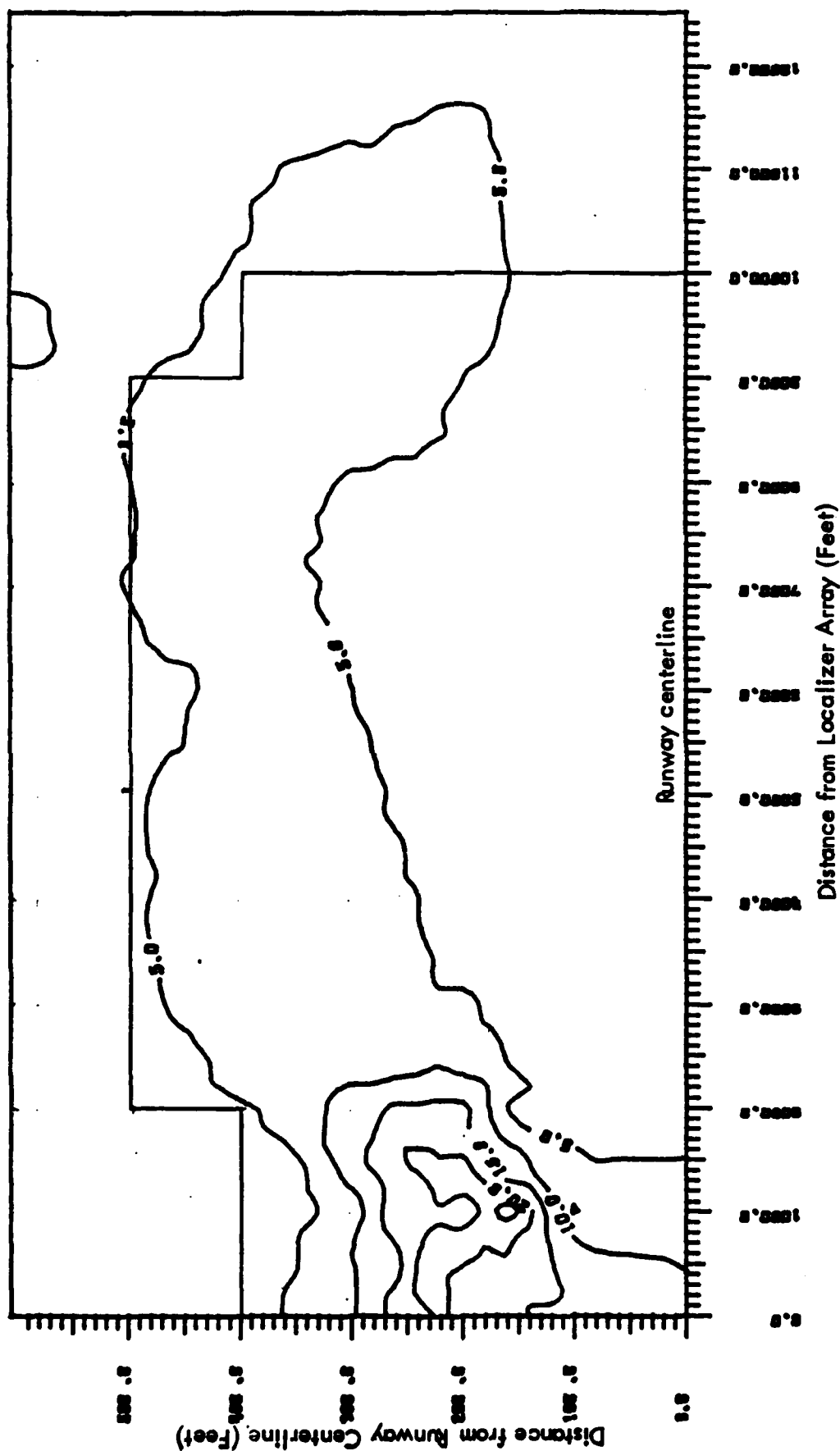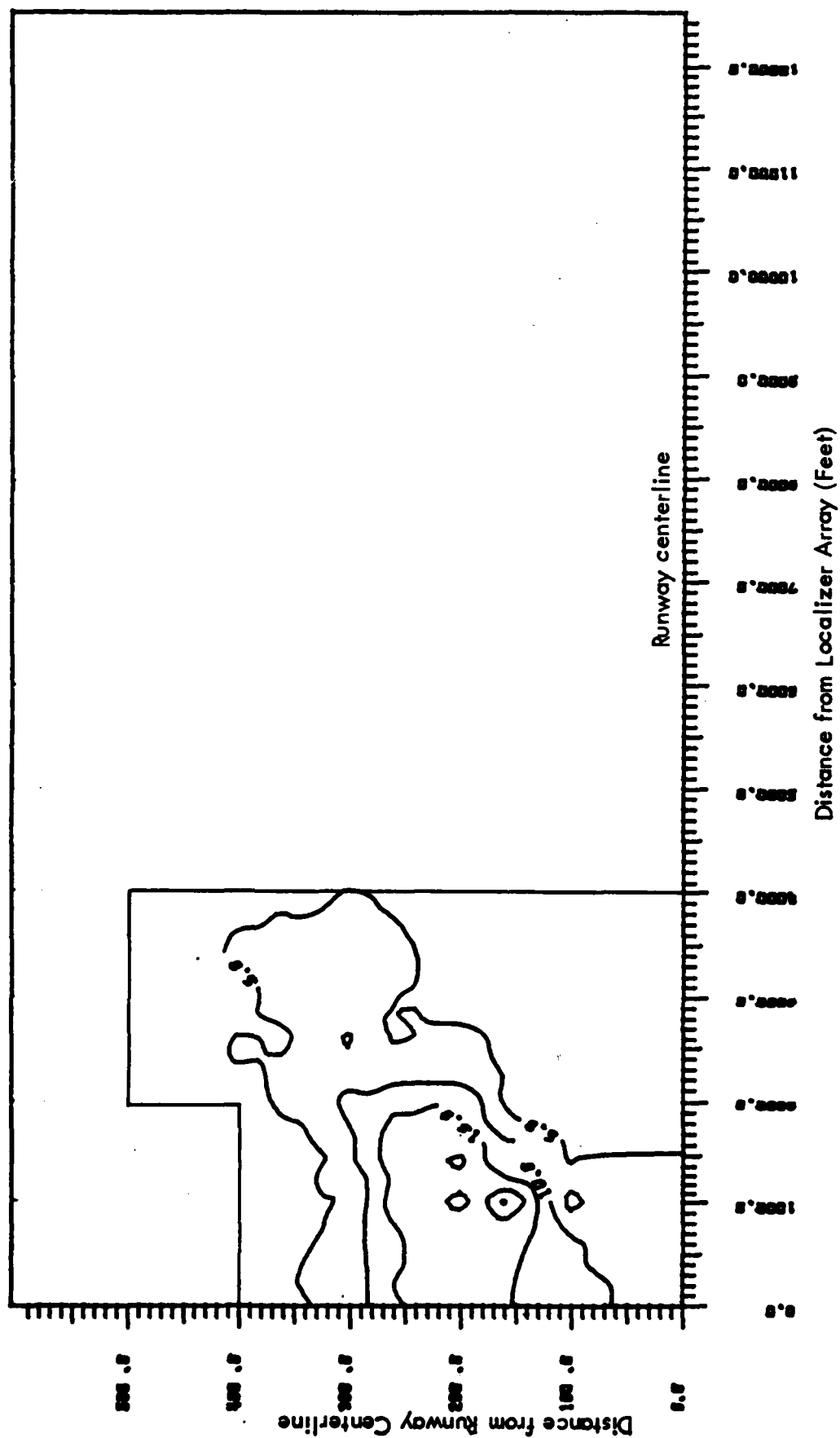
Figure 3. B-747 Perpendicular to the Centerline with the Nose of the Aircraft Towards Centerline. Peak CDI Between ILS Points D and E. Simulated approach speed of 200 ft/sec.
Note: Localizer structure "In tolerance" beyond solid line.

-5-

Distance from Runway Centerline (Feet)

Runway centerline
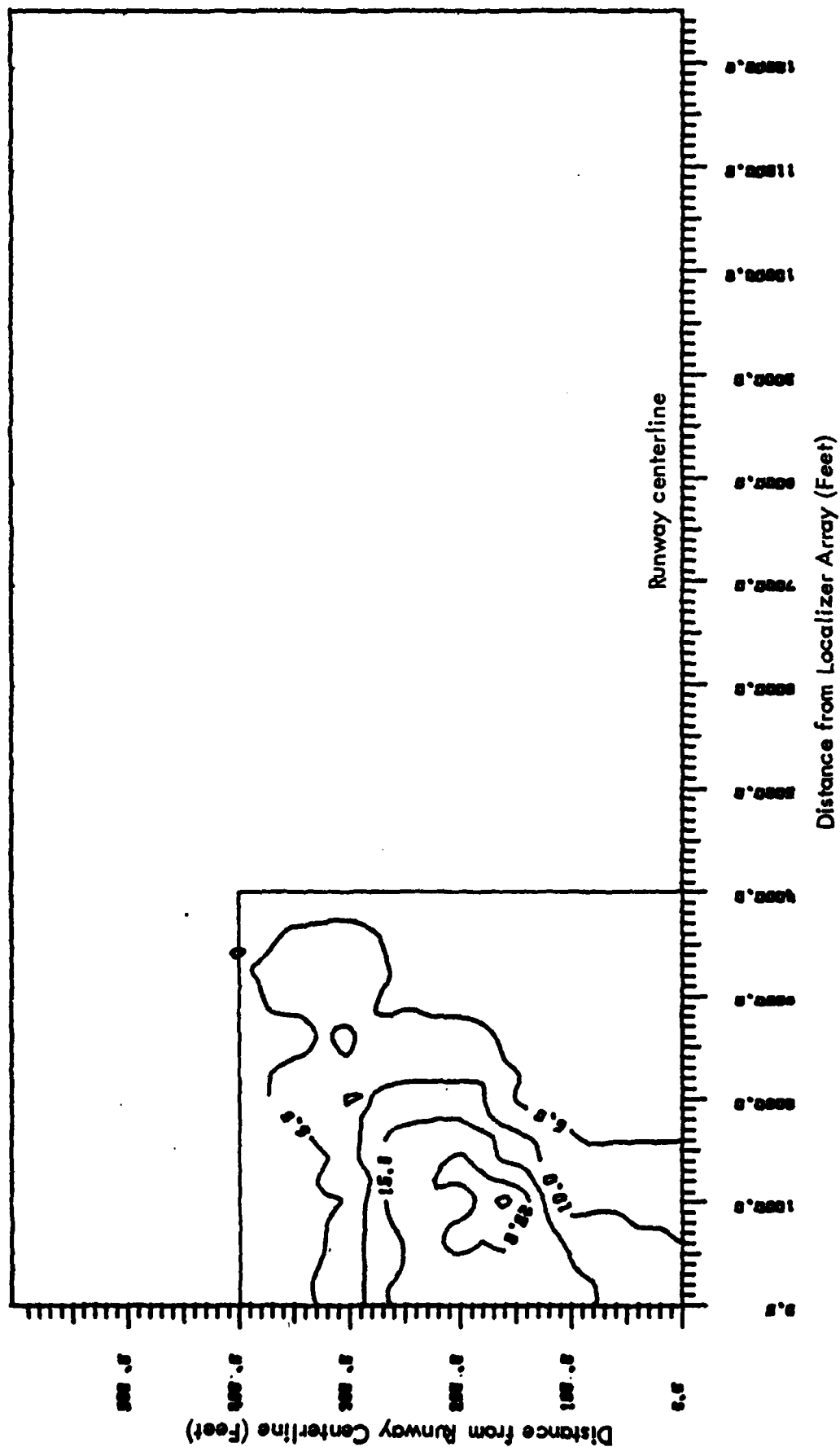
Distance from Localizer Array (Feet)

Figure 4. B-747 Perpendicular to the Centerline with the Nose of the Aircraft Towards Centerline. Peak CDI Between ILS Points C and D. Simulated approach speed of 200 ft/sec.

Note: Localizer structure "In Tolerance" beyond solid line.

Runway centerline

Distance from Localizer Array (Feet)

Distance from Runway Centerline (Feet)

Figure 5. B-747 Perpendicular to Centerline With Nose of the Aircraft Towards Centerline. Peak CDI Between ILS Points B and C. Simulated approach speed of 200 ft/sec.

Note: Localizer structure "In Tolerance" beyond solid line.

Figure 6. B-747 Perpendicular to the Centerline With the Tail of the Aircraft Towards Centerline. Peak CDI Between ILS Points D and E. Simulated approach speed of 200 ft/sec.
Note: Localizer structure "In Tolerance" when aircraft is located beyond solid line.

-8-

Figure 7. B-747 Perpendicular to the Centerline with the Tail of the Aircraft Towards Centerline. Peak CDI Between ILS Points C and D. Simulated approach speed of 200 ft/sec.
Note: Localizer structure "In Tolerance" when aircraft is located beyond solid line.

Figure 8. B-747 Perpendicular to the Centerline With the Tail of the Aircraft Towards Centerline. Peak CDI Between ILS Points B and C. Simulated approach speed of 200 ft/sec.

Note: Localizer structure "In Tolerance" when aircraft is located beyond solid line.

Distance from Localizer Array (Feet)

Distance from Runway Centerline

Figure 9. B-747 Perpendicular to the Centerline with the Tail of the Aircraft Towards Centerline. Peak CDI Between ILS Points A and B. Simulated approach speed of 200 ft/sec.
Note: Localizer structure "In Tolerance" when aircraft is located beyond solid line.

These were selected to be:

        1. Representative of actual aircraft locations
            during normal operations.

        2. Positions which would have the most pronounced
            effects on the localizer course structure without
            obstructing the runway.

        3. Positions easily located.

EXPERIMENTAL RESULTS.

The localizer course CDI values along the centerline simlulating a flight
inspection aircraft approach were computed for each of nine B-747 loca-
tions. These same nine locations were then measured on October 13 and 14,
1982 at the Dallas-Ft. Worth Airport. The results of both the measured and
computed CDI values are plotted in figures 10 through 18. The specific
aircraft locations and orientations are shown in appendix A.

Extremely good correlation is noted in 7 of the 9 locations measured. In
each of these cases the maximum bends and scalloping of the localizer
course occur very near the predicted locations and have very similar magni-
tudes. In the two cases where the correlation is not as readily discer-
nable (positions 2 and 6) the calculated magnitude is equal to or greater
than that measurement.

FAR-FIELD MONITOR MEASURMENTS.

Coincident with the airborne measurements of the localizer system with the
B-747 located at the previously mentioned positions, far-field monitor
measurements were conducted. These measurements were recorded for both the
normal far-field monitor in place for runway 17L at the Dallas-Ft. Worth
Regional Airport and for a new design vector far-field monitor built by
Westinghouse (reference 5).

The vector far-field monitor is designed to detect both quadrature and
scalar ddm quantities and is therefore more sensitive to reflected sideband
energies which may cause course abberations. Both units were located at
the current far-field monitor site at the middle marker for runway 17L.
Table 1 summarizes the results of these measurements.

RECOMMENDATIONS

CRITICAL AREA RECOMMENDATIONS.

Using the contour maps it is now possibe to establish an estimate of where
the critical areas should be located. Another criteria other than the peak
deviation must be included in the analysis of localizer stucture. This is
the application of paragraph 217.41 of the U.S. Flight Inspection Manual
(reference 4). Essentially this is as follows:

    a. Where course/path structure is out-of-tolerance in any region of
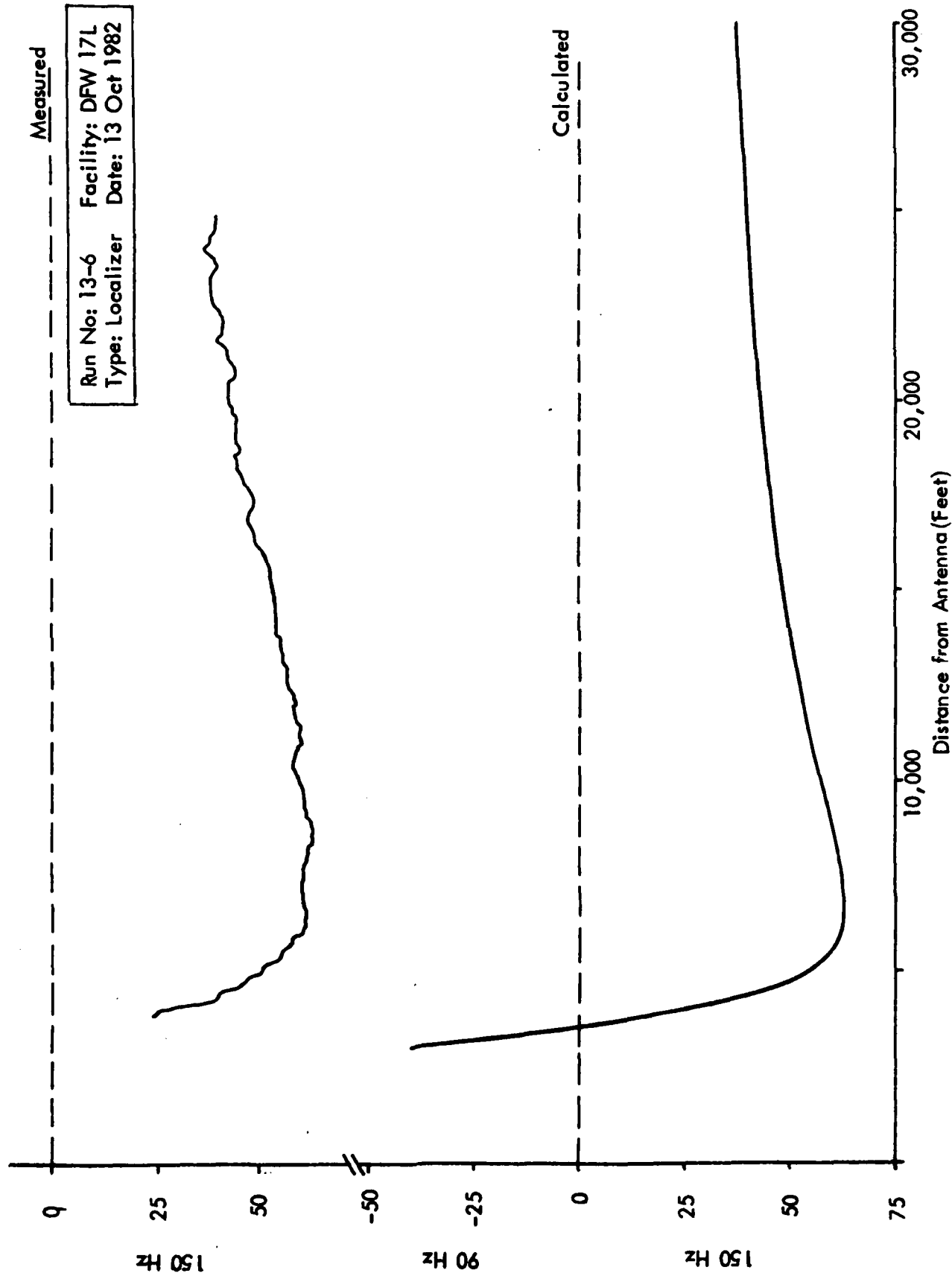the approach, the flight recordings will be analyzed in distance intervals

Figure 10. Plots of Measured and Calculated Localizer CDI with B-747

Measured

Calculated

Run No: 13-6   Facility: DFW 17L
Type: Localizer   Date: 13 Oct 1982

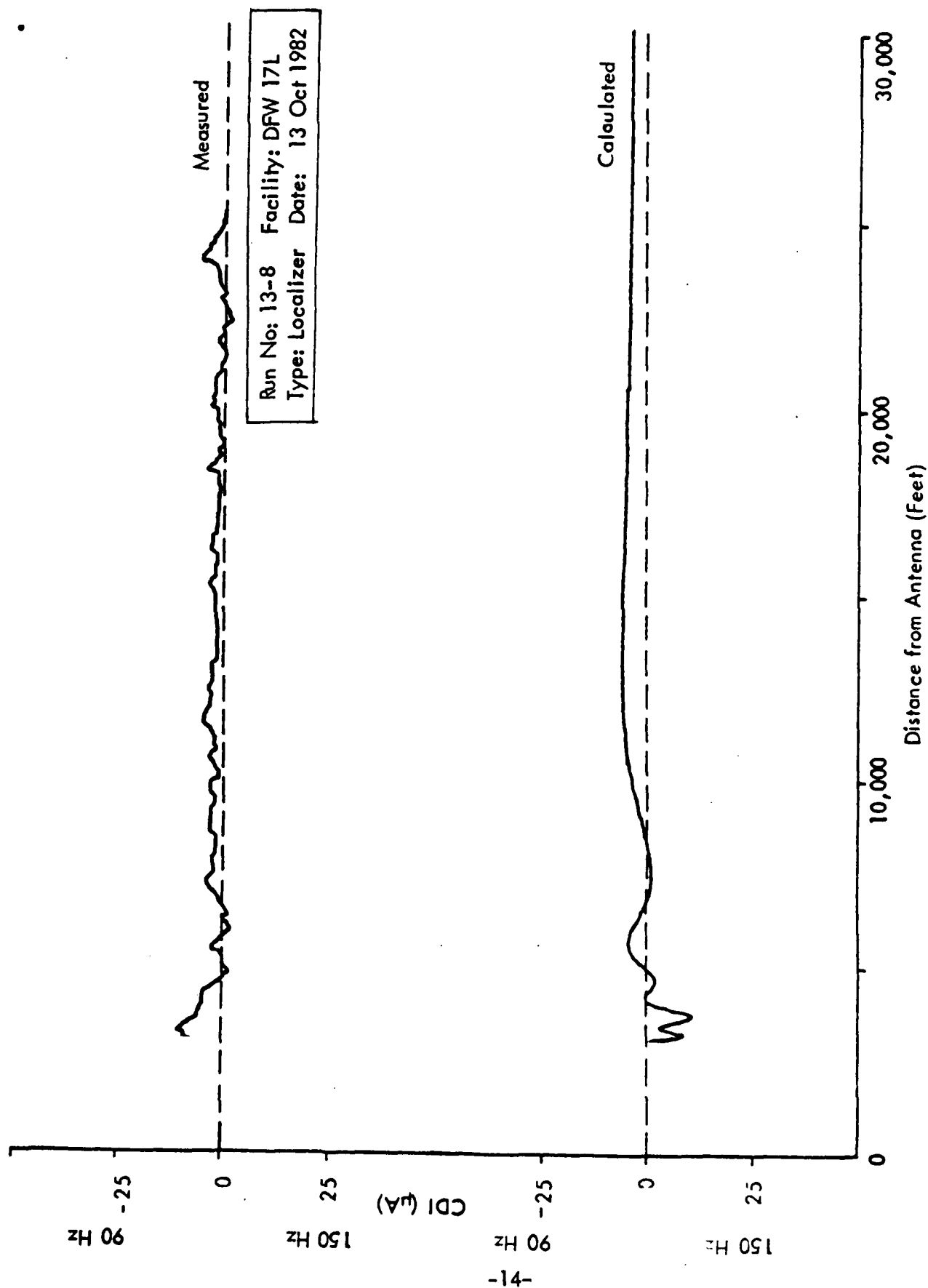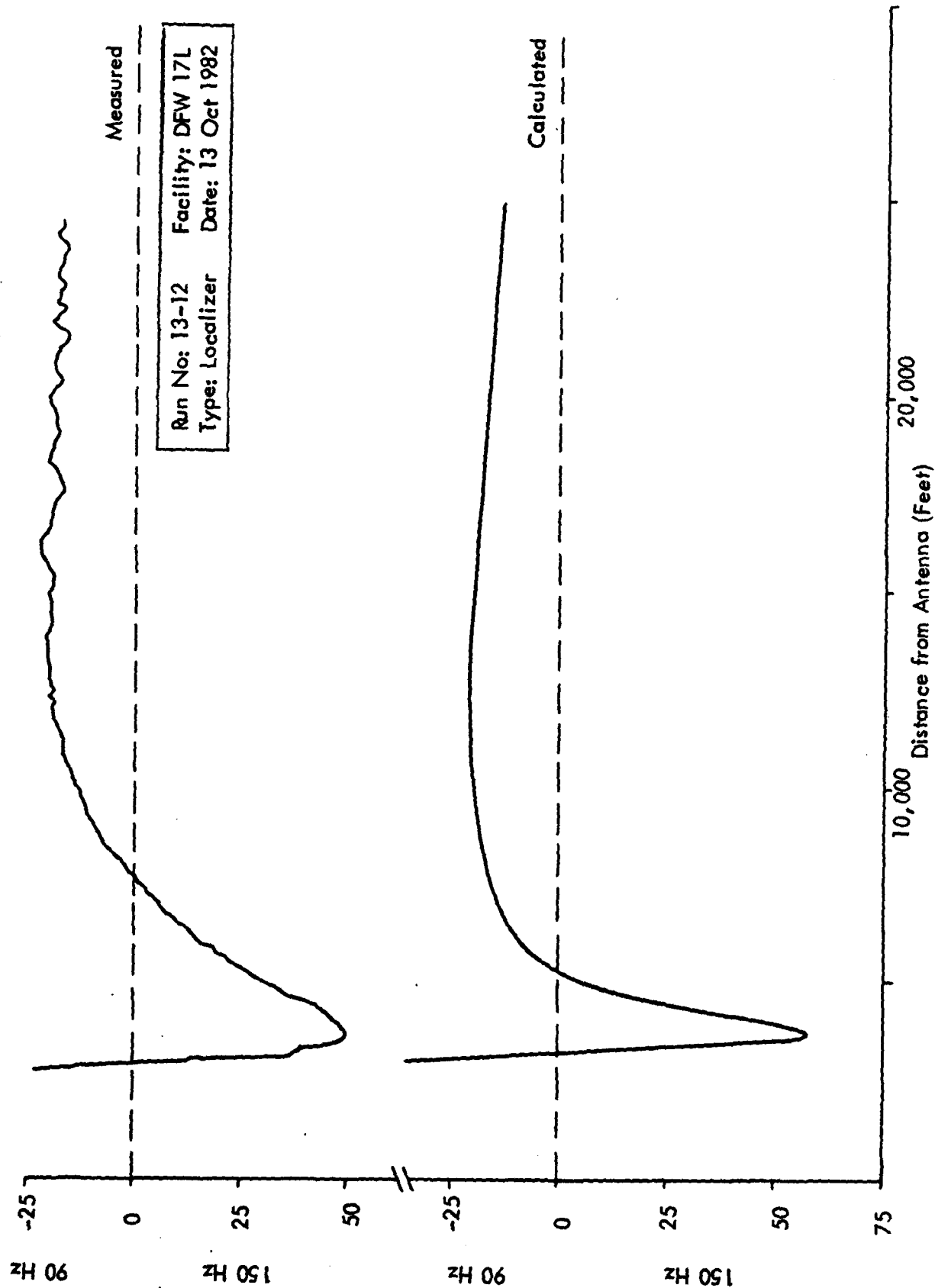Distance from Antenna (Feet)

150 Hz

90 Hz

150 Hz

Figure 11. Plots of Measured and Calculated Localizer CDI with B-747 Located at Position No.2.

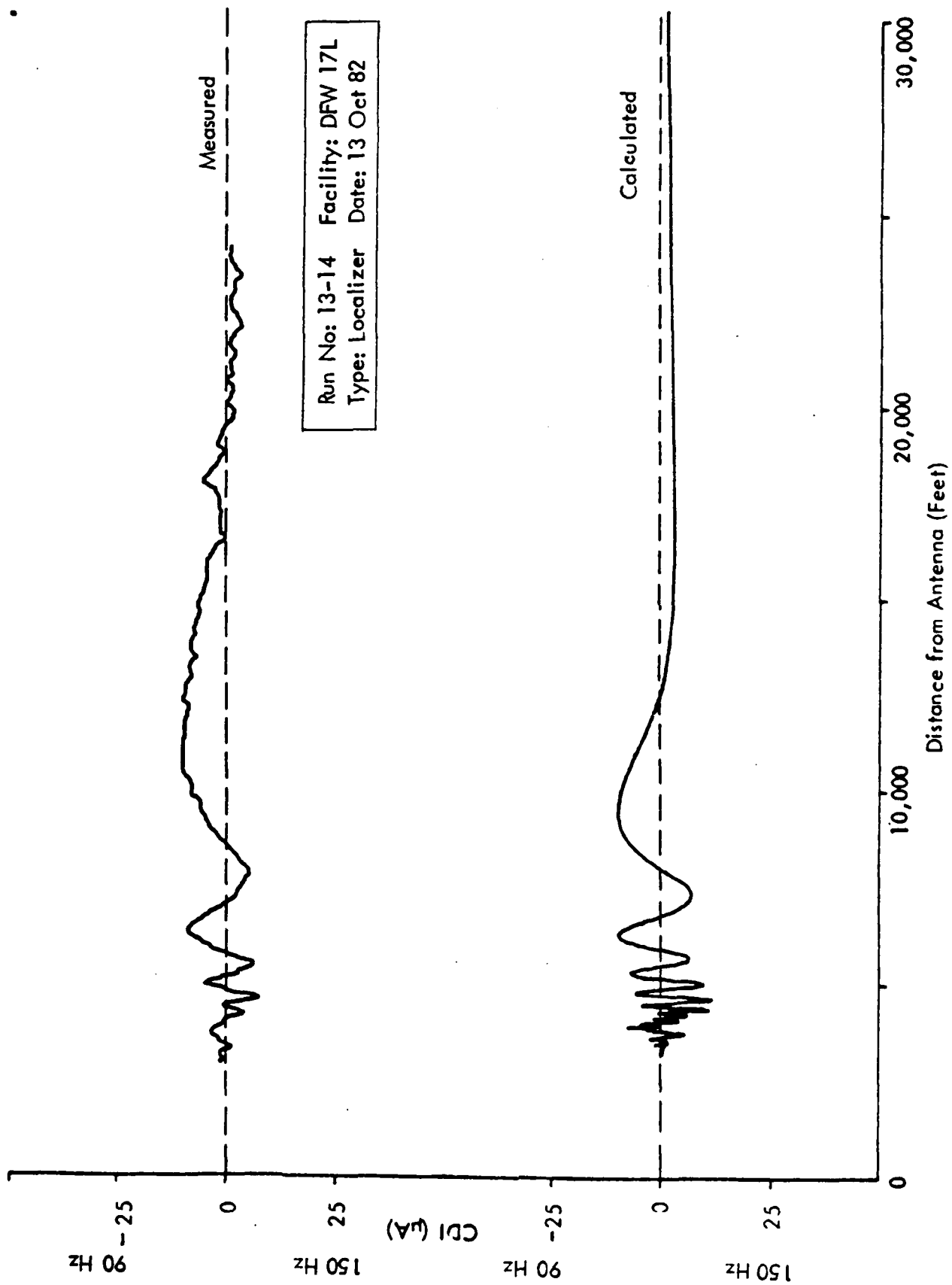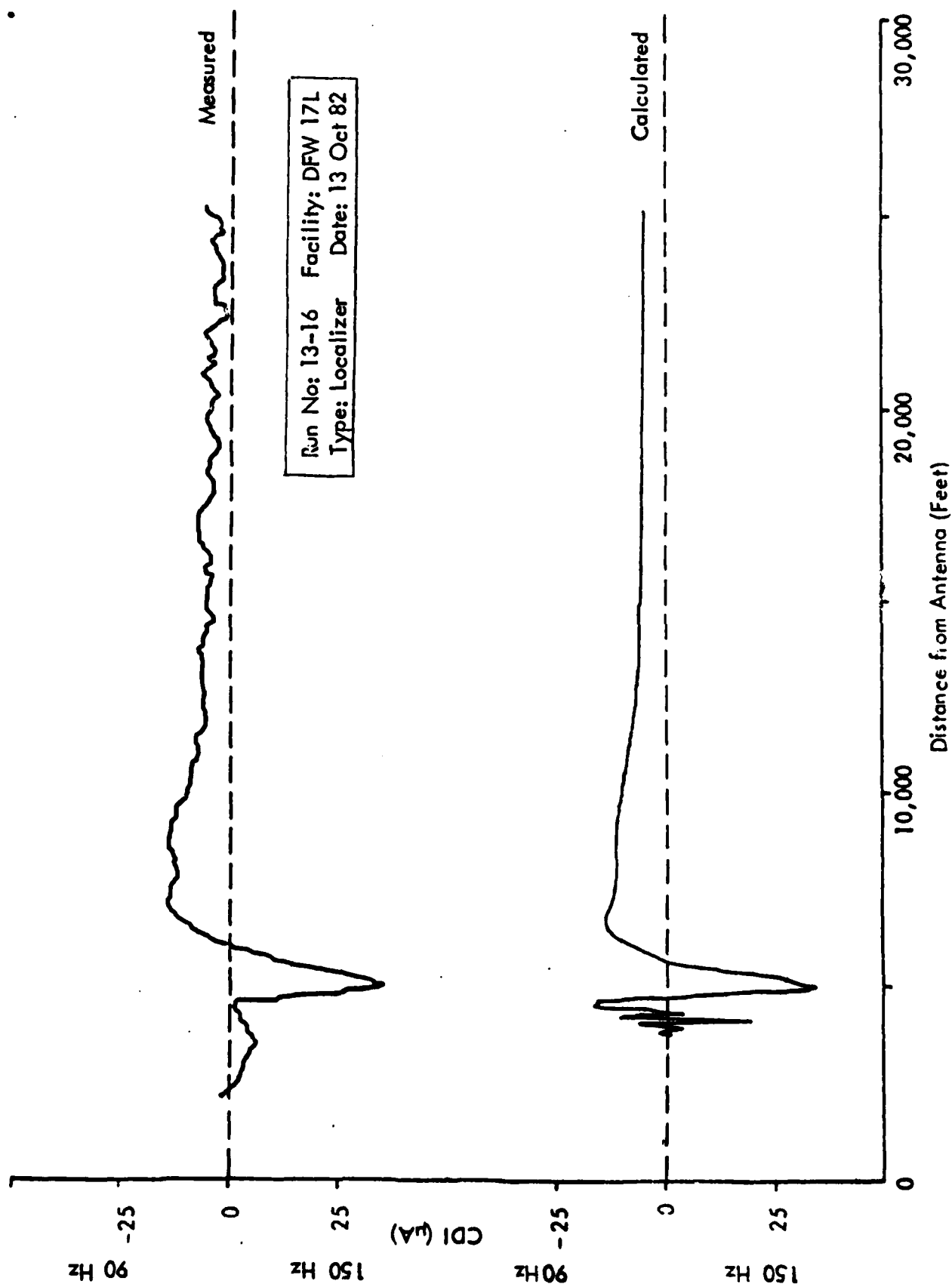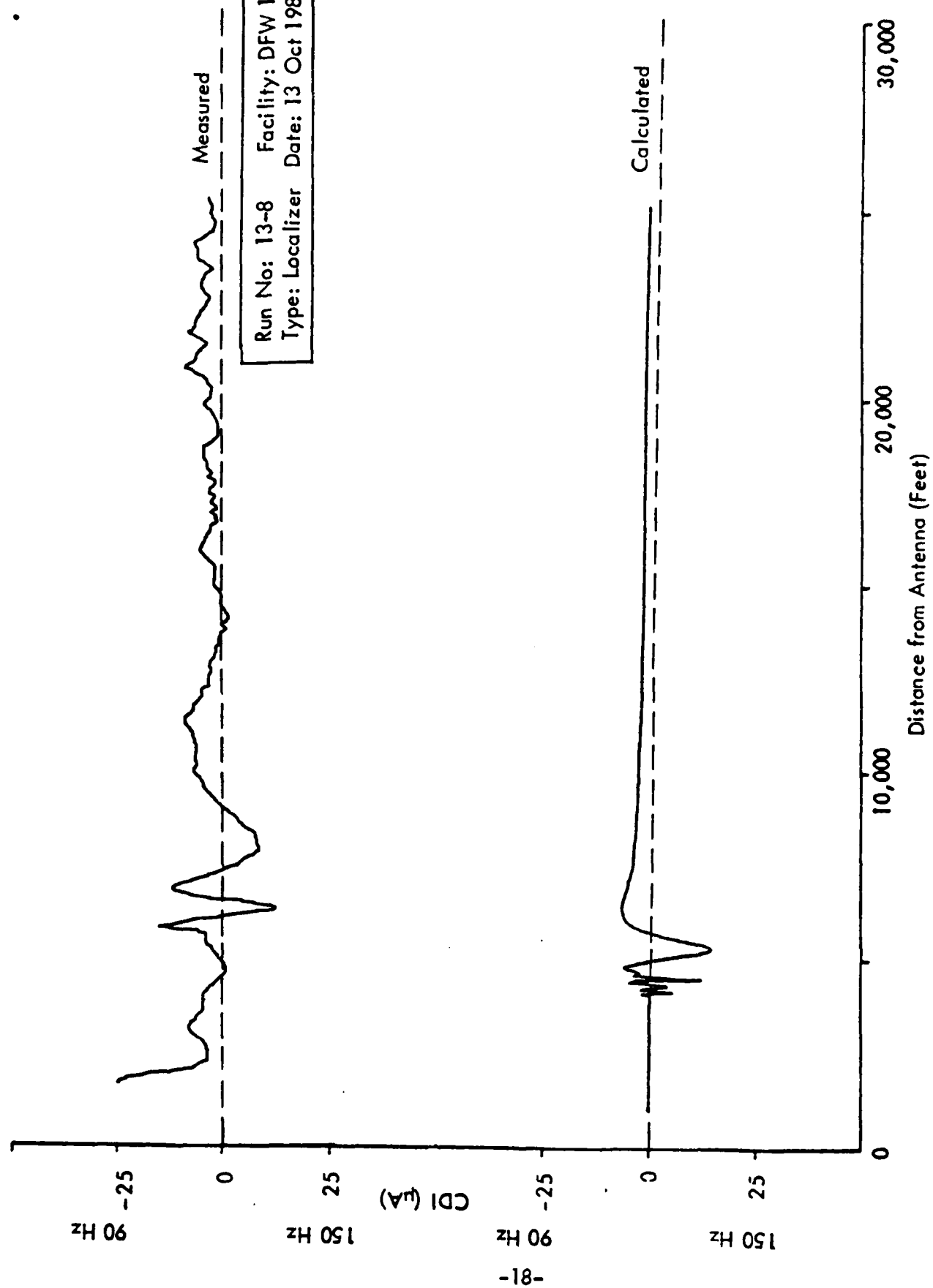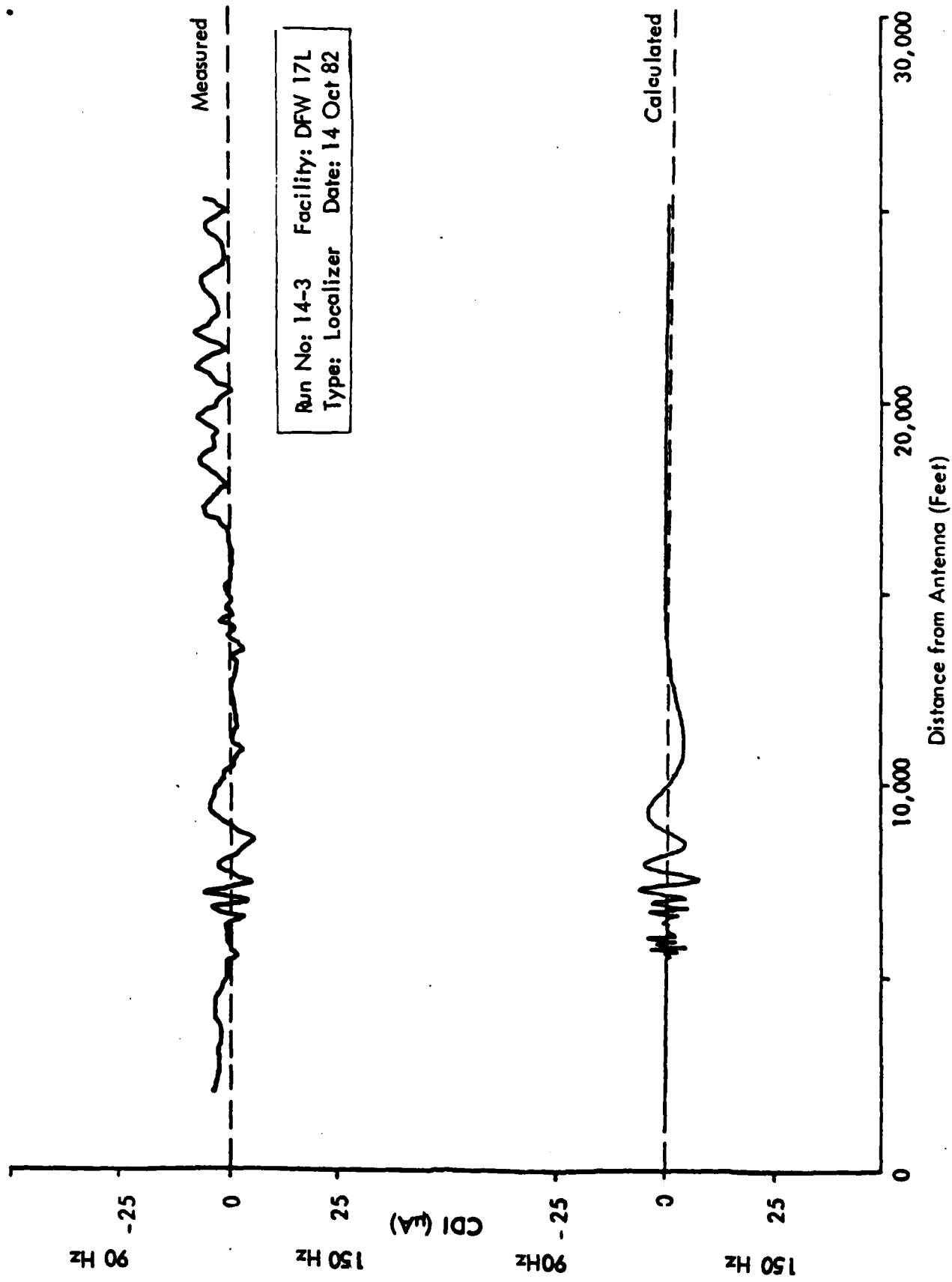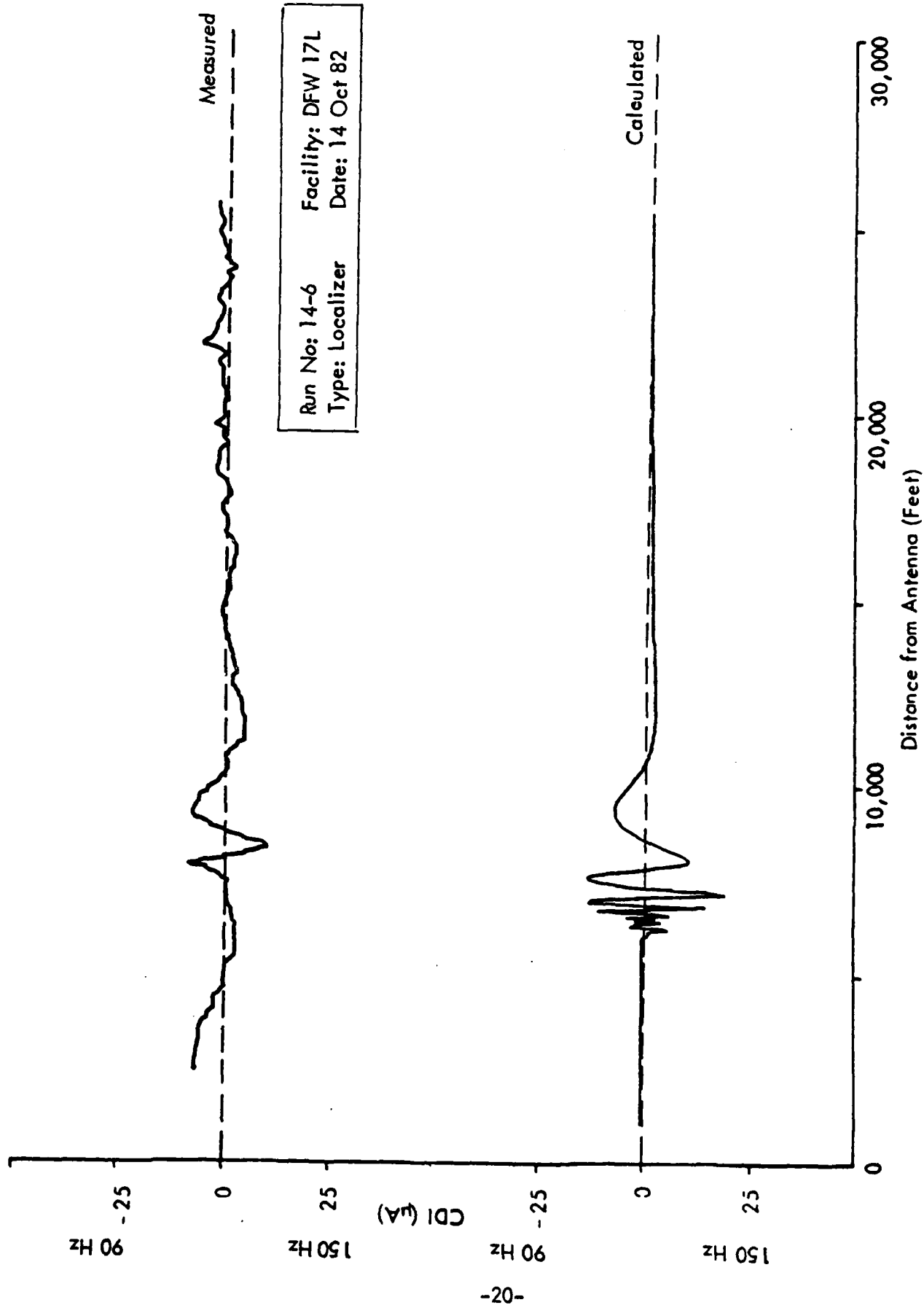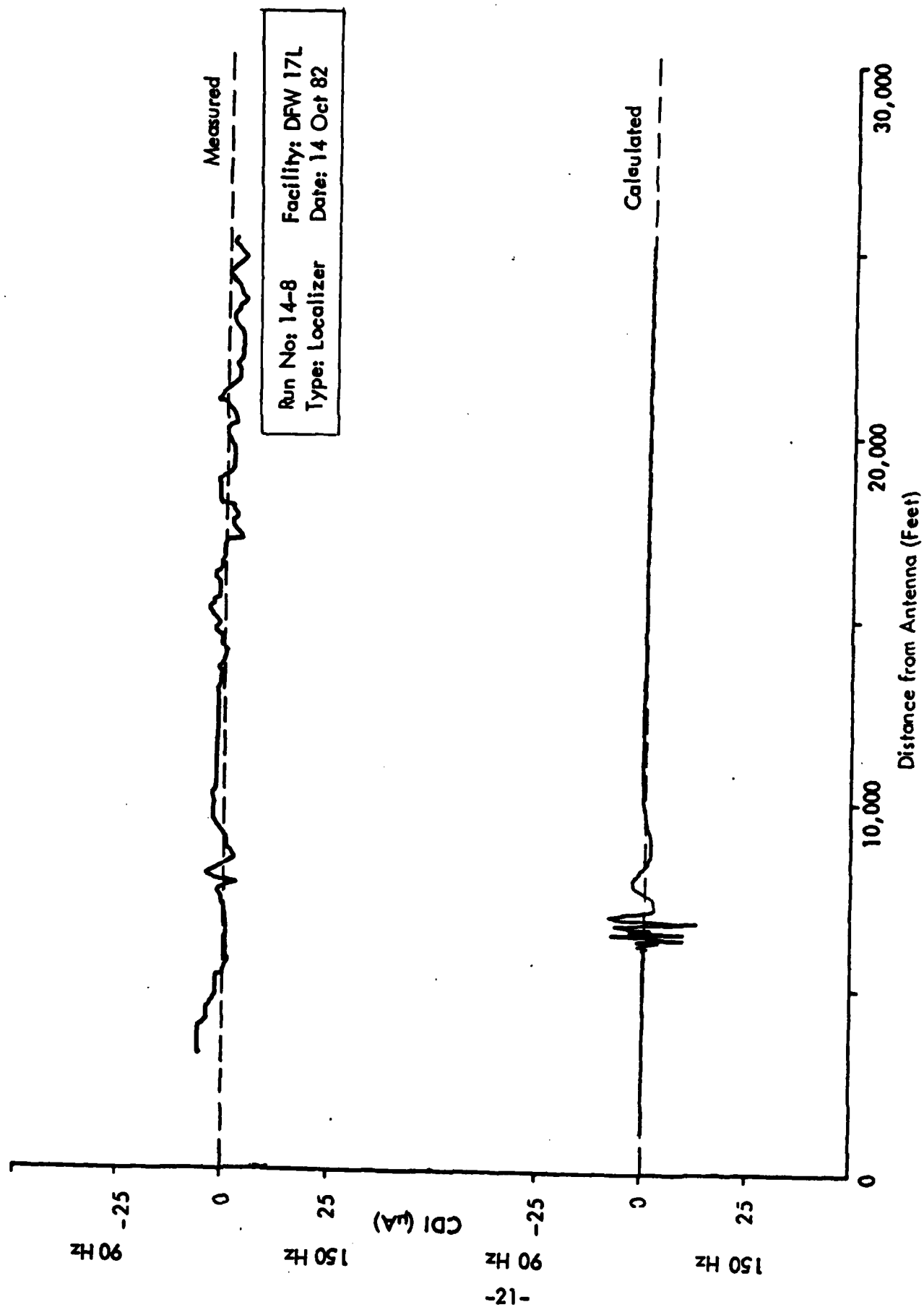Figure 12. Plots of Measured and Calculated Localizer CDI with B-747 Located at Position No. 3.

Figure 13. Plots of Measured and Calculated Localizer CDI with B-747 Located at Position No. 4.

Run No: 13-14   Facility: DFW 17L
Type: Localizer   Date: 13 Oct 82

Measured

Calculated

Distance from Antenna (Feet)

CDI (μA)

90 Hz   150 Hz   90 Hz   150 Hz

Figure 14. Plots of Measured and Calculated Localizer CDI with B-747

Run No: 13-16   Facility: DFW 17L
Type: Localizer   Date: 13 Oct 82

Distance from Antenna (Feet)

CDI (μA)

Figure 15. Plots of Measured and Calculated Localizer CDI with B-747 Located at Position No. 6.

Run No: 13-8   Facility: DFW 17L
Type: Localizer   Date: 13 Oct 1982

Measured

Calculated

Distance from Antenna (Feet)

CDI (μA)

90 Hz   150 Hz   90 Hz   150 Hz

-25   0   25   -25   0   25

0   10,000   20,000   30,000

-18-

Run No: 14-3   Facility: DFW 17L
Type: Localizer   Date: 14 Oct 82

Measured

Calculated

Distance from Antenna (Feet)

CDI (μA)

90 Hz   150 Hz   90Hz   150 Hz

-25   0   25   -25   0   25

0   10,000   20,000   30,000

Figure 17. Plots of Measured and Calculated Localizer CDI with B-747 Located at Position No. 8.

Figure 18. Plots of Measured and Calculated Localizer CDI with B-747
Located at Position No. 2

Aircraft Position #	Vector FFM Values		FFM Values	Peak CDI recorded by flight measurement
	(Q + 1) Vector	(J) Scalar		
Normal Sys.	2.5(90)	2.5(90)	1(150)	3(90)
Position 1	65(150)	65(150)	22(150)	65(150)
Position 2	8(90)	5(90)	2(150)	8(90)
Position 3	12(90)	12(90)	4(90)	20(90)50(150)
Position 4	13(90)	9(90)	0	8(90)
Position 5	31(90)	9(90)	2(90)	12(90)30(150)
Position 6	18(90)	4(90)	.5(150)	16(150)
Position 7	9(90)	6(90)	1(90)	7(90)
Position 8	7(90)	5(90)	.5(90)	10(90)
Position 9	10(90)	7(90)	.5(90	5(90)
Normal	9(90)	5(90)	1(90)	3(90)
Monitor right alarm limits	15(90)	15(90)	4(90)	----
Monitor left alarm limits	10(150)	10(150)	4(150)	----

Table 1. Comparison of Far-Field Monitor, Vector Far-Field Monitor and Measured Responses to B-747 Locations.

of 7089 feet (1.17 NM) centered about the region where the out-of-tolerance condition(s) occurs. Two 7089-foot areas will not overlap.

  b. Where necessary to avoid averlap, centering the interval about the out-of-tolerance region may be disregarded.

  c. It is not permissible to extend the 7089-foot segment beyond the area checked, i.e., service volume or ESV whichever is greater or the point closest to the runway where analyzation stops.

  d. The course/path structure is acceptable if the aggregate structure is out-of-tolerance for a distance equal to or less than 354 feet within each 7089-foot segment (reference 4).

The recommended critical areas are based upon both the contour maps and the abovementioned analyzation criterion. An example of the application of the flight inspection criteria and the contour maps to obtain the recommended critical area is presented in appendix B.

Based upon these requirements critical areas for each aircraft orientation have been drawn. Figure 19 shows the Category III critical region with the B-747 perpendicular to and heading towards the runway centerline; figure 20 shows the region with the aircraft perpendicular to and heading away from the runway centerline and figure 21 shows the region with the aircraft parallel to the runway centerline.

A worst case critical area is now established from those of figures 19 through 20. This is shown in figure 22. This region as established for the single frequency V-ring localizer array is shown in figure 23. Note that there is little difference in the recommended areas. This is due mainly to the fact that the course width for the V-ring calculation was 5.0° and for the GRN27 this value was 3.0°. The reflecting aircraft is essentially always in the course sector of the two-frequency localizer system. As this is the case then no real advantage is gained through the use of the two-frequency system as far as the effects of taxiing aircraft are concerned. It must be pointed out, however, that the dual-frequency localizer system will usually have a much better structure if no large aircraft are present and hence a compound effect of taxiing aircraft and reflections from buildings will not be as likely to occur.

CONCLUSIONS

The two-frequency localizer model utilized in this effort is a valid method of determining the derogation of localizer signals caused by a reflector the size of a Boeing 747 aircraft. This also provides the validity for use of this model in critical area determinations.

The measurements of the localizer far-field monitor on runway 17L at the Dallas Ft. Worth Airport indicate that the monitor is not always capable of detecting intrusions into the localizer critical areas.

The measurements of the Westinghouse vector far-field monitor indicate that the deviations in the approach area are more likely to be detected by the VFFM than by the GRN-27 far-field monitor.
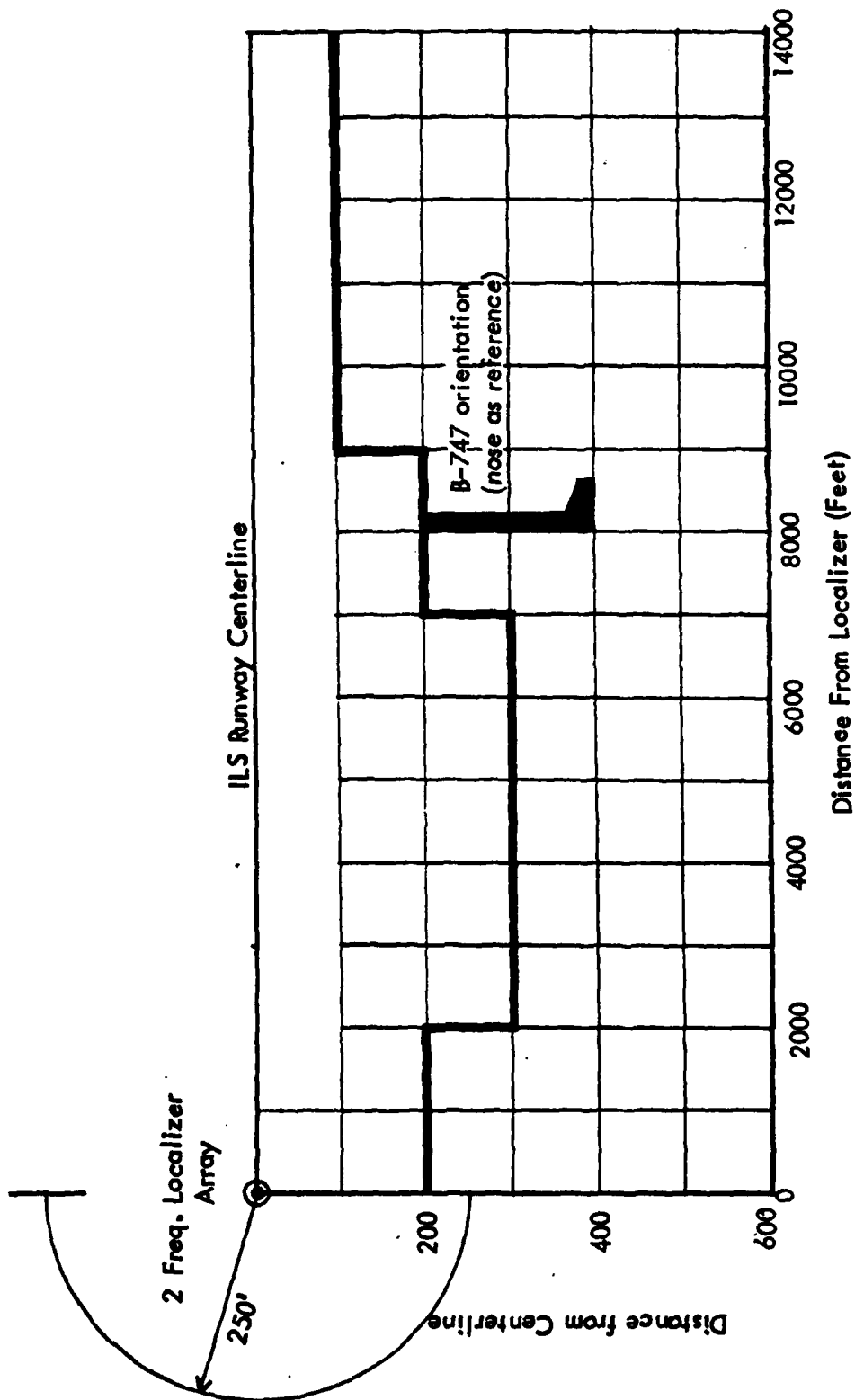
Figure 19. Localizer Cat III Critical Area. B-747 Perpendicular to Runway Centerline with Nose Toward Centerline.
Note: Critical area established with the nose of the aircraft located on the critical area lines.
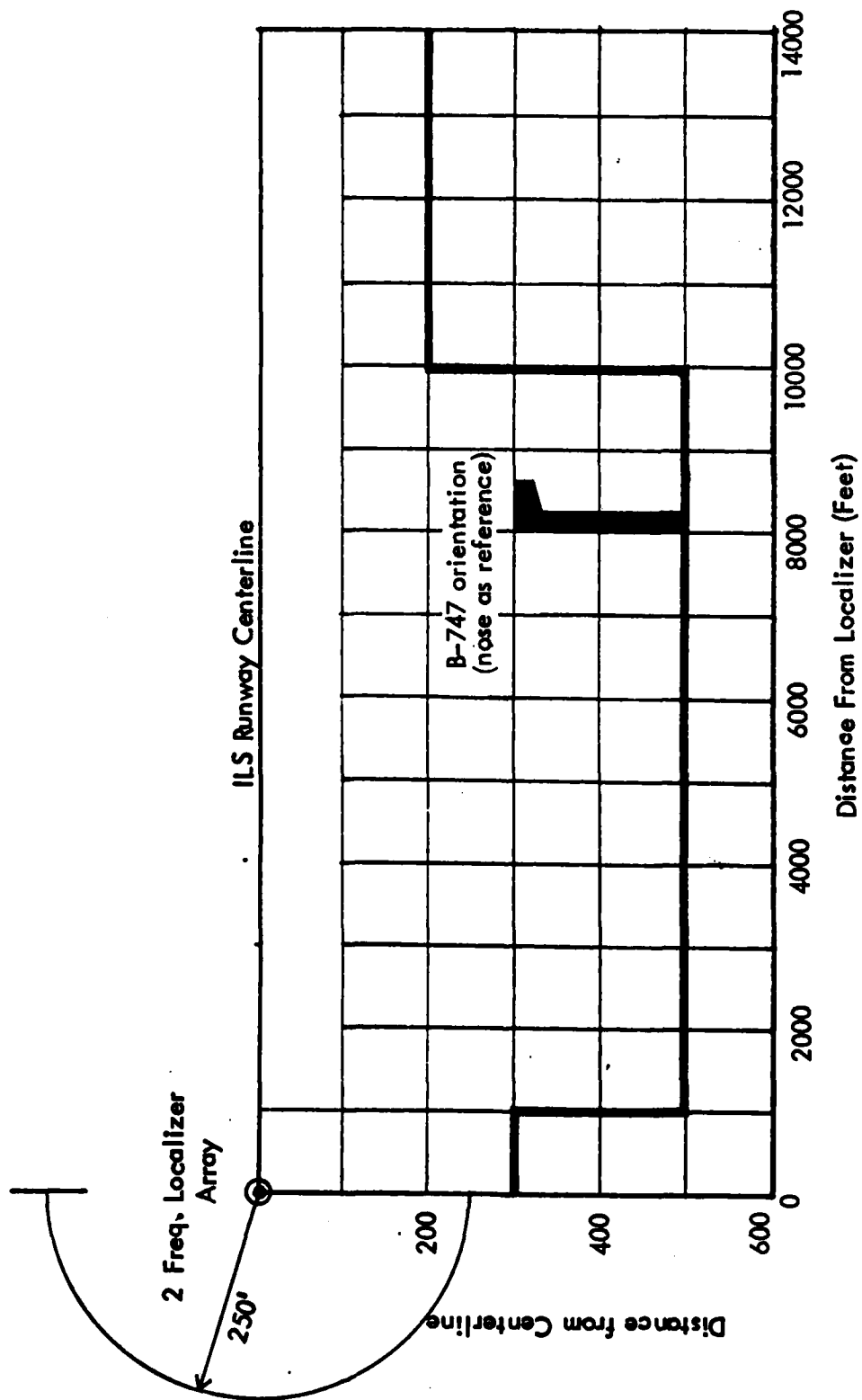
Figure 20. Localizer Cat III Critical Area. B-747 Perpendicular to Centerline with Tail Toward Centerline.
Note: Critical area established with the nose of the aircraft located on the critical area lines.
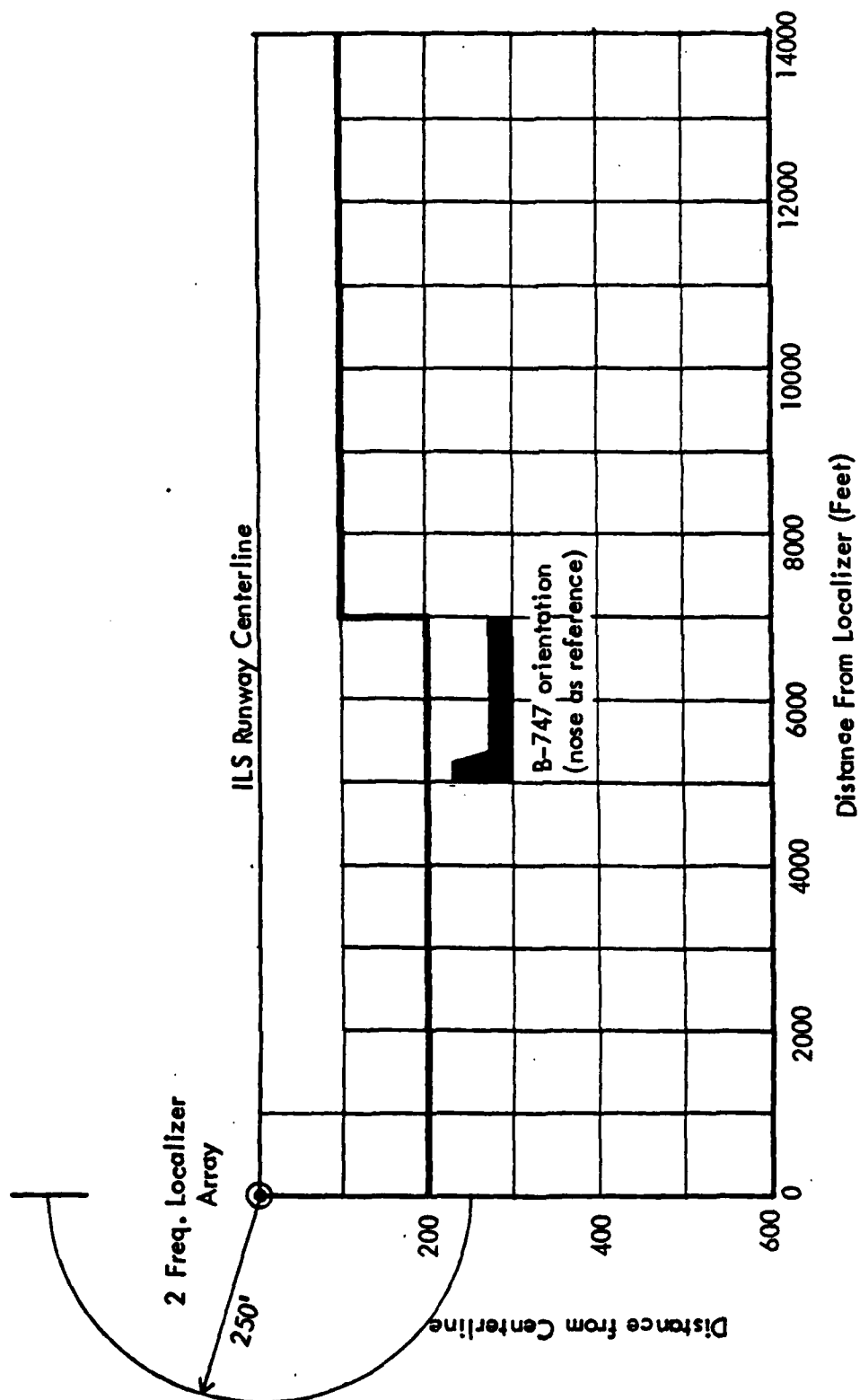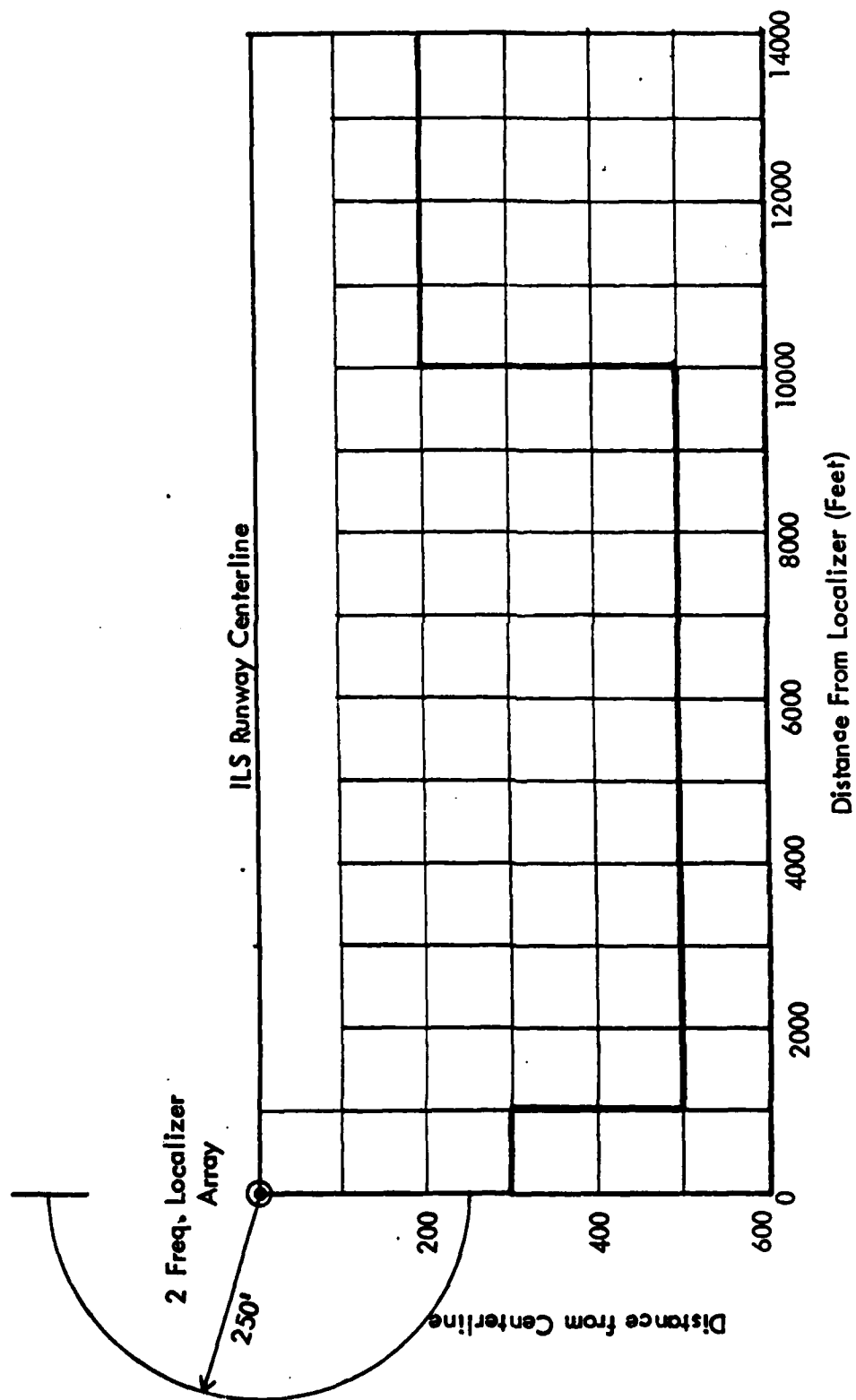
-25-

Figure 21. Localizer Cat III Critical Area. B-747 Parallel to Centerline.

ILS Runway Centerline

2 Freq. Localizer Array

250'

Distance From Localizer (Feet)

Distance from Centerline

B-747 orientation (nose as reference)

Figure 22. Proposed Worst Case Localizer Cat III Critical Areas.
Note: Critical area established with the nose of the aircraft located on the critical area lines.

-27-
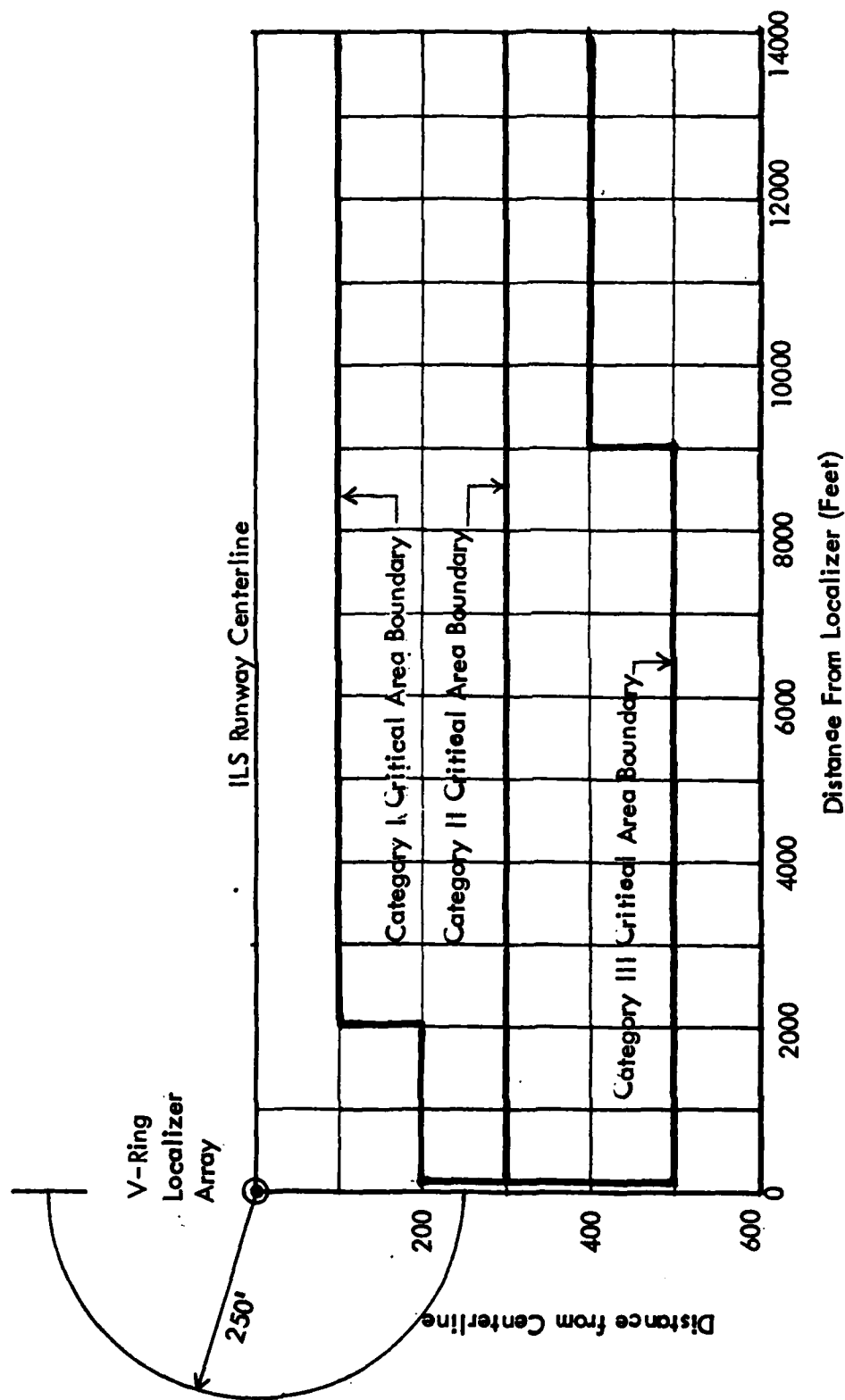
Figure 23. Worst Case – Proposed Localizer Critical Area.
for V-Ring Localizer Array (reference 6).
Note: V-ring course width was 5° for calculation.

ACKNOWLEDGEMENTS

REFERENCES

1. Localizer Critical Areas for the 747 Aircraft, Avionics Engineering Center, Ohio University, Athens, Ohio, SRDS Report FAA-RD-73-137

2. Rondini, R. A., McFarland, R. H., Experimental Validation of Boeing 747 ILS Signal Scattering Calculations for Critical Area Determination, Final Report, OU/AEC/EER 18-1, Report No. FAA-RD-74-57, Contract DOTFA74WA-3361, Avionics Engineering Center, Ohio University, Athens, Ohio, January 1974.

3. McFarland, R. H., Longworth, J. D., Phipps, W. D., Investigations of Array Changes and Terrain Modifications to Provide for Category III Quality Localizer Course Structure at Los Angeles International Airport, OU/AEC/EER 55-1, Avionics Engineering Center, Ohio University, Athens, Ohio, prepared for Airway Facilities Division, Western Pacific Region, Federal Aviation Administration, Los Angeles, CA., April 1982.

4. Final Engineering Report on the Vector Far-Field Monitor System, Westinghouse Electric Corporation, Defense and Electronic Systems Center, Baltimore, Maryland, Contract DTFA01-80-C-10134 for Federal Aviation Administration, ARD-320.

5. United States Standard Flight Inspection Manual, FAA OAP 8200.1, Change 32, April 1980.

6. Rondini and McFarland, op. cit., p. 13.

APPENDICES

Appendix A

Aircraft Specification, Location and Orientation for Dallas-Ft. Worth
Localizer Measurements. Figure A-1 shows the size specification of the
Boeing 747 used in the experimental work at the Dallas-Ft. Worth airport.
The aircraft was located at nine points along the runway. The points and
the aircraft orientations for each are shown in figure A-2.

In addition, the drawing in figure A-3 represents the combination of
theoretical plate reflectors estimated from the aircraft specifications.

Appendix B

Critical Area Determination Based Upon Contour Maps and Flight
Inspection Tolerances. This appendix demonstrates the technique utilized
to obtain the recommended critical areas from the computed contour maps and
the application of flight inspection tolerances.

Figure B-1 will be used as an example. First, the CDI value at the points
(X, Y locations) which exceed the allowable tolerance levels are annotated.
The localizer course structure is then computed with the aircraft located
at each point for each ILS zone. Flight inspection tolerances (max struc-
ture roughness, duration of out-of-tolerance condition) are then applied as
appropriate. See figure B-2. If the resultant analysis of the structure
measurement is within tolerance, this location of the reflecting aircraft
is not considered to derogate the structure.

The process is repeated for all points which exceed the max roughness cri-
teria for the zone in question. Following this, lines are drawn for each
zone on a grid. These lines represent the recommended critical area lines
for each zone. The critical areas for each of the zones are then combined
to form one critical area map for each aircraft orientation.
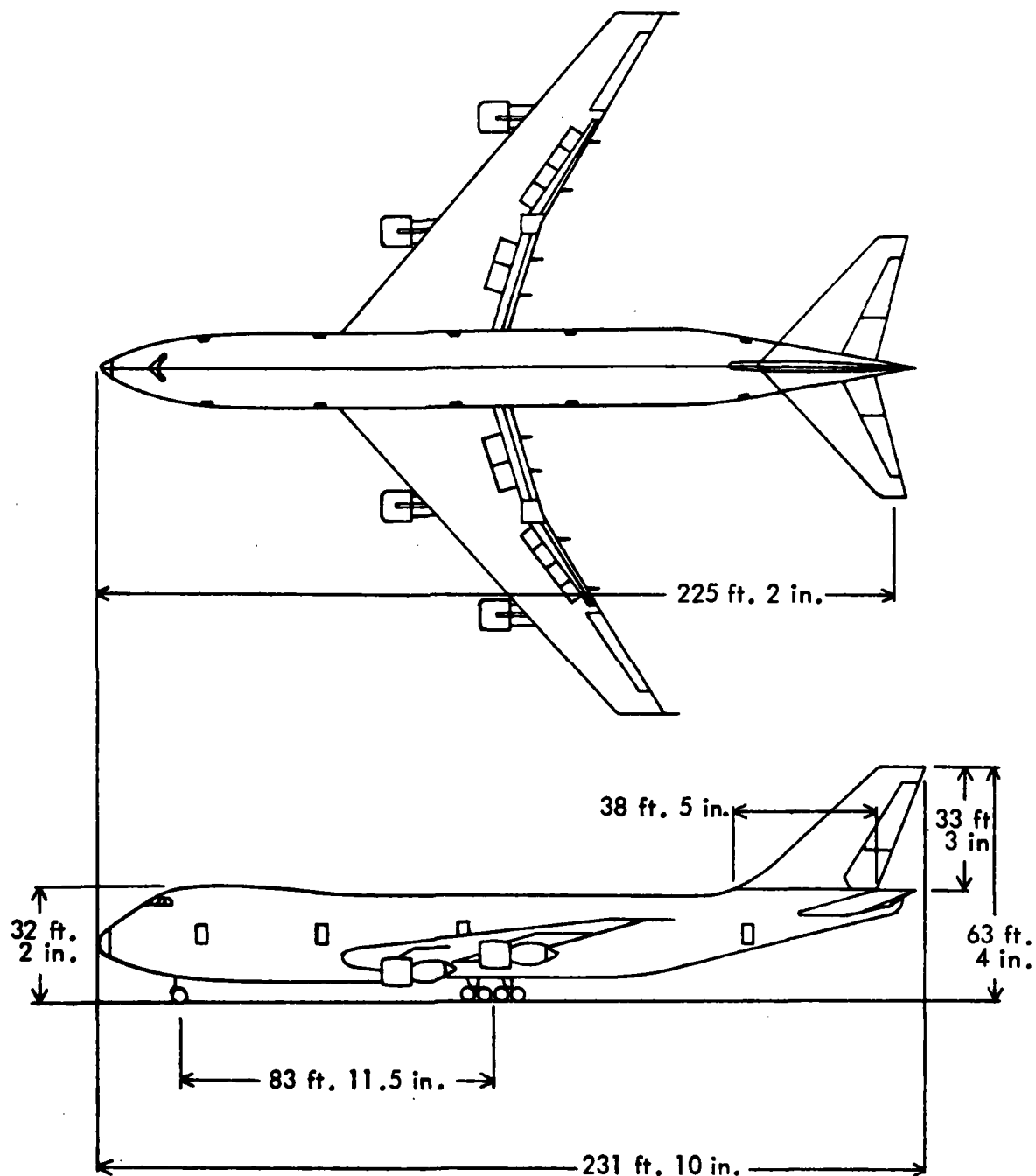
Figure A-1. Physical Dimensions of Boeing 747 Used in Critical Area
Measurements at Dallas-Ft. Worth Airport October 1982.

Reference Point ⟶ o

POSITION	X	Y	Z	ALPHA	DELTA
Tail ②	1050	300.	+4.2	−90	0
Head ②	1825	125.5	+3.7	−90	0
Tail ③	1825	300.	+1.7	−90	0
Head ④	3350−3210	125.5	+4.2	−90	0
Tail ⑤	3350−3210	300.	+4.2	−90	0
Tail ⑥	4100	200.	+4.2	−29.5	0
Head ⑦	5870	225.	+5.2	−30	0
Tail ⑧	6045	322.	+5.7	−152	0
Parallel ⑨	5763.5	230	+5.2	0	0
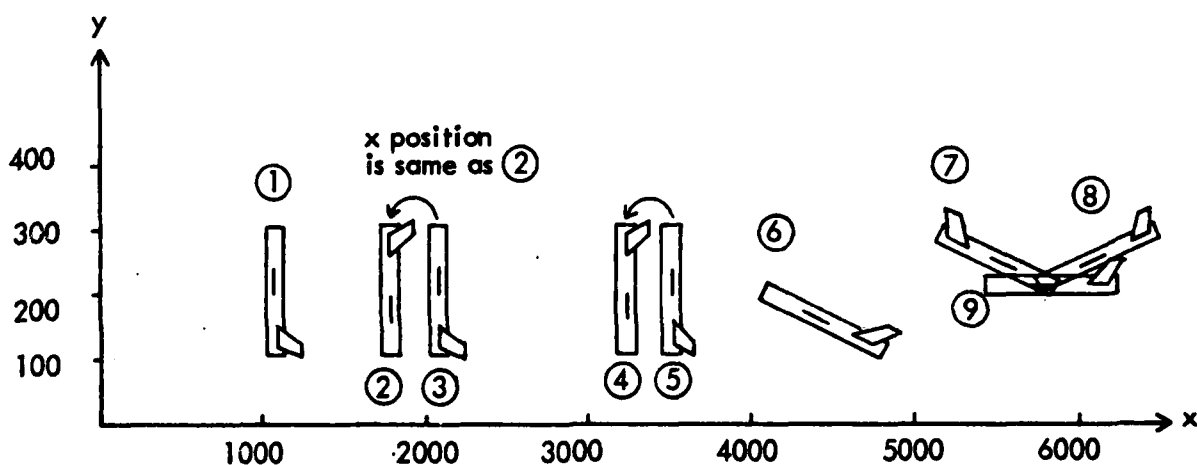
Figure A-2. Aircraft Location and Orientation Measured in Localizer Critical Area Experiments at Dallas-Ft. Worth Airport October 1982.
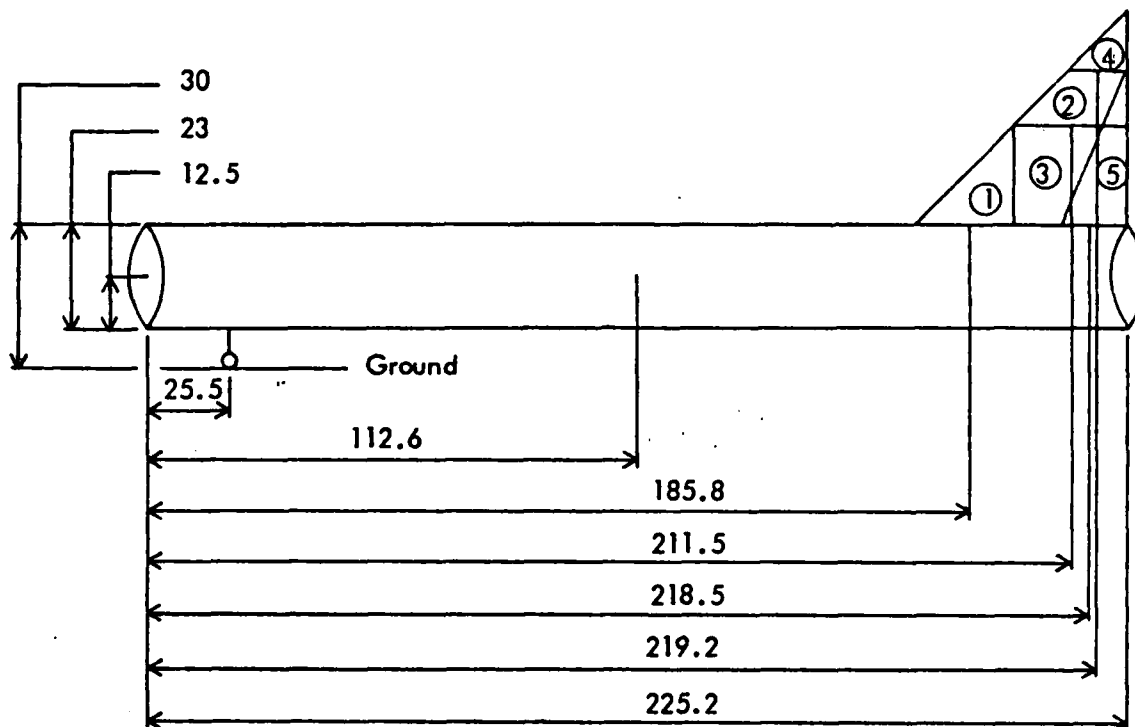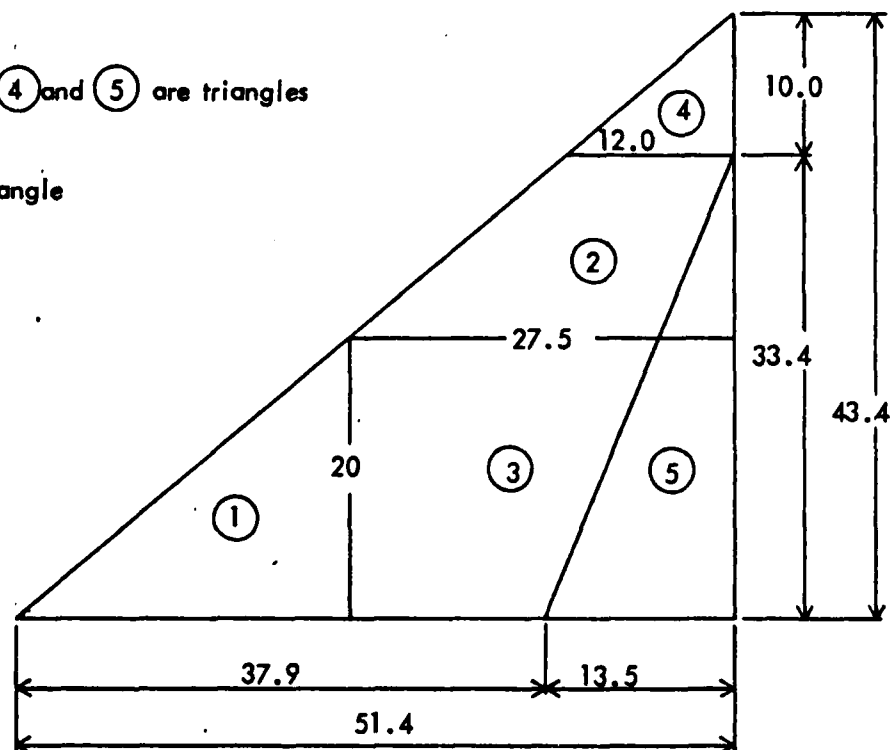
Figure A-3. Theoretical Plate Reflector Simulating the Boeing 747 of
Figure A-1.
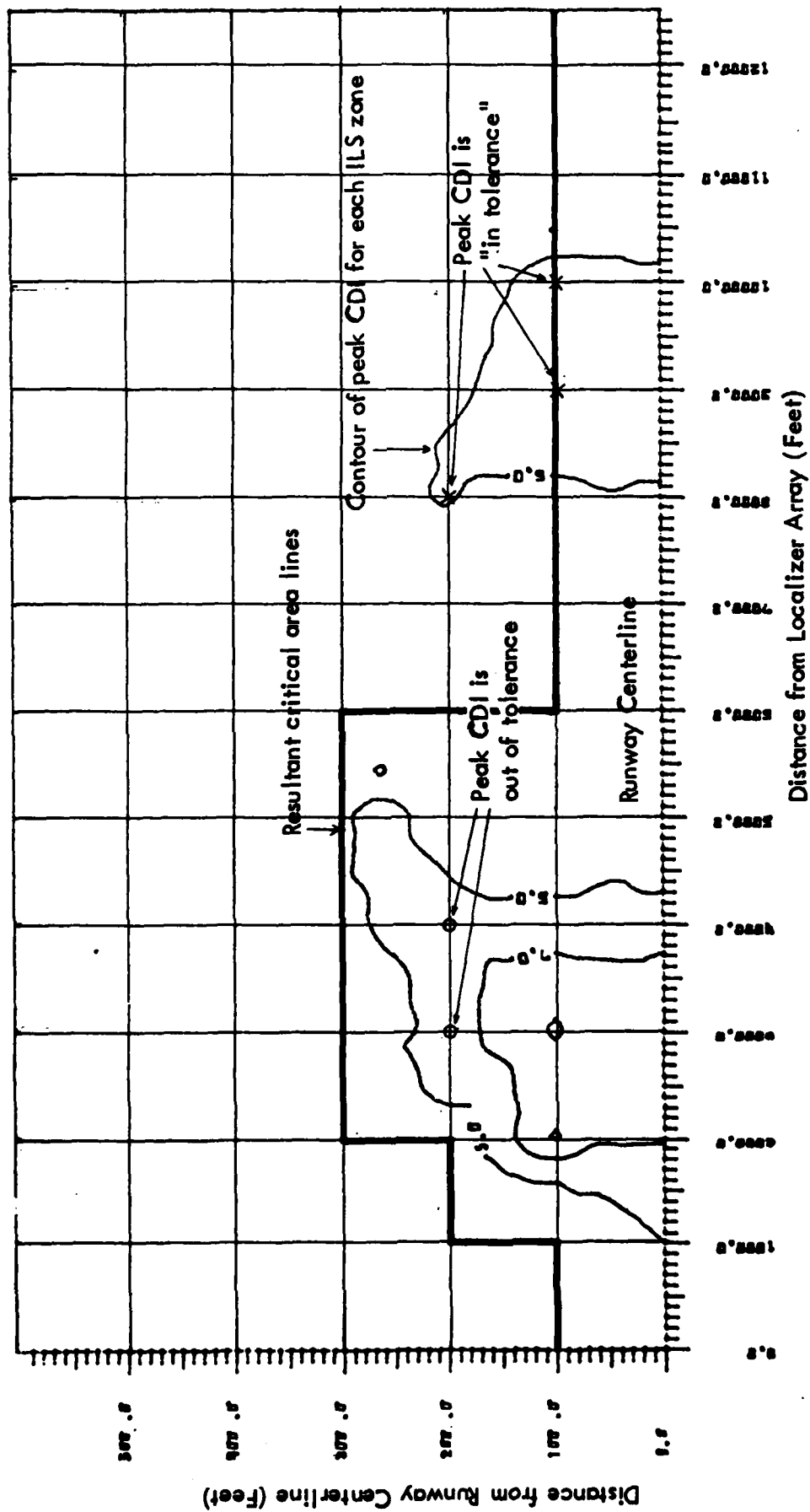
Figure B-1. Example of Critical Area Determination Based Upon Contour Maps and Application of Flight Inspection Criteria.

-34-
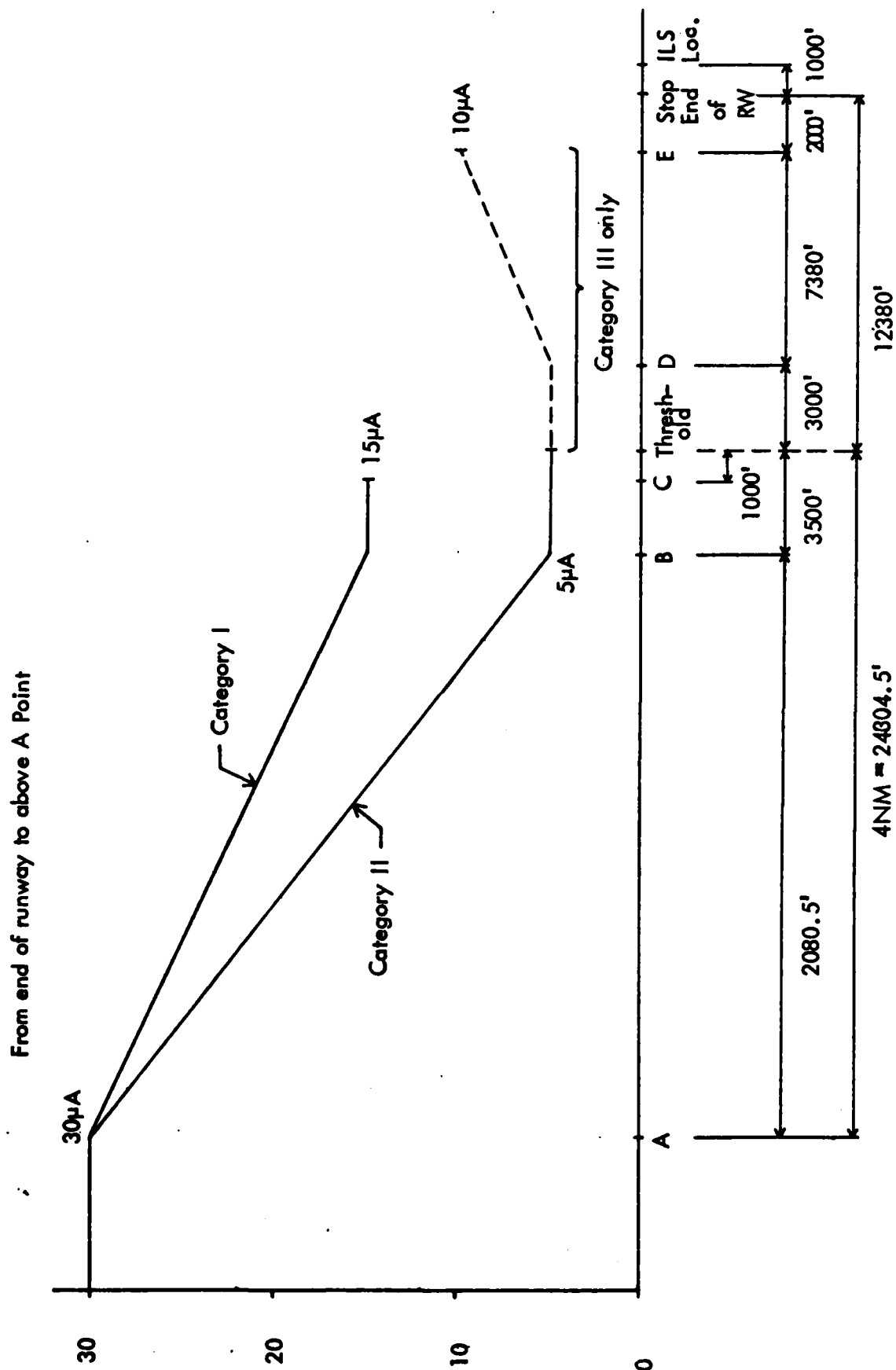
Figure B-2. Localizer Course Maximum Bend Amplitude Criteria (Dallas-Fort Worth Airport).

PHASE II

THEORETICAL INVESTIGATION OF WIDE-BODY AIRCRAFT SINGLE-FREQUENCY

8- AND 14-ELEMENT LOCALIZER SIGNAL SCATTERING

FOR CATEGORY III CRITICAL AREA DETERMINATION

by

Joe D. Longworth

FEBRUARY 1983
(Revised March 1983)
(2nd Revision August 1983)

TABLE OF CONTENTS

List of Figures

List of Figures (Continued)

PAGE

List of Figures (Continued)

List of Figures (Continued)

I.   INTRODUCTION

A. <u>Purpose</u>. Recent requests, both within the FAA and from commercial users to utilize single-frequency localizer systems which meet Category-III tolerances for azimuth guidance in Category-III approaches, have led to a request for an extension of previous single-frequency investigations (reference 1) and dual-frequency investigations (reference 2) to include the 14-element, O-ring and LPD arrays and the 8-element LPD array. These arrays are of a more directional nature than the previously investigated V-ring array (reference 3). Being more directional, it is anticipated that with carefully defined critical areas the arrays could be used in a Category-III approach system.

B. <u>Background</u>. In 1974 Ohio University performed both a theoretical and experimental study to recommend critical areas for the ILS localizer and glide-slope systems. This study utilized a single-frequency computer model of the V-ring localizer array and field measurements of the same array. In the current contract effort, the investigations of the 1974 work were used to upgrade the computer model to a two-frequency system and both a theoretical and experimental study were conducted for this system. The two-frequency system using the traveling-wave type of antenna has again been modified to calculate the signal scattering due to large aircraft for two directional single-frequency localizer cases.

II. DISCUSSION

A. Contour Maps of the Fourteen-element Array. Contour maps of the
CDI deviations for the 14-element, single-frequency array have been gener-
ated. The specific aircraft locations and orientations are those of the
two-frequency effort which are with the aircraft parallel to the runway
centerline, with the aircraft perpendicular to the centerline and the nose
toward the centerline and, with the aircraft perpendicular to centerline
and the tail toward the centerline. As in the previous reports, the three
orientations have drastically differing effects upon the localizer perfor-
mance. In addition, all ILS points and zones are defined assuming the
length of Dallas-Ft. Worth airport runway 17L.

The 14-element array has an aperture of 86 feet and is considered to
be a directional array. The resultant contour maps plotting the CDI indi-
cation show this to be the case. These maps are shown in figures 1 through
12. Note that individual maps are provided for each aircraft orientation
and for each ILS zone in which an out-of-tolerance condition was recorded.

To show the correlation with previous work, contour maps of ILS zone
5 with the aircraft tail toward centerline are shown in figures 13, 14 and
15 for the 14-element, single-frequency array, the V-ring array and the
14-element, two-frequency array. The V-ring array contour map peak CDI
deviations are for the entire length of the approach while those of the
single-and dual-frequency directional arrays are for the specified ILS zone
only. Comparing the three contour maps, it is noted that the more direc-
tional the array, the lower the peak CDI variations in zone 5.

On each of the contour maps the x-axis is aligned along the runway
centerline with the distance in feet from the localizer array annotated.
The y-axis is the perpendicular distance in feet from the localizer array
and, the contour lines indicate the peak CDI excursions for the indicated
aircraft positions. It should also be noted that the calculations were
made assuming a 3° localizer course width.

B. Contour Maps of the Eight-element Array. Calculations of the
peak CDI excursions for the same aircraft locations and orientations were
repeated for the 8-element LPD localizer array. The contour maps for these
positions are shown in figures 16 through 27. Again, the maps are gener-
ated for each orientation and for each ILS zone in which an out-of-tolerance
condition exists. These calculations were also made assuming a 3° local-
izer course width.

Referring back to the contour maps for the V-ring localizer and the
two-frequency system in figures 14 and 15 respectively, it is noted that
the peak deviations in ILS zone 5 for the 8-element (figure 23) are some-
what more severe than those of either the V-ring, the 14-element, single-
frequency, or the two-frequency system. It should be noted that the 8- and
14-element calculations assume a 3° course width while those of the V-ring
array were made based upon a 5° course width. This results in a smaller
CDI value for the V-ring versus those of the 8- and 14-element arrays.

Figure 1. B-747 Parallel to the Runway Centerline. Peak CDI between ILS points D and E, 14-element array. Calculations assuming constant approach speed of 200 ft/sec. Note: all aircraft locations result in an "in tolerance" localizer structure when flight inspection tolerances are applied.

Runway Centerline

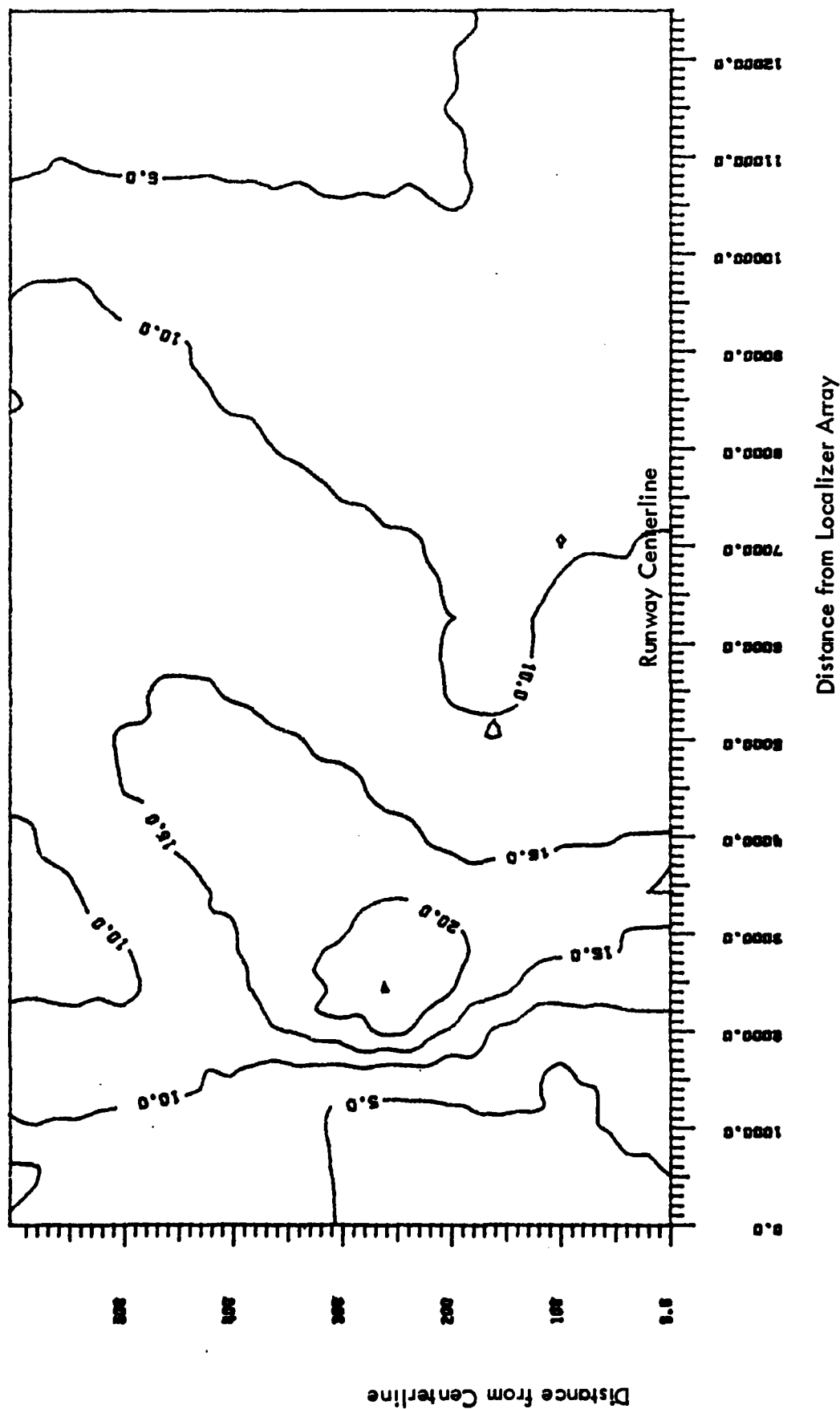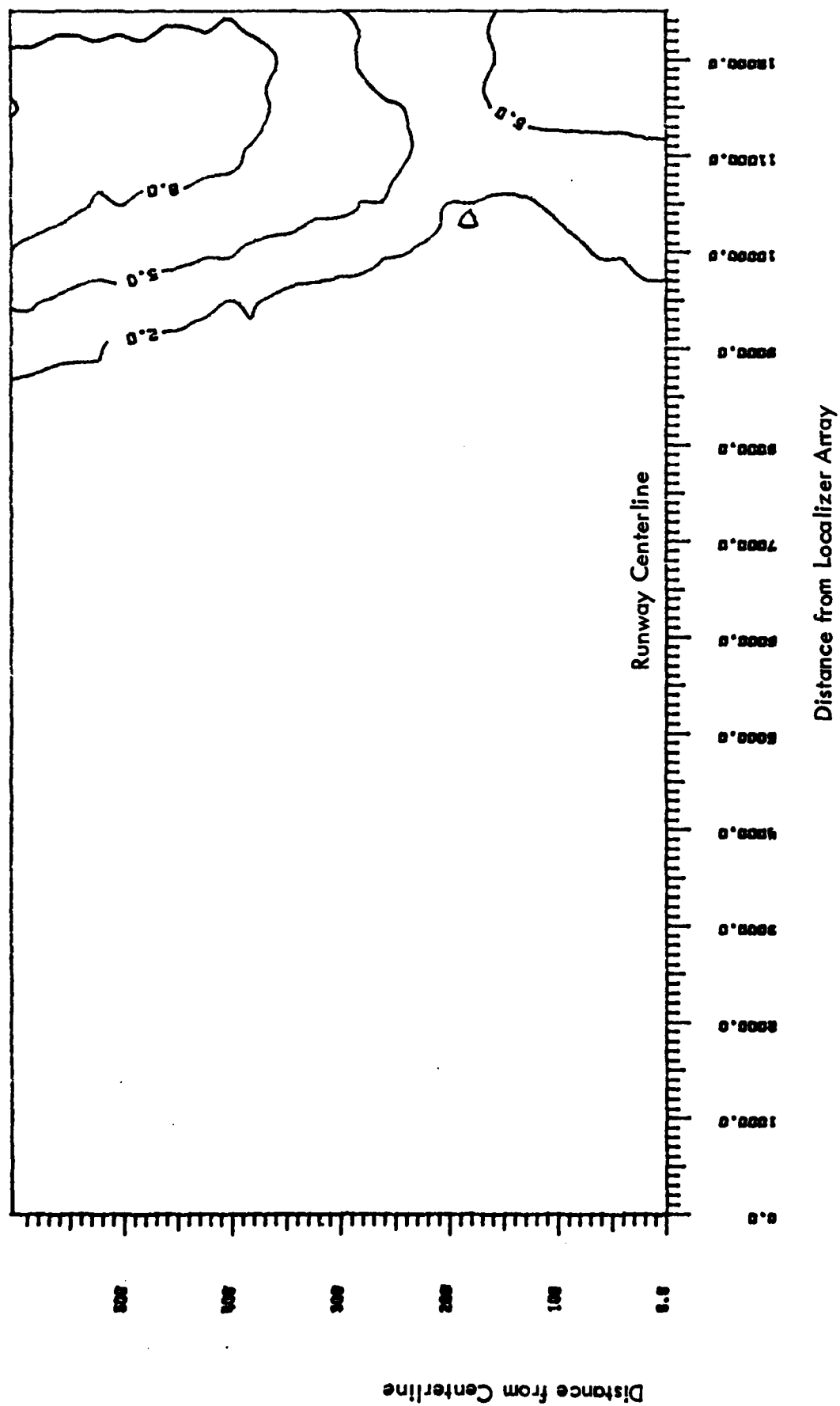Distance from Localizer Array

Distance from Centerline

Figure 2. B-747 Parallel to the Runway Centerline. Peak CDI between ILS points C and D, 14-element array. Calculations assuming constant approach speed of 200 ft/sec.

Figure 3. B-747 Perpendicular to the Runway Centerline with the Nose of the Aircraft Toward Centerline. Peak CDI between ILS points D and E, 14-element array. Calculations assuming constant approach speed of 200 ft/sec. Note: all aircraft locations result in an "in tolerance" localizer structure when flight inspection tolerances are applied.

-40-

Figure 4. B-747 Perpendicular to the Runway Centerline with the Nose of the Aircraft Toward Centerline. Peak CDI between ILS points C and D, 14-element array. Calculations assuming constant approach of 200 ft/sec.
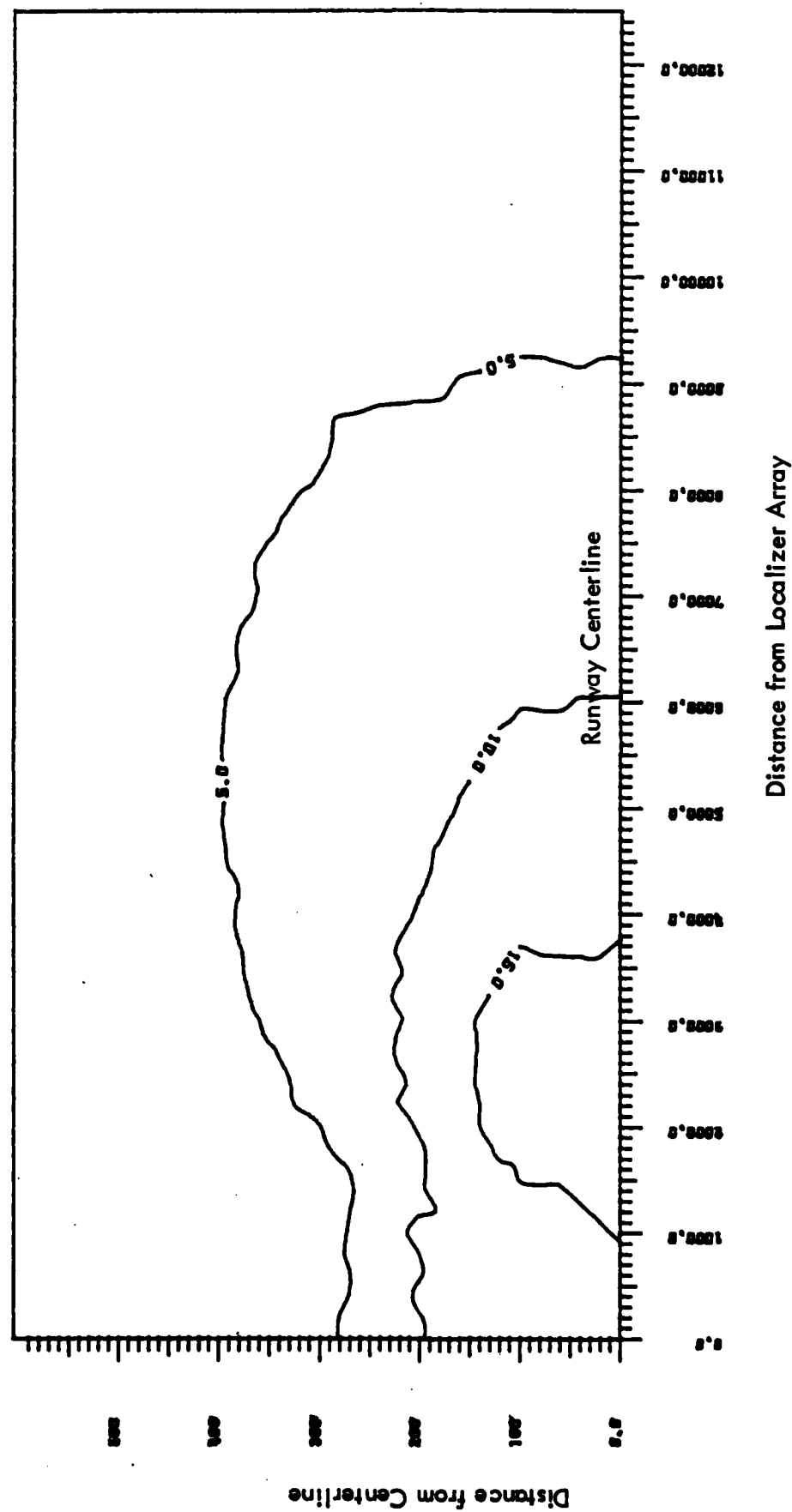
-41-

Figure 5. B-747 Perpendicular to the Runway Centerline with the Nose of the Aircraft Toward Centerline. Peak CDI between ILS points B and C, 14-element array. Calculations assuming constant approach speed of 200 ft/sec.
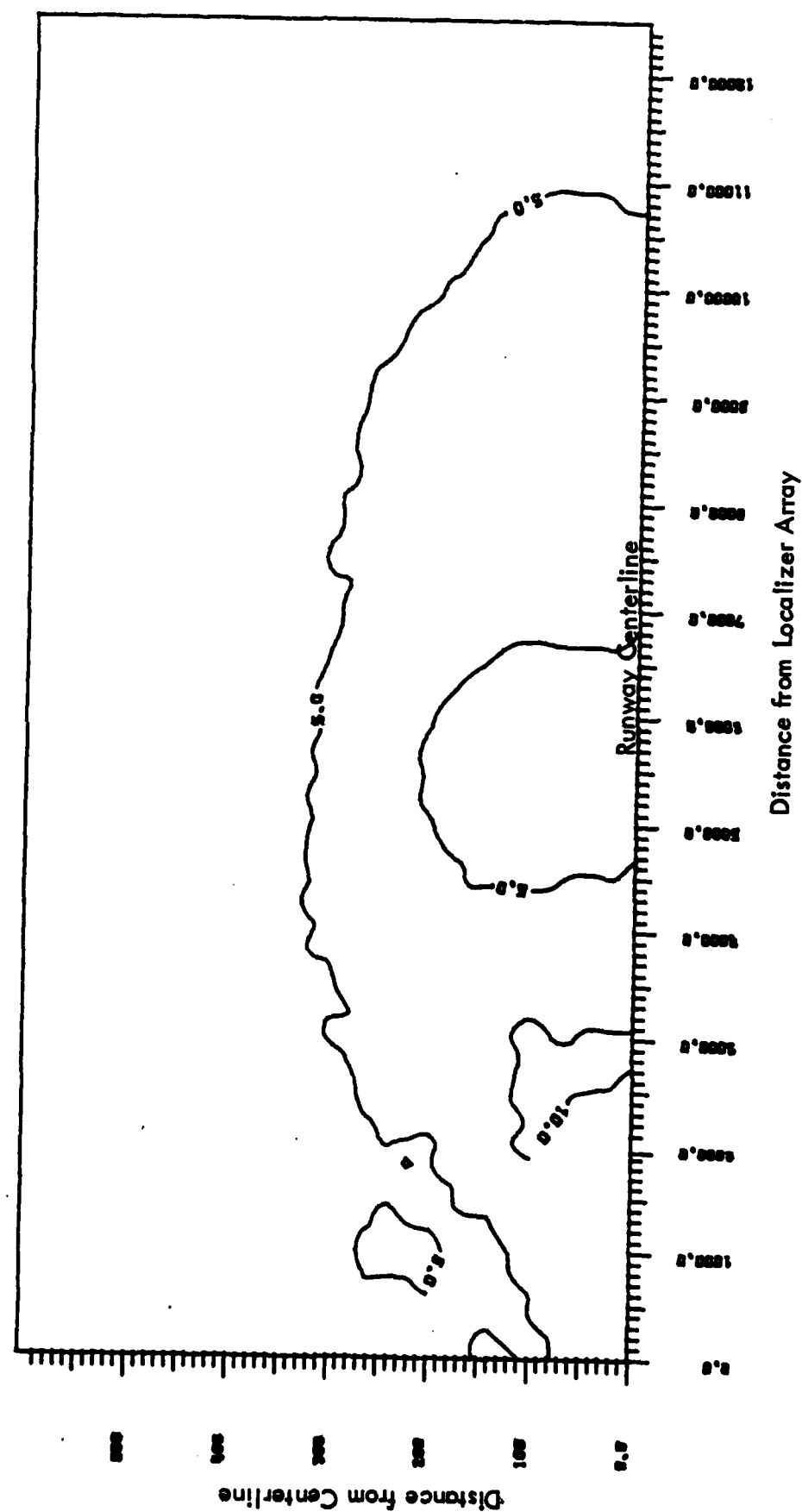
-42-

Figure 6. B-747 Perpendicular to the Runway Centerline with the Nose of the Aircraft Toward Centerline. Peak CDI between ILS points A and B, 14-element array. Calculations assuming constant approach speed of 200 ft/sec.

-43-

Figure 7. B-747 Perpendicular to the Runway Centerline with the Nose of the Aircraft Toward Centerline. Peak CDI beyond ILS point A, 14-element array. Calculations assuming constant approach speed of 200 ft/sec.

Figure 8. B-747 Perpendicular to the Runway Centerline with the Tail of the Aircraft Toward Centerline. Peak CDI between ILS D and E, 14-element array. Calculations assuming constant approach speed of 200 ft/sec.
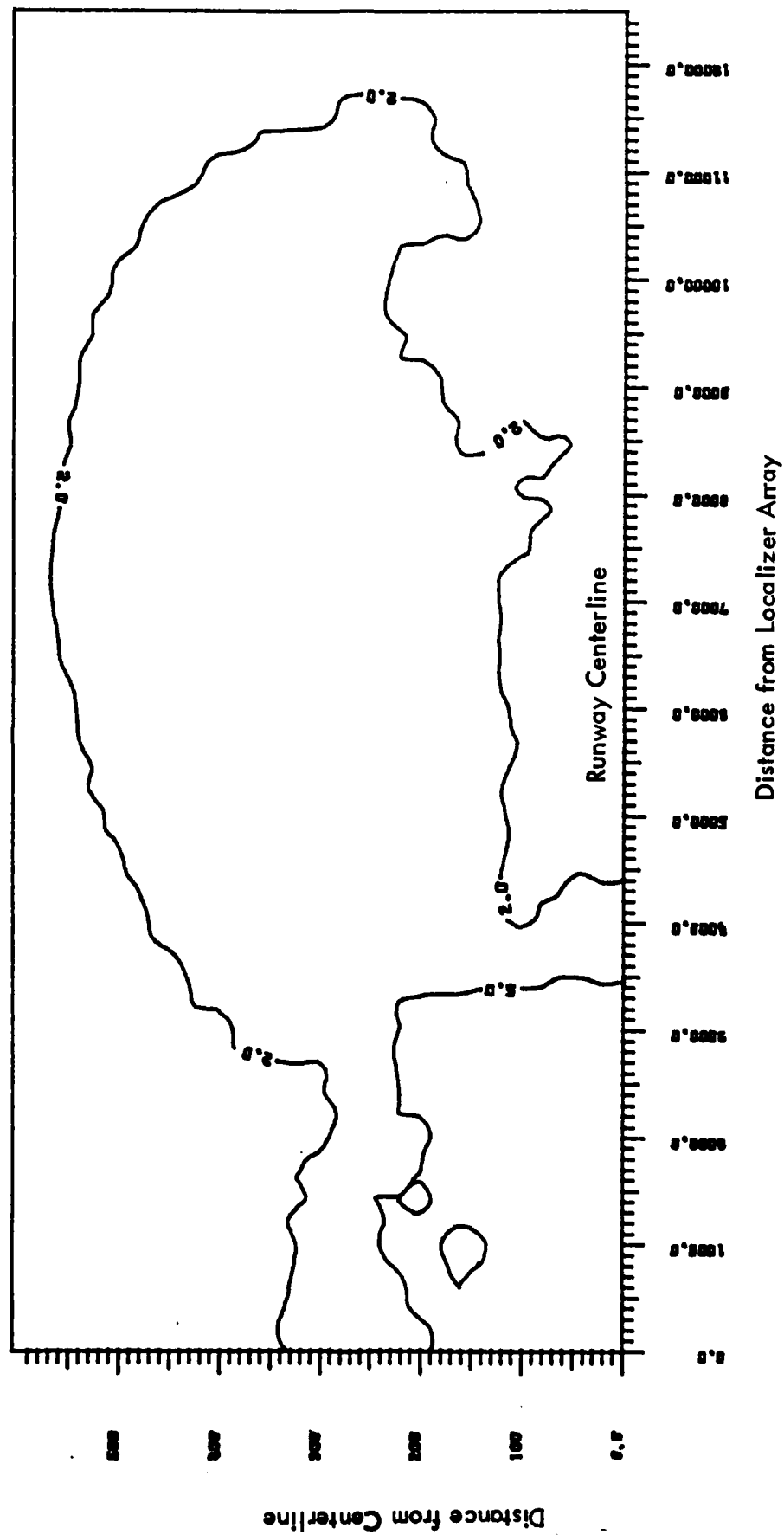
-45-

Figure 9. B-747 Perpendicular to the Runway Centerline with the Tail of the Aircraft Toward Centerline. Peak CDI between ILS points C and D, 14-element array. Calculations assuming constant approach speed of 200 feet/second.
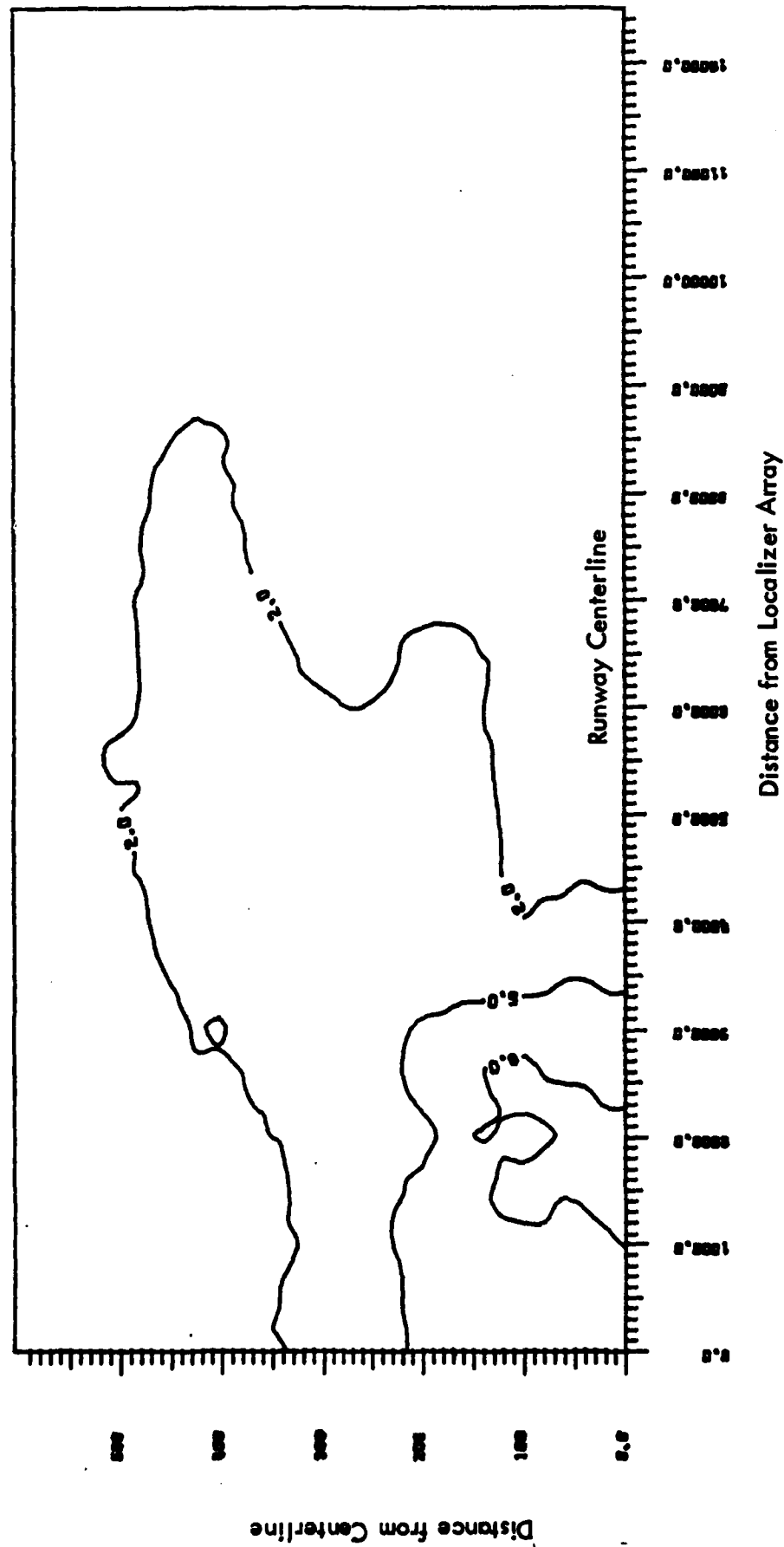
-46-

Distance from Localizer Array

Runway Centerline

Distance from Centerline

Figure 10. B-747 Perpendicular to the Runway Centerline with the Tail of the Aircraft Toward Centerline. Peak CDI between ILS points B and C, 14-element array. Calculations assuming constant approach speed of 200 feet/second.
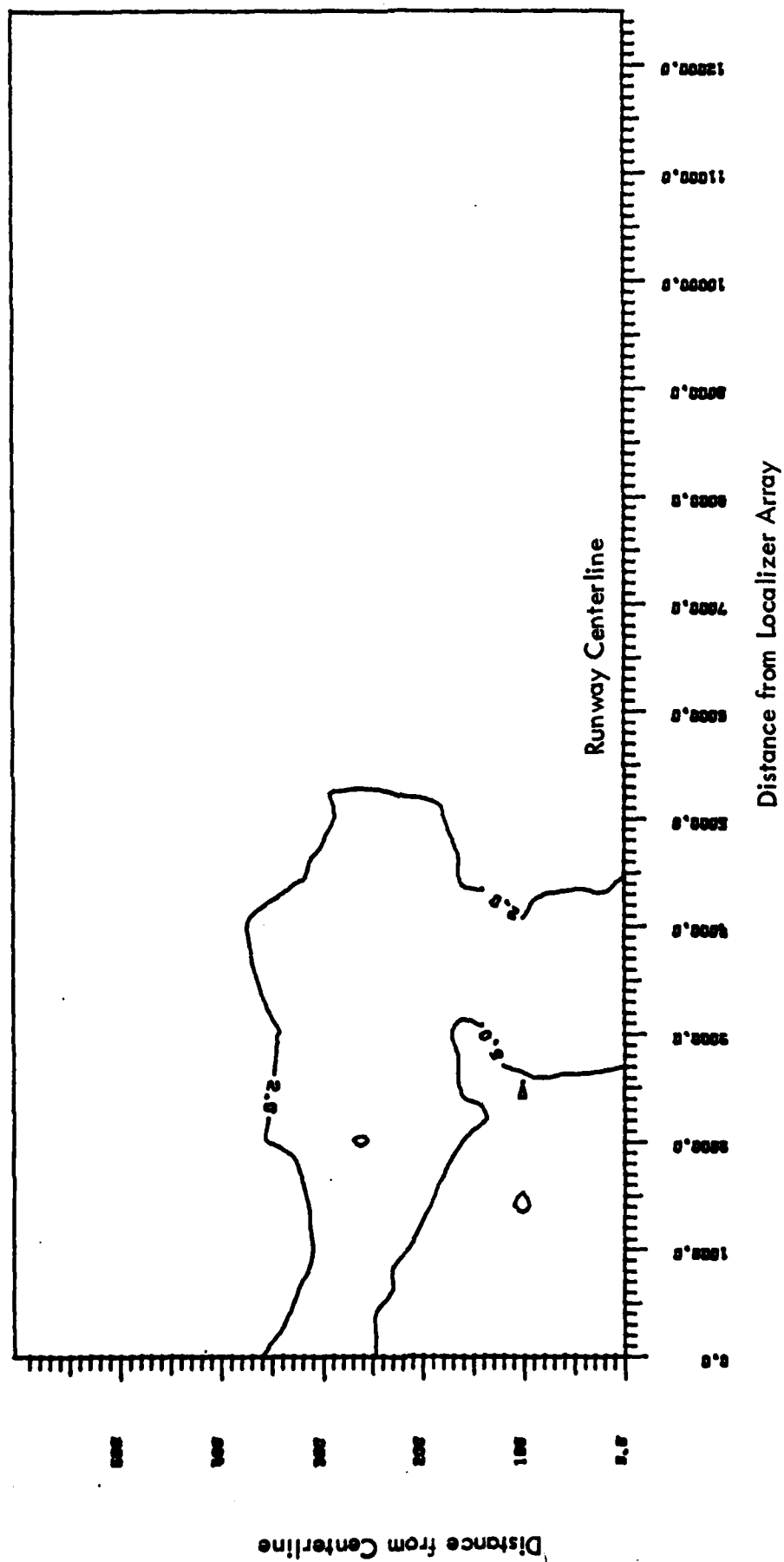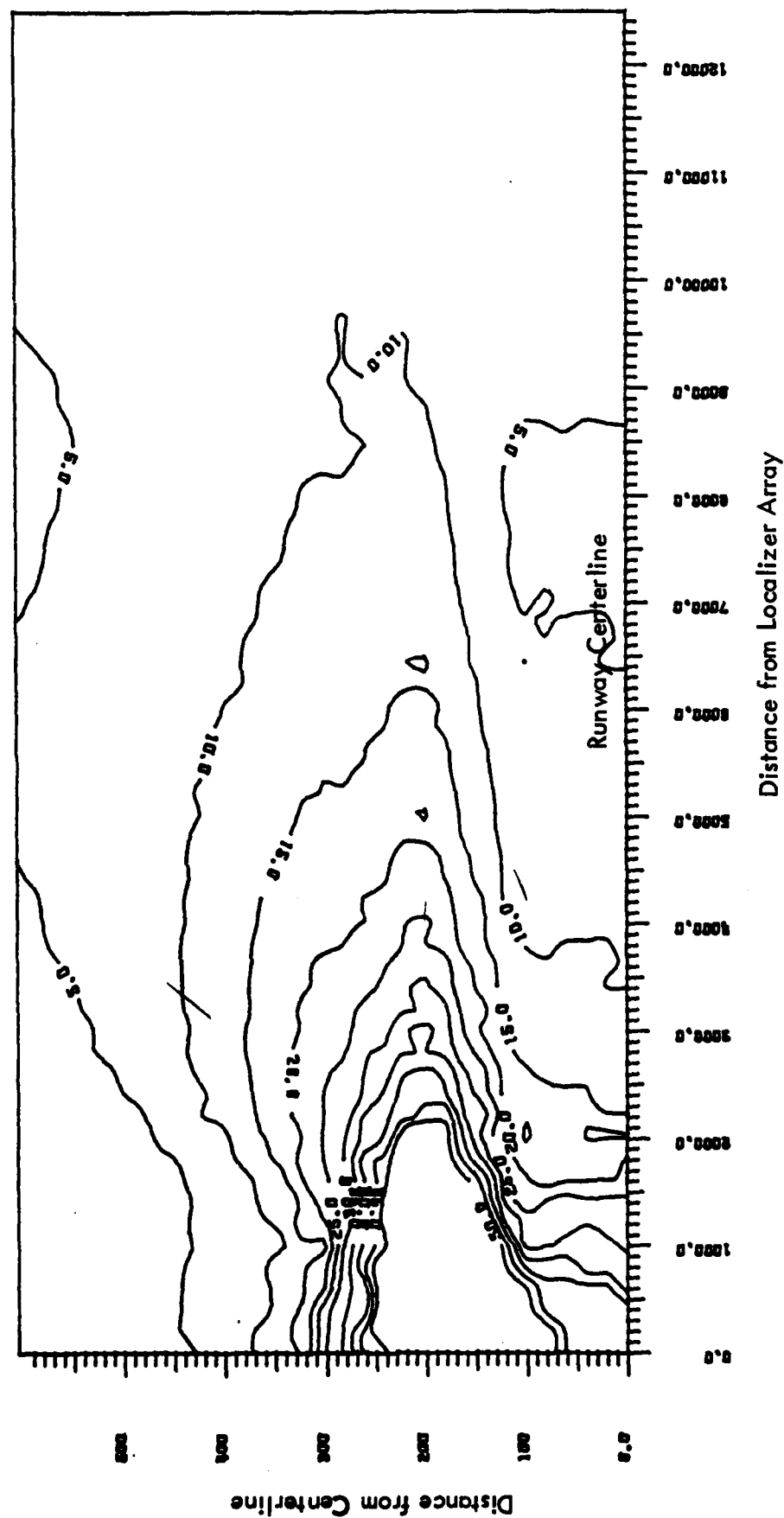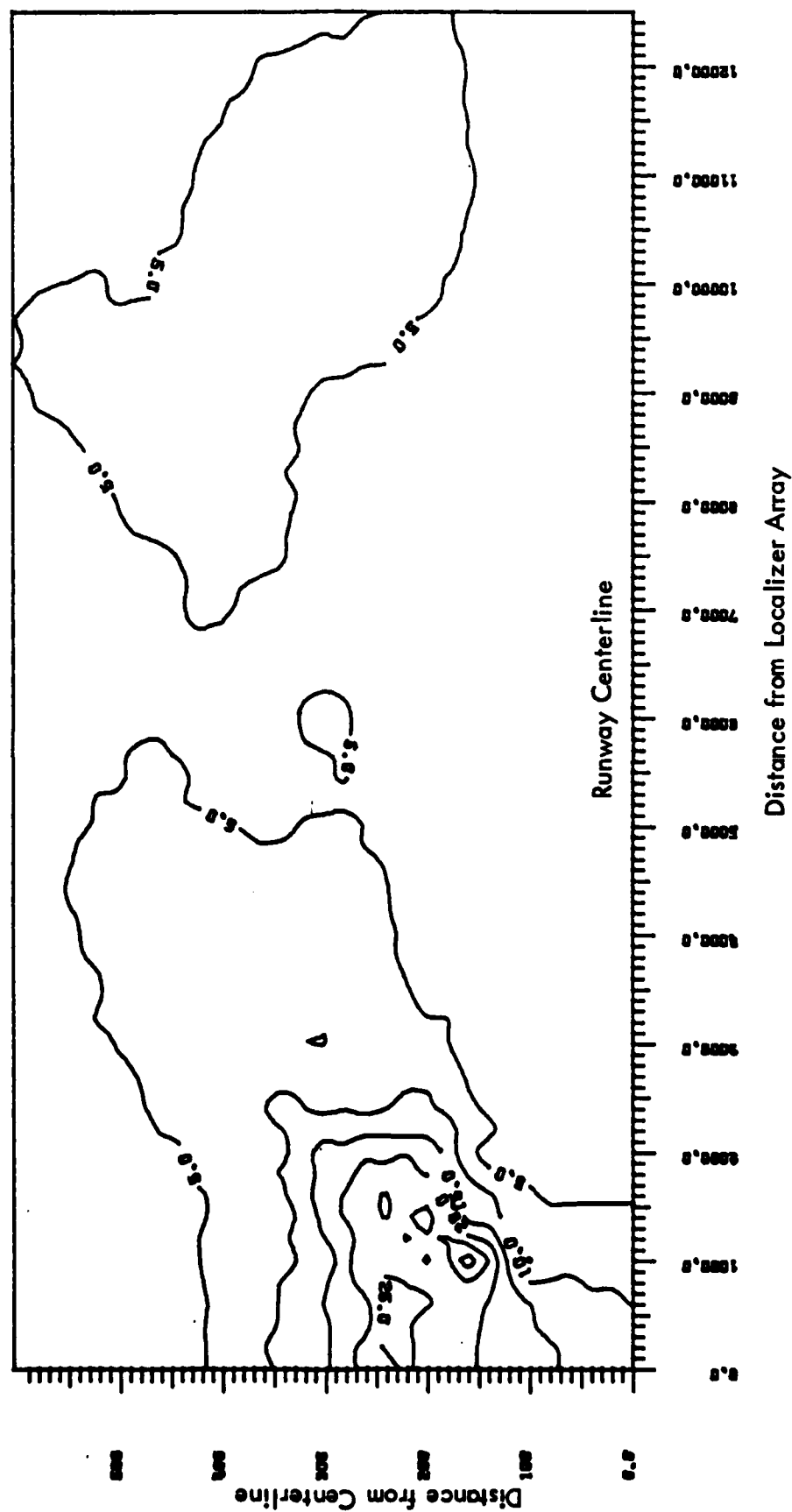
Figure 11. B-747 Perpendicular to the Runway Centerline with the Tail of the Aircraft Toward Centerline. Peak CDI between ILS points A and B, 14-element array. Calculations assuming constant approach speed of 200 feet/second.
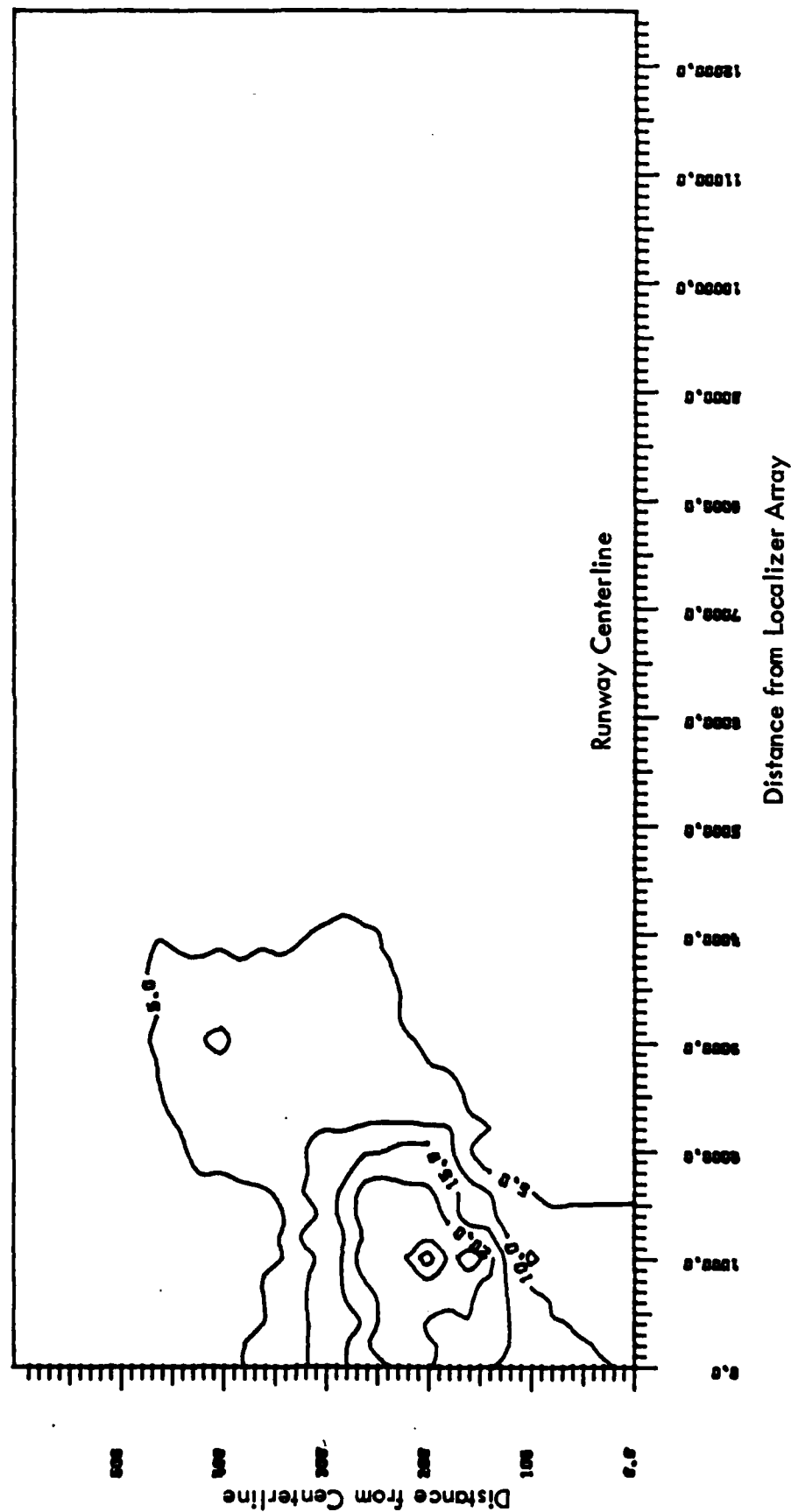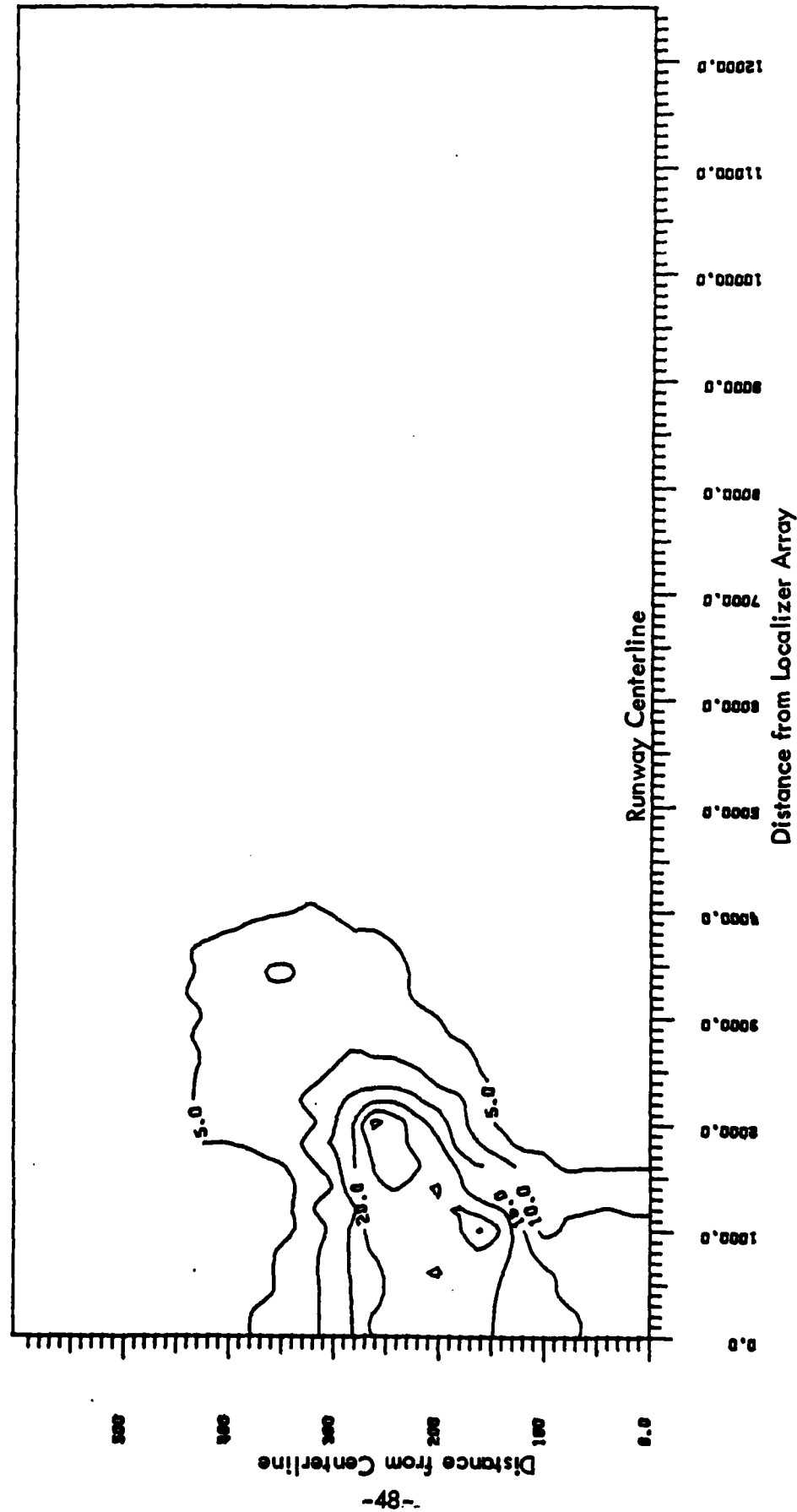
-48-

Figure 12. B-747 Perpendicular to the Runway Centerline with the Tail of the Aircraft Toward Centerline. Peak CDI beyond ILS point A, 14-element array. Calculations assuming constant approach speed of 200 feet/second.

-49-

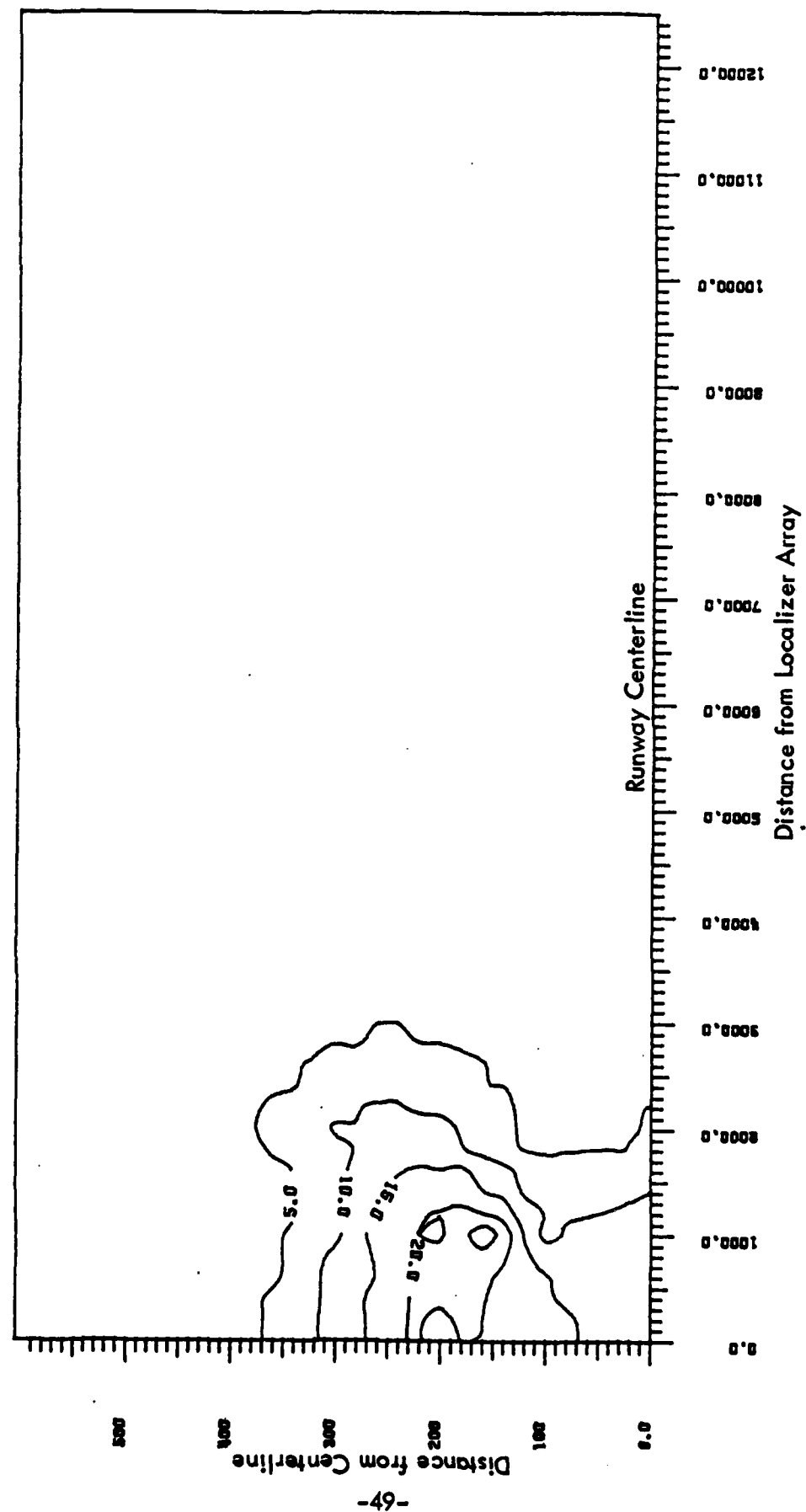Figure 13. B-747 Perpendicular to the Runway Centerline with the Tail of the Aircraft Toward Centerline. Peak CDI in ILS Zone 5. 14-element, single-frequency localizer array. Calculations assuming a constant approach speed of 200 feet/second.

-50-

Figure 14. B-747 Perpendicular to the Runway Centerline with the Tail of the Aircraft Toward Centerline. Peak CDI along entire approach. V-ring localizer array [4]. Calculations assuming a dynamic approach speed with touchdown at 200 feet/second.
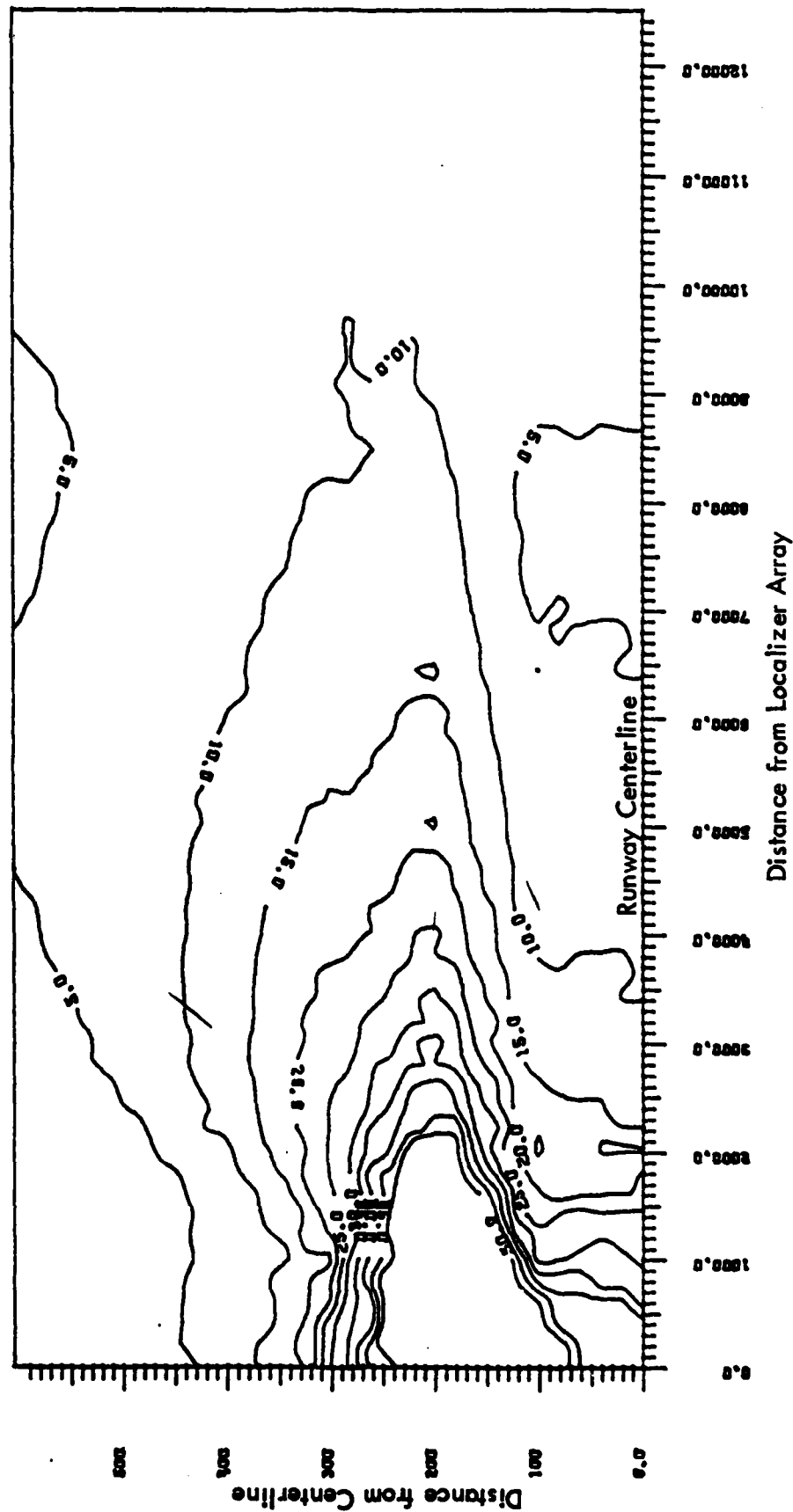
-51-
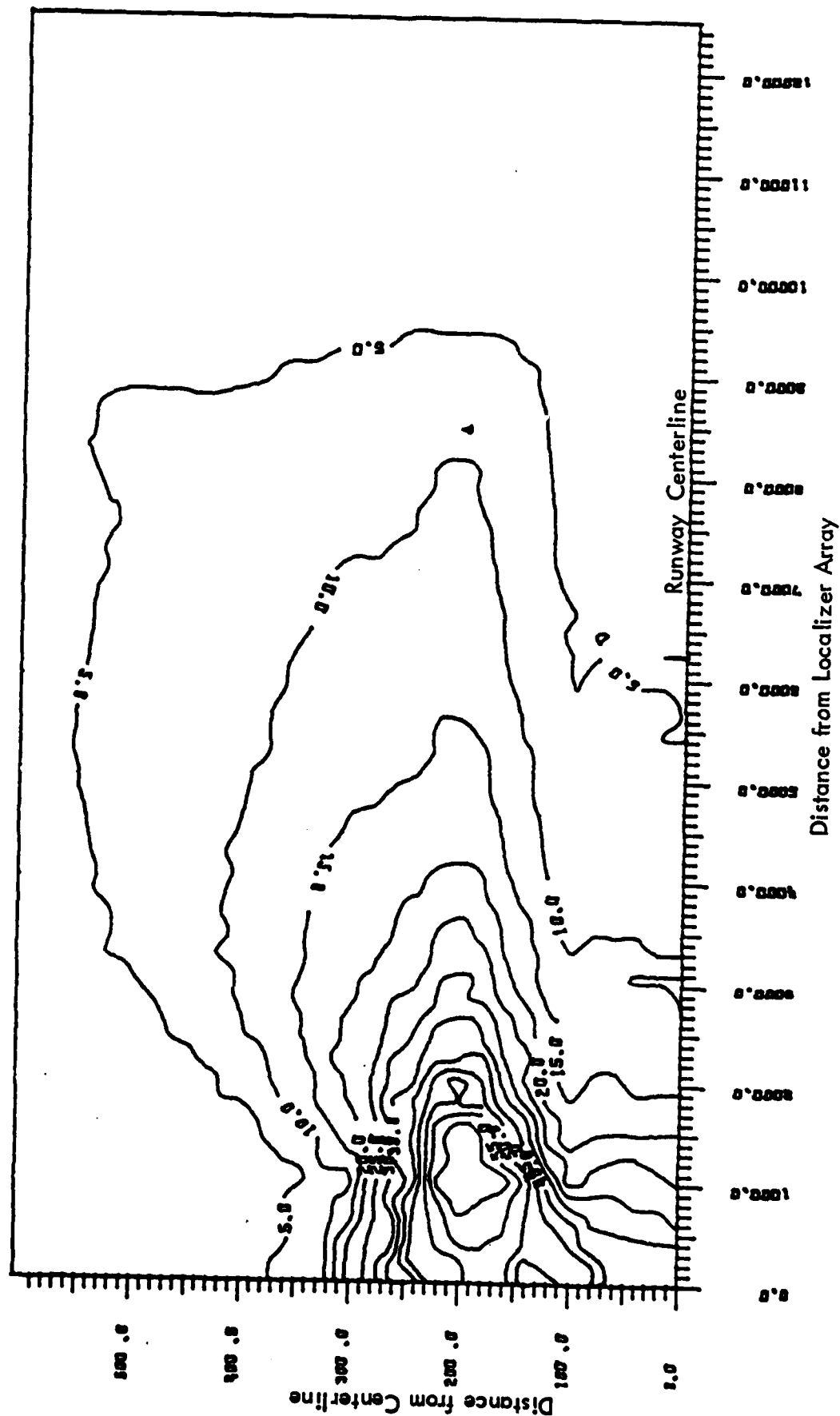
Figure 15. B-747 Perpendicular to the Runway Centerline with the Tail of the Aircraft Toward Centerline. Peak CDI in ILS Zone 5. 14-element, dual-frequency localizer array. Calculations assuming a constant approach speed of 200 feet/second.
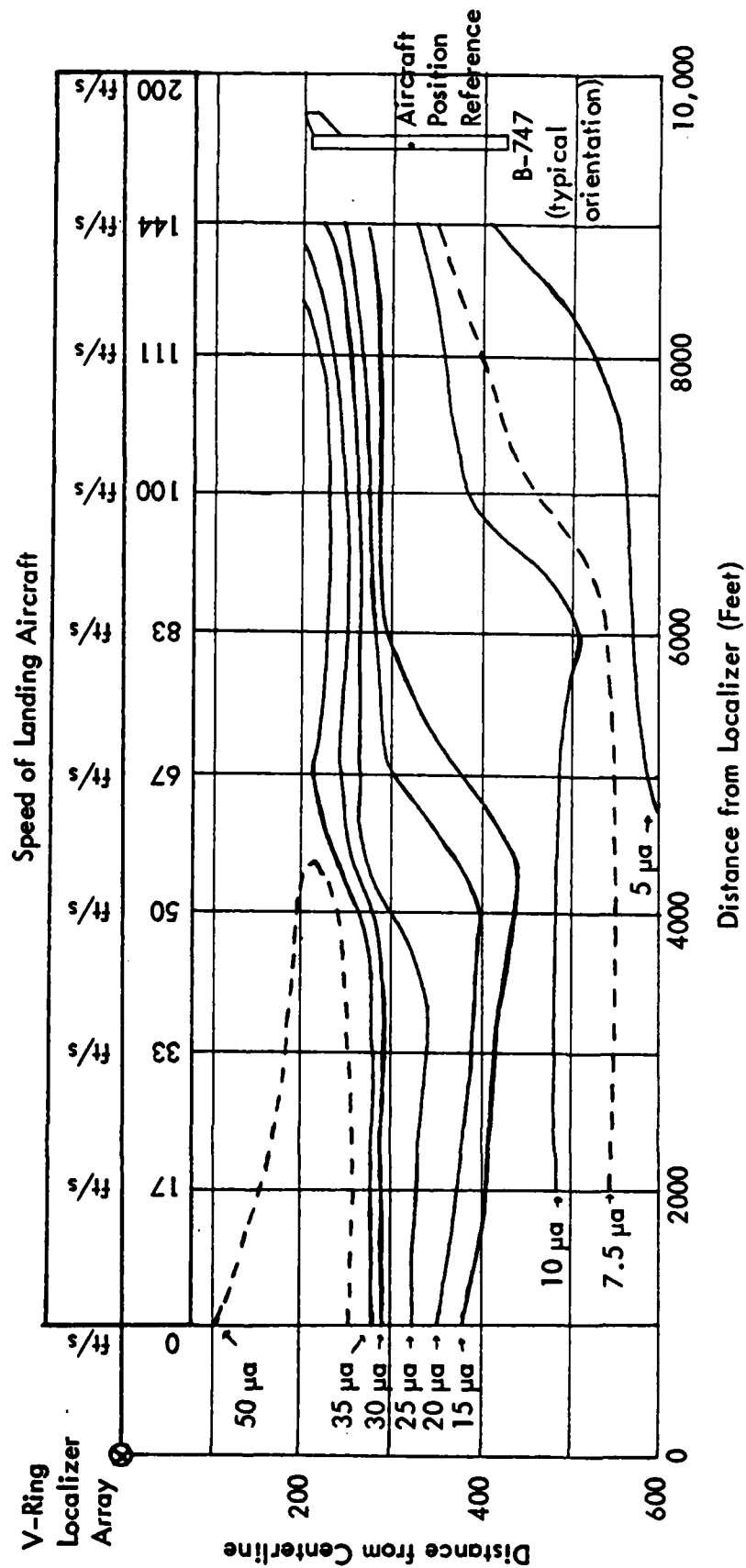
-52-

Figure 16. B-747 Parallel to the Runway Centerline. Peak CDI between ILS points D and E, 8-element array. Calculations assuming constant approach speed of 200 feet/second.

-53-

Figure 17. B-747 Parallel to the Runway Centerline. Peak CDI between ILS points C and D, 8-element array. Calculations assuming constant approach speed of 200 feet/second.

Figure 18. B-747 Perpendicular to the Runway Centerline with the Nose of the Aircraft Toward Centerline. Peak CDI between ILS points D and E, 8-element array. Calculations assuming constant approach speed of 200 feet/second.

-55-
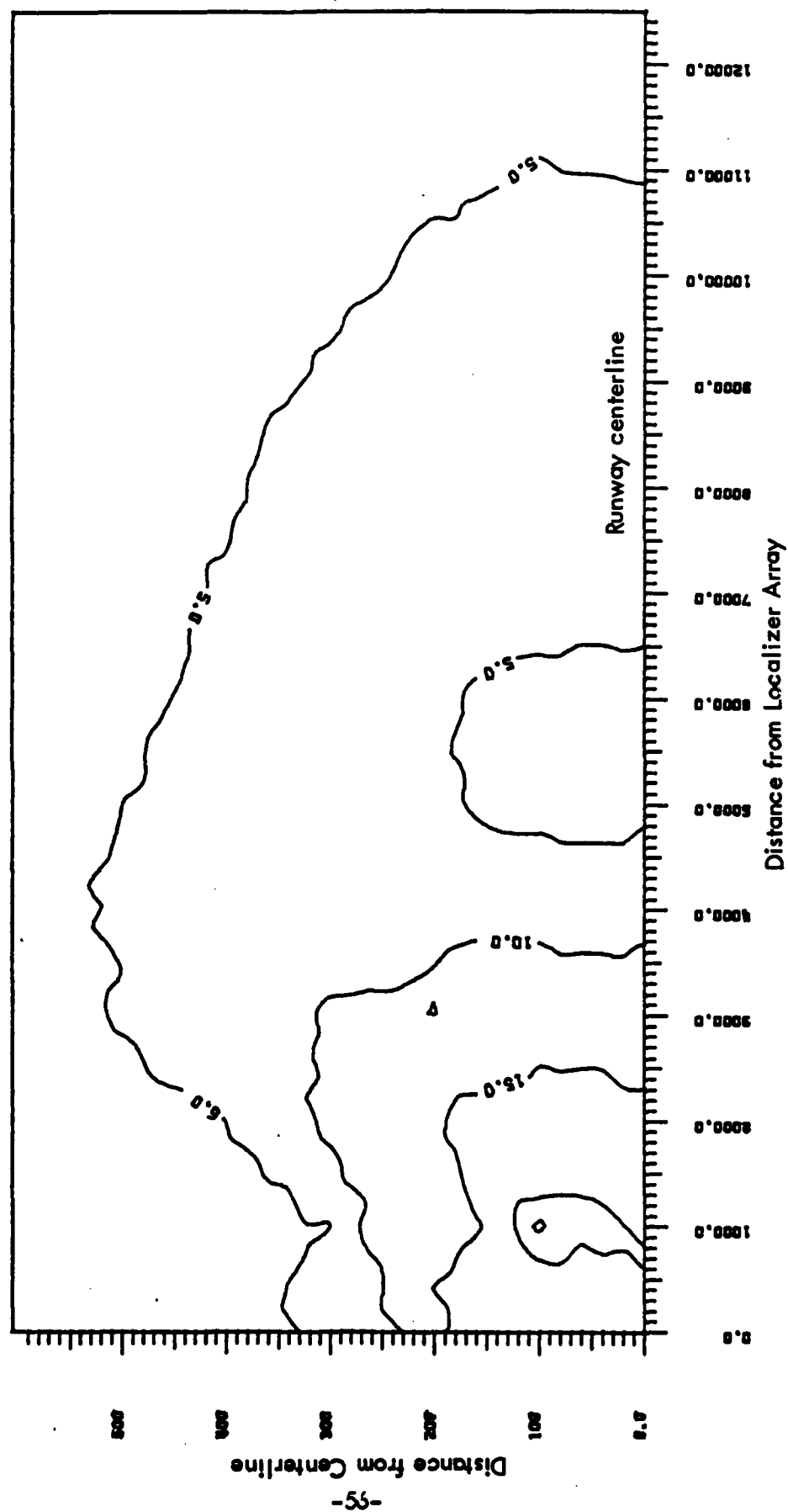
Figure 19. B-747 Perpendicular to the Runway Centerline with the Nose of the Aircraft Toward Centerline. Peak CDI between ILS points C and D, 8-element array. Calculations assuming constant approach speed of 200 feet/second.

-55-
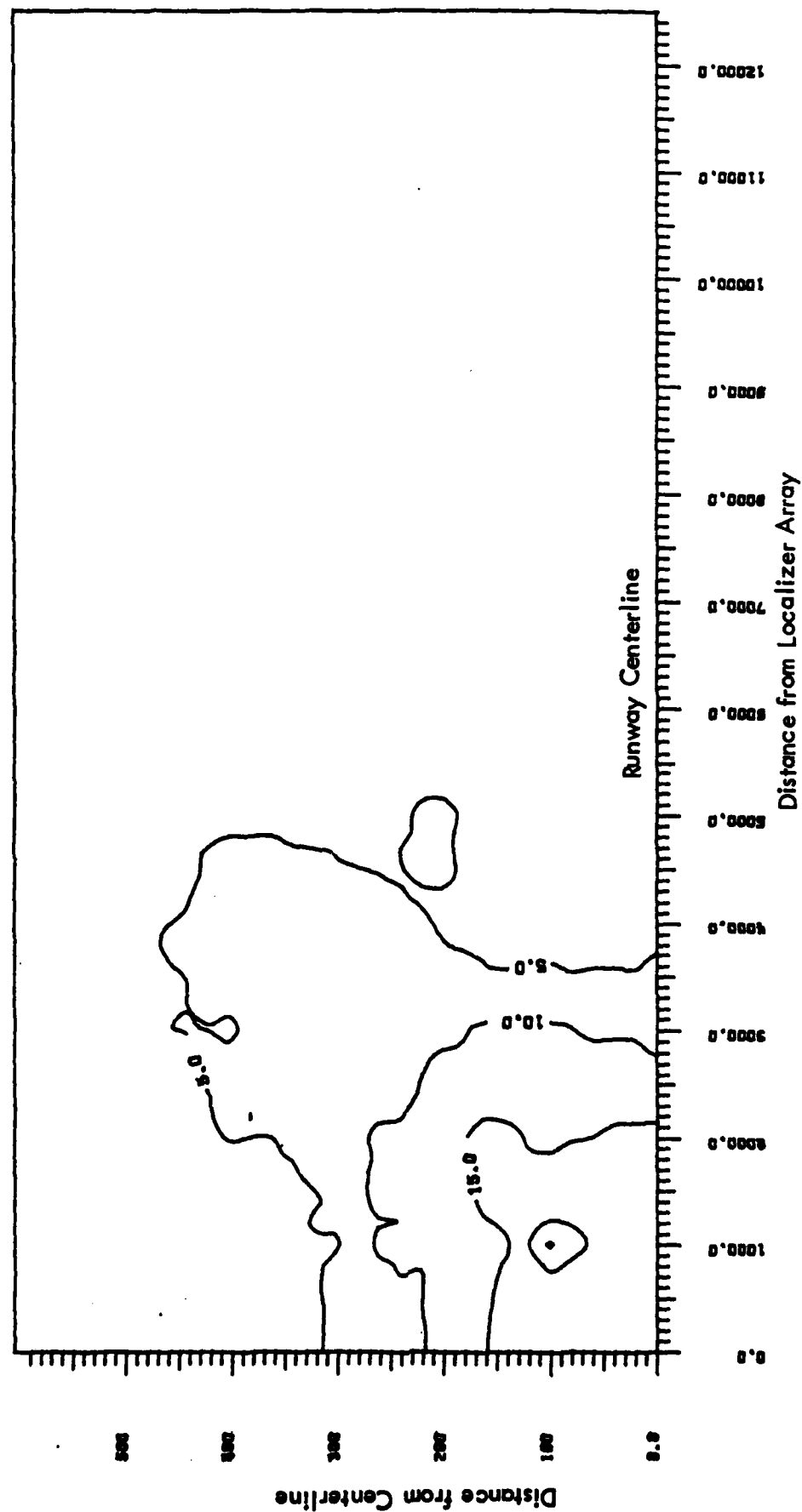
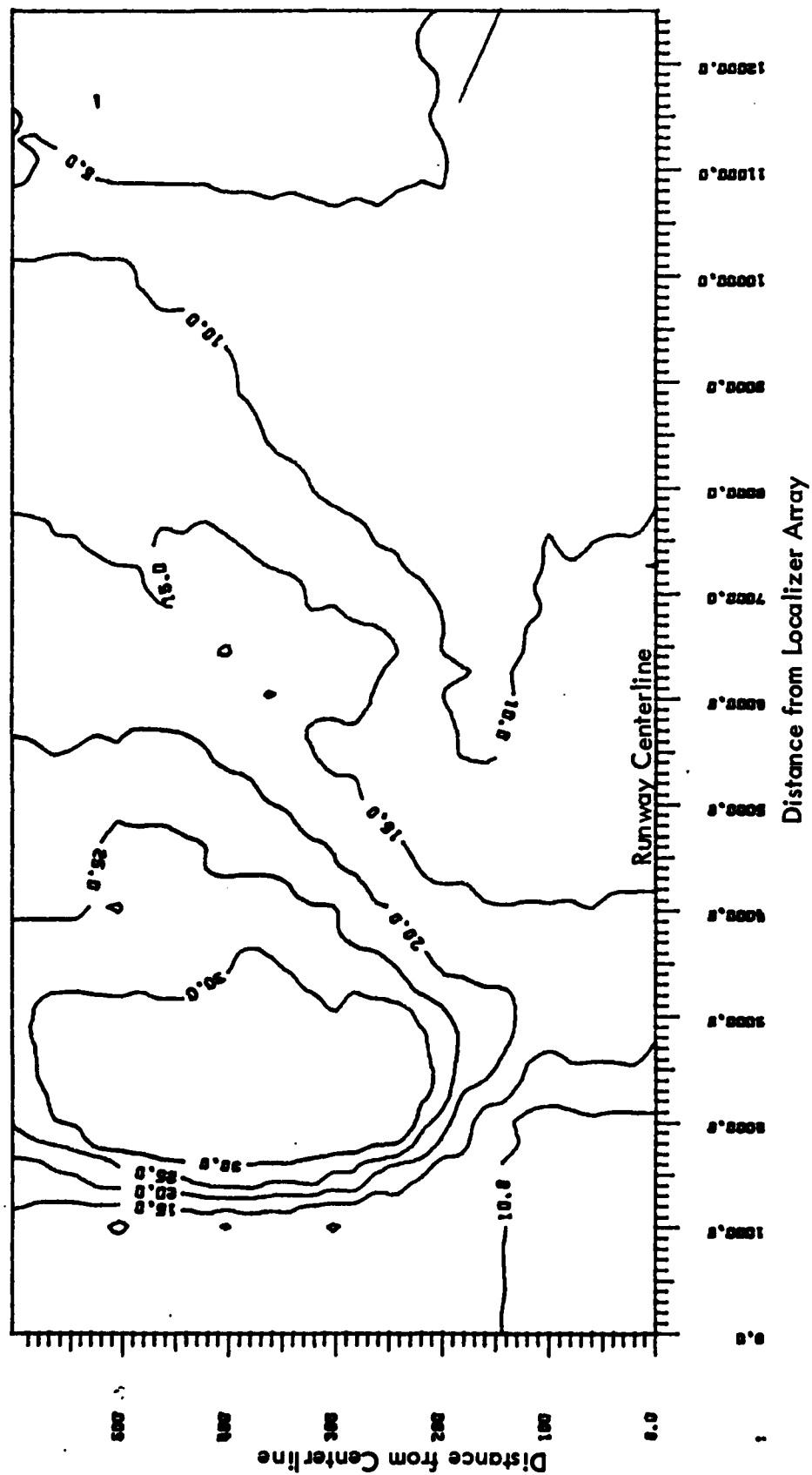Figure 20. B-747 Perpendicular to the Runway Centerline with the Nose of the Aircraft Toward Centerline. Peak CDI between ILS points B and C, 8-element array. Calculations assuming constant approach speed of 200 feet/second.

-57-

Figure 21. B-747 Perpendicular to the Runway Centerline with the Nose of the Aircraft Toward Centerline. Peak CDI between ILS points A and B, 8-element array. Calculations assuming constant approach speed of 200 feet/second.
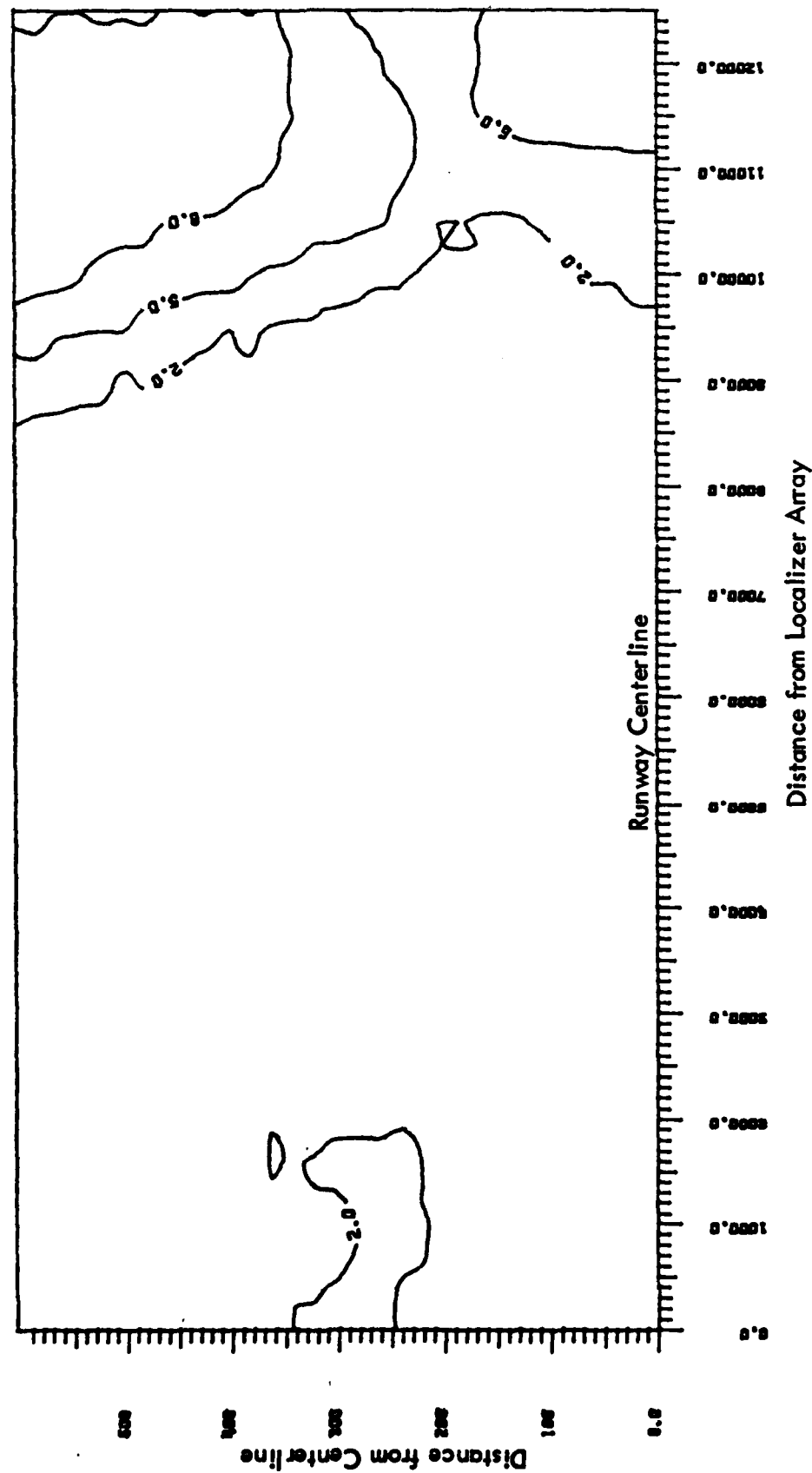
Figure 22. B-747 Perpendicular to the Runway Centerline with the Nose of the Aircraft Toward Centerline. Peak CDI beyond ILS point A, 8-element array. Calculation assuming constant approach speed of 200 ft/sec.
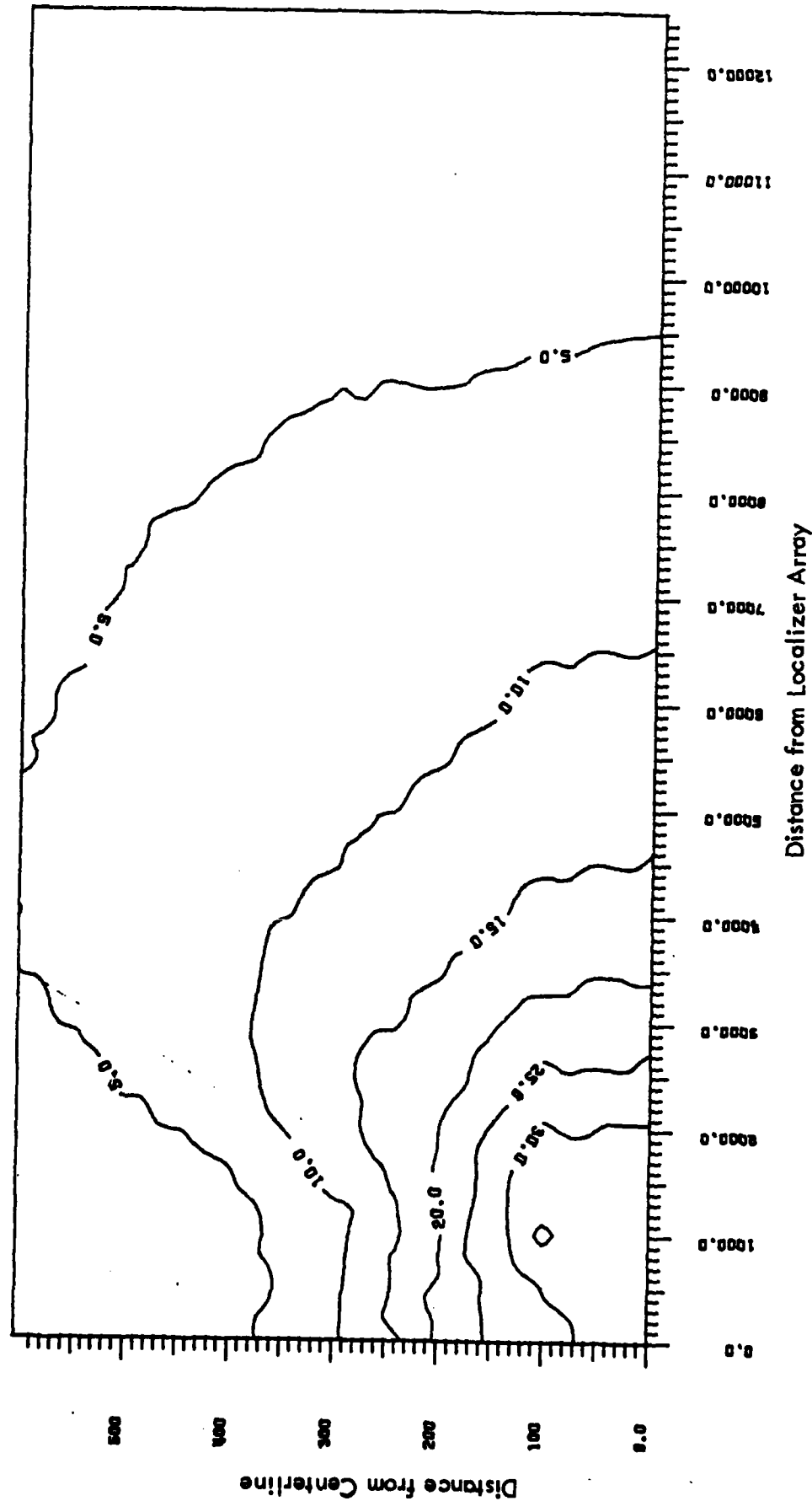
Figure 23. B-747 Perpendicular to the Runway Centerline with the Tail of the Aircraft Toward Centerline. Peak CDI between ILS points D and E, 8-element array. Calculations assuming constant approach speed of 200 ft/sec.

-60-

Figure 24. B-747 Perpendicular to the Runway Centerline with the Tail of the Aircraft Toward Centerline. Peak CDI between ILS points C and D, 8-element array. Calculations assuming constant approach speed of 200 ft/sec.

-61-

Runway Centerline

Distance from Localizer Array

Distance from Centerline

6.0

5.0

10.0

15.0

18.0

22.0

18.0

25.0

18.0

40.0

40.0

0.0

1000.0

2000.0

3000.0

4000.0

5000.0

6000.0

7000.0

8000.0

9000.0

10000.0

11000.0

12000.0

Figure 25. B-747 Perpendicular to the Runway Centerline with the Tail of the Aircraft Toward Centerline. Peak CDI between ILS points B and C, 8-element array. Calculations assuming constant approach speed of 200 ft/sec.

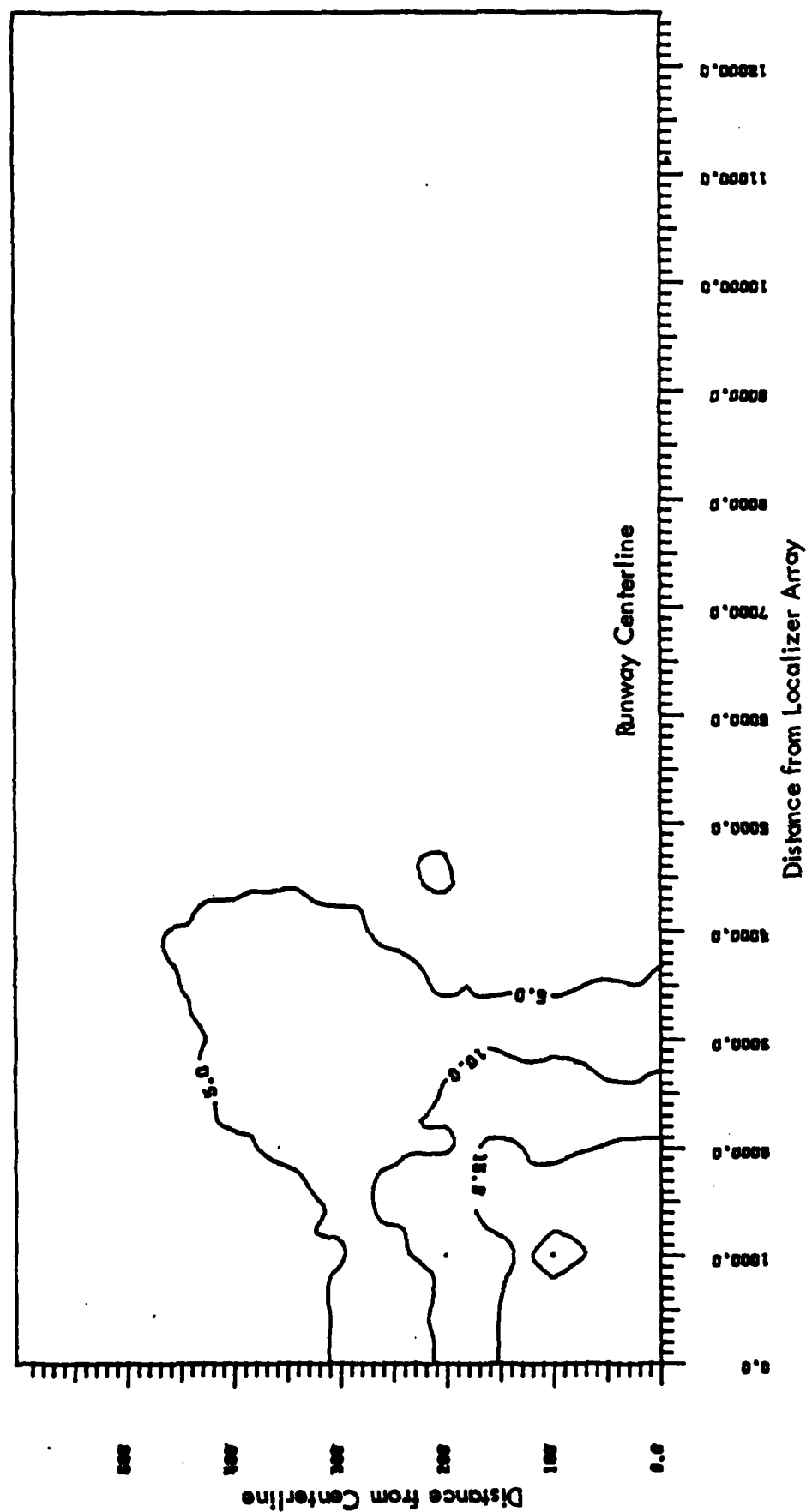Figure 26. B-747 Perpendicular to the Runway Centerline with the Tail of the Aircraft Toward Centerline. Peak CDI between ILS points A and B, 8-element array. Calculations assuming constant approach speed of 200 ft/sec.
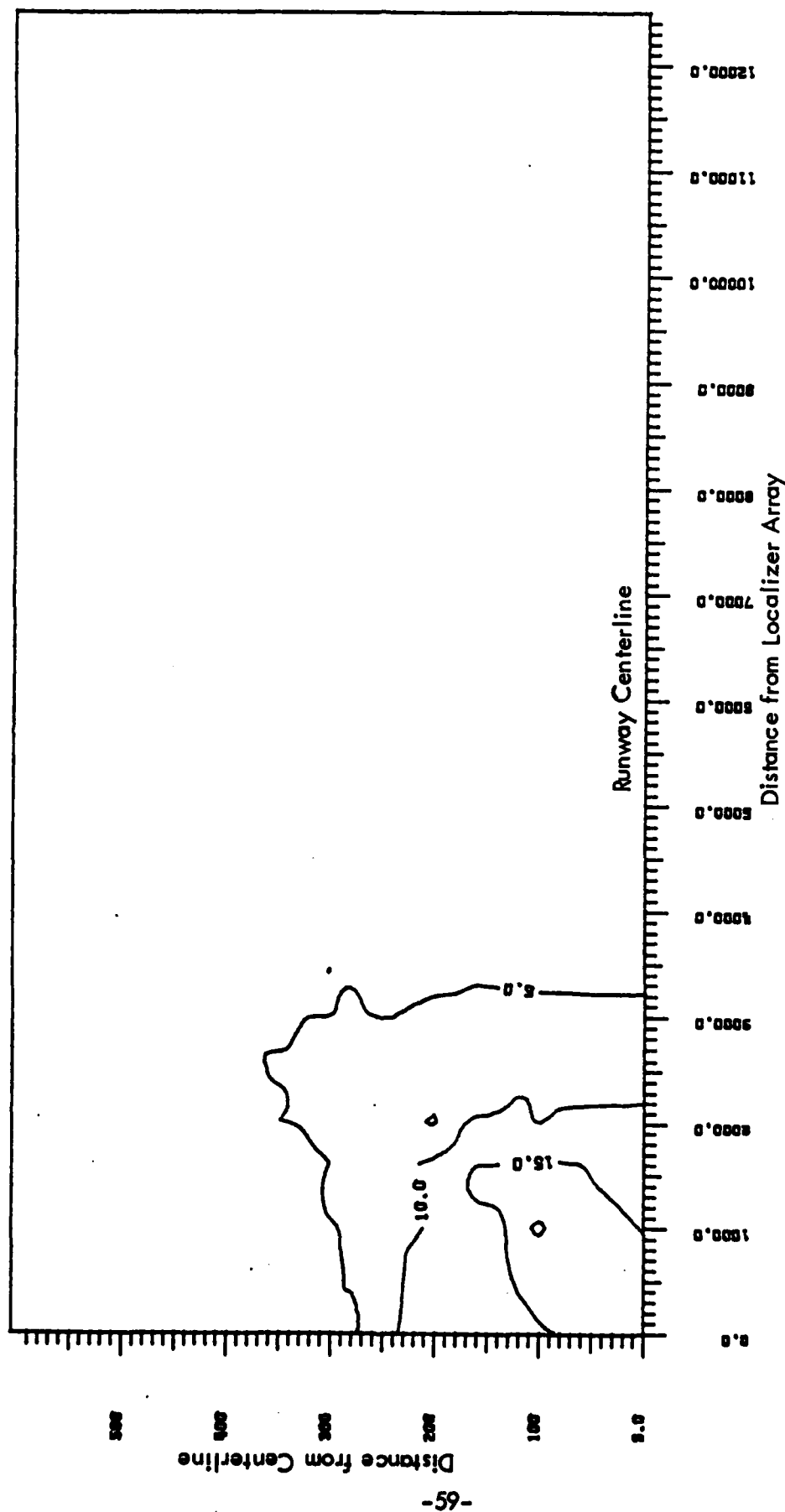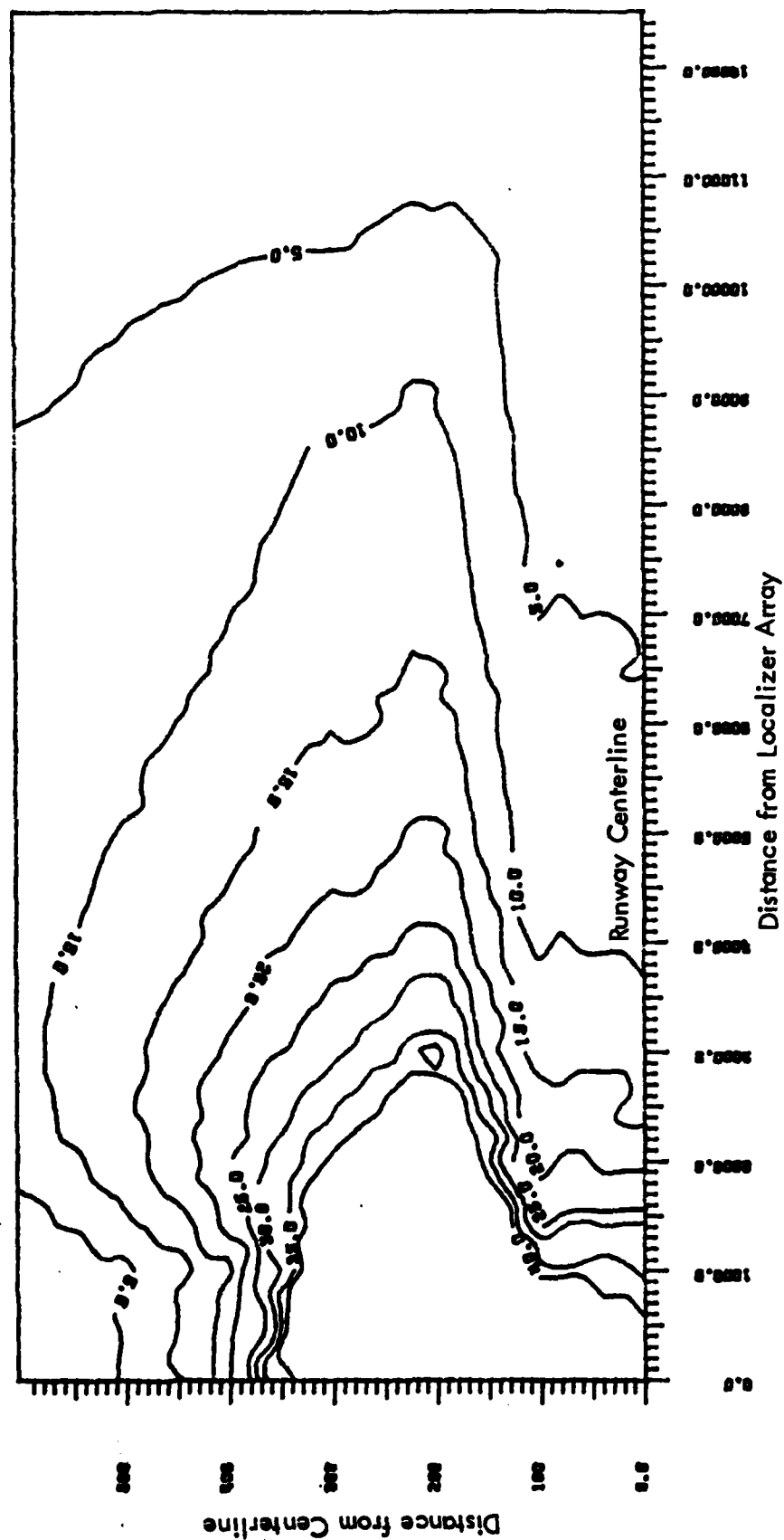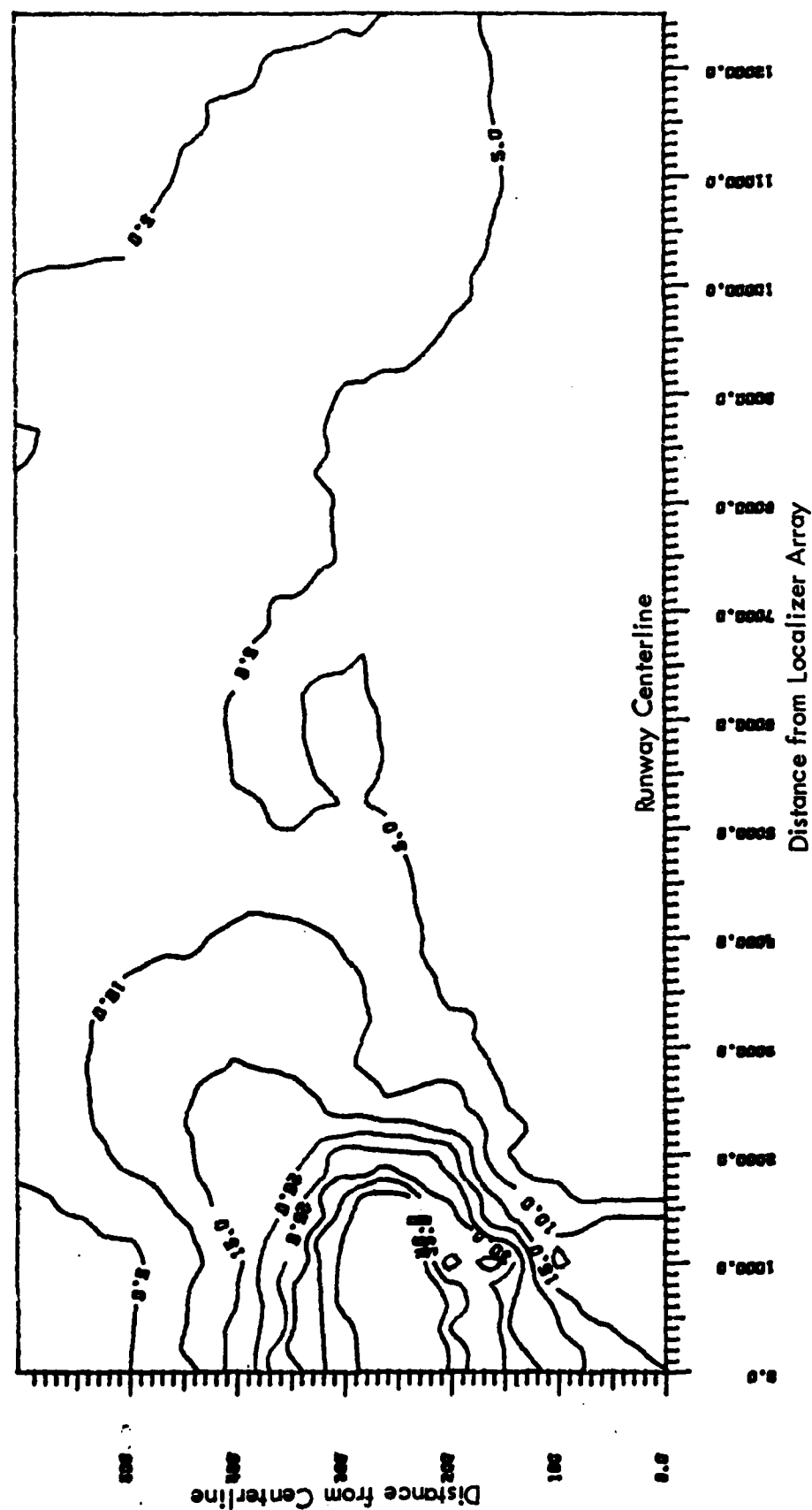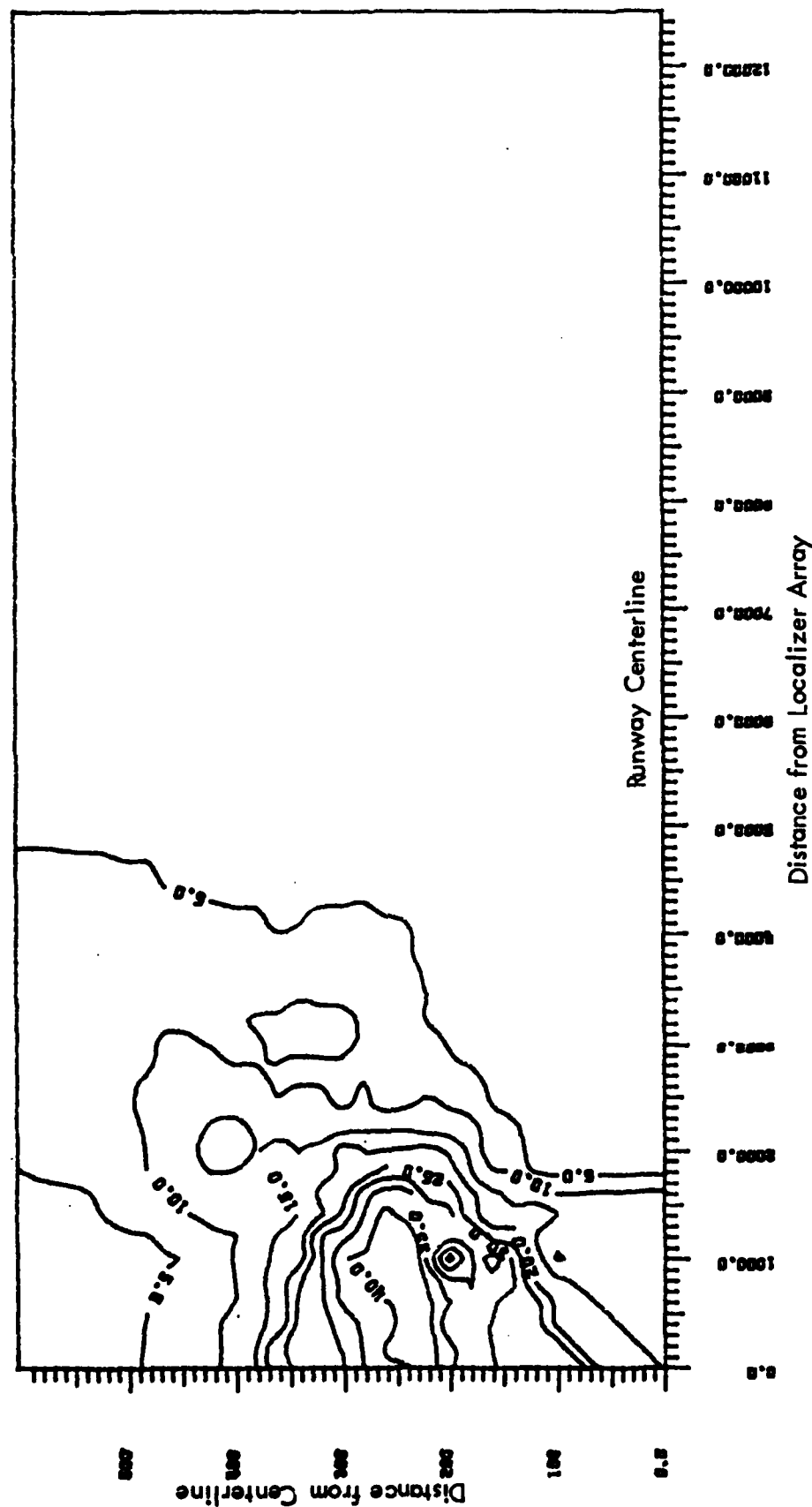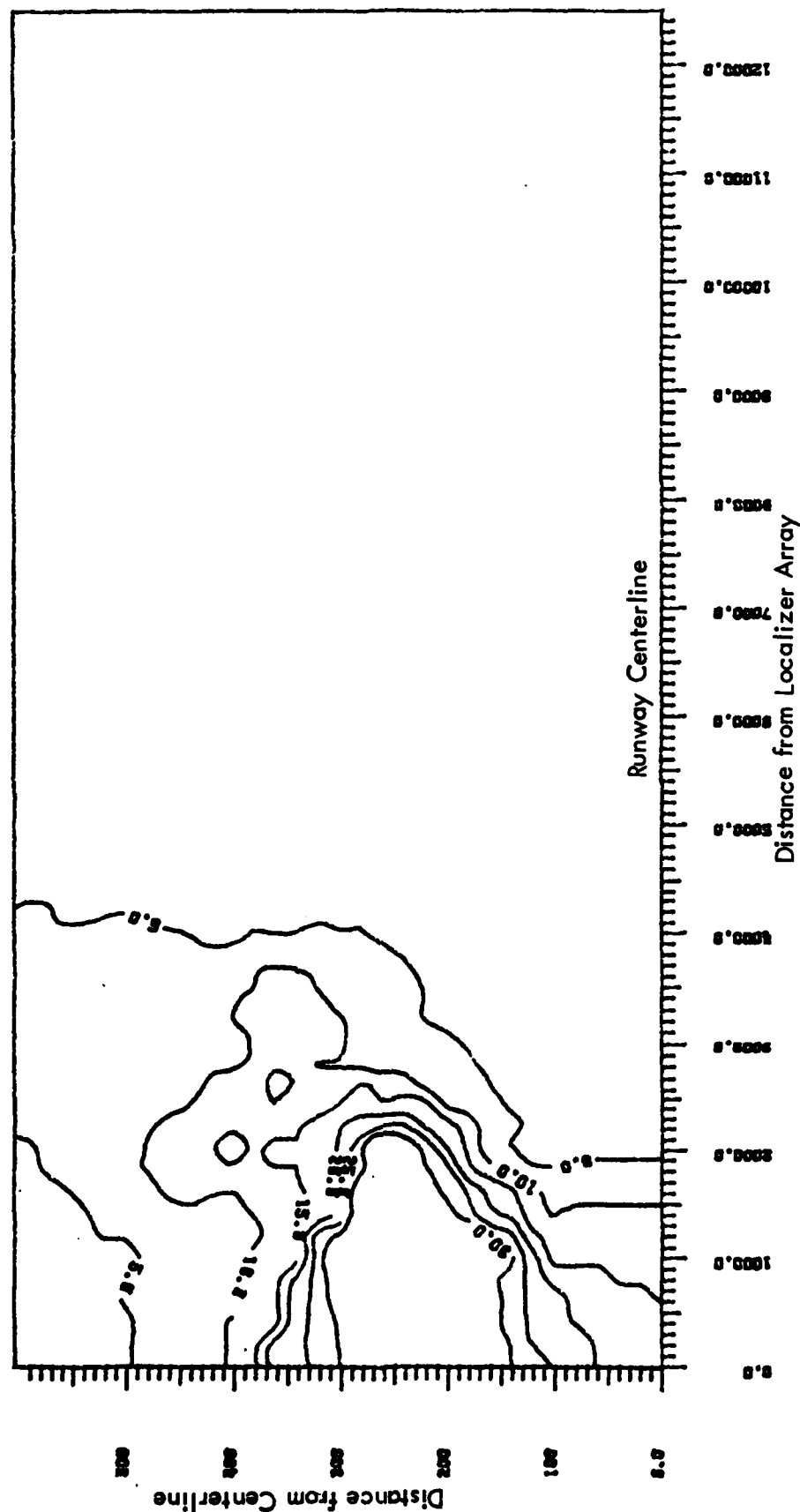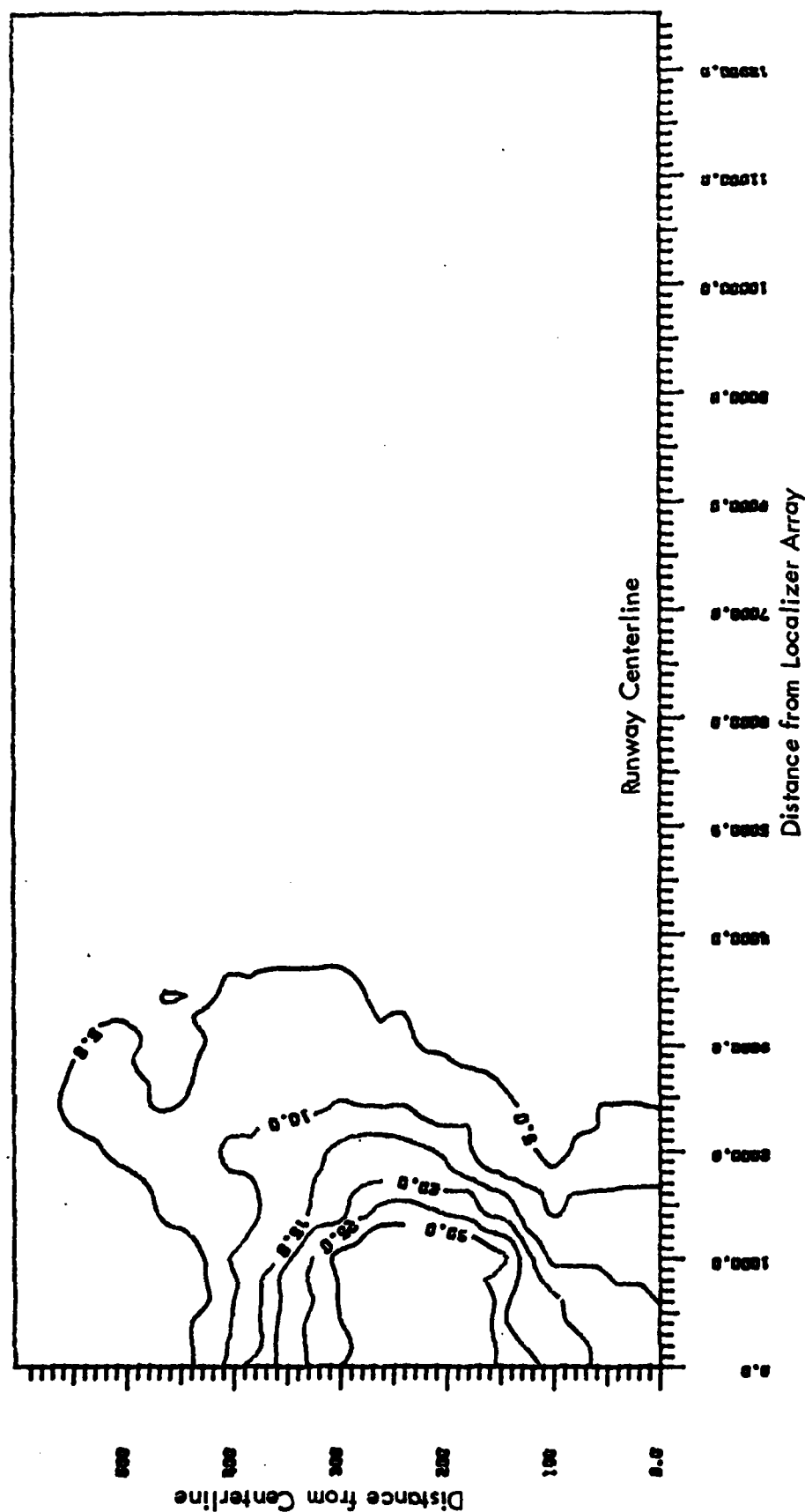
-63-

Figure 27. B-747 Perpendicular to the Runway Centerline with the Tail of the Aircraft Toward Centerline. Peak CDI beyond ILS point A, 8-element array. Calculations assuming constant approach speed of 200 ft/sec.

-64-

C. __Application of Contour Maps for Smaller Aircraft.__ The previously generated contour maps were calculated based upon the worst case size aircraft, the Boeing 747. At this time, the Boeing 747 series aircraft is not a certified Category-III carrier in the United States. With this in mind, the contour maps may indicate a more severe critical area than would be required, based upon currently certified CAT-III aircraft.

Specific locations have been calculated with the size of the aircraft reduced to that of a Lockheed L-1011, a certified Category-III carrier. These calculations resulted in the following:

1. If the tail position and orientation for the Boeing 747 and Lockheed L-1011 are identical, a reduction in the localizer peak deviations is noted for the smaller aircraft. See figures 28 and 29.

2. Using the nose of the aircraft as the reference point for calculations of critical areas results in a greater deviation in the localizer on-course signal for the smaller aircraft when the aircraft is perpendicular to centerline with the nose toward the centerline. The fuselage of the L-1011 is shorter than that of the 747. This results in the tail of the aircraft being approximately 45 feet closer to the centerline than for the 747. See figures 30 and 31.

Figure 28. On-Course Structure Calculation with Boeing 747 Nose Wheel Positioned Approximately 100 Feet from Centerline, 2000 Feet from Localizer Array Perpendicular to Centerline and Nose Toward Centerline. 14-element, single-frequency localizer.
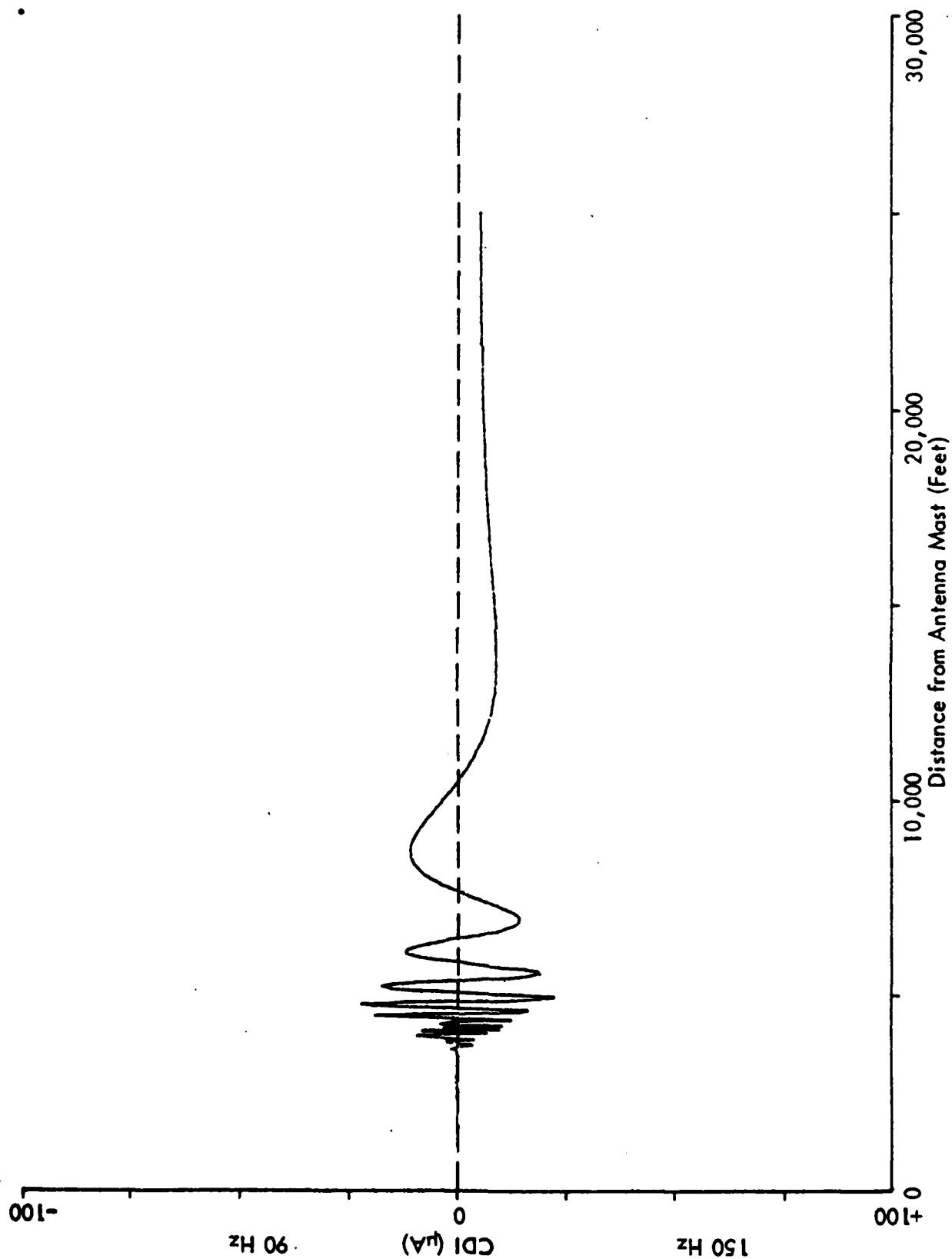
Figure 29. On-Course Structure Calculation with L-1011 Positioned Approximately 100 Feet from Center-line 2000 Feet from Localizer Array (same tail location as figure 28). Aircraft is perpendicular to centerline with nose toward centerline. 14-element, single-frequency localizer.
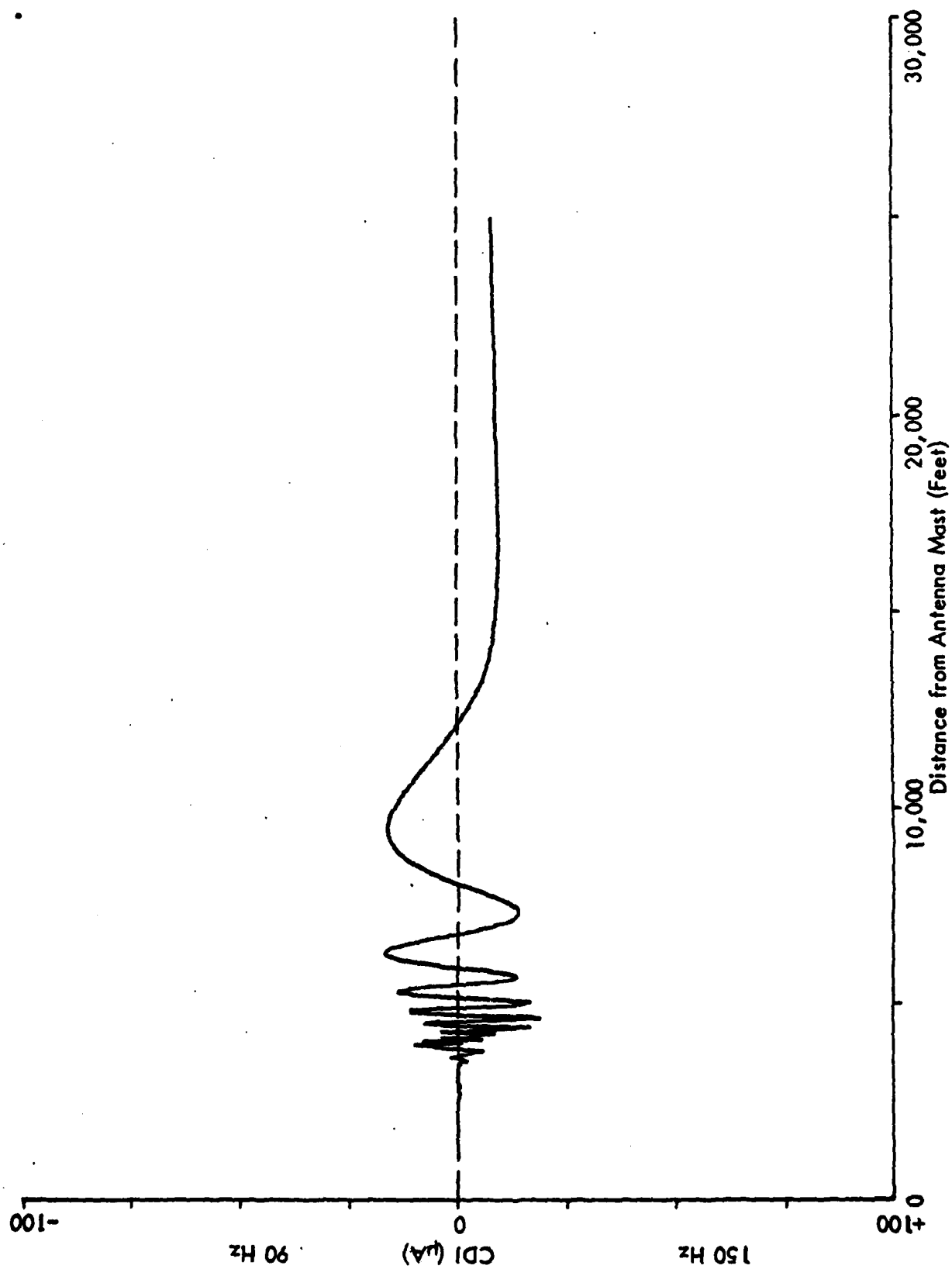
Figure 30. On-course Structure Calculation with Boeing 747 Positioned Approximately 100 Feet from Centerline and 2000 Feet from Localizer. Nose wheel is reference position. Aircraft is perpendicular to centerline with nose toward centerline. 14-element, single-frequency localizer.

Figure 31. On-course Structure Measurement with L-1011 Positioned at 100 Feet from Centerline and 2000 Feet from Localizer (Nose wheel as reference). Aircraft is perpendicular to center-line with nose toward centerline. 14-element, single-frequency localizer.

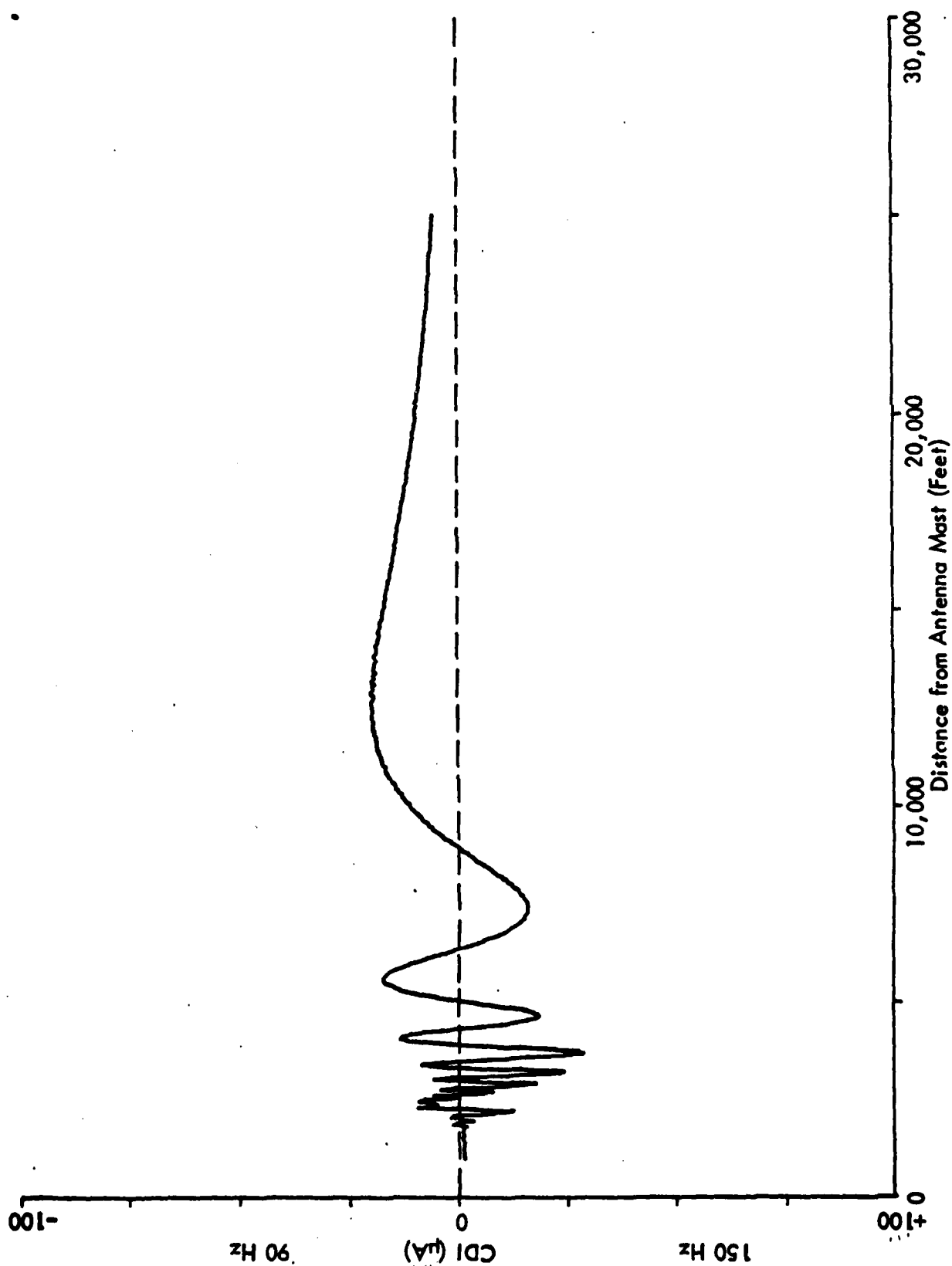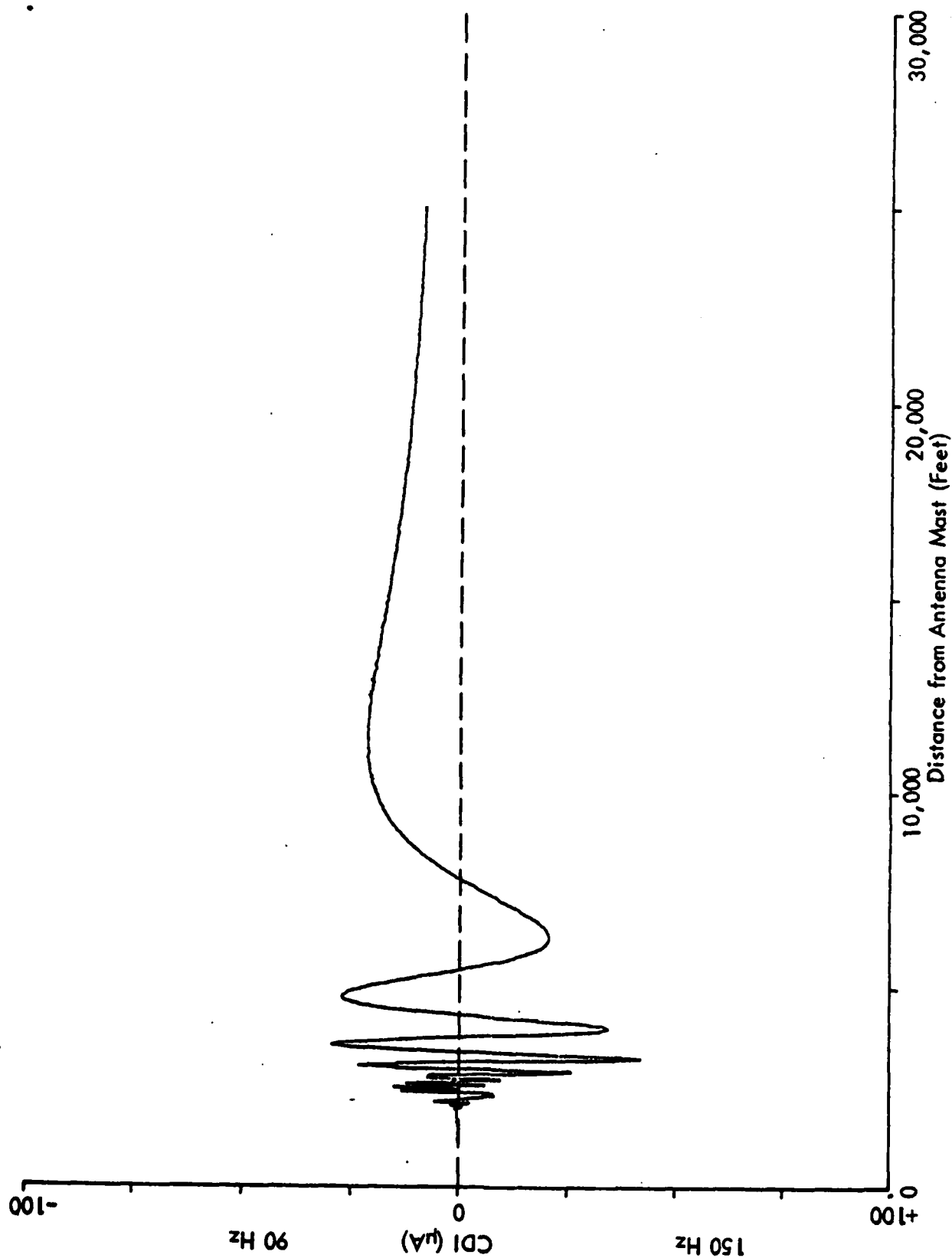## III. CATEGORY-III CRITICAL AREA RECOMMENDATIONS

Critical area in the following recommendations is defined as the area outside of which the nose of the aircraft must lie. Using the above contour maps, it is now possible to establish an estimate of the critical areas. As in the previous two-frequency effort (reference 5), the application of flight inspection tolerances (reference 6) is required. Based upon flight inspection tolerances on the contour maps, the worst critical areas for each aircraft orientation may be drawn. Figures 32 through 34 show the critical area regions for the 14-element, single-frequency localizer system with figure 35 showing the combined worst case. These figures were drawn using the maps generated from the 747 calculations.

The recommended critical areas for the 8-element array are indicated in figures 36 through 39 for each aircraft orientation and for the combined worst case. In addition the worst case critical areas for the 8-, 14- and dual-frequency arrays are shown in figure 40.

The method used to obtain the critical areas shown in figures 32 through 39 from the contour maps and the application of flight inspection tolerances is demonstrated by the following example.

Example 1:

From figure 1 (zone 5) it is noted that the 10 A contour occurs beyond 1000 feet from the localizer and 450' from centerline. Using this map only, would result in a critical area greater than 600' from centerline; however, when the flight inspection tolerances of reference 6 are applied it is found that none of the peak CDI variations are out-of-tolerance for more than 354' out of a 7089' span along the approach. This then allows the critical area to be reduced to the edge of the runway for this ILS zone.

To obtain the overall critical area for this orientation, the above procedure is applied to all ILS zones. The greatest resulting critical area is that recommended for the particular orientation.

Figure 32. Localizer Cat III Critical Area. B-747 Parallel to Runway Centerline. 14-element, single-frequency localizer array.

Figure 33. Localizer Cat III Critical Area. B-747 Perpendicular to Runway Centerline with Nose Toward Centerline. 14-element, single-frequency localizer array.

Figure 34. Localizer Cat III Critical Area. B-747 Perpendicular to Runway Centerline with Tail Toward Centerline. 14-element, single-frequency localizer array.

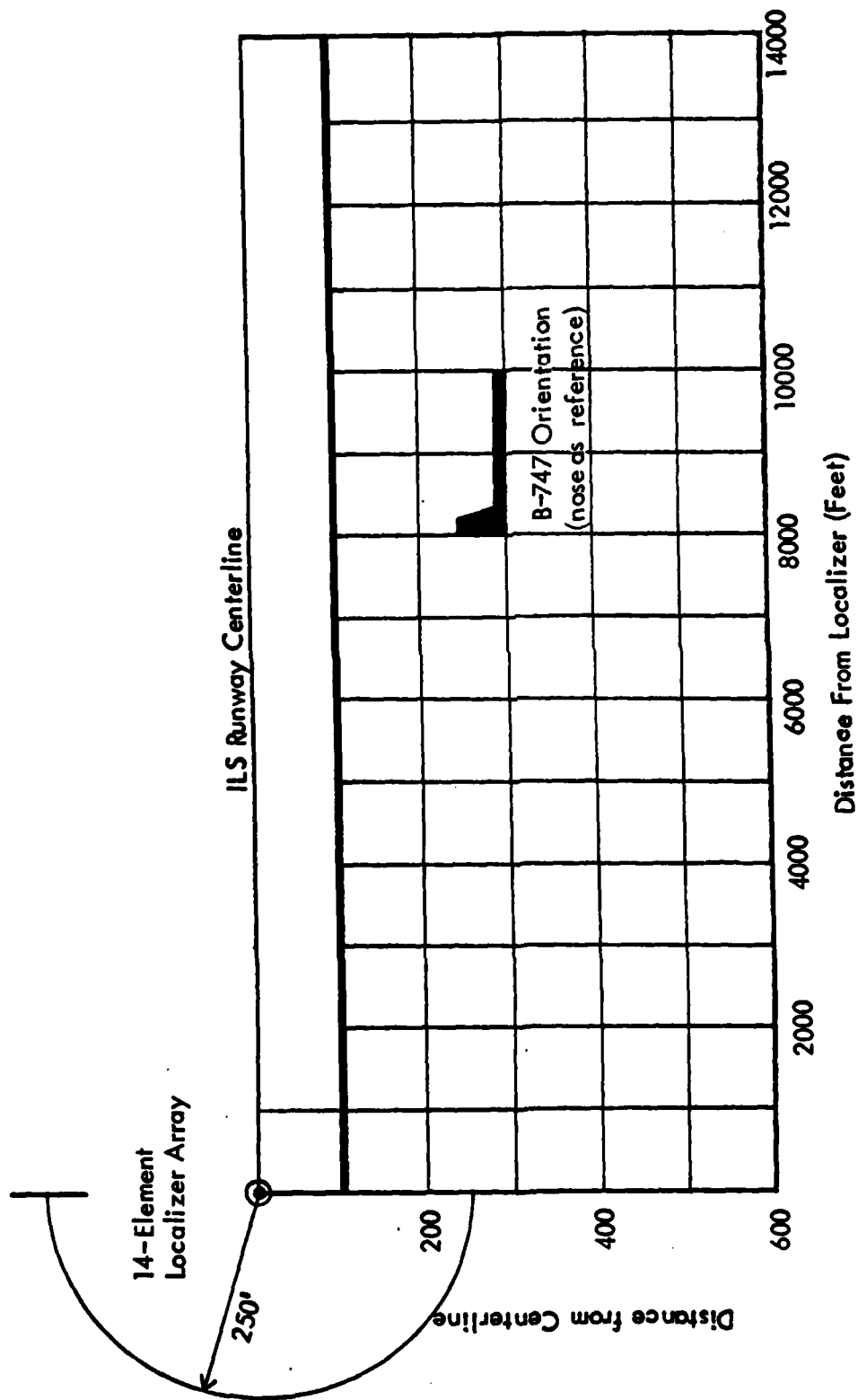Figure 35. Localizer Cat III Critical Area. Worst Case Critical Area. 14-element, single-frequency localizer array.

-74-
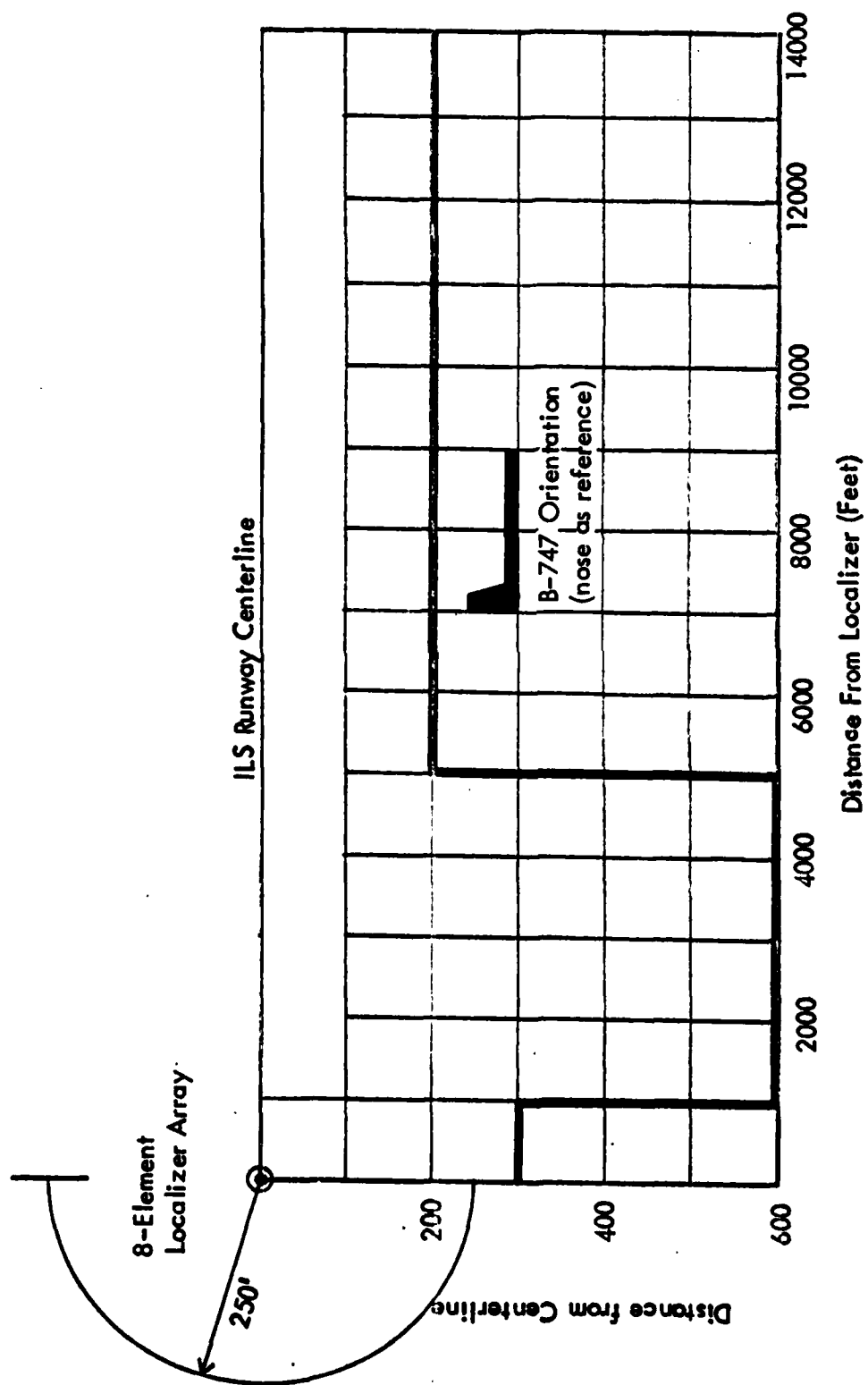
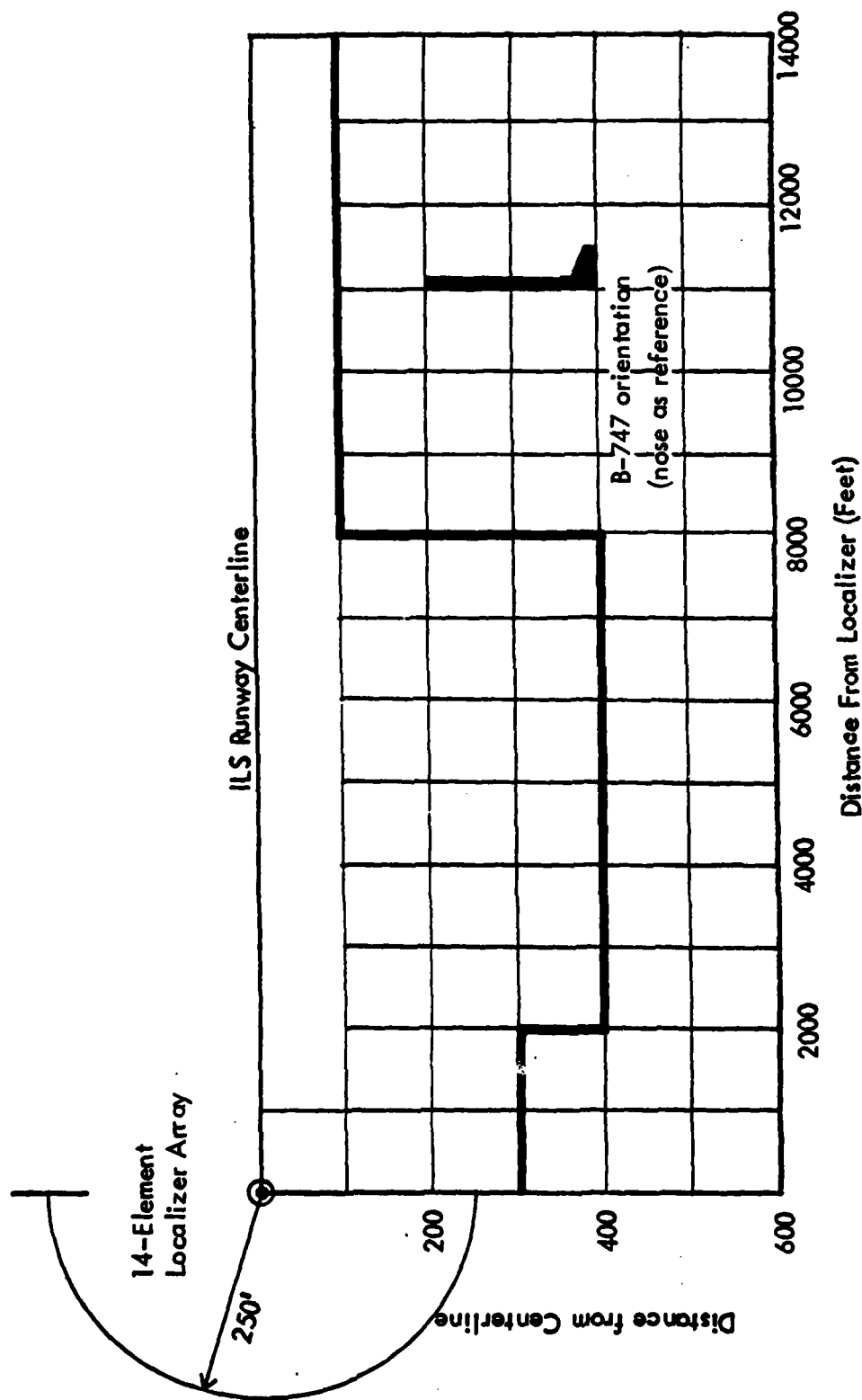Figure 36. Localizer Cat III Critical Area. B-747 Parallel to Runway Centerline. 8-element, LPD array.
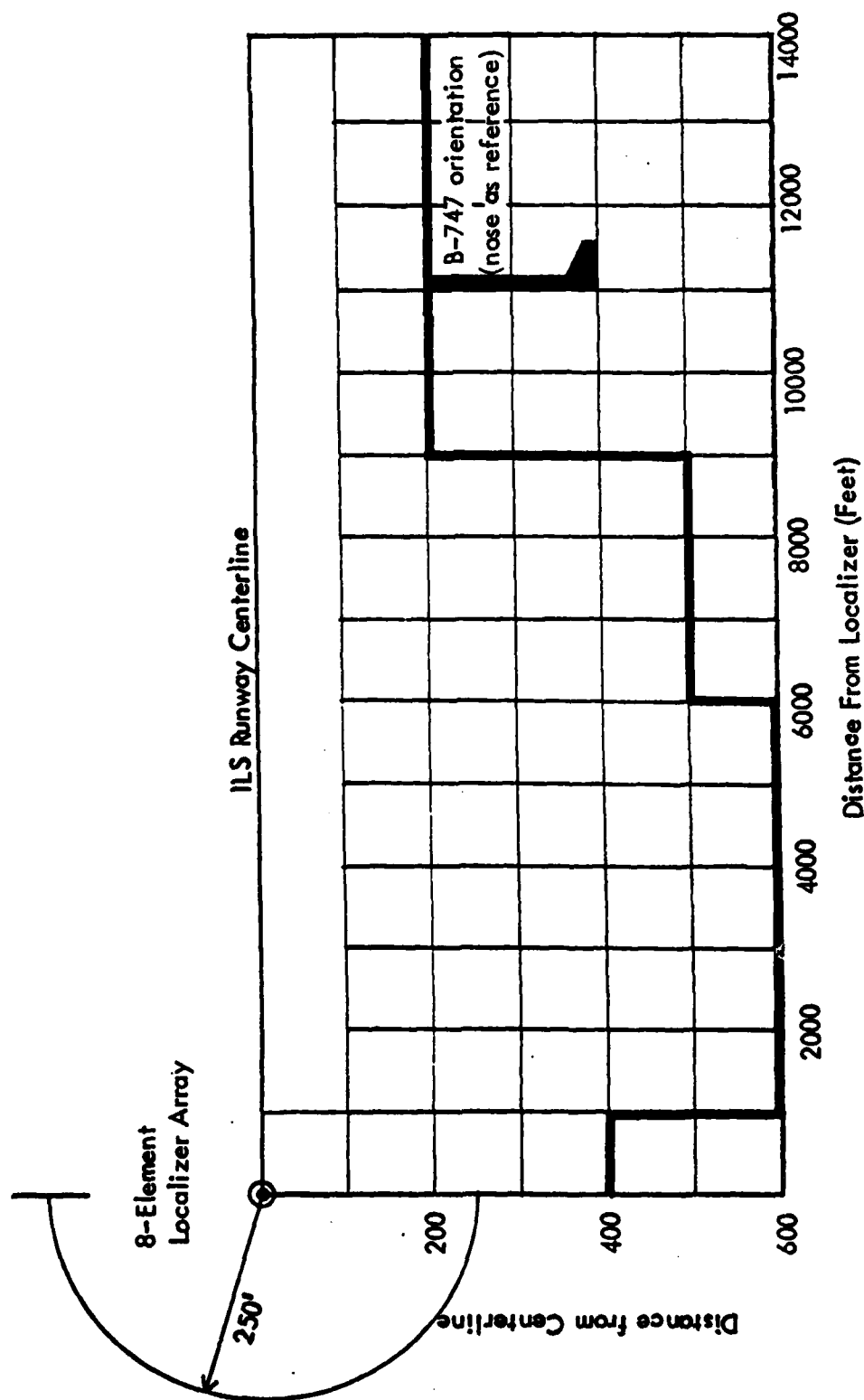
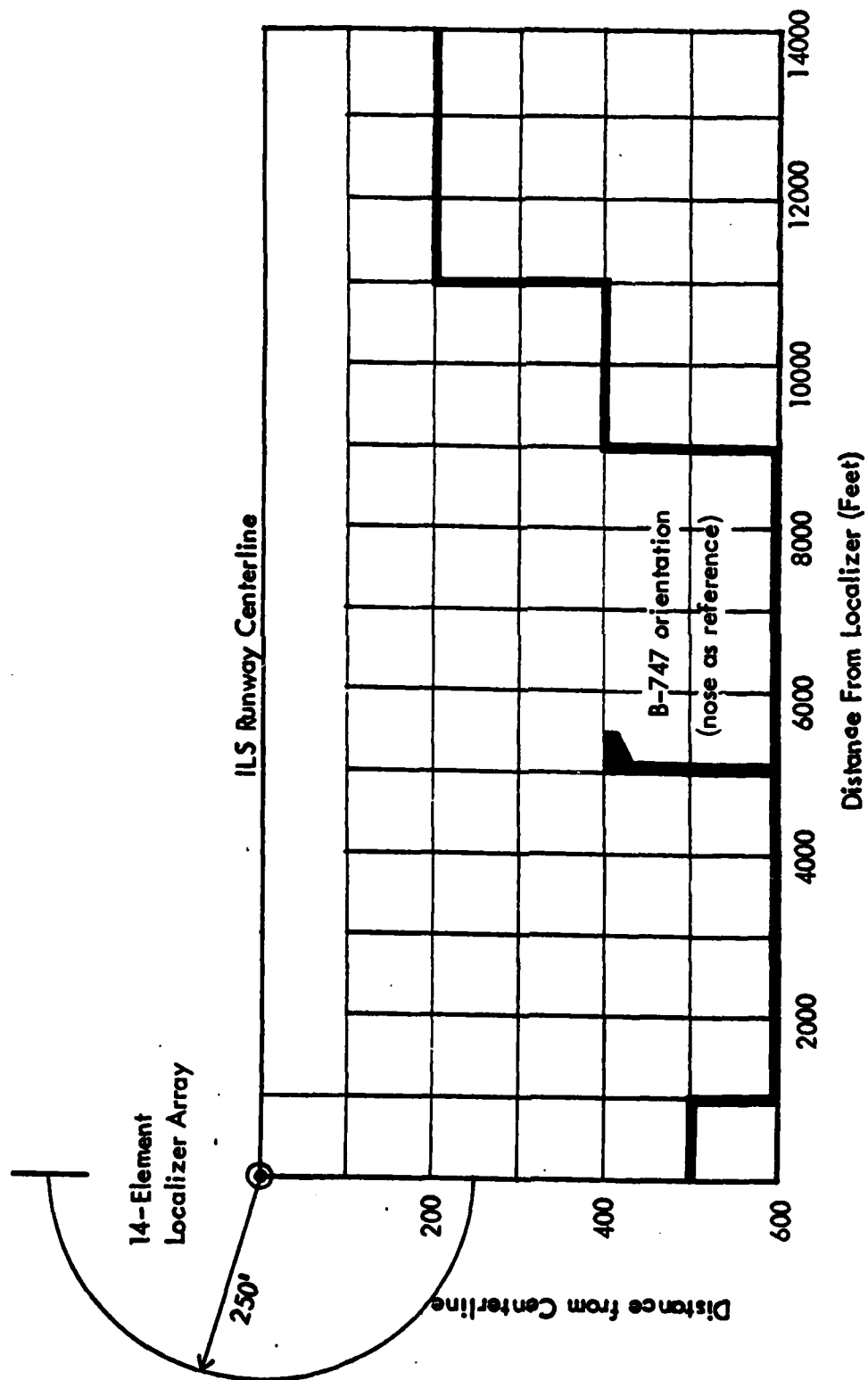Figure 37. Localizer Cat III Critical Area. B-747 Perpendicular to Runway Centerline with Nose Toward Centerline. 8-element, LPD array.

-76-
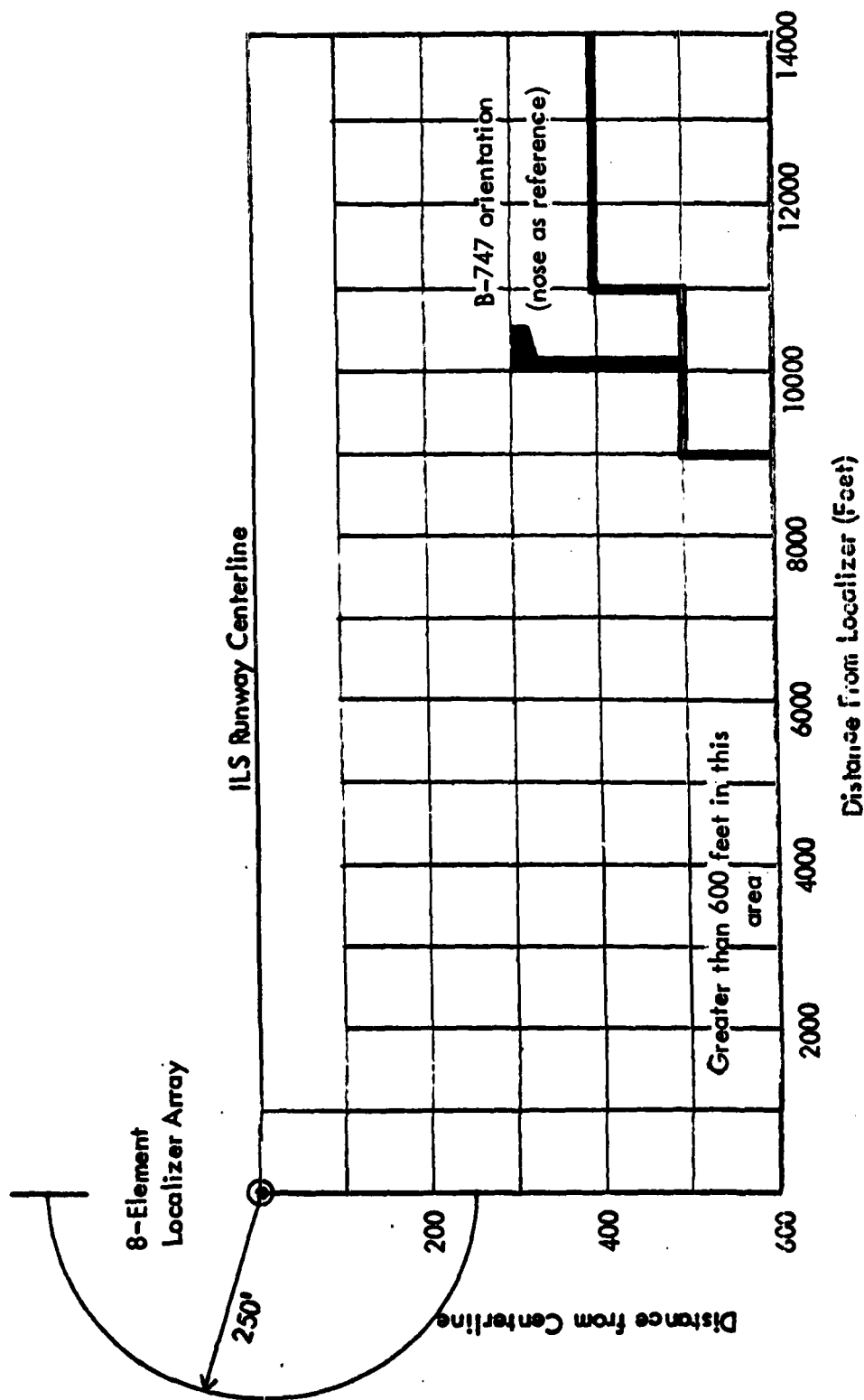
Figure 38. Localizer Cat III Critical Area. B-747 Perpendicular to Runway Centerline with Tail Toward Centerline. 8-element, LPD array.
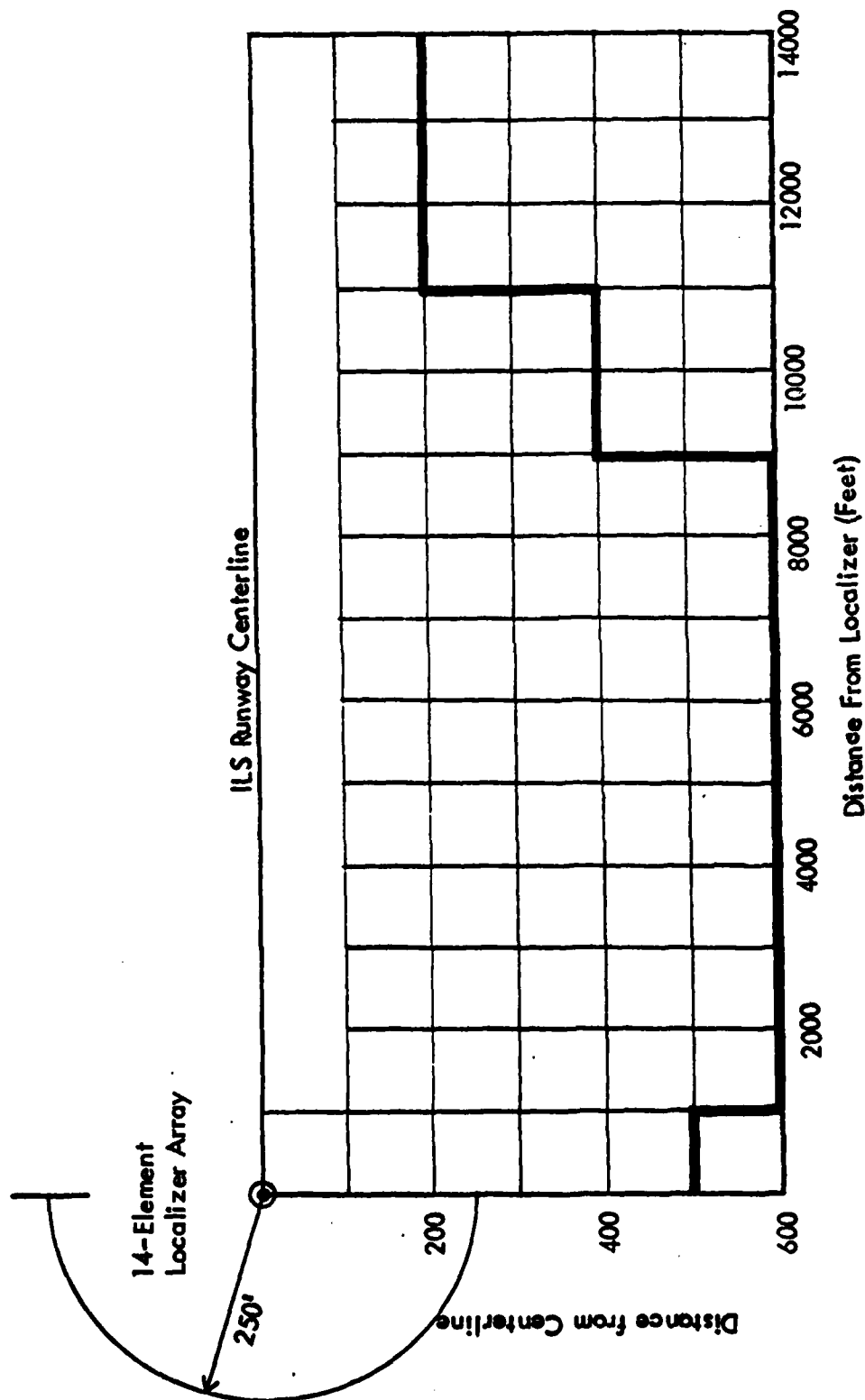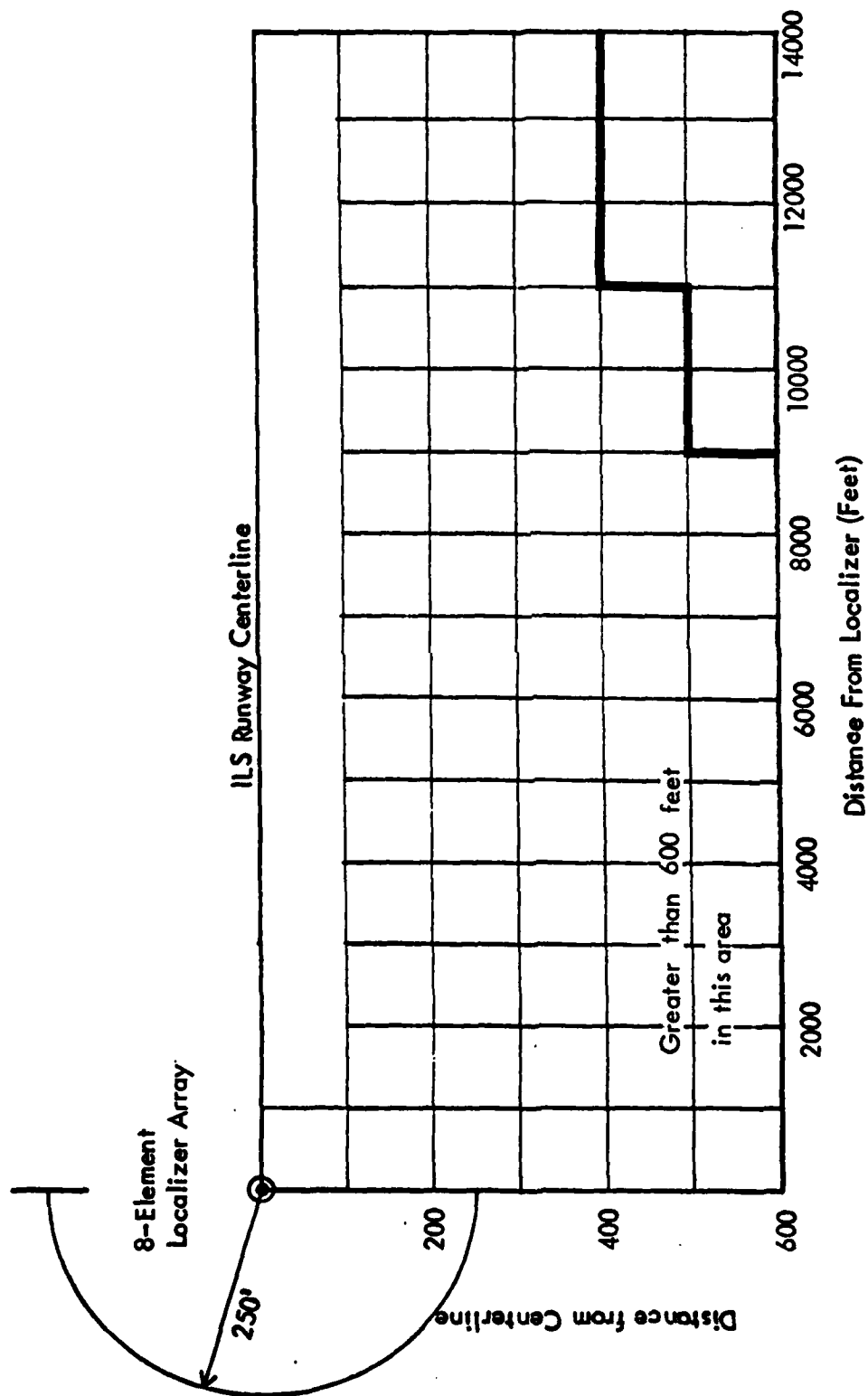
Figure 39. Localizer Cat III Critical Area. Worst Case for 8-element, single-frequency, LPD array.
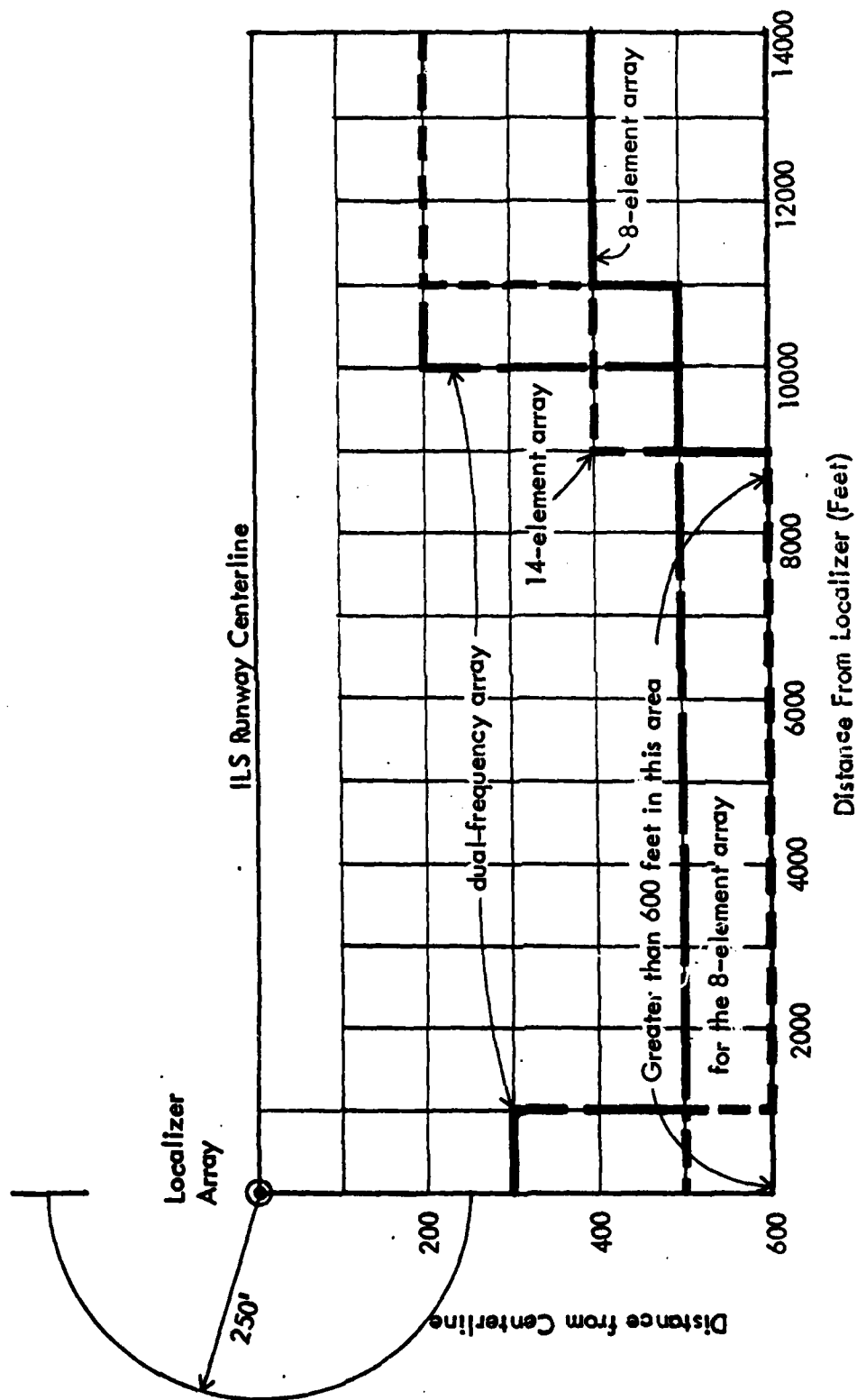
Figure 40. Localizer Cat III Critical Area. Worst Case for 8-element, single-frequency, LPD array, 14-element, single-frequency, LPD array, and the 14-element dual frequency array.

-79-

IV. AKNOWLEDGEMENTS
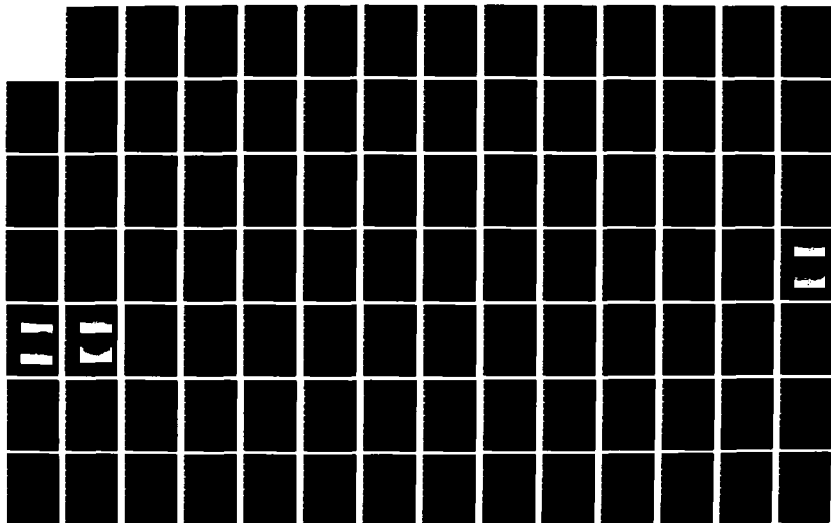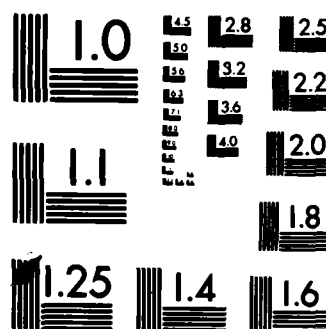
MICROCOPY RESOLUTION TEST CHART
NATIONAL BUREAU OF STANDARDS-1963-A

V. REFERENCES

[1] Rondini, R.A. and R.H. McFarland, "Experimental Validation of Boeing 747 ILS Signal Scattering Calculations for Critical Area Determination", Final Report, SRDS No. FAA-Rd-74-57/EER 18-1, Avionics Engineering Center, Ohio University, Athens, Ohio, Janaury 1974.

[2] Longworth, Joe D., "Theoretical and Experimental Investigation of Boeing 747 Dual-frequency Localizer Signal Scattering for CAT-III Critical Area Determination", OU/EER/AEC 59-1, Avionics Engineering Center, Ohio University, Athens, Ohio, November 1982.

[3] Rondini and McFarland, op. cit.

[4] Ibid.

[5] Longworth, op. cit.

[6] U.S. Standard Flight Inspection Manual, FAA OA P 8200.1.

PHASE III

CRITICAL AREA DETERMINATION FOR NULL-REFERENCE

GLIDE SLOPE CONSIDERING GENERAL

AVIATION TYPE AIRCRAFT

by

Richard H. McFarland, Ph.D.

September 1983

TABLE OF CONTENTS

LIST OF FIGURES

List of Figures (Continued)

List of Figures (Continued)

List of Figures (Continued)

List of Table

I.   CONCLUSIONS

The following conclusions are based on both theoretical and experimental work performed to examine the effects on the ILS glide slope performance of small and medium aircraft parked near the transmitting antennas. Considerable interest is justified in what sensitive or critical areas may exist for parking or taxiing general aviation-type aircraft in particular. At airports serving such aircraft it is typical that real estate is limited, and a number of aircraft may exist in a critical area waiting for departure. Some remarkable findings have been obtained, some being contrary to the intuition of some who are not intimately familiar with the theory of ILS.

Basically, three distinct types of aircraft are considered in this study. They are small size, exemplified by a Piper PA-28 Cherokee; medium size, exemplified by a Rockwell Commander, and a large size, represented by a Convair 440. Jumbo Jet aircraft, for example, the Boeing 747, were not considered since they have been the subject of previous studies.

When defining a critical area at a particular glide slope site the principal conclusions are:

1.   Consideration must be given to the inherent noise produced by the specific site. This noise is a base to which the perturbations produced by the aircraft must be added. For simplicity discussions in this report consider this noise to be zero, which is not true for practical sites.

2.   The placement of any of the small, medium, or large aircraft in any practical fashion, given common taxiway complexes serving an ILS runway, does not produce an unflyable glide slope or one that leads to a destination other than to the runway. In all practical cases the path remains within Category I tolerances. Only when the large aircraft might be parked close to the transmitting antennas, conflicting with the area where monitor detector probes would be normally found, are significant perturbational influence produced.

3.   The ILS glide slope is found to be remarkably unaffected by placement of general aviation-type aircraft on a typical taxiway complex. This is consistent with facts acquired informally over the long period of time that ILS glide slopes have been operating satisfactorily with aircraft taxiing and parking in front of the transmitting antennas.

4.   Below-path structures with parked aircraft in front of the antennas have not been found to deteriorate significantly. The finding is that the path perturbation is generally replicated at lower levels. This would be masked to the pilot since a variation or oscillation of a fly-up command from say, 200 to 150 microamperes cannot be observed by the pilot. This is due, of course, to the full scale of the pilot's indicator being 150 microamperes.

5.   Width and symmetry indications for a rough path can be expected to vary depending on how the measurement is made. A level cut would be the ·

least desirable means of obtaining a value since it is dependent on determination by identifying two discrete values. If width measurements are made by flying an approach above and below the on-course by 75 microamperes, then these will be subject to similar perturbational influence as seen on course. Appropriate averaging techniques will resolve repeatability problems in a manner similar to when rough terrain is producing problems in path structure.

6. Math models using physical optics predict quite well the behavior of the glide slope with certain specific aircraft parked at specified locations. Deviations with measured values appear to be on the conservative side, i.e., the predictions are for equal or greater perturbations than those observed.

7. The precise position but importantly not the size of the perturbation or peak scallop in space is altered significantly by lateral movement of the reflecting aircraft. That is to say, the effect of the displacement of the reflecting aircraft from the runway centerline is more noticeable in the path structure than a small percentage movement of the target to and from the antennas. This assumes the starting point is out in front of the antennas some 1000 feet such as a typical taxiway might be. Sensitivity is therefore with lateral rather than longitudinal movement of aircraft from the antennas.

8. Positioning of additional airplanes in a taxiway queue does not increase the magnitude of the path perturbations linearly. Because the addition of the signal in space is not simply scalar, but rather phasor type addition, only in very special cases could the perturbation produced by n aircraft be n times that for one. Contributing to this also is the fact that additional aircraft cannot occupy the same real estate. Thus, if the first aircraft is at the worst location for producing path roughness, another aircraft added will produce a lesser effect. The converse must be recognized also, that being if the first aircraft is at an insensitive location, then the second aircraft can contribute more path roughness by being at a more critical location.

9. A test with two medium and two small aircraft parked 1000 feet directly in front of the transmitting antennas as if on an entry taxiway to the ILS runway produced perturbations that were imbedded in the 5 microampere-peak noise in the recording. A Convair 440 parked in the same location produced path perturbations equaling only 50% of Category I tolerance limits.

10. An example of a critical area delineation is given making use of the contour maps to provide the definition for a Category I operation. See figure 1.
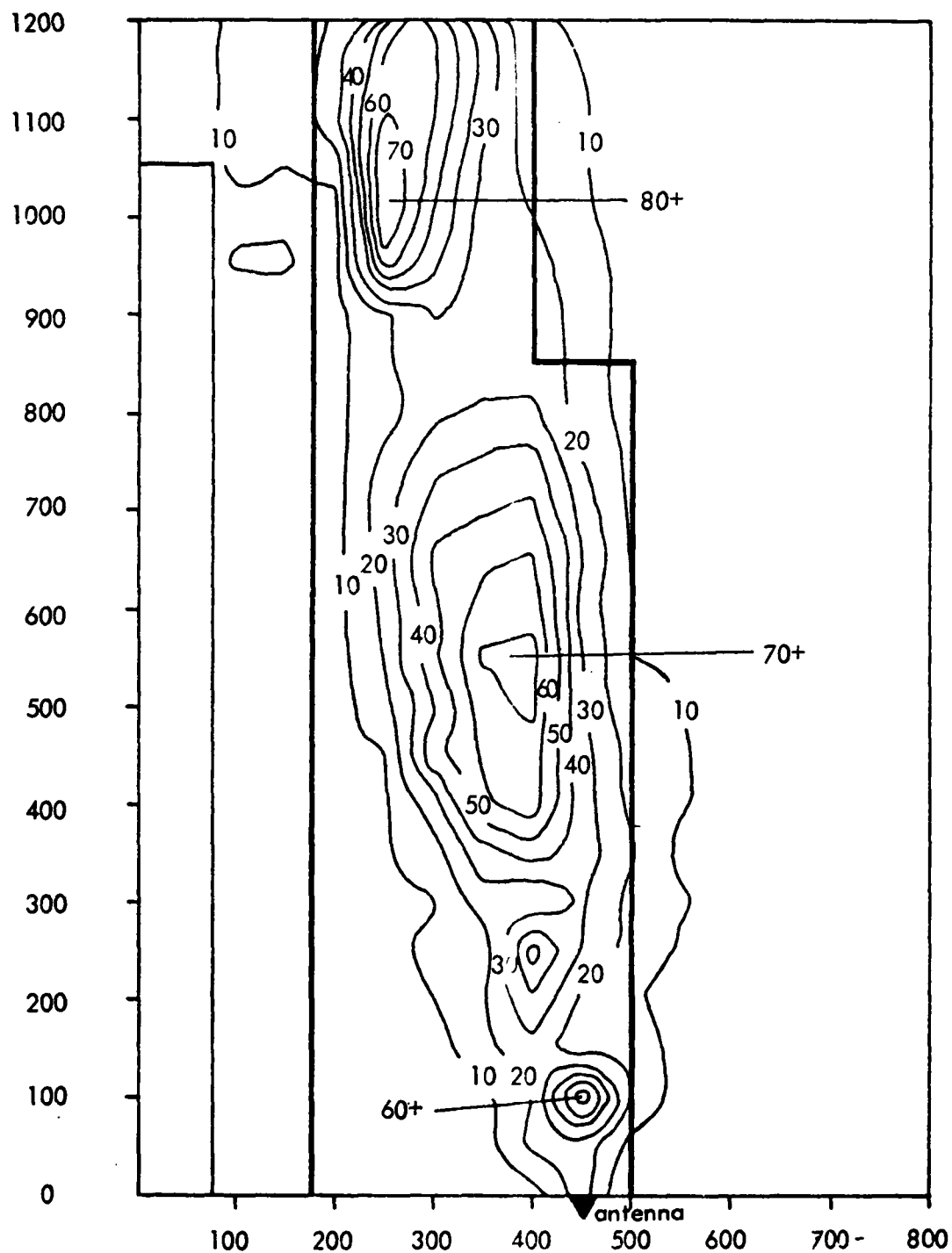
Figure 1. A critical area delineation making use of the contour maps to provide the definition for a Category I operation for a general aviation airport condition. See figure 7 also.

II. INTRODUCTION AND BACKGROUND

The term "critical area" is defined for purposes of this work, as that area which, when aircraft are parked there or are transiting the area, allows significant aberrations in the signals radiated by the specific navigational aid. Significant is taken to mean large, i.e., at least 50% or more of the tolerances for the facility specified in the U.S. Flight Inspection Handbook 8200.1. The navigational aid of particular interest in this investigation is the null-reference, image glide slope, operating with non-directional antennas.

Intuitively, the critical area is the area close to the transmitting antennas. Obviously, large conducting objects placed near any antenna transmitting electromagnetic signals will have some effect on the transmitting system and its radiation patterns.

In recent years aircraft have grown larger and more numerous and this prompted numerous experimental investigations, both in the U. S. and abroad [1][2], to examine the effects of such aircraft near the localizer and glide slope transmitting arrays. In 1974 Ohio University published the first comprehensive work on mathematical modeling of large aircraft near the ILS transmitting antennas which were validated with on-site measurements using the Boeing 747 and the Lockheed C-5A.

It is clear to even the most casual observer that ILS installations are no longer restricted to commercial airports where jumbo jet aircraft are commonly found, but they are serving many general aviation airports as well. These airports typically are not populated with the very large aircraft but do have many aircraft of varying sizes taxiing at any one time. These may, at certain of these airports, move to locations near ILS transmitting facilities. Thus it is necessary to determine what restrictions or what prohibitions should be imposed to insure that the ILS signals in space, serving user aircraft on an approach, are adequate and safe. In other words, what areas should be restricted and what efforts should be made to prevent aircraft from taxiing into the area especially when an aircraft is on an instrument approach. While this question has been addressed in previous work [3] for the case of a single, very large aircraft, the case for smaller aircraft (e.g. typical general aviation type aircraft) and for numbers greater than one have not been studied extensively up to this time.

The intent of this work has been to address these cases of numerous, smaller aircraft that might be expected to exist at a typical general aviation airport served by an ILS. Because the glide slope component of the ILS is the most critical in terms of safety relative to path alignment, structure and width, this investigation has focused exclusively on the glide slope.

The approach to a solution has been along the same lines used in the earlier ILS studies, i.e., produce a mathematical model which will predict the effects of signal scattering from an aircraft and use this model to predict the path characteristics, particularly structure, throughout the

approach zone. To insure accuracy and realism, real world path measurements have been made while general aviation aircraft were parked at specific locations suggested by the calculations as being important and at other locations representative of commonly found taxiway orientations.

The pilot flying an instrument approach using a glide path is critically depending on several characteristics of the path being within certain tolerance values. The path angle should be such that it is flyable (not too steep) and high enough that it affords adequate terrain clearance. Implicit in this statement is that there is sufficient fly-up command signal below path such that there is no information other than full-scale fly-up occurring at elevation angles lower than $\theta - 0.9$ degrees where θ is the path angle. Absent the full-scale fly-up, a flag must occur at the low angles.

Generally, also, irregularities in the on-course structure must be such that they do not cause the pilot or autopilot to adjust inappropriately the descent path to other than the nominal angle minus 7 1/2%. This points to the need to regard the spatial frequency of any path perturbation because short period aberrations or noise will result in only control motion noise which, though undesirable, is in most cases not dangerous. Longer periods produce path following errors which, if path tolerance limits are exceeded, produce undesirable, and in extremes, unsafe conditions.

Presently accepted technical definitions for control motion noise (CMN) and path following error (PFE) can be found in Appendix A.

From an intuitive standpoint the image glide path is particularly sensitive to reflecting obstacles in front of the antenna. Not only is the object capable of producing reflected signal (multipath) which degrades performance, but it also may be capable of disrupting the earth-reflected signal which is essential for the proper path formation. Commonly, the treatment of this reflected energy utilizes optical concepts such as Fresnel zones. However, because precise quantitative predictions are necessary for accurate determination of critical areas, a more elaborate method is required. Investigations of modeling techniques involving aircraft have been performed by Gorman [4], Kwon [5], and Rondini [6]. All of these were successful. Work on modeling techniques for the glide path were also performed by Chin, et al. at the Transportation System Center in the early 1970's [7]. Because of this rich background of material it was possible to prepare quickly a capability for predicting glide slope performance when an obstacle was not only producing blockage of some of the desired ground-reflecting area but was producing classical multipath problems as well.

The basic model for this presentation of technical results is similar to that used by Chin, et al. and by Rondini and McFarland [8] in which critical areas were fundamentally determined in terms of contour maps. These maps were based on calculations and experimental validations. Earlier considerations of critical areas are evident in the FAA Manual on Siting Criteria [9]. This work was accomplished prior to 1971 and involved hand

-86-

calculations. The formulations in the manual, therefore, have not taken into account either the intricacies associated with the complex conducting shapes of aircraft or these later works.

III. OBJECTIVE OF WORK

The specific objective of the work presented in this report has been to identify areas of the earth's surface near the glide slope transmitting antennas which when aircraft are parked therein produce certain quantities of glide path roughness. This identification process consists of using a mathematical model, which has been validated through the use of flight measurements, to predict specific values of path roughness. Given a specific type aircraft, its location, and orientation, specific path roughness in space will occur with a null reference glide slope antenna system. Of interest is the magnitude of the roughness and its location. By considering the maximum value for a specific ILS zone [10] or for the entire approach path, a scalar value can be determined and related to the point where the aircraft is located.

Numerical values can thus be determined for a grid of points in the area of interest and these constitute a scalar field for which a set of contours can be drawn. Because flight inspection path structure tolerances are given in microampere units, the contour lines are therefore constructed isopleths in units of microamperes for convenience. Therefore, if one wishes to consider what an aircraft placed in a certain location with a certain orientation will produce in terms of maximum path perturbation, one can search out the appropriate page from the contour maps, hypothetically place the aircraft on the map and read directly the maximum value that this aircraft placement would produce for an aircraft making an approach through the particular zone.

If an airport designer wants to consider where to place hold lines, he first determines the maximum allowable path irregularity for the path in space, notes the orientation of taxiways and from the maximum allowable contour lines places the hold sign at that point on the taxiway. The assumption will be that an aircraft will not be perpendicular to the taxiway.

The final objective is to be able to define a critical area, especially with respect to taxiways so that it may be identified clearly for pilots thus allowing them and the air traffic controllers to take appropriate holding and restructive actions which will prevent path anomalies from occurring in space which are in fact out of tolerance path conditions.

IV. APPROACH TO SOLUTION

Clearly, there are an infinite number of points that could be considered for aircraft placement. To make the problem tractable the area for placement is broken into a grid and a value determined for each element of the grid. The area of principal interest is in front of the transmitting array. The glide-slope array is assumed to have bent-dipole antennas such that a conservative critical area would be determined, i.e., there would be no particular antenna type for which great protection would be needed. Because of the several parameters involved, it is important to specify them for case considerations. They are:

1. Aircraft type. This implies size, shape and, in particular, height and size of the tail.

2. Orientation of aircraft. This involves the two discrete cases of the reflecting aircraft being parked either parallel or perpendicular to the runway centerline. For the perpendicular case with the glide slope the tail end of the aircraft is always taken to be further from the runway.

3. Number of aircraft. Consideration is given to the effects on path structure of a plurality of aircraft in the vicinity of a grid point.

4. ILS Zone of interest. Predictions are made with respect to specific ILS Zones, viz, 1, 2 and 3 [11]. Since different tolerances are sometimes applied for different zones, this distinction is considered desirable. There is no consideration given to Zone One because of the small effects expected and its distance of greater than four miles from the airport.

V. MATHEMATICAL MODEL DESCRIPTION

Mathematical modeling of ILS systems has long been recognized as a useful tool in the siting of localizer and glide slope systems. In addition, the previous critical area tasks performed at Ohio University in 1974 utilized both localizer and glide slope models to compute the effects of aircraft located near the radiating systems. The current computational effort has been completed through the use of an updated version of the 1974 model used by Rondini [12] and earlier by Chin et.al. [13]. The following is a description of this model.

This model operates using the physical optics principles by considering the aircraft as a target or reflector. This type of object can be satisfactorily modeled by considering it as a collection of flat plates, whose profile is that of the specific aircraft. Experimental evidence obtained previously [14] demonstrates this fact. A flat plate which has been found to adequately represent the aircraft is assumed to be perfectly conducting and located with a specified orientation at a specific location on the airdrome, i.e., in the space through which the glide slope signals are propagating.

The flat plate may be divided up into arbitrarily small areas, each of which is receiving incident electromagnetic radiation from the glide slope transmitting antennas. The incident signals arrive at the respective incremental area with a specific amplitude and phase. These are dependent on the phase and amplitude of the source currents in the glide slope antennas and the path length from the antennas to the incremental area on the plate. The fields are in effect terminated by currents in the conducting surface so that the boundary conditions at the conducting surface are met. These currents flowing in the incrementatal plate thus become source currents for the scattering signal. Boundary conditions are imposed by the structure itself.

The predicted radiation is calculated assuming an array of incremental, flat-plate antennas each with its own radiation pattern. There is radiation which takes place to some extent in most all directions. An integration or summation of the contributions in the form of radiation produced by the incremental plates is accomplished and summed with direct and image-produced radiation from the glide slope.

This physical optics approach while requiring a large number of computations can be made to represent the real world radiation patterns quite well. Each point of interest in space, usually taken as a locus in a straight line out from the glide slope at 3 degrees on the localizer centerline requires a calculation of the difference in depth of modulation. Another calculation follows to determine the course deviation indication in microamperes as seen by the pilot. The result is that obtained from the superposition of all signals arriving at the point the aircraft occupies in space. Points are taken each 50 feet to form the locus.

It is important to note that antenna offsets and positioning are automatically taken into account through the calculational process. One must be careful in the practical validation work to insure that the antennas are indeed where they are taken to be for the calculation. A slight tilt in the tower could reposition the upper antenna several electrical degrees from where the calculation assumed it to be and one would then suffer the inconsistency in the comparison of calculated and measured data even though all considerations except the antenna locations had been taken into account.

The plates representing the aircraft may be placed either parallel, perpendicular, or at other required angles which might be required to represent taxiway locations. The height of the aircraft above ground level may also be taken into account.

Some limitations do exist with this particular model; however, the resultant errors due to these limitations or assumptions are very small. One limitation in the model is that only reradiation from the target aircraft is considered. No interaction between the reflectors is taken into account (i.e., the effects of the multiple reflectors are summed together). Another limitation is the assumption that the terrain is level and perfectly smooth. This suggests that some means of subtracting out terrain effects is appropriate when making model and measured data comparisons.

VI. CALCULATION WORK

The final product of this work is intended to be a set of contour maps which can be generally applied to any airport and any taxiway complex for the purpose of delineating critical areas. Preparation of these contour maps requires many data points. Because of the expense of collecting experimental data, a calculational approach has been found to be the most efficient and effective. In this section the results of using the mathematical model discussed in section V are presented. Calculations are performed which give a description of the glide-slope structure for conditions of one or more aircraft parked in various positions in front of the glide-slope transmitting antennas.

Once a calculation has been performed maximum values of the path deviation or perturbation can be ascertained either by inspection from the plot or by the computer for which software has been written to determine maximum values.

Because tolerances are specified as a function of distance from the threshold, i.e., ILS zones, analyses for maximum values have been accomplished based on the range, viz., ILS Zone 2 (range from runway threshold 3500 feet to 24,300 feet); first section of ILS Zone 3 applied to Cat I qualifications (range approximately 900 feet to 3500 feet) and finally the second section of Zone 3 (threshold to approximately 900 feet range).

The approach has been to take a grid of points in front of the antennas amounting to as many as 240 points and develop a scalar field of values from the calculations. This allows a contour map to be drawn. Specifications for the map then are type of aircraft, number of aircraft and the ILS zone of interest, each zone having different specifications on tolerance given by 0 AP 8200.1.

The first work involved a single Piper PA28 Cherokee Arrow. Structures were plotted for 240 locations of this aircraft. Samples of these plots can be found in figures in the following sections where comparisons are made with the measured data.

Figure 2 shows the grid for the 240 points. Each of these points will have associated with it that maximum perturbations for one of the three zones of interest.

In addition to the consideration of the small Piper PA28 Cherokee-type aircraft similar calculations were performed for larger aircraft viz, Rockwell Aero Commander AC-6T which can be regarded as a medium-size general aviation type aircraft and a Convair 440 (CV-44) which represents a large general aviation aircraft. Finally, to examine the effects of multiple aircraft parked in areas which might affect glide slope performance the condition for four aircraft in the field is examined.

Examples of the results of the calculations for determining effects on the total glide path structure are given in the figures contained in the next section on comparisons.

aircraft orientation and outline

X
└─ -Y

Threshold

20 40 60 80 100 120 140 160 180 200 220 240

1000
900
800
700
600
500
400
300
200
100
0

GPI, RPI
0,0,0

+

1   21   41   61   81   101 121 141 161 181 201 221
                                      +

0   50 100 150 200 250 300 350 400 450 500 550 600
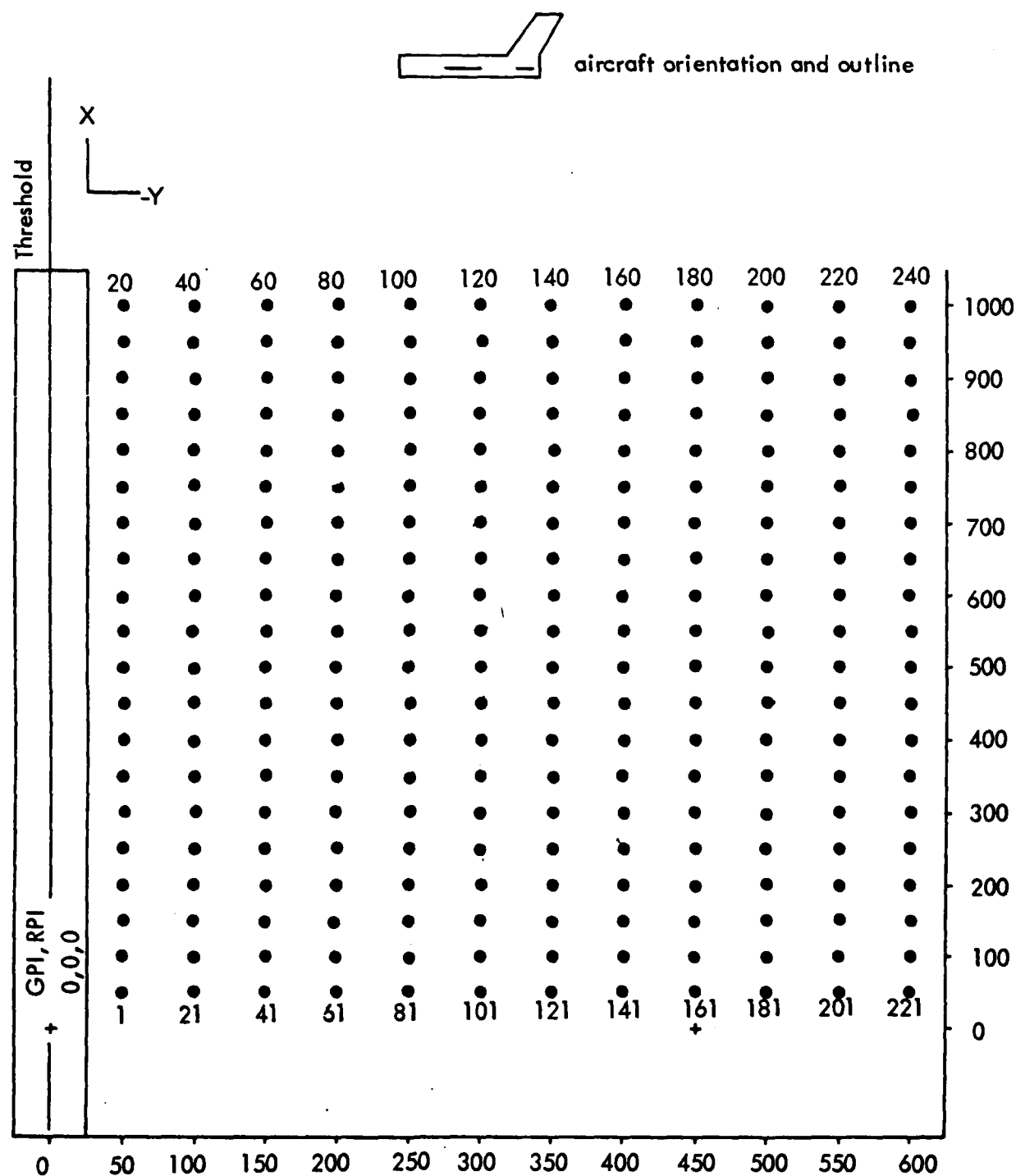
Figure 2. Definition of grid points which define the locations for placing the center of the reflecting aircraft used in producing the perturbations in the glide path structure. Final calculations produced a single number at each point representing the maximum perturbation in a given ILS zone. These became the values because the scalar field were the basis for the contour plots.

The contour maps which have been generated through the multitude of calculations follow. In general, the appearance is what one might expect from intuition. The smaller the aircraft, the smaller the perturbation, for example. In fact, the perturbations produced by the Piper PA 28 are really of no concern for operational purposes.

Following are 24 (figures 3 - 26) contour maps which can be duplicated by a user to produce a transparent overlay. This overlay can be used with a map of the same scale to identify specific locations where hold lines or signs should be placed near the taxiway to prevent aircraft from entering the critical areas. The contour maps are organized as follows.

Large General Aviation Aircraft (Convair 440)
Orientation parallel To Runway
ILS Zone 2
ILS Zone 3 (Pt. B to Pt. C.)
ILS Zone 3 (Pt. C to Threshold)

Orientation perpendicular to Runway
ILS Zone 2
ILS Zone 3 (Pt. B. to Pt. C.)
ILS Zone 3 (Pt. C. to Threshold)

Medium-Size General Aviation Aircraft (Rockwell Commander AC-6T)
Orientation parallel to Runway
ILS Zone 2
ILS Zone 3 (Pt. B to Pt. C)
ILS Zone 3 (Pt. C to Threshold)

Orientation perpendicular to Runway
ILS Zone 2
ILS Zone 3 (Pt. B to Pt. C)
ILS Zone 3 (Pt. C to Threshold)

Small General Aviation Aircraft (Piper Cherokee PA-28)
Orientation parallel to Runway
ILS Zone 2
ILS Zone 3 (Pt. B to Pt. C)
ILS Zone 3 (Pt. C to Threshold)
Orientation perpendicular to Runway
ILS Zone 2
ILS Zone 3 (Pt. B to Pt. C)
ILS Zone 3 (Pt. C to Threshold)

Plurality of General Aviation Aircraft (Four)
(Rockwell Commander AC-6T, Beechcraft King Air
BE-90, Two Piper Cherokee PA-28)
Orientation parallel to Runway
ILS Zone 2
ILS Zone 3 (Pt. B to Pt. C)
ILS Zone 3 (Pt. C to Threshold)
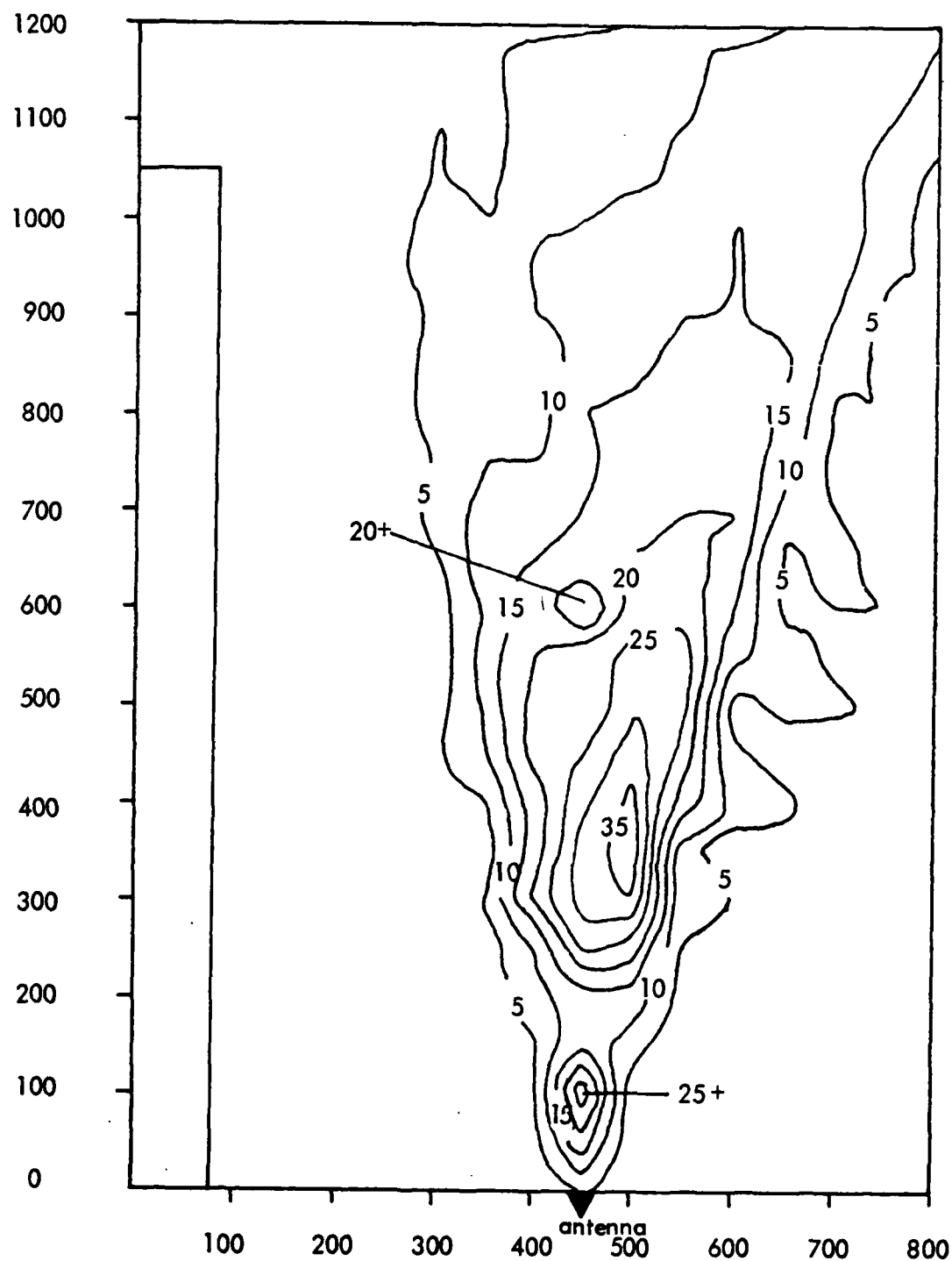
Figure 3. Contours of maximum values of CDI produced in ILS Zone 2 for a large general aviation type aircraft, specifically a Convair 440, parked parallel to the runway.

Figure 4. Contours of maximum values of CDI produced in ILS Zone 3
to point C for a large, general aviation type aircraft,
specifically a Convair 440, parked parallel to the runway.

Figure 5. Contours of maximum values of CDI produced in ILS Zone 3
to the threshold for a large, general aviation type aircraft,
specifically a Convair 440, parked parallel to the runway.
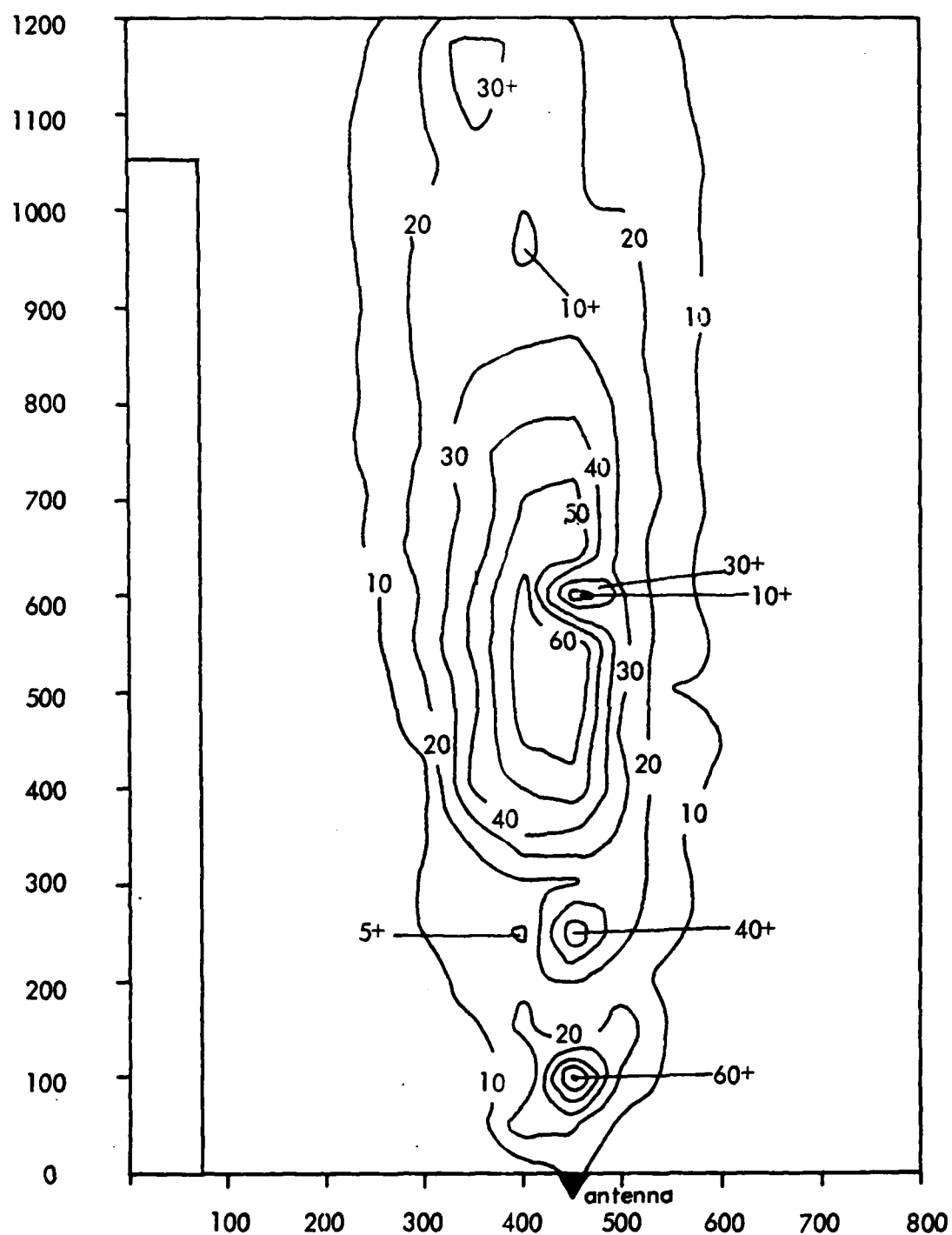
Figure 6. Contours of maximum values of CDI produced in ILS Zone 2
for large, general aviation type aircraft, specifically a
Convair 440, parked perpendicular to the runway.

Figure 7. Contours of maximum values of CDI produced in ILS Zone 3 to point C for a large, general aviation type aircraft, specifically a Convair 440, parked perpendicular to the runway.

Figure 8. Contours of maximum values of CDI produced in ILS Zone 3 to the threshold for a large, general aviation type aircraft, specifically a Convair 440, parked perpendicular to the runway.

Figure 9. Contours of maximum values of CDI produced in ILS Zone 2
for medium, general aviation type aircraft, specifically a
Rockwell Commander, parked parallel to the runway.

Figure 10. Contours of maximum values of CDI produced in ILS Zone 3 to point C for a medium, general aviation type aircraft, specifically a Rockwell Commander, parked parallel to the runway.

-102-

Figure 11. Contours of maximum values of CDI produced in ILS Zone 3 to the threshold for a medium, general aviation type aircraft, specifically a Rockwell Commander, parked parallel to the runway.

Figure 12. Contours of maximum values of CDI produced in ILS Zone 2 for a medium, general aviation type aircraft, specifically a Rockwell Commander, parked perpendicular to the runway.

Figure 13. Contours of maximum values of CDI produced in ILS Zone 3 to point C for a medium, general aviation type aircraft, specifically a Rockwell Commander, parked perpendicular to the runway.

Figure 14. Contours of maximum values of CDI produced in ILS Zone 3 to the threshold for a medium, general aviation type aircraft, specifically a Rockwell Commander, parked perpendicular to the runway.
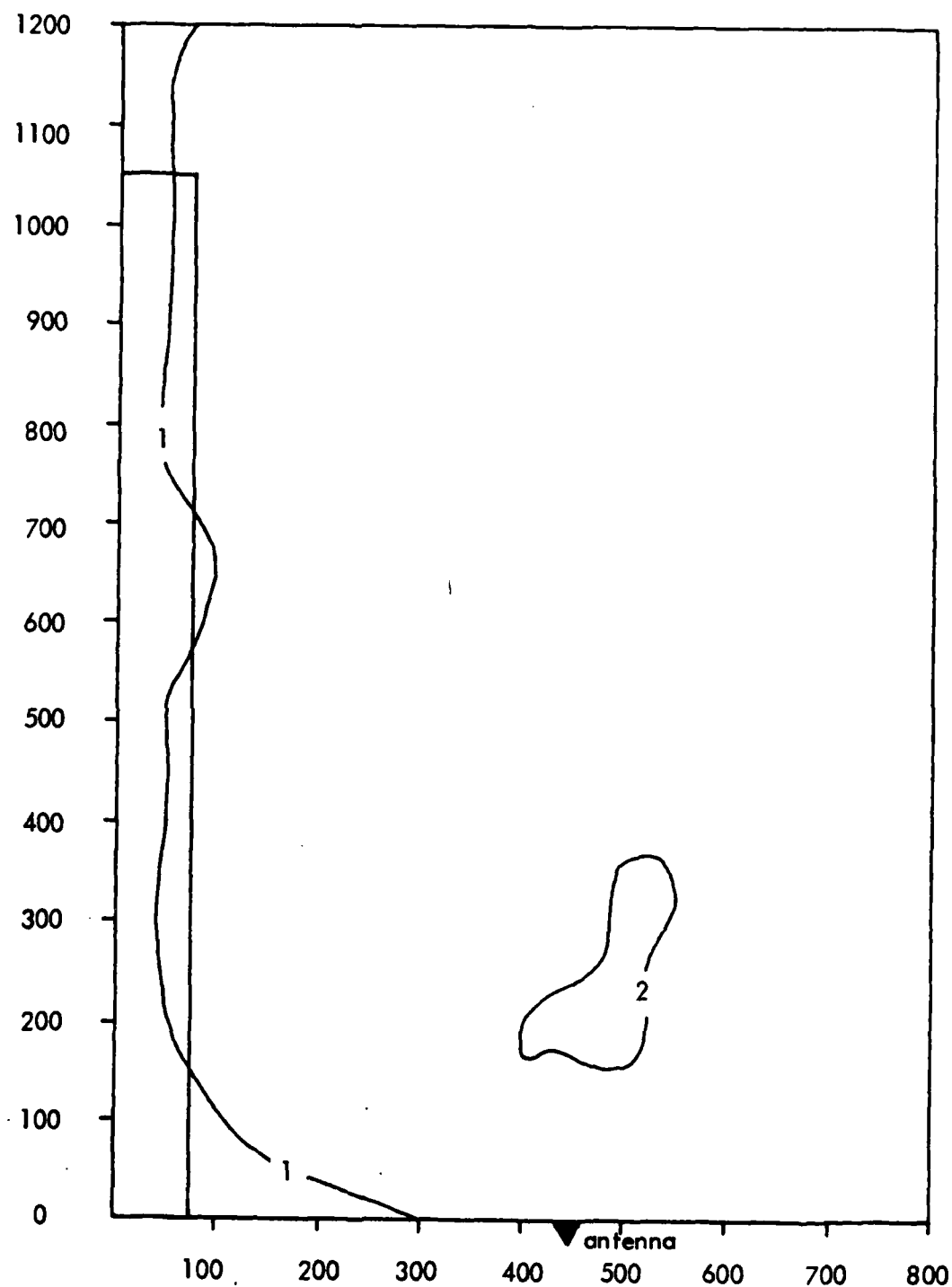
Figure 15. Contours of maximum values of CDI produced in ILS Zone 2 for small aircraft, specifically a Piper Cherokee, parked parallel to the runway.
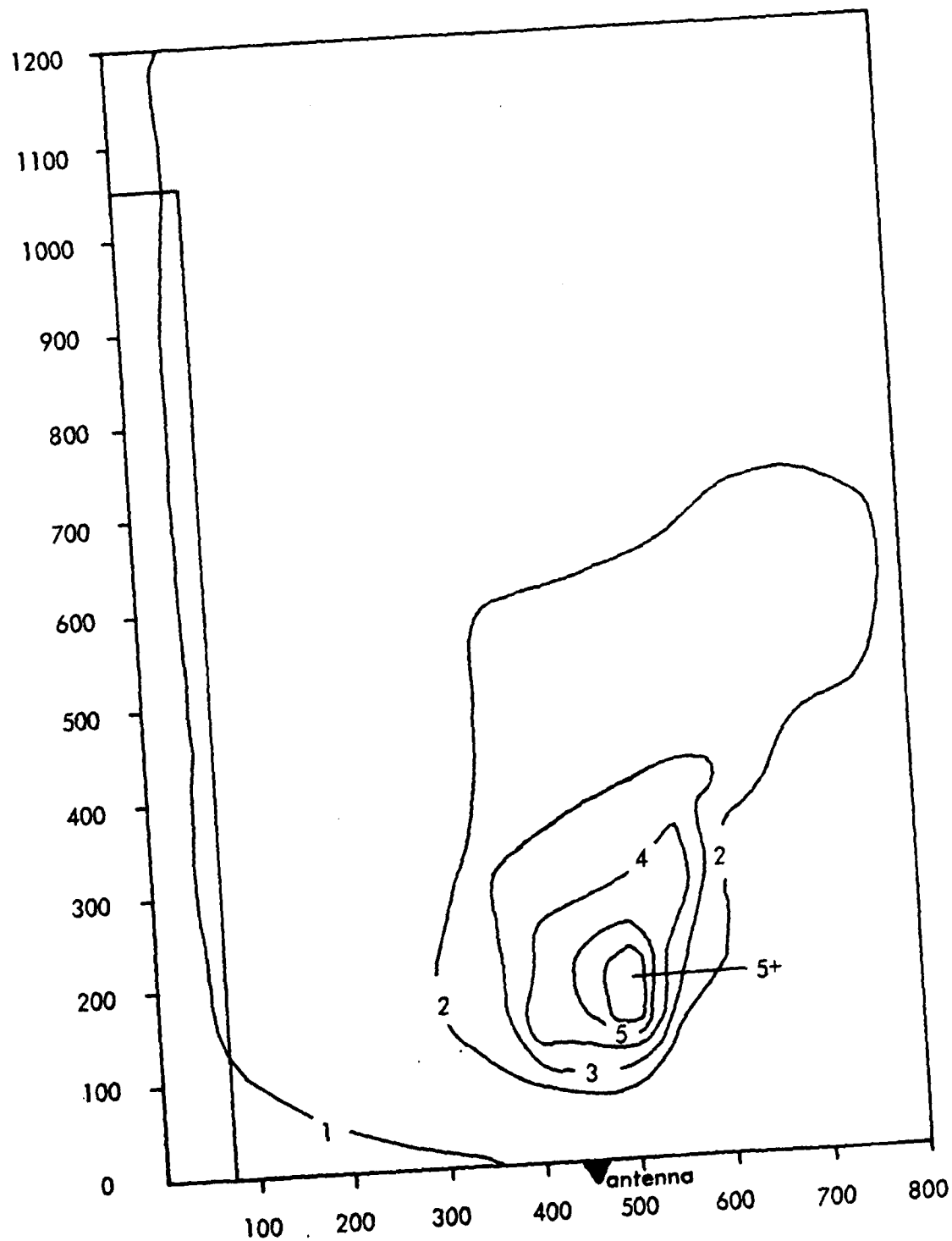
Figure 16. Contours of maximum values of CDI produced in ILS Zone 3 to point C for small aircraft, specifically a Piper Cherokee, parked parallel to the runway.
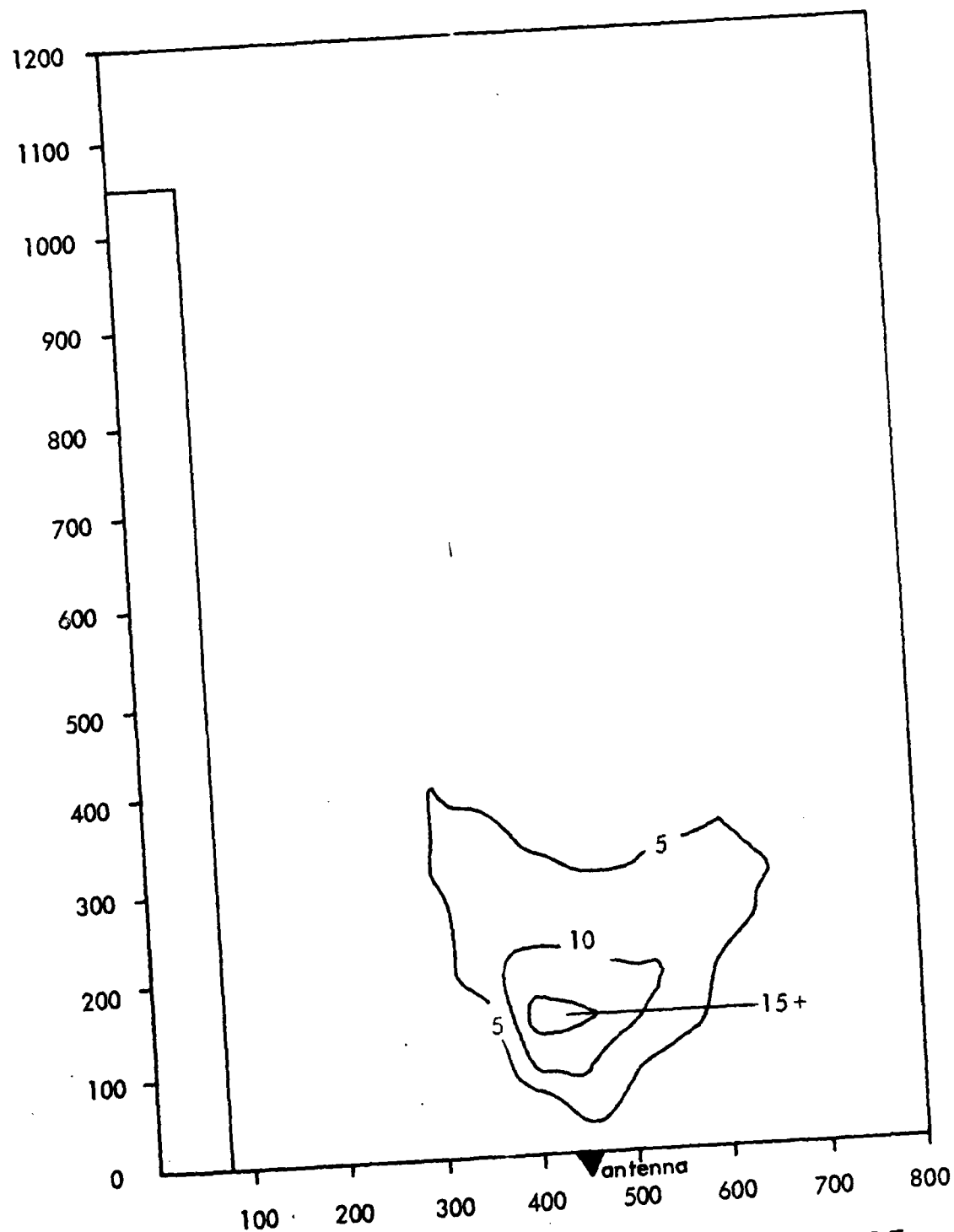
Figure 17. Contours of maximum values of CDI produced in ILS Zone 3 to the threshold for small aircraft, specifically a Piper Cherokee, parked parallel to the runway.
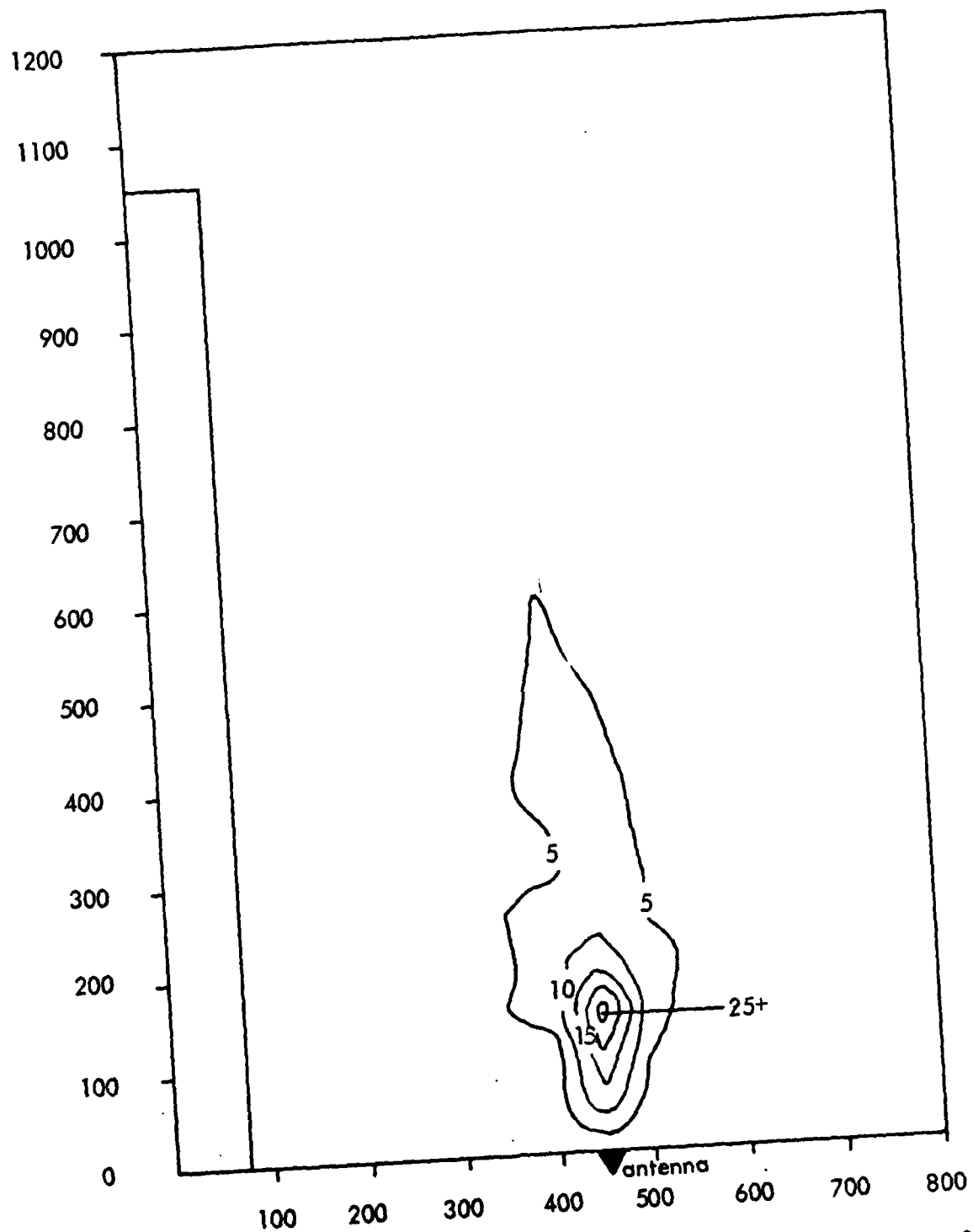
Figure 18. Contours of maximum values of CDI produced in ILS Zone 2 for small aircraft, specifically a Piper Cherokee, parked perpendicular to the runway.
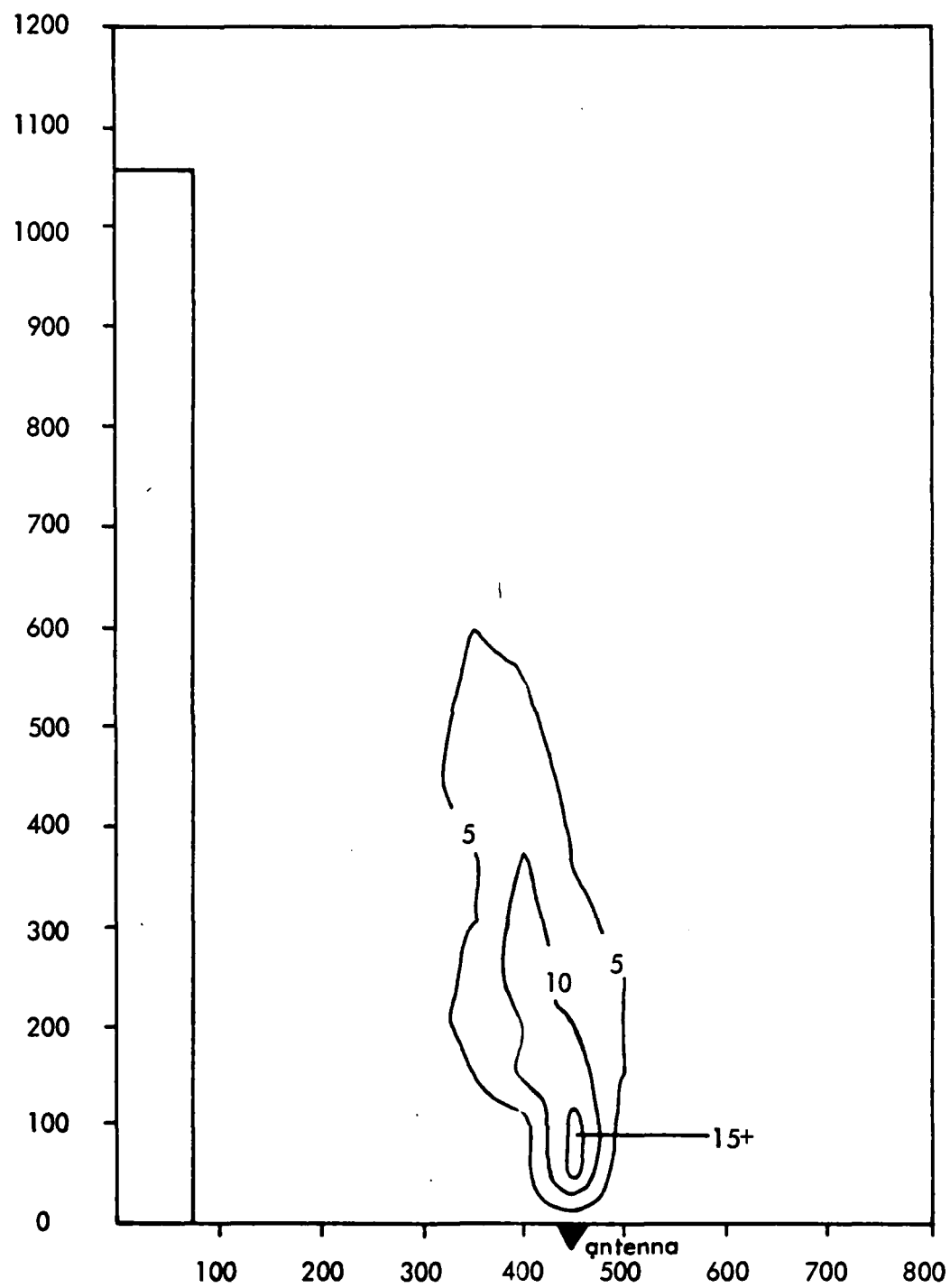
Figure 19. Contours of maximum values of CDI produced in ILS Zone 3
to point C for small aircraft, specifically a Piper Cherokee,
parked perpendicular to the runway.
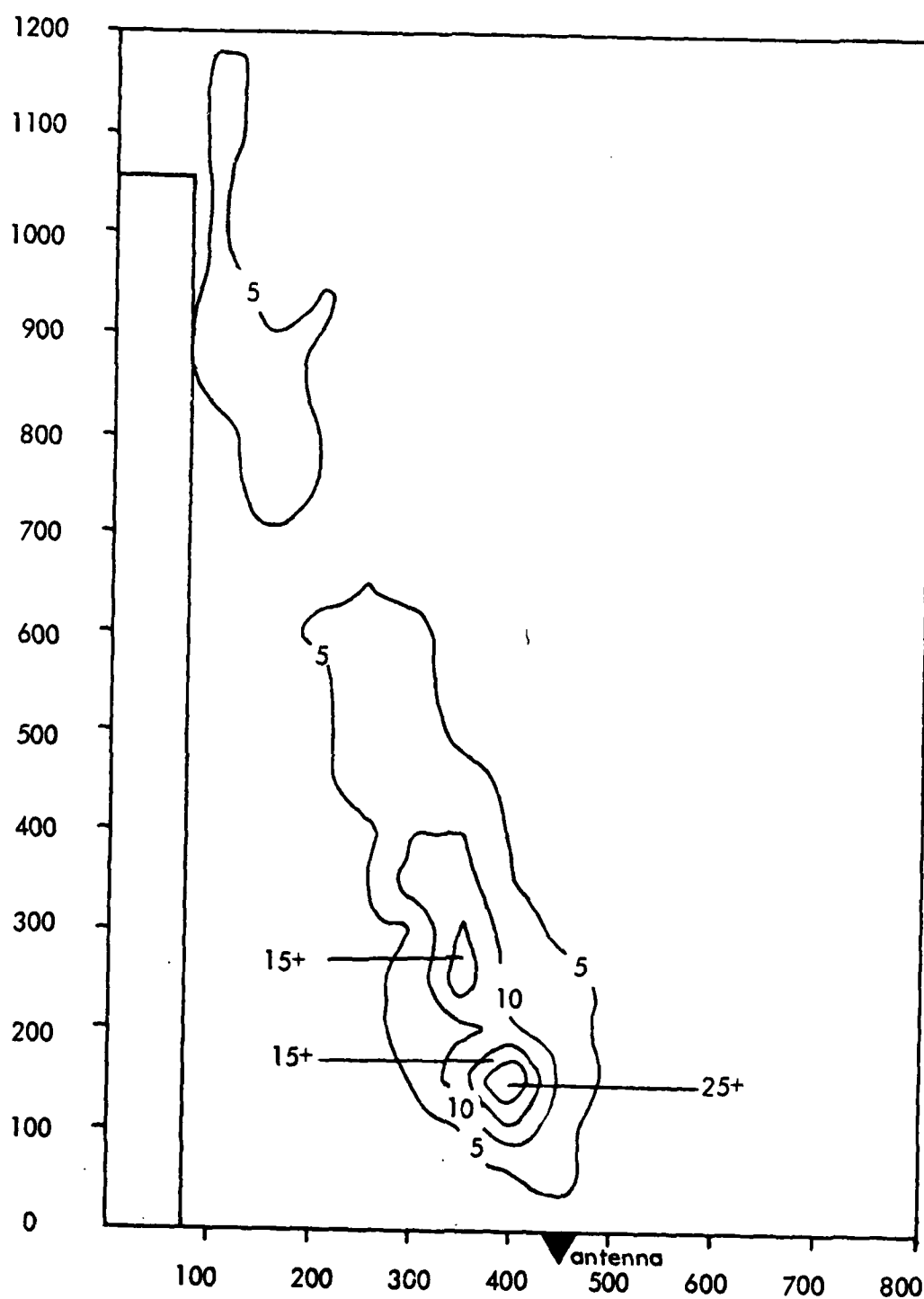
Figure 20. Contours of maximum values of CDI produced in ILS Zone 3 to the threshold for small aircraft, specifically a Piper Cherokee, parked perpendicular to the runway.
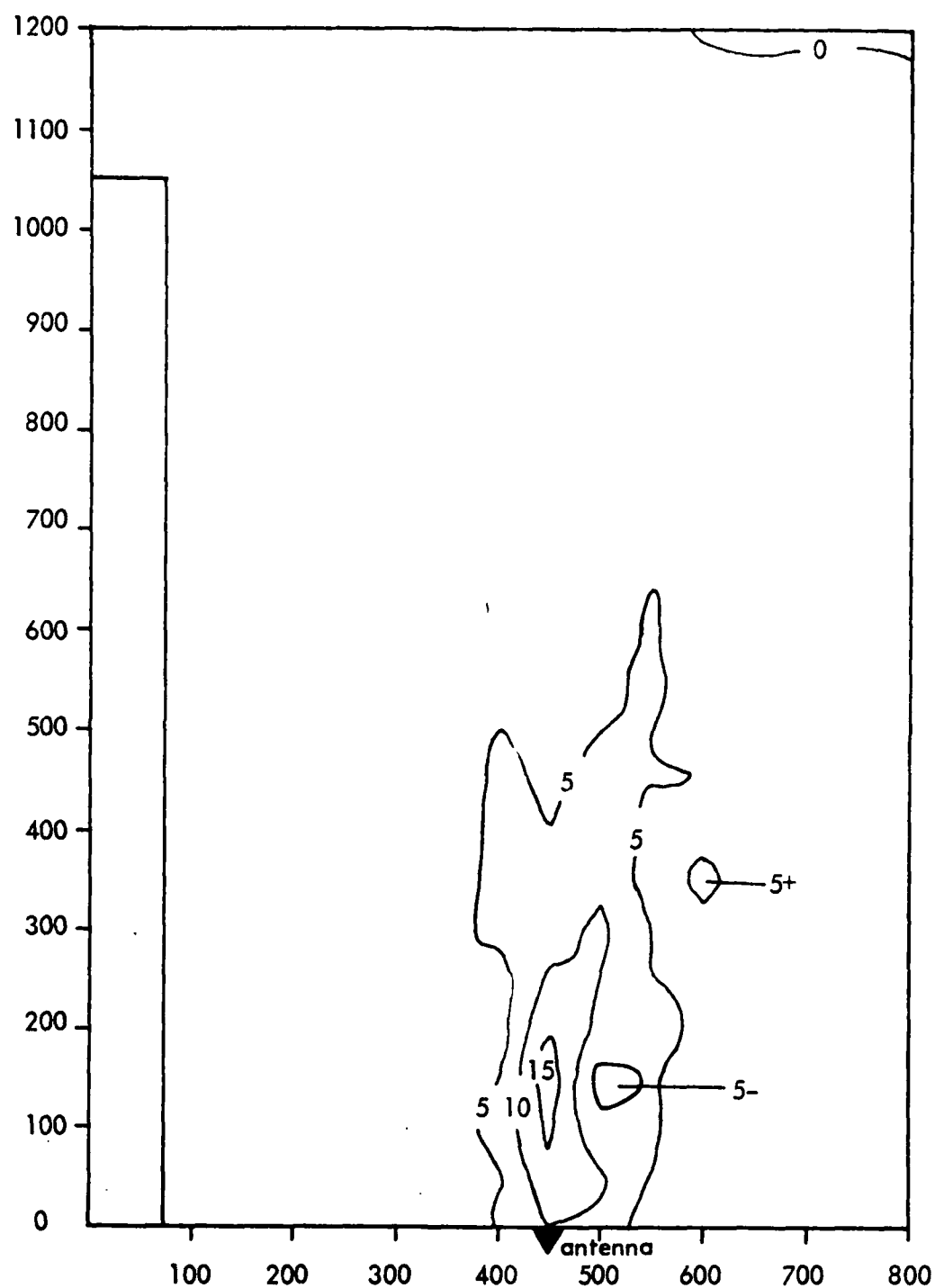
Figure 21. Contours of maximum values of CDI produced in ILS Zone 2 for four general aviation type aircraft, specifically a Rockwell Commander, Beechcraft King Air and 2 Piper Cherokees, all in trail, aligned parallel to the runway.
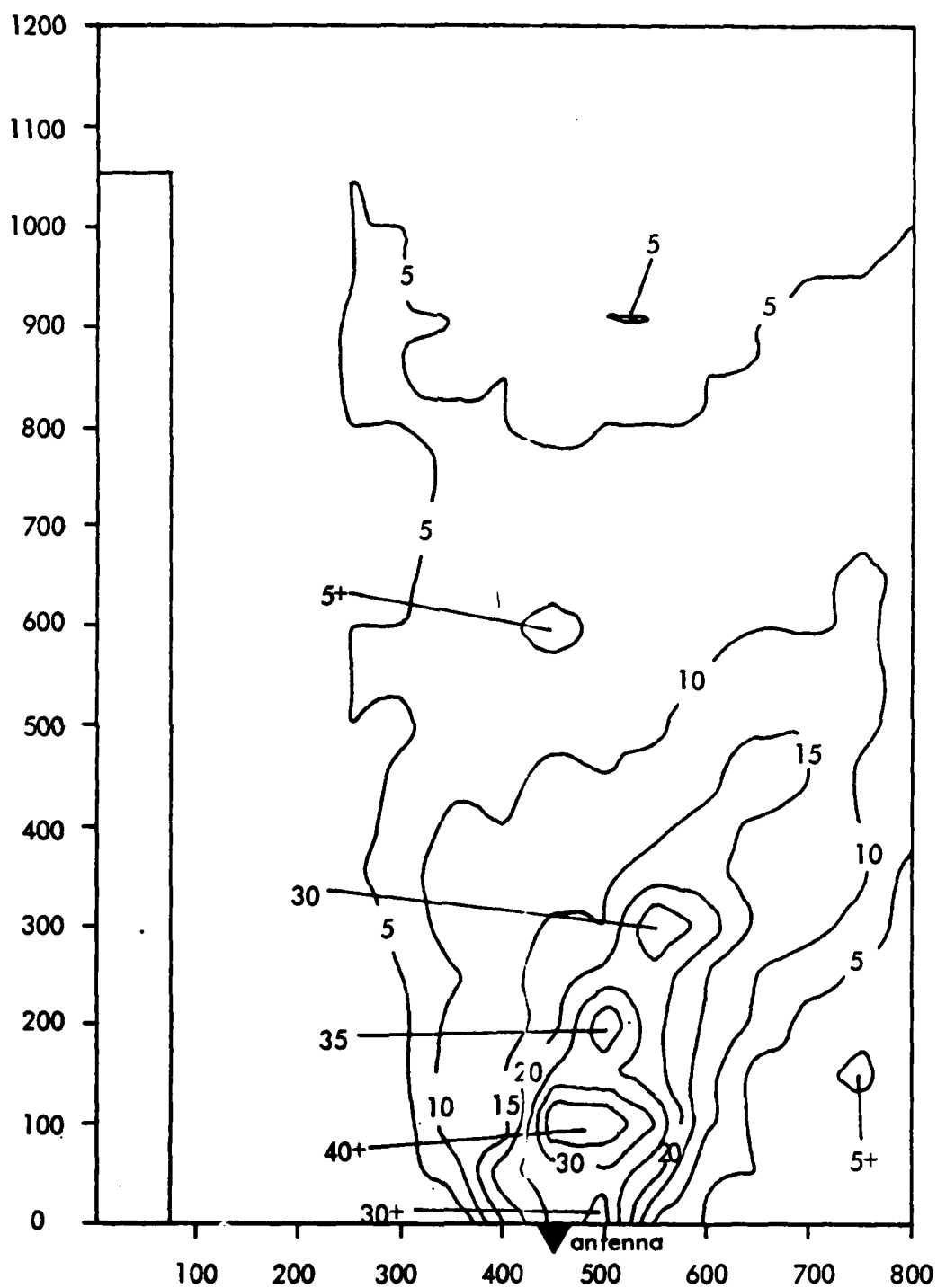
Figure 22. Contours of maximum values of CDI produced in ILS Zone 3 to point C for four general aviation type aircraft, specifically a Rockwell Commander, Beechcraft King Air and 2 Piper Cherokees, all in trail, aligned parallel to the runway.

-114-

Figure 23. Contours of maximum values of CDI produced in ILS Zone 3
to the threshold for four general aviation type aircraft, specifi-
cally a Rockwell Commander, Beechcraft King Air and 2 Piper
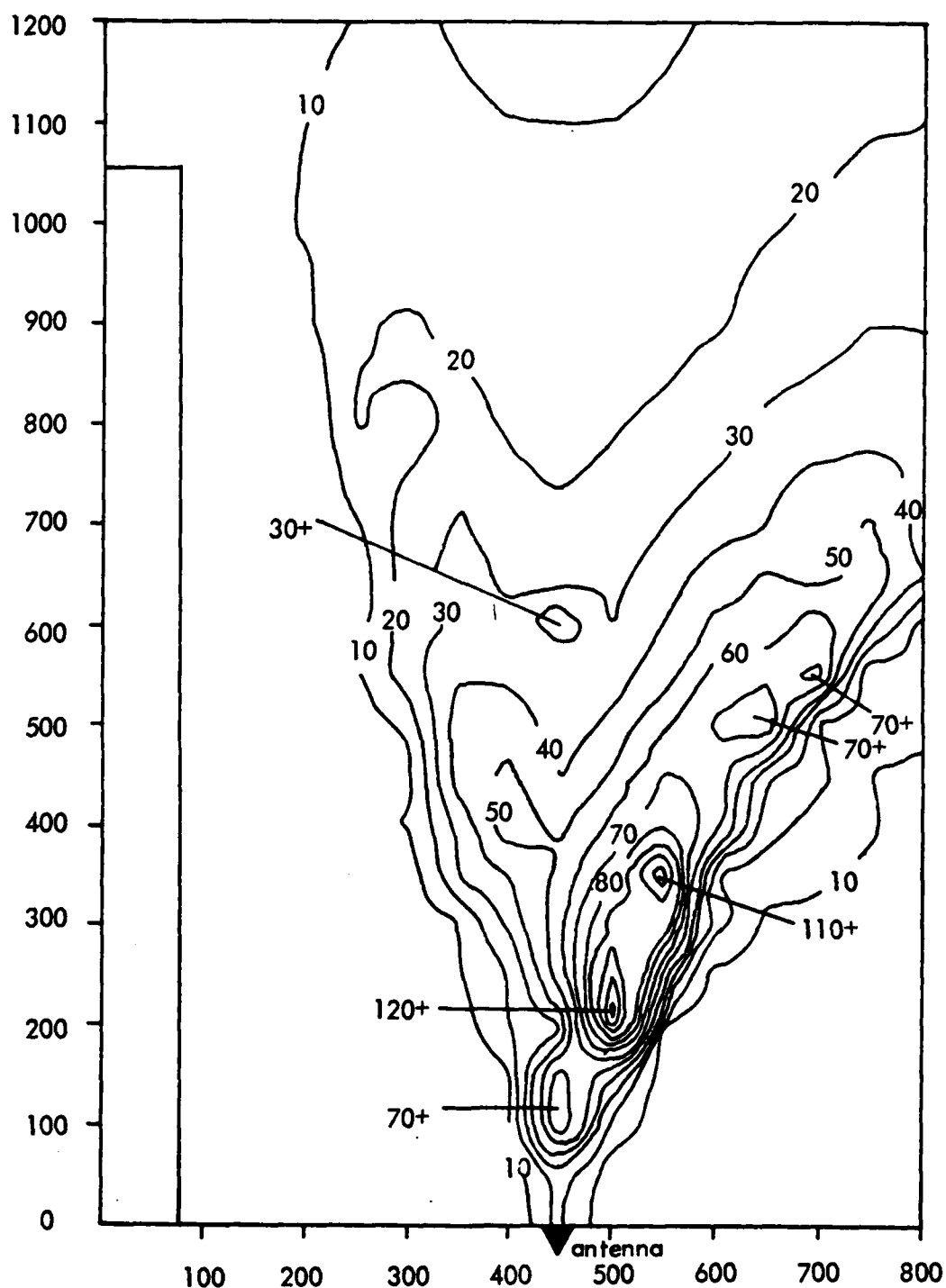Cherokees, all in trail, aligned parallel to the runway.
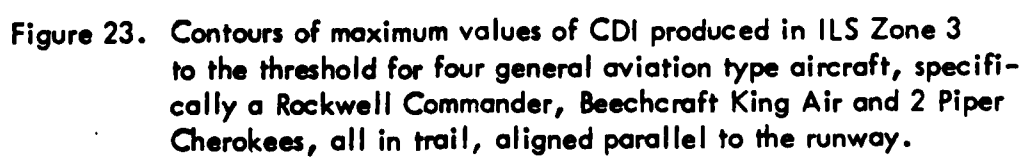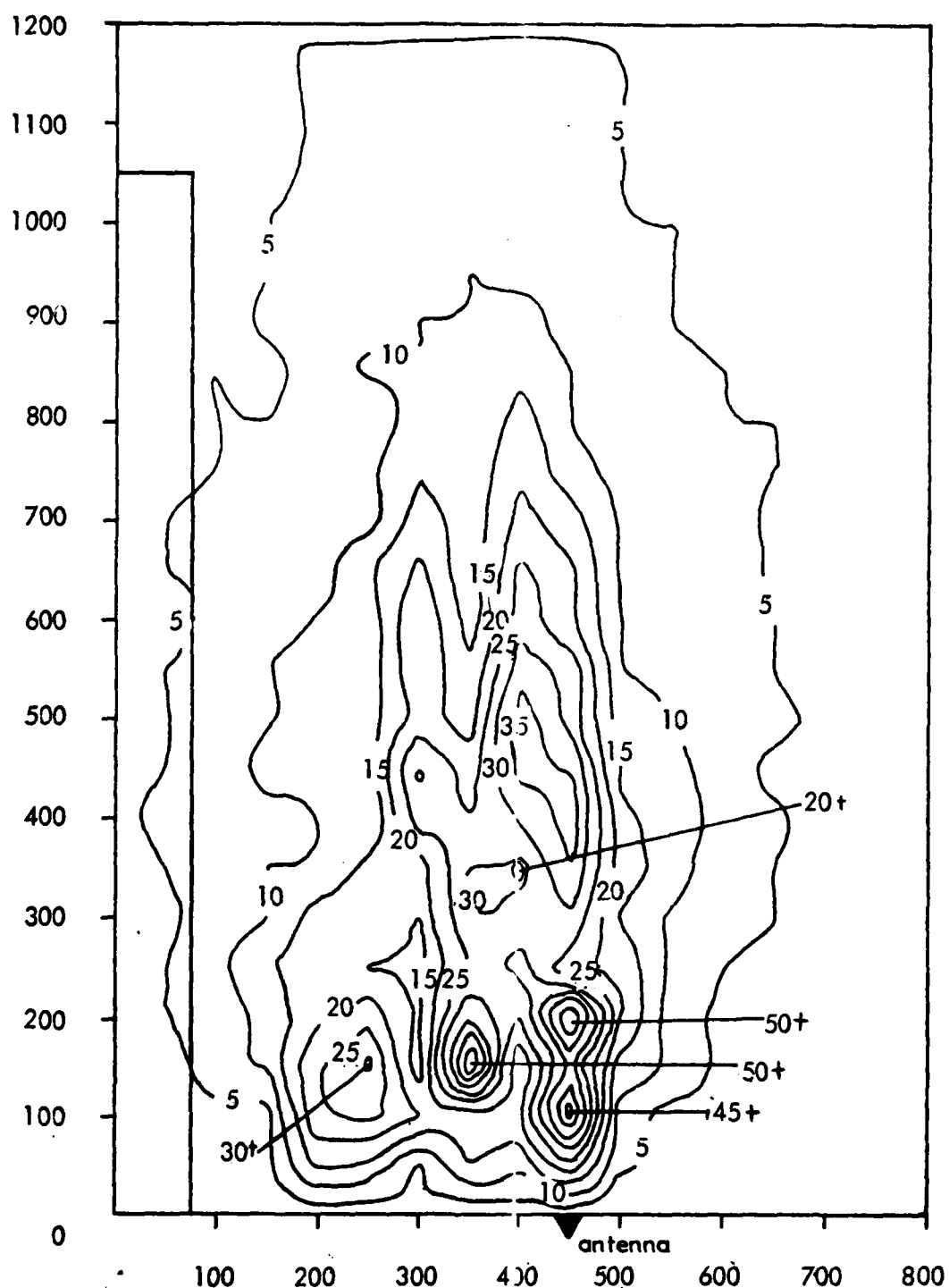
Figure 24. Contours of maximum values of CDI produced in ILS Zone
2 for four general aviation type aircraft, specifically
a Rockwell Commancer, Beechcraft King Air and 2 Piper
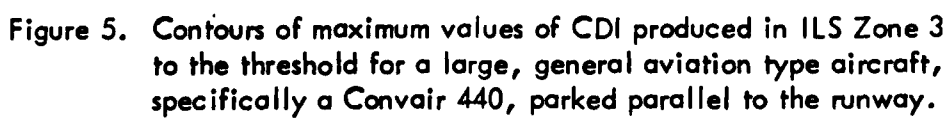Cherokees, all in trail, aligned perpendicular to the
runway.
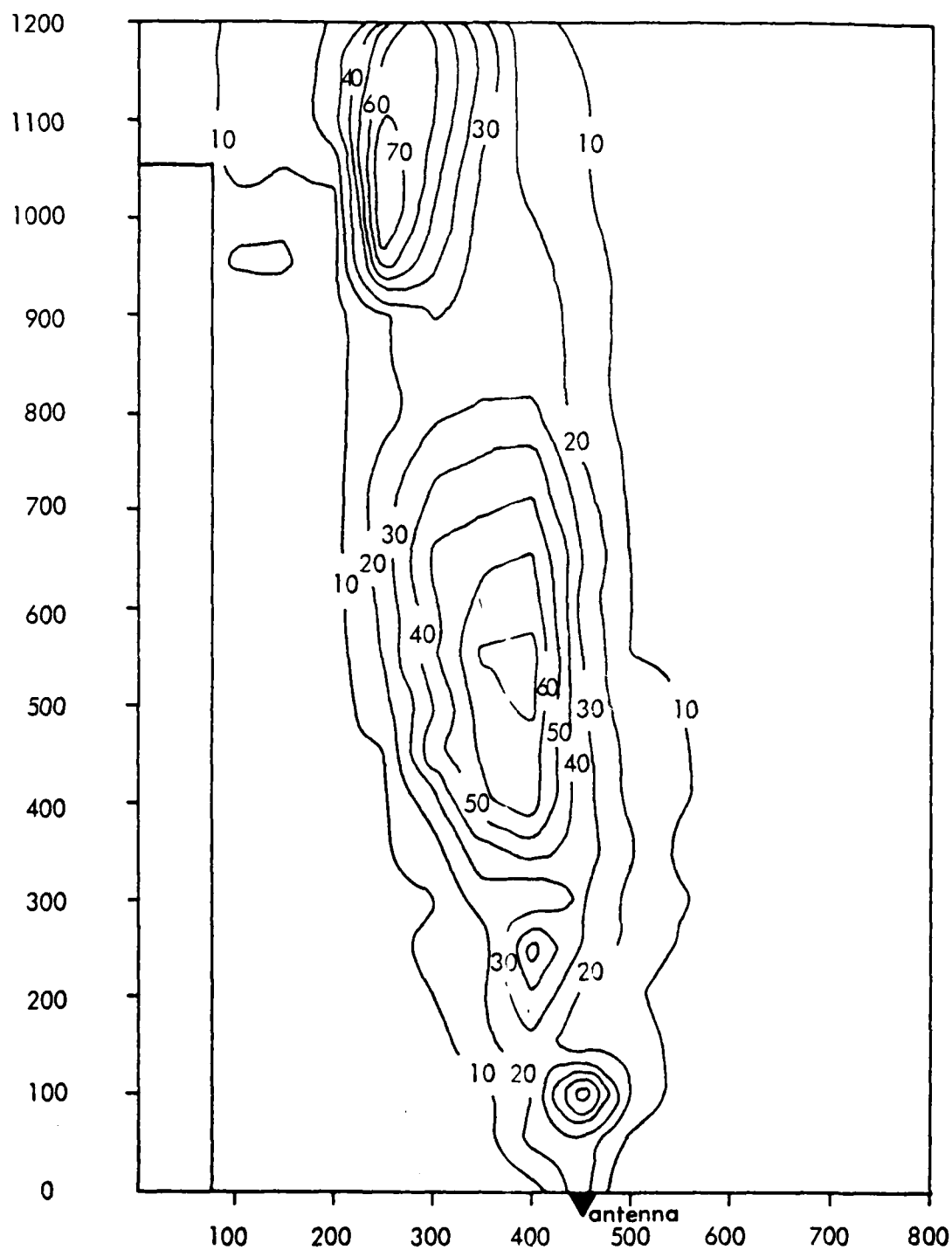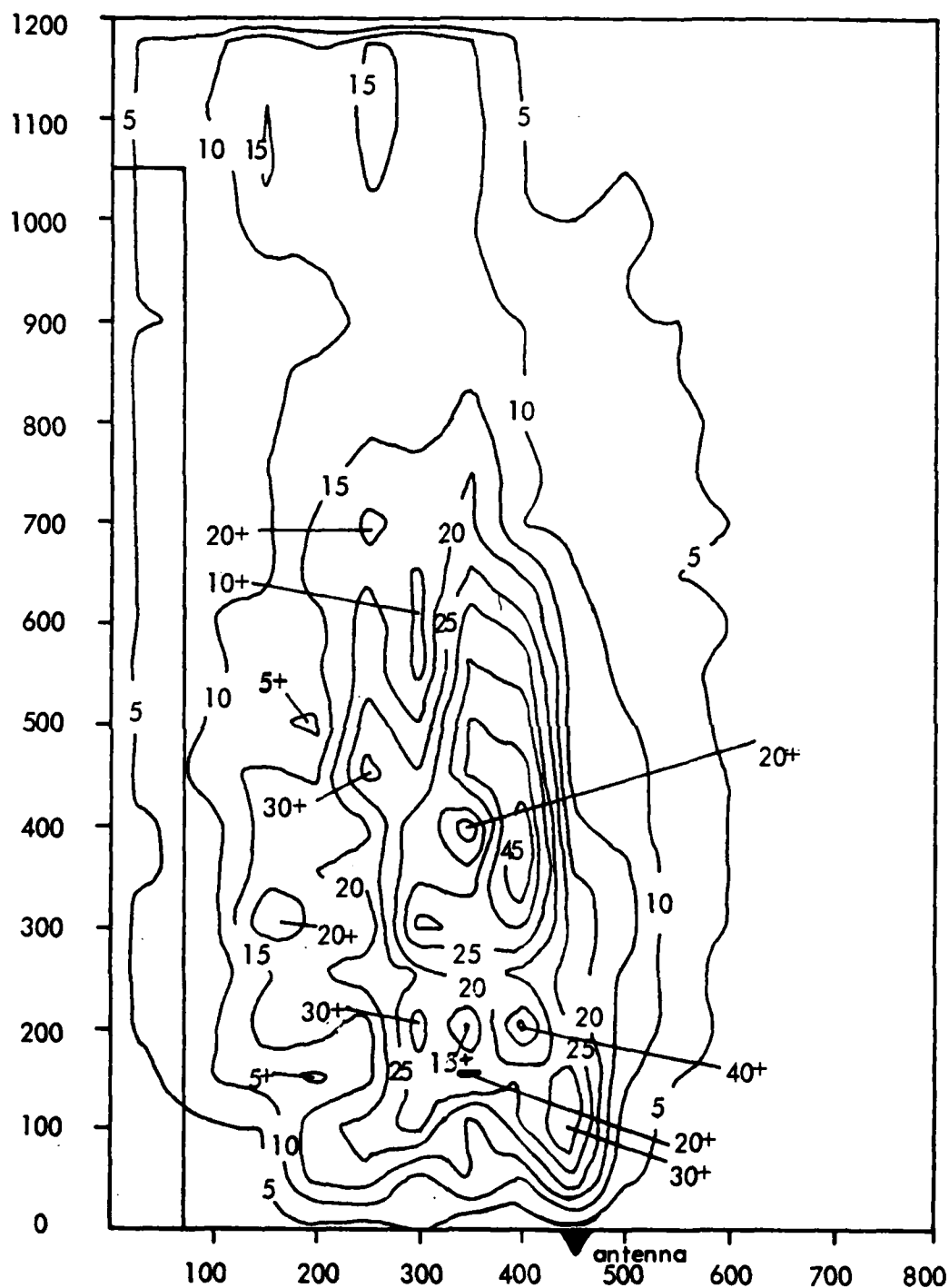
Figure 25. Contours of maximum values of CDI produced in ILS Zone 3 to point C for four general aviation type aircraft, specifically a Rockwell Commander, Beechcraft King Air and 2 Piper Cherokees, all in trail, aligned perpendicular to the runway.
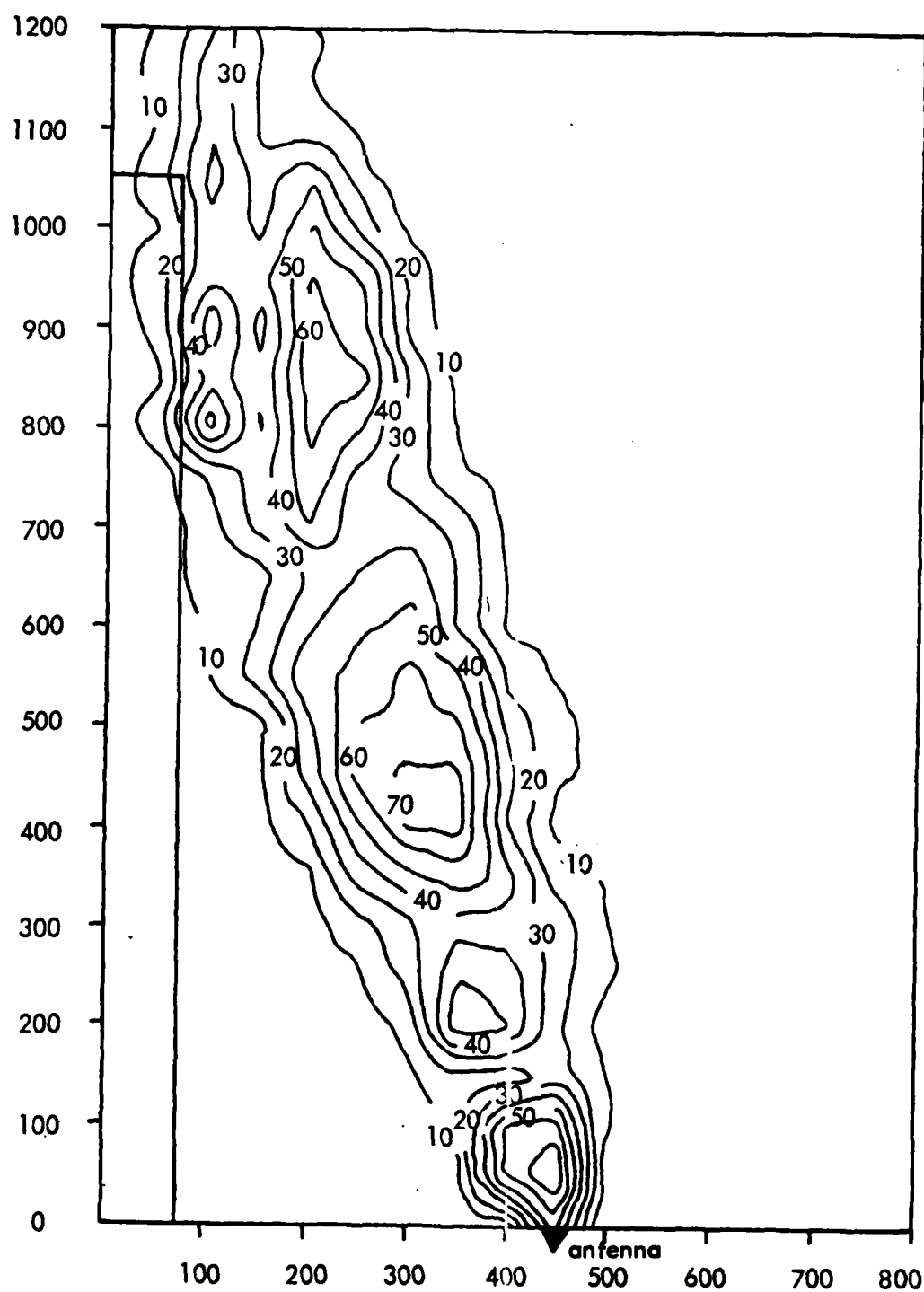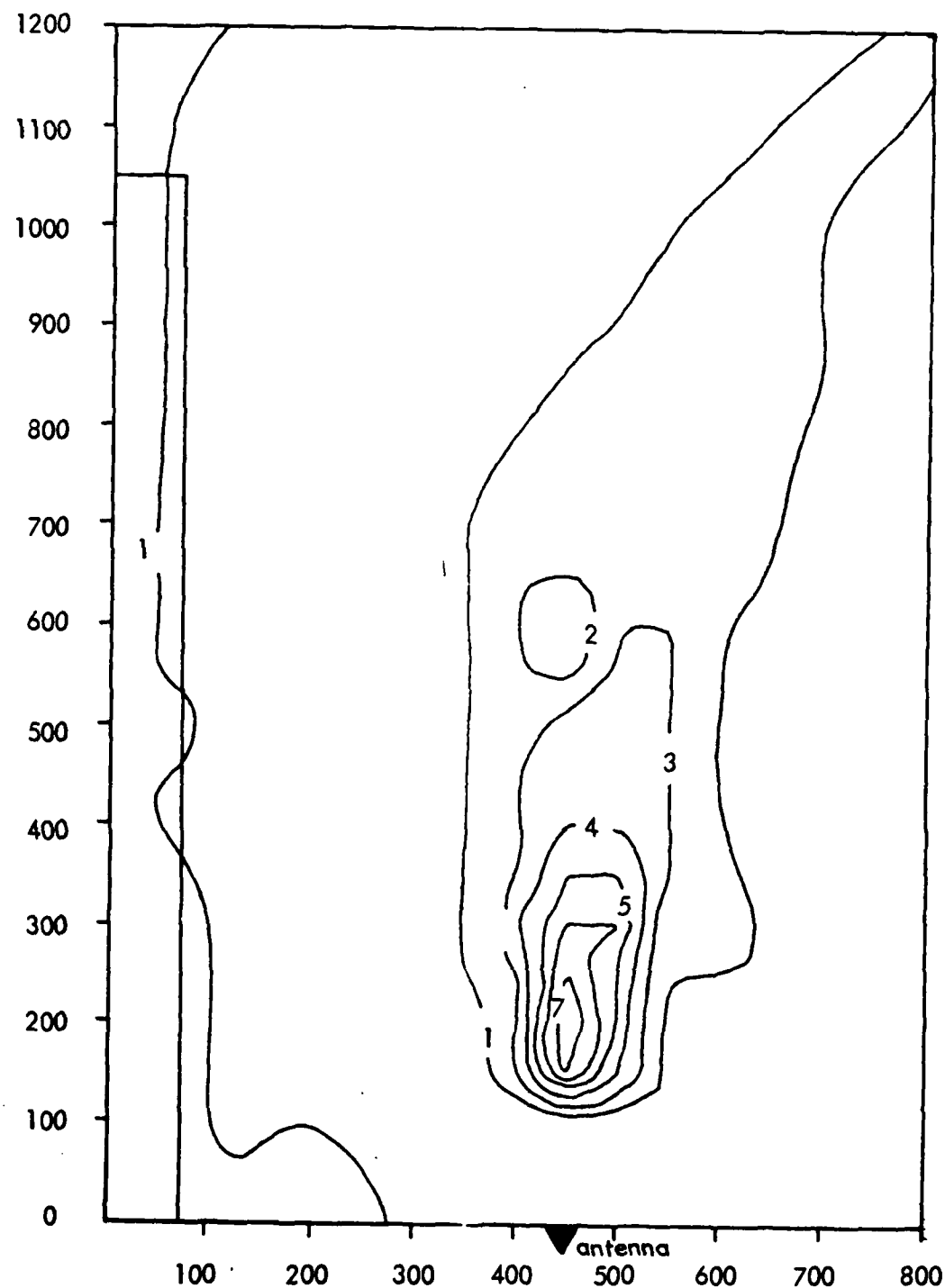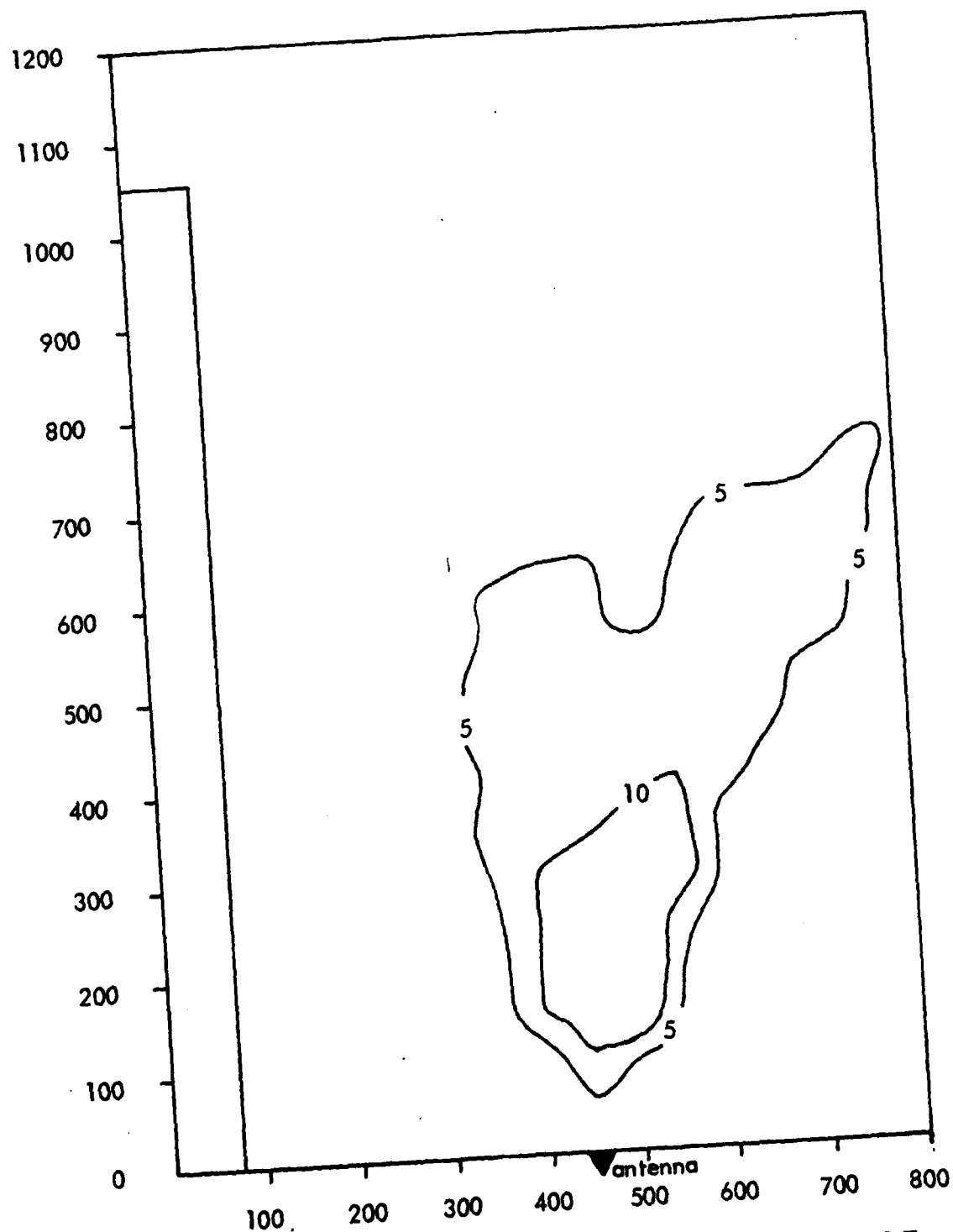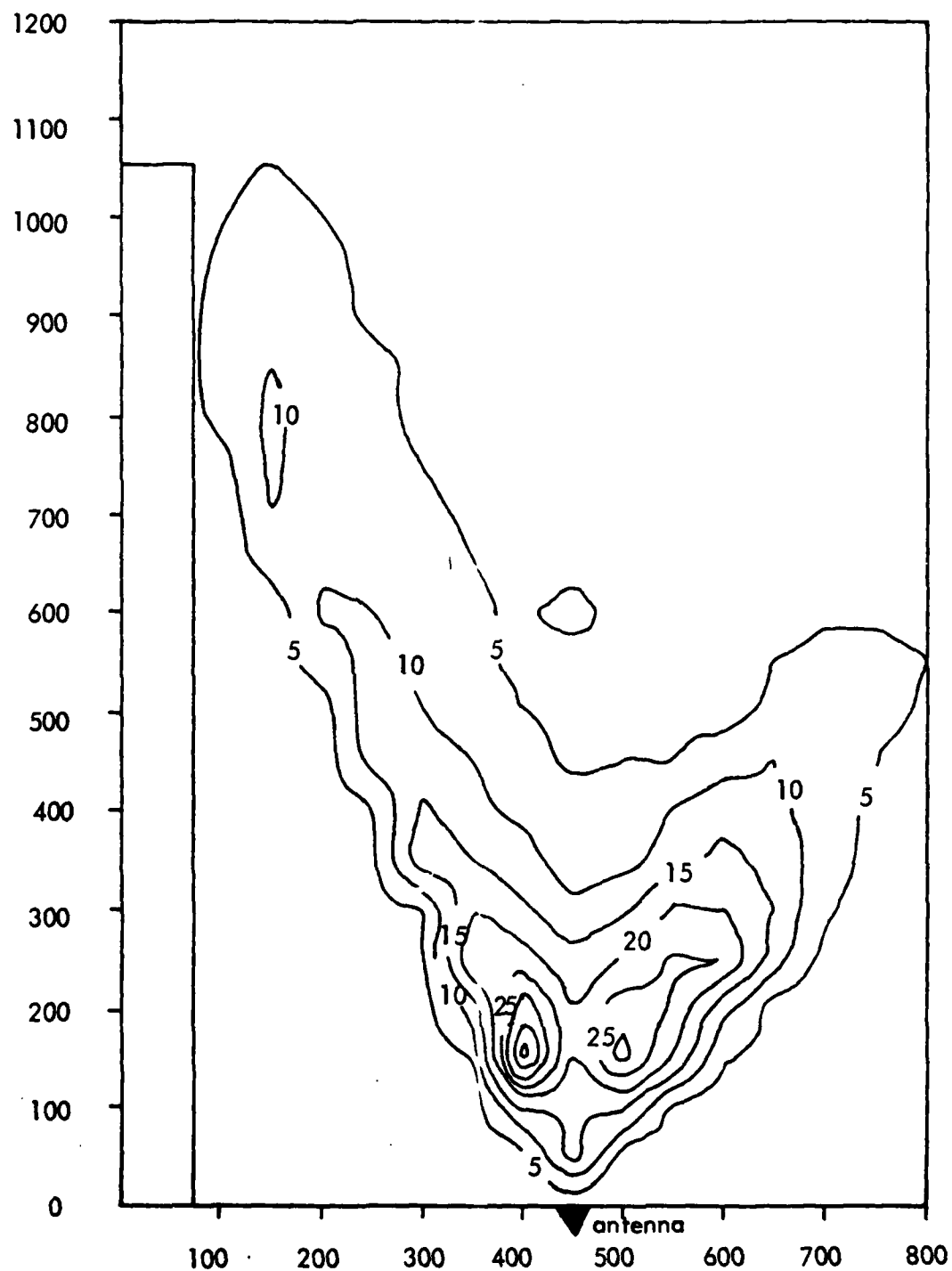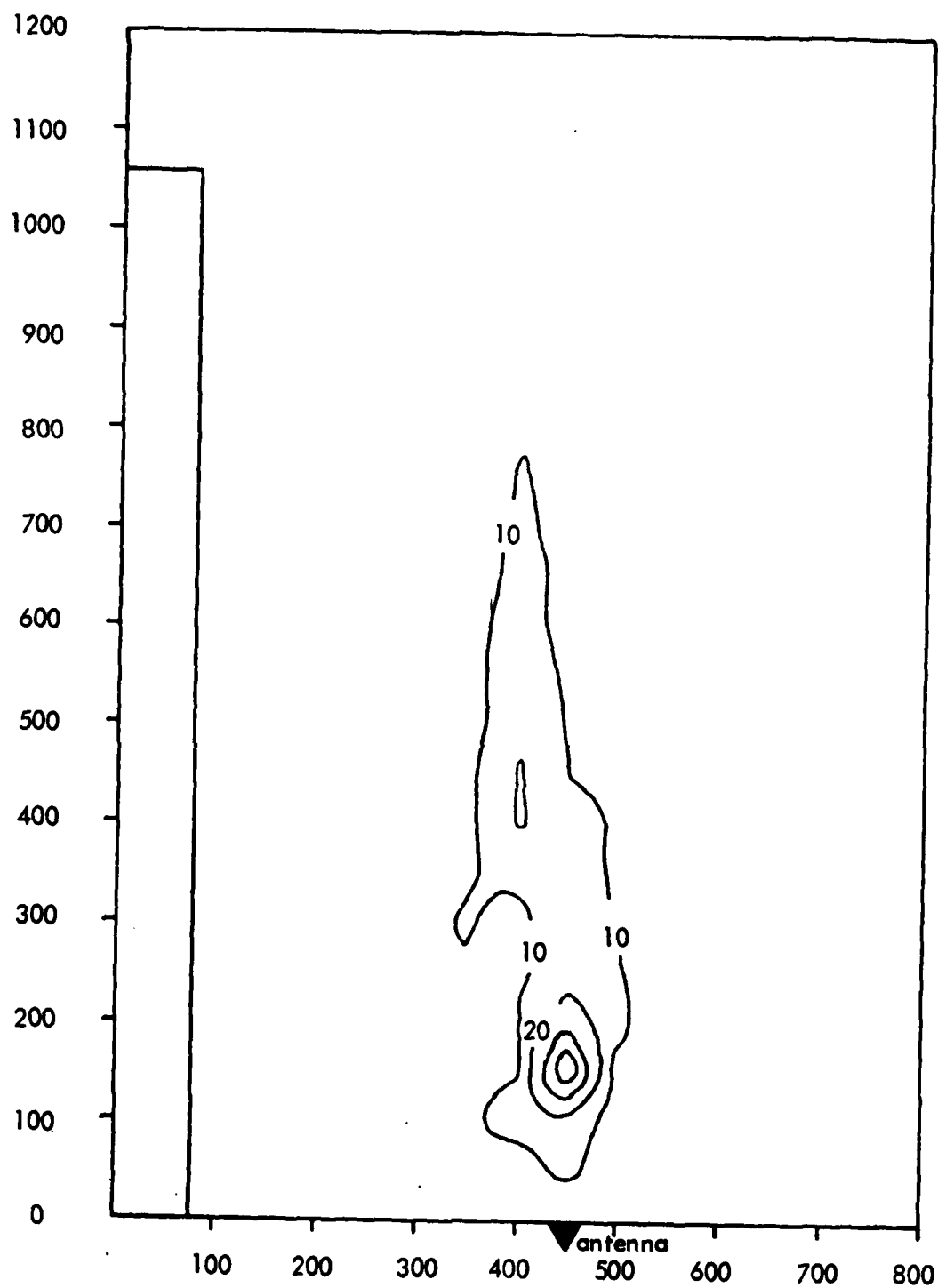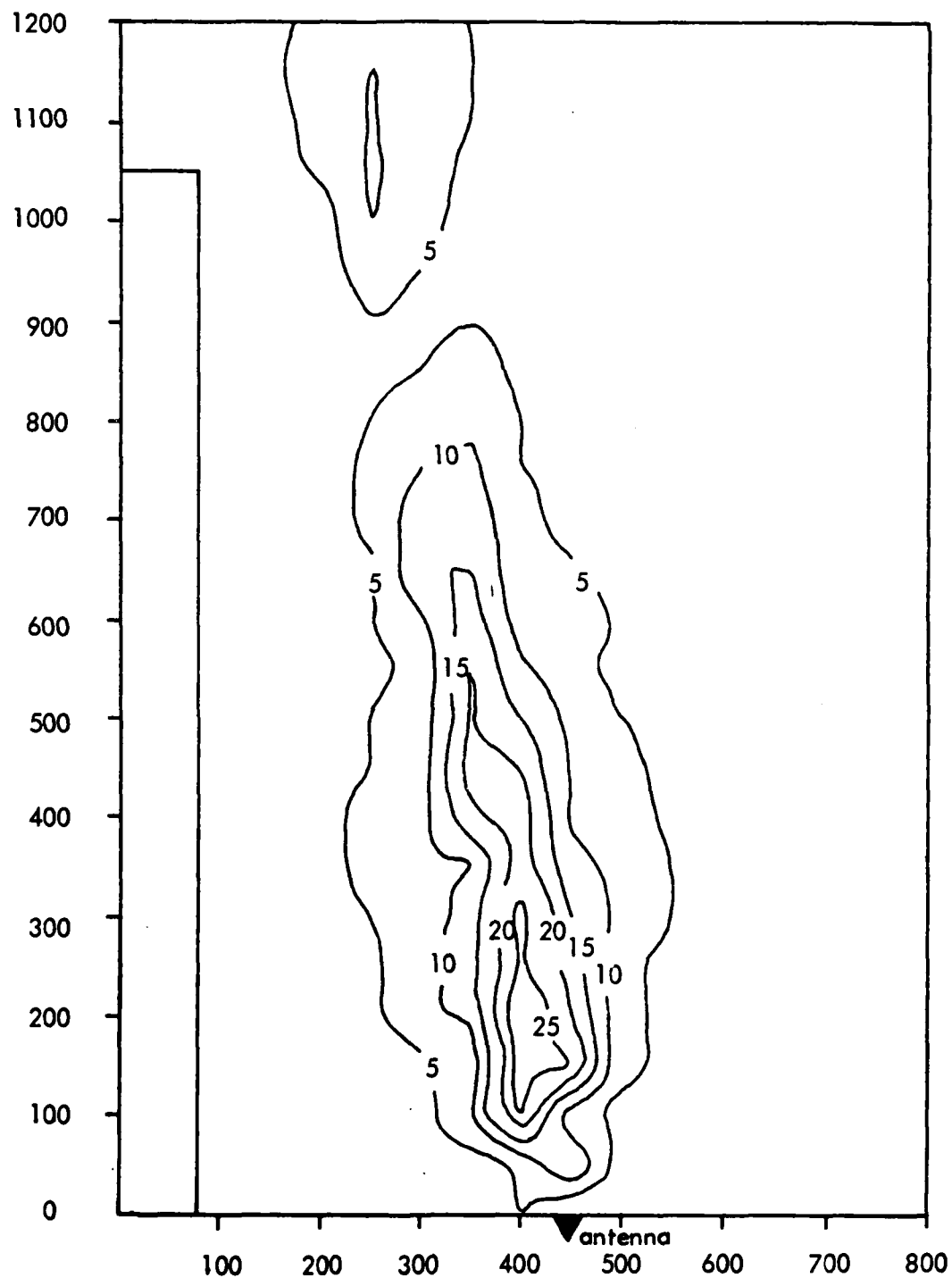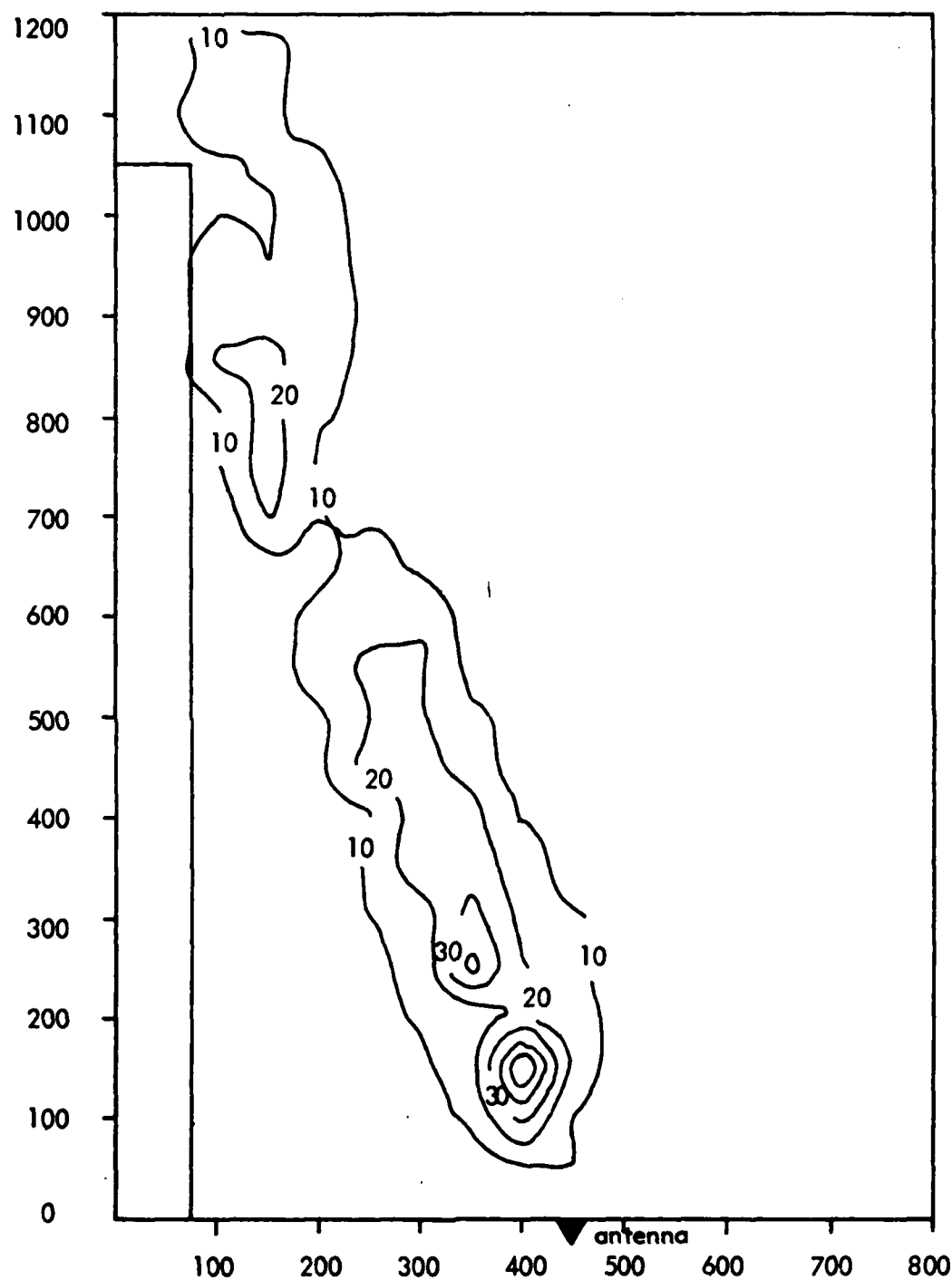
-117-
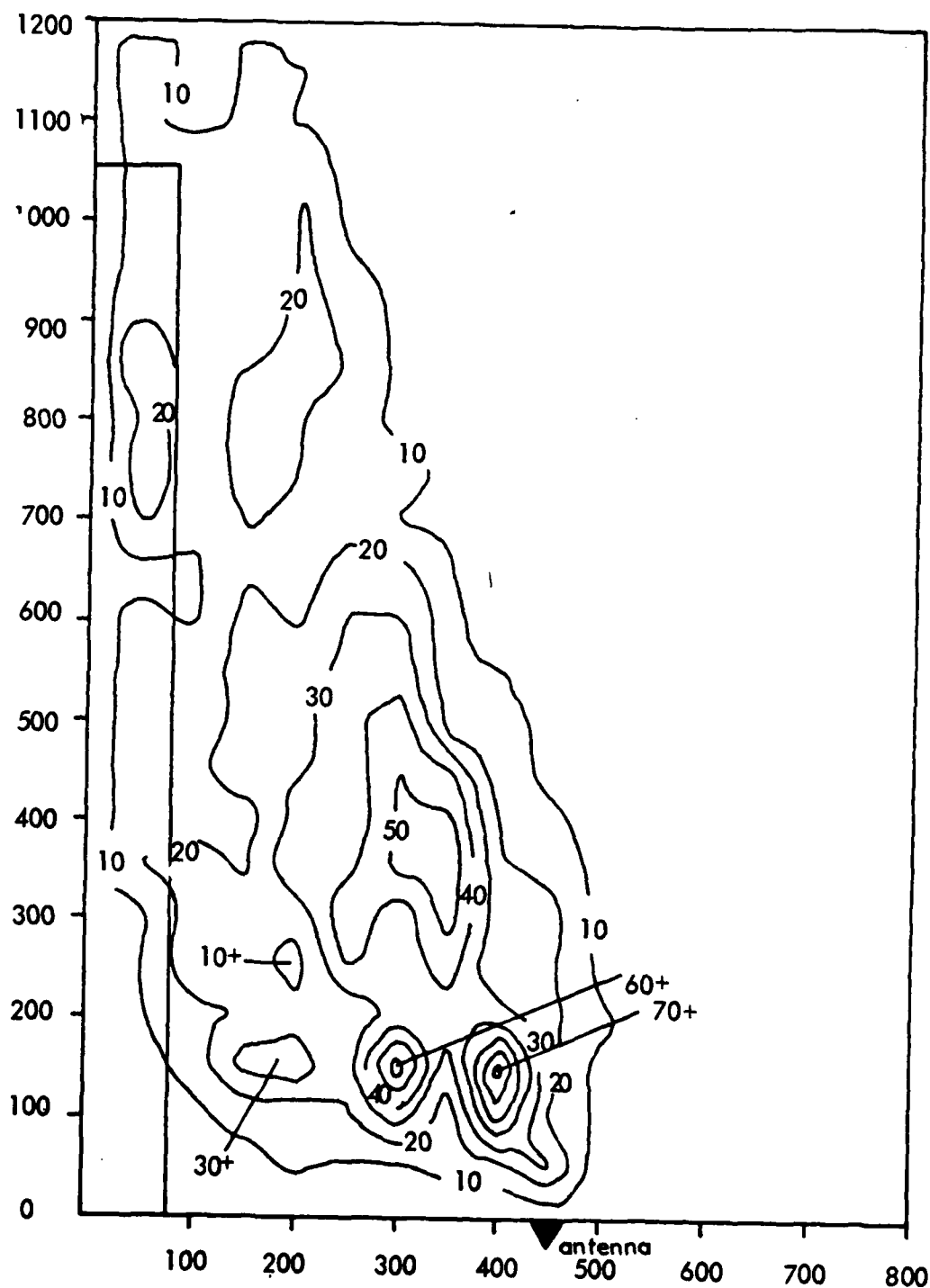
Figure 26. Contours of maximum values of CDI produced in ILS Zone 3 to the threshold for four general aviation type aircraft, specifically a Rockwell Commander, Beechcraft King Air and 2 Piper Cherokees, all in trail, aligned perpendicular to the runway.

-118-

Orientation perpendicular to Runway
        ILS Zone 2
        ILS Zone 3 (Pt. B to Pt. C.)
        ILS Zone 3 (Pt. C to Threshold)

As one may expect, the largest effect is produced by the Convair aircraft either in a parallel or perpendicular orientation in their parked position. Calculations show that this aircraft is theoretically capable of producing perturbations of 200 microamperes for certain positions close to the antenna.

By inspection of the contour plots the reader can see that most of the critical location of the target aircraft follows along the line connecting the transmitting antennas to the user aircraft. Interestingly and importantly, the maximum perturbations are only 50 to 70 microamperes for practical locations which is rather remarkable when considering the size of the reflecting aircraft. The term "practical locations" is used to mean those areas where a taxiway might be expected to exist. For example, 250 feet directly in front of a glide slope transmitting antenna mast would not be practical because fixed monitor probes are physically located in this vicinity.

The contours for the large, general aviation-type aircraft effects indicate that critical areas would not have to be as large as presently defined, provided the site being considered is a good one, i.e., the glide-path structure produced is smooth. The reader should note, however, that the contours are for a noise-free environment. The values should be added to known existing path structure noise meaning a very small contour value may be sufficient to place the resulting path structure beyond tolerance limits.

When considering medium-size general aviation aircraft such as the Rockwell Commander AC-6T, the Beech King Air BE90 or 100 series, the Falcon Jet, Cessna Citation, the Jet Commander, Rockewell Saberliner and others, the taxiway locations appear to be non critical. From the contours shown in figures 10 and 11 aircraft of this size located anywhere on a practical taxiway location are expected to produce no more than 25 microamperes. Given a good basic site, this should mean that this size aircraft would not produce out-of-tolerance conditions for path structure.

Location of small aircraft such as a Piper Cherokee, Piper Arrow, Beechcraft Bonanza, Mooney M20 or 21, Cessna single-engine series is non critical. No parallel or perpendicular location produces more than 15 microamperes of path roughness. This is an important finding inasumch as at smaller general aviation airports real estate is often limited and when an installation of an ILS is accomplished, protection of large areas from taxiing aircraft is difficult to provide.

The addition of the effects of several aircraft allows for an infinite number of possibilities. To approach a solution considering a reasonable situation a case of four aircraft, two medium, and two small aircraft. was calculated and measured.

-119-

A maximum perturbation of 70 microamperes of path perturbation was calculated whereas the maximum for just one of the aircraft was 60 microamperes. From the contours it is clear that these very sensitive areas are small in dimension and cannot accommodate more than one aircraft; hence addition of other aircraft in the queue does not produce effects anywhere near double that for the one aircraft. This is another fortuitous circumstance. Multiple aircraft by the very nature of their necessary physical arrangement cannot produce doubling or tripling of the resultant perturbation.

Following is a table showing the maximum perturbation produced by various aircraft and ensembles of aircraft. It is noteworthy that only in extreme, impractical cases is the performance of the ILS glide slope impacted significantly. Practical refers to a 100-foot wide taxiway feeding the runway at the threshold (1050 and running 200 feet on center alongside the glide-slope antenna mast.

TABLE 1

Aircraft	Location Longit., Lateral X,Y	Peak μa perturbation	Orientation	Range from the threshold
Cherokee				
Practical	1070,100	5	Perpendicular	Within 900'
Any	150,450	25	Perpendicular	3500-24,300'
Rockwell Commander				
Practical	210,600	25	Parallel	Within 900'
Any	130,400	40	Parallel	Within 900'
Convair 440				
Practical	350,650	140	Parallel	Within 900'
Any	150,500	240	Parallel	Within 900'
2 Medium + 2 small				
Practical	1000,200	20	Perpendicular	Within 900'
Any	150,400	70	Perpendicular	Within 900'

In general, the contour maps point to very small peak areas where, if aircraft are parked therein, noticeable path noise will be produced; however, an important result is that only for aircraft approaching the Convair will significant perturbations be evident, and these will not be of great concern unless the site is poor (producing inherent path noise) or a taxiway is placed within 500 feet of the transmitting antennas.

VII. EXPERIMENTAL WORK

The experimental work was conducted at the Ohio University ILS test site at the Tamiami Airport, Miami, Florida. A null-reference glide slope system was established using bent-dipole antennas 28.3 and 14.1 feet above the earth's surface. An eight-inch lateral offset was used. The result was a path angle of 3.01 degrees with a width of .70 degree. The structure is as shown in figure 27.

On March 25 and March 26, 1983, an initial series of measurements was accomplished using a Piper Cherokee Arrow as the target aircraft. Ten different locations for the target aircraft were used for the measurements. These positions are shown in the sketch contained in figure 28. The motivation for selecting these particular locations was to provide opportunities to measure worst case conditions and to replicate locations that might be expected should typical taxiways exist alongside of and in front of the glide slope transmitting antennas.

A Beechcraft Model 36 was used to collect the flight data. The Ohio University Mark IIIa minilab was used on board the aircraft to receive and process the data. A Warren-Knight WK-83 radio telemetering theodolite was used with a Reaction Instruments telemetry transmitter to provide the references for the measurements. Each run was performed at least twice and repeatability was confirmed before succeeding measurements were made.

Using the reference signal telemetered from the ground, it was possible to read out in real time the difference between the observed CDI value and the reference. This is commonly referred to as the differential amplifier output and is representative of the position of the on-course signal in space independent of the pilot-induced deviations of the aircraft from this path.

The flight tracks were made by intercepting the path outside a five-mile fix. Because the CDI was being flown and recorded, below-path fly-up indications were also observed. No significant abnormalities in the below-path clearance at low elevation angles were observed in any of the runs.

No attempt was made to execute the usual level runs for determining vertical path width. This was because when perturbations are caused by reflectors they are most always manifest in scalloping of the path. These lead to ambiguous and rather meaningless width values made from level runs.

The results of the measurements of the structures produced when the Cherokee was at the various locations are shown along with the calculated curves in the next section. The plots of the Tamiami data shown are reproductions of the flight records which have been digitized.

The maximum path perturbation due to the Cherokee at any point was found to be 30 microamperes, and that occurred in Zone 2 (Cat I) for the case where the Cherokee was 250 feet in front of the antennas and 350 feet from the centerline. Even for this worst case the path remained within Category I tolerance limits.
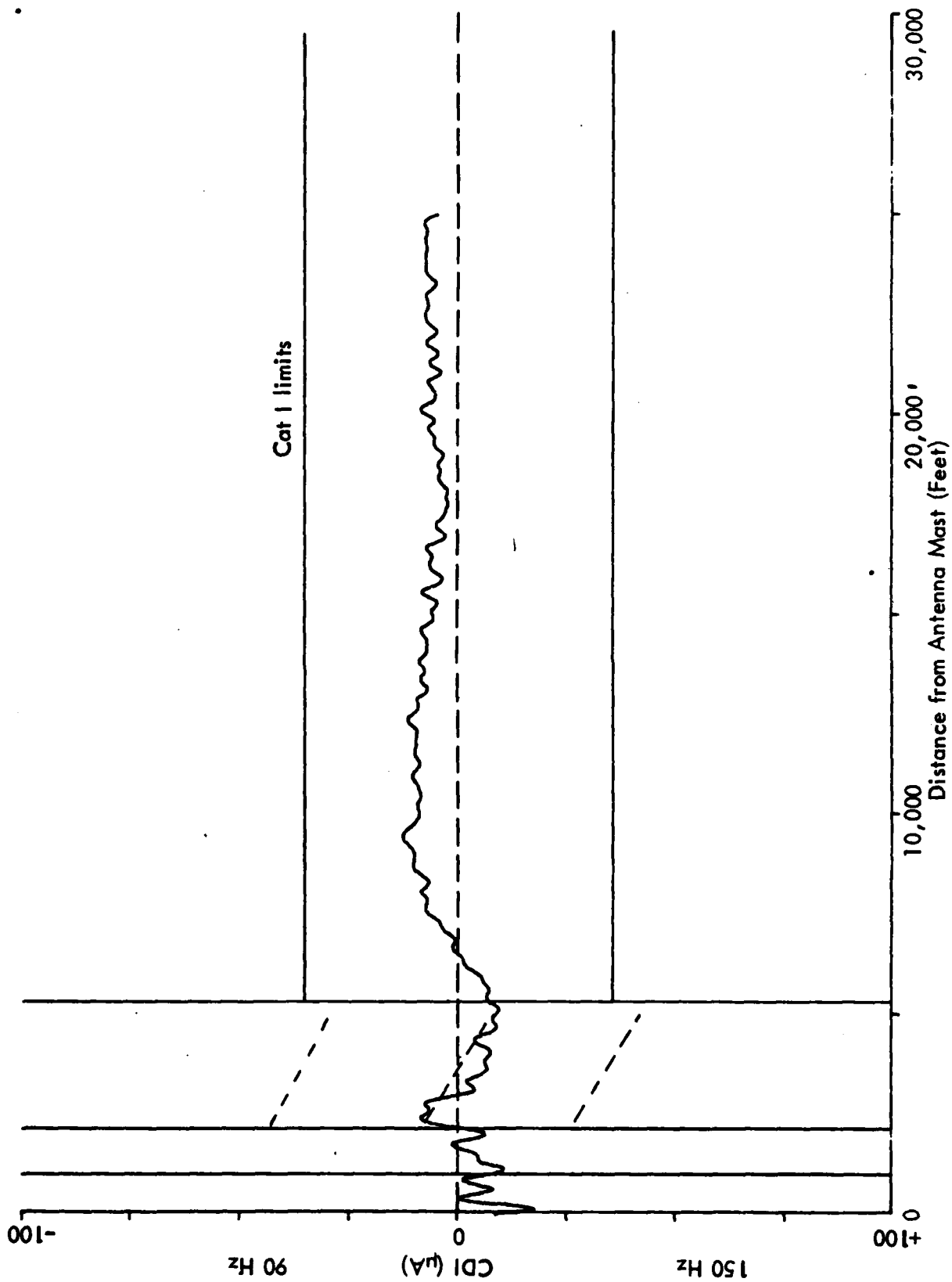
Figure 27. Digitized flight recording of the normal glide slope system made on April 25, 1983. This path exhibits greater than normal inherent noise for the Tamiami site, and no specific cause can be given.
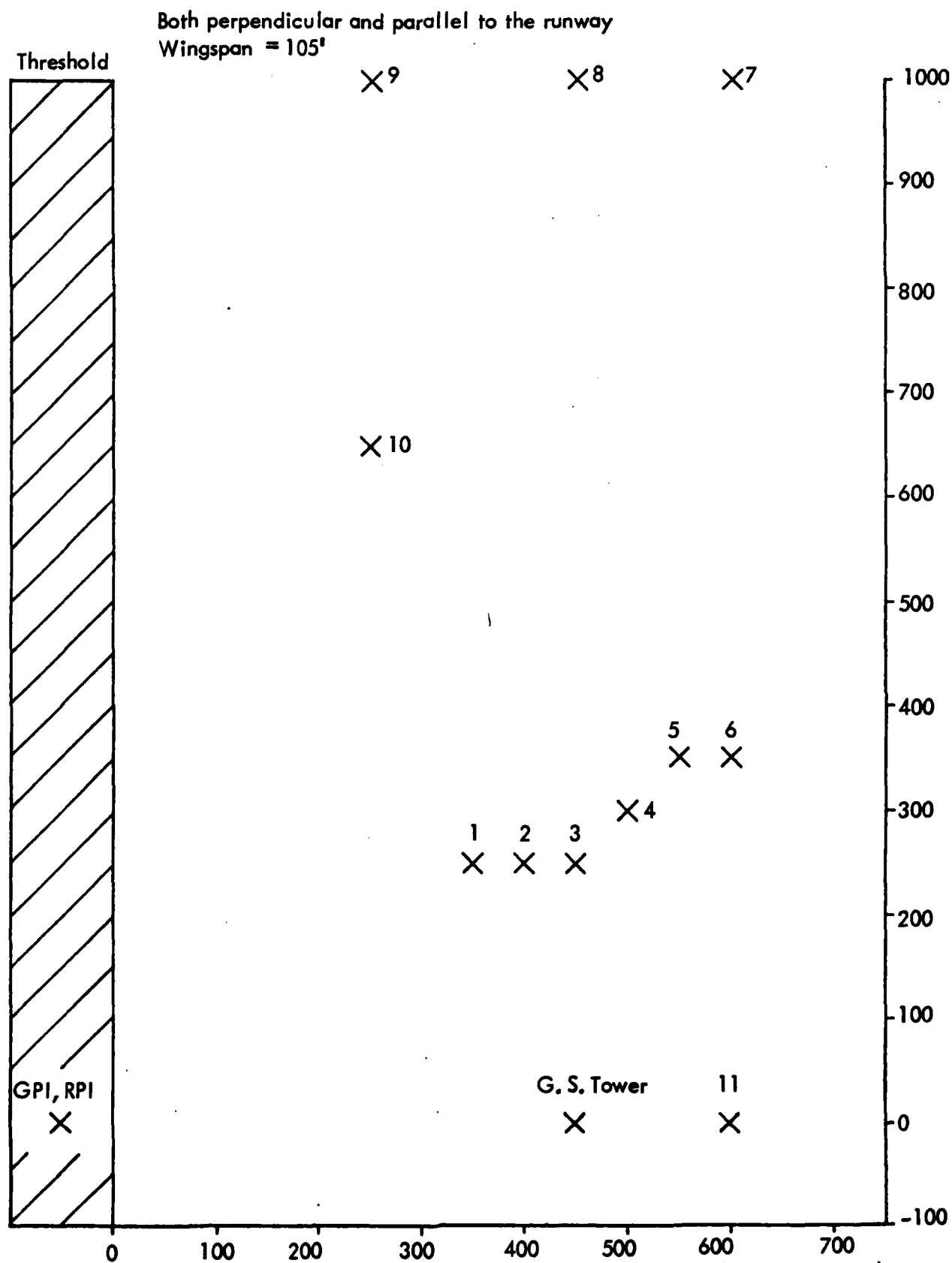
Figure 28. Definition of positions for the Cherokee aircraft for experimental examination of the effects on glide-path structure.

On April 13 and 14, 1983, measurements were made of the Convair 440 alone, the Rockwell Aero Commander alone, the Commander with a Beechcraft King Air, and finally, the case with the Commander, King Air plus two Piper PA-28 Cherokees. Again, positions were selected to provide for the most interesting results with respect to maximum effects and practical taxiway considerations. The time availability of the various aircraft prevented more combinations of testing; however, sufficient data were obtained to indicate the adequacy of the model to predict conservatively.

The digitized flight records showing the structures produced with the various aircraft at the selected locations are contained in the next section. From these one can see that the maximum perturbation was 45 microamperes produced by the Convair only 250 feet directly in front of the antennas. This, of course, is an unrealistic position considering usual taxiway complexes. When the Convair is moved out to 1000 feet, a more representative location, the maximum perturbation is reduced to 20 microamperes. This is within Category I limits. A practical position parallel to the runway, 150 feet to the side of the antennas, produced a maximum of 13 microamperes of path deviation. This simulated a position on the taxiway next to the glide slope mast.

Another set of measurements involved the Rockwell Commander which has a relatively high tail at the same locations as for the Convair. A maximum of 30 microamperes of path deviation was observed when the aircraft was 250 feet in front of the antennas. This is 61 percent of that for the Convair.

Adding a King Air, another popular, medium size, general aviation aircraft, making a two-aircraft ensemble 1000 feet from the antennas produced perturbations of only 20, this occurring in Zone 3 for positioning of the two aircraft 1000 feet in front of the antennas. Much of this appears to be recorder noise, however.

For assessment of the effects due to a plurality of aircraft parked on a taxiway, four aircraft, viz., the Commander, the King Air, and 2 Cherokees were parked in what might be considered normal taxiway situations. These 2 cases were: (a) 4 aircraft, nose to tail, perpendicular to the runway 1000 feet in front of the antennas, and (b) 4 aircraft nose to tail, parallel to the runway centerline, abeam and extending forward in front of the antennas as if on a parallel taxiway. Perturbations to path structure due to four aircraft located as indicated were 15 microamperes maximum in Zone 3. The path angle bias due to the recorder was removed.

It was possible in all of the cases for the pilot to fly successfully the CDI indication to the runway threshold and maintain the needle on scale. While in some cases the path was out of tolerances specified by the U.S. Flight Inspection Handbook O AP 8200.1, the path was not deformed to such an extent that it could not be flown to the intended destination.

To make it possible to reproduce the data in this report each recording of the differential amplifier output was digitized and plotted on a Hewlett-Packard Model 7203A plotter.

Some photographs of the experimental setup are shown in figures 29 through 34. Captions provide the details for interpreting the photos.

Figure 29. View Looking Out into the Approach Region from the Glide Slope
at Tamiami. Evident is the very flat terrain forming the glide slope
reflecting plane. The equipment used for tracking and the telemetry
are shown in place.

Figure 30. To the Left is the Model 36 Beechcraft Used for Gathering the Flight
Data. Behind and to the right is the Beechcraft BE-90 King Air used
as one of the target airport.

Figure 31. View from the Cockpit Taken During a Measurement Flight With the Commander and King Air in place 1000 feet Forward of the Glide Slope Transmitting Antennas.

Figure 32. Convair 440 Being Tugged into Position in Front of the Glide Slope.

Figure 33. Rockwell Aero Commander AC-6T Located in Front of the Glide Slope
Ready for Measurement Process to Begin. The glide slope mast is
evident as is the King Air which is being stowed behind the mast
awaiting a future measurement.

Figure 34. Aerial View of the Glide Slope Site With the Commander and King Air
in Place for Measurements.

VIII. COMPARISONS

The confidence which the reader can place in the predictions given by the contour maps in the preceding sections is related directly to the correlation of the measured and calculated structure perturbations produced by the subject aircraft. In this section the predicted and measured path structures obtained in this work are compared and discussions provided concerning the degree of replication.

For each of the 20 physically different cases of aircraft position a calculated and measured structure plot is provided in figures 35 to 54. The reader is encouraged to inspect these and determine to his or her own satisfaction the correlation.

Experience with the base line data taken on other occasions at Tamiami suggests that the inherent noise of the traces for these measurements is greater than normal for some undetermined reason. One possibility is telemetry noise which decreases the quality of the correlation and should be taken into account when making judgements. An example of the excessive noise is evident in figure 39. With the generally small effects produced by the parked aircraft, the noise was especially troublesome.

In general the correlation is acceptable. Outstanding examples are found in figures 35 and 47 where the inherent noise does not complicate the correlation. Here the noise is sufficiently diffused so as not to mask the character of the perturbations which are produced by the reflecting aircraft.

These plots of both calculated and experimental data indicate clearly that the mathematical model is predicting well and conservatively.

The traces which have been taken from an analog to digital conversion of the data do appear to have more noise in this form than on the original strip charts due solely to the compression of the time axis by more than a factor of three. This compression was necessary, of course, in order to eliminate fold-outs in the final report form.

In each of the calculated traces the principal area of perturbation due to the aircraft can be observed. Although small in many cases, it is evident in the traces because the inherent noise of the system is zero. In some cases, notably figure 45 with the large aircraft close to the antennas, there is a path displacement in addition to the fast oscillations called scalloping.

In figures 50 and 51 there is some evidence that an apparent phase displacement exists between the small perturbations of the calculated and measured structures. A question was raised as to the precision of the placement of the reflecting aircraft. Unfortunately, placement was not surveyed and some difference can reasonably be expected to exist between that called out in the measurement and that calculated. In order to evaluate how critical this was, a sensitivity analysis was performed to examine the effects of differences in placement.

A calculational exercise was performed in which the four aircraft were considered as a unit and moved with respect to a reference point. Thirteen different locations of the unit were considered as shown in Appendix B. The reference point was 1000 feet in front of the antennas and 450 feet from centerline. The results of the sensitivity analysis indicate there is very little effect that can be observed as a result of moving the reflectors closer or farther from the antennas by a small amount (say 10%); however, lateral movement to or from the runway by the same small amount does not change the magnitude of the perturbation but can alter its phase with respect to the reference. The phase referred to is the relations of the peaks in the sinusoidal scalloping produced by the reflecting aircraft. One can therefore conclude that displacement in the peaks of the measured path perturbation with respect to the calculated is most likely due to the imprecise placement of the subject reflecting aircraft. The fundamental cause thus is an inconsistency between the input data for the calculation and the true location.

Figure 35. Calculated and measured on-course positions for the null-reference glide slope with a Piper Cherokee parked perpendicular to the runway 400 feet from the centerline and 150 feet in front of the antennas.

Figure 36. Calculated and measured on-course positions for the null-reference glide slope with a Piper Cherokee parked perpendicular to the runway 450 feet from the centerline and 250 feet in front of the antennas.

Figure 37. Calculated and measured on-course positions for the null-reference glide slope with a Piper Cherokee parked perpendicular to the runway 400 feet from the centerline and 250 feet in front of the antennas.
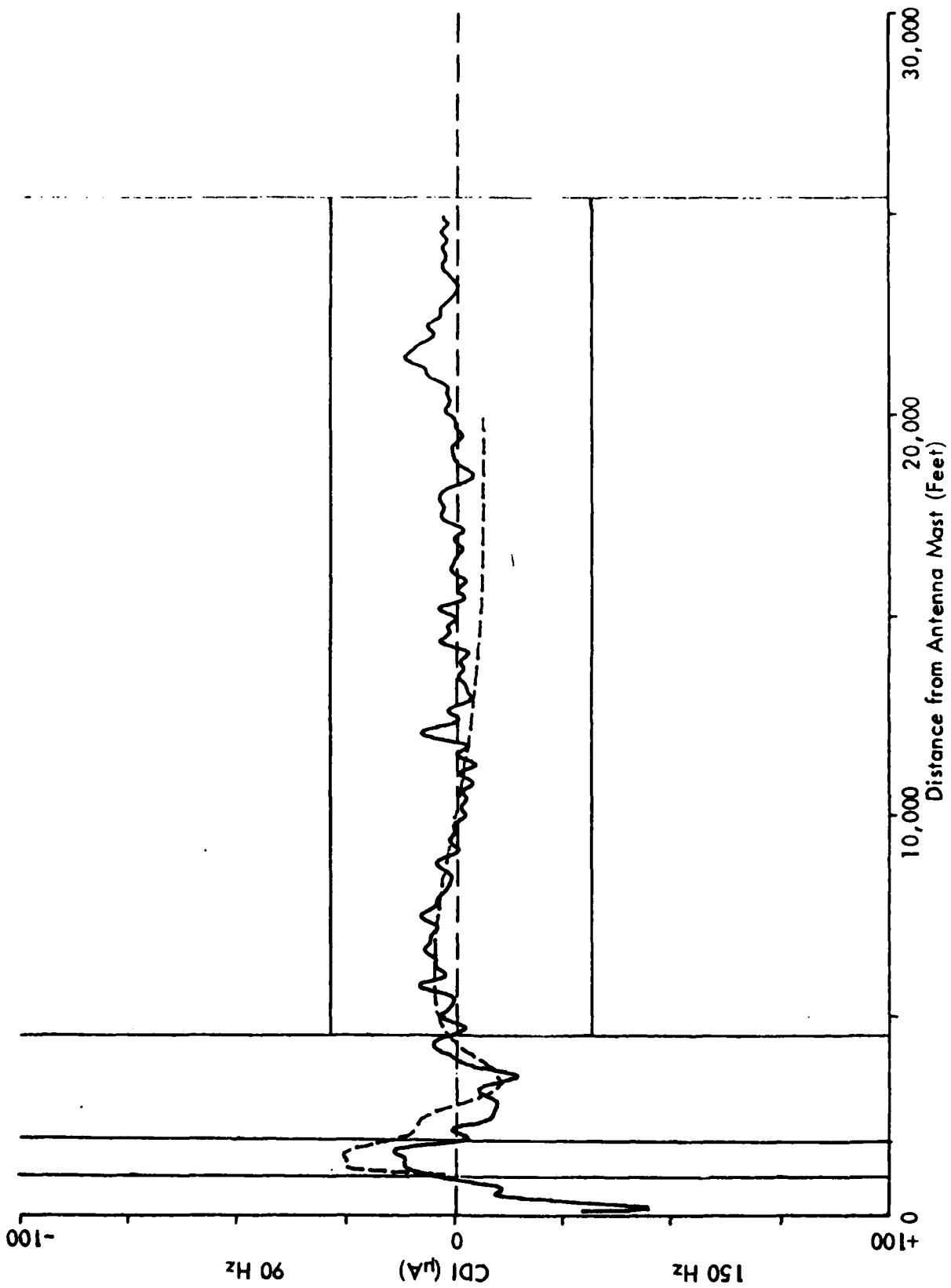
-133-

Figure 38. Calculated and measured on-course positions for the null-reference glide slope with a Piper Cherokee parked perpendicular to the runway 350 feet from the centerline and 250 feet in front of the antennas.

-134-

Figure 39. Calculated and measured on-course positions for the null-reference glide slope with a Piper Cherokee parked parallel to the runway 400 feet from the centerline and 250 feet in front of the antennas.
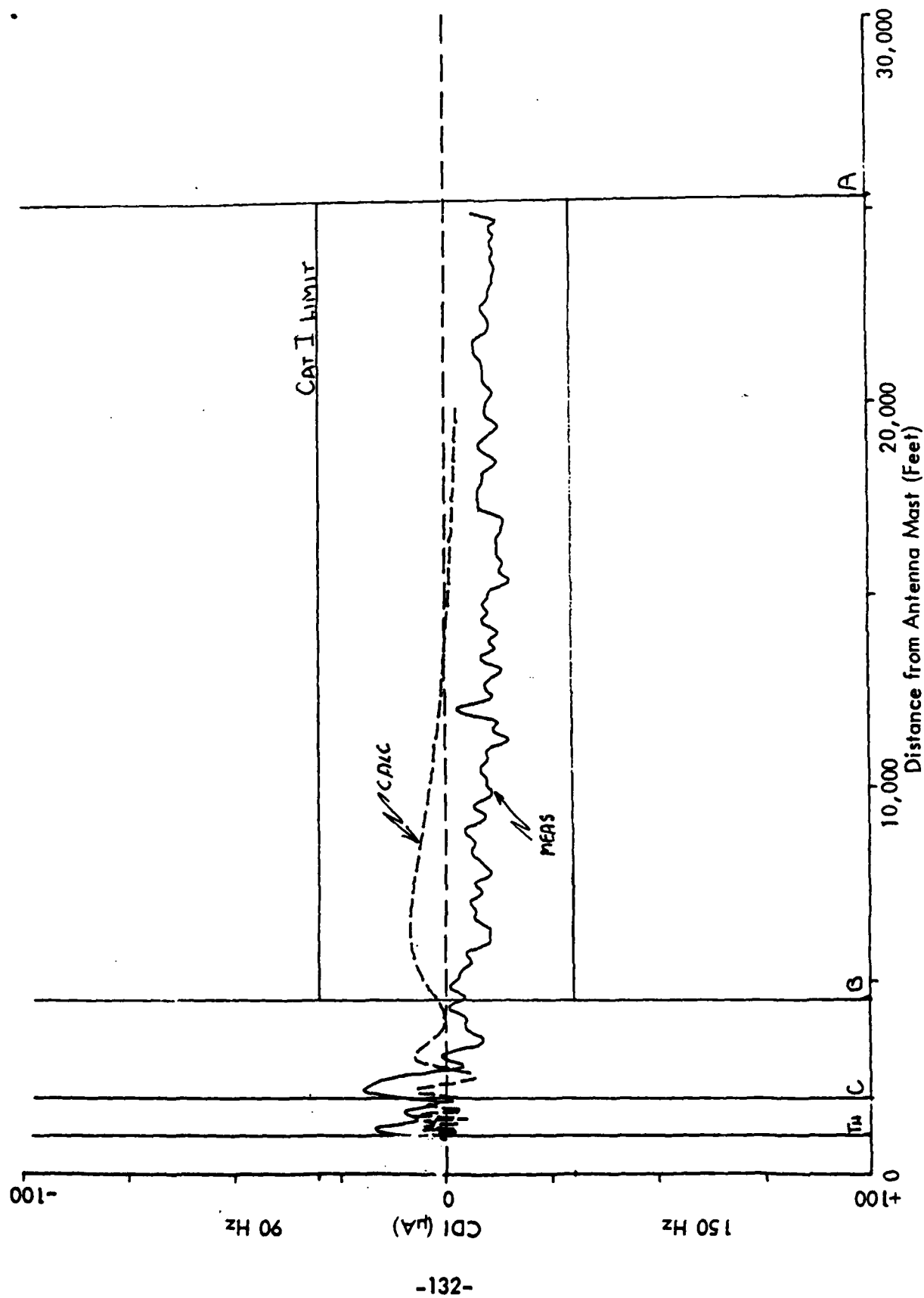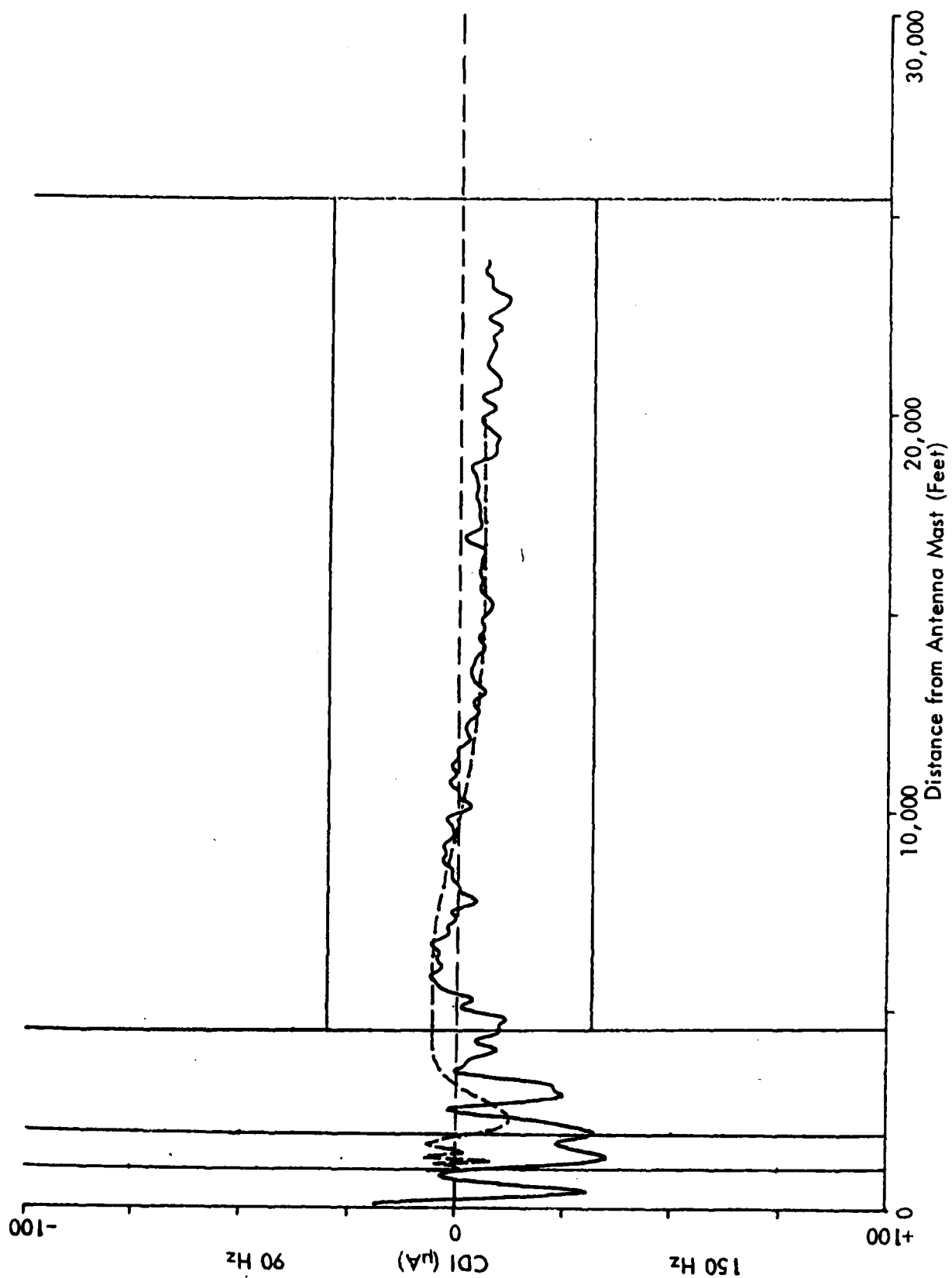
-135-

Figure 40. Calculated and measured on-course positions for the null-reference glide slope with a Piper Cherokee parked perpendicular to the runway 500 feet from the centerline and 300 feet in front of the antennas.

Figure 41. Calculated and measured on-course positions for the null-reference glide slope with a Piper Cherokee parked parallel to the runway 600 feet from the centerline and 350 feet in front of the antennas.

Figure 42. Calculated and measured on-course positions for the null-reference glide slope with a Piper Cherokee parked perpendicular to the runway 600 feet from the centerline and 0 feet in front of the antennas.
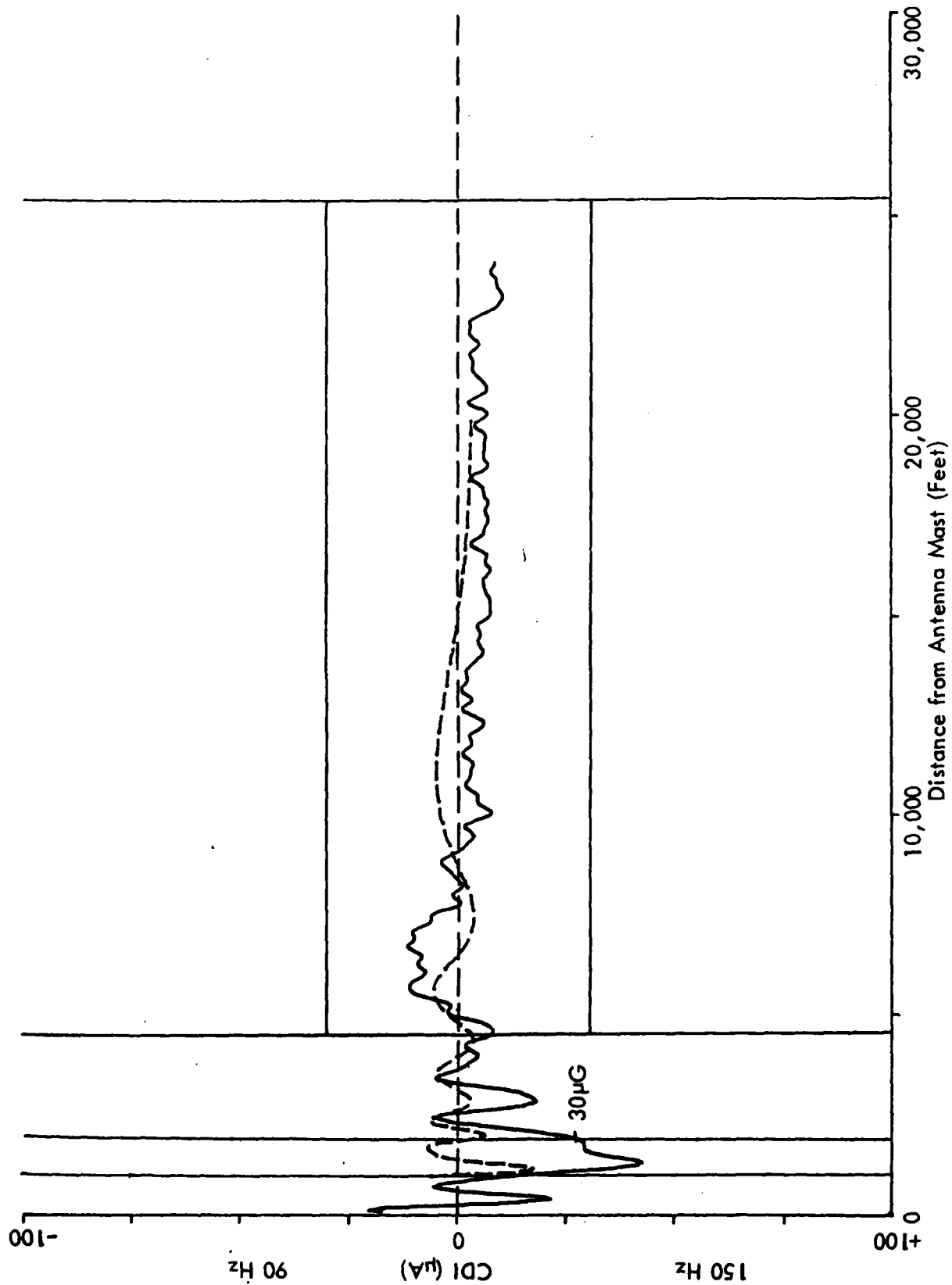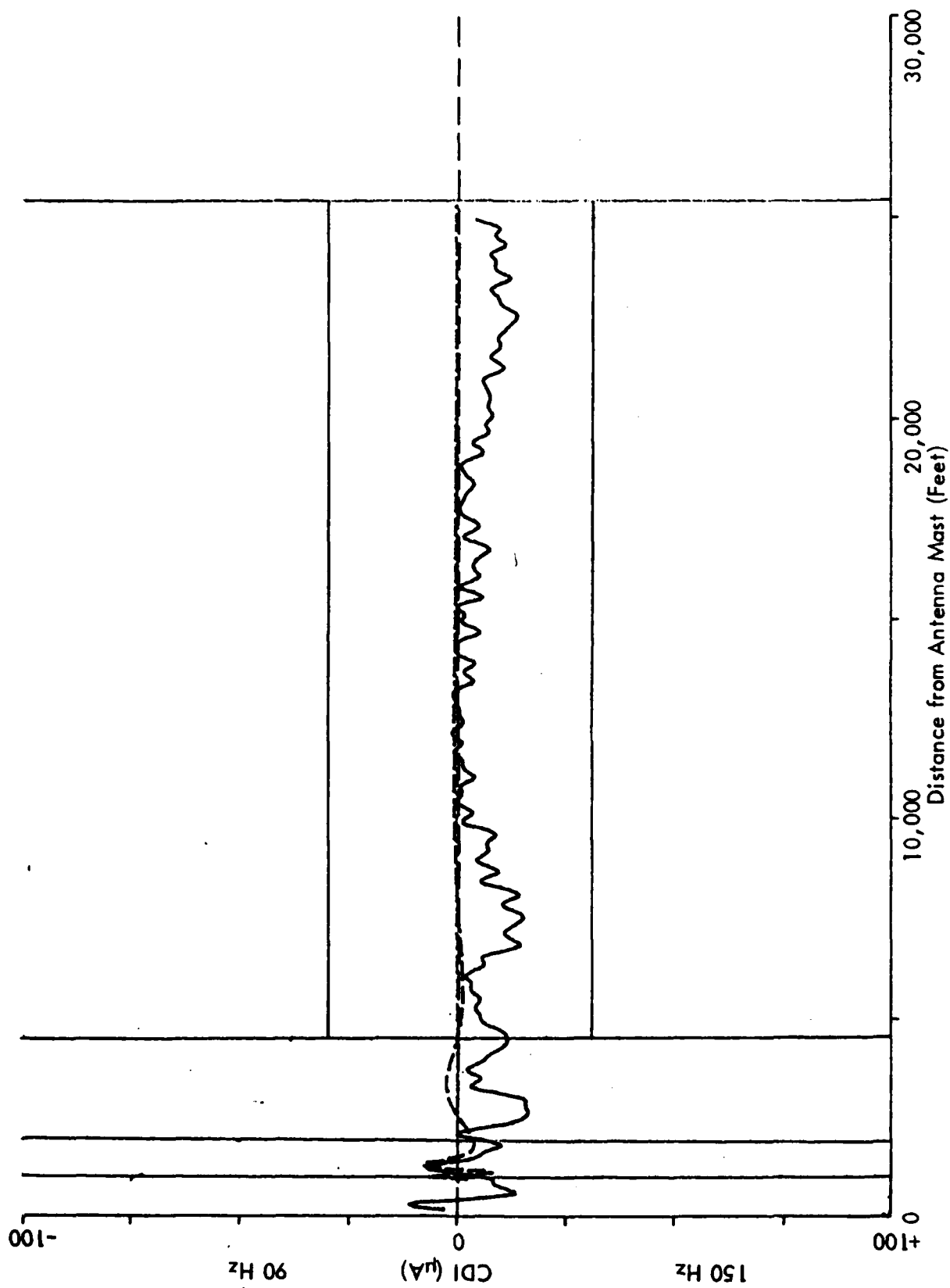
-138-

Figure 43. Calculated and measured on-course positions for the null-reference glide slope with a Piper Cherokee parked parallel to the runway 600 feet from the centerline and 0 feet in front of the antennas.
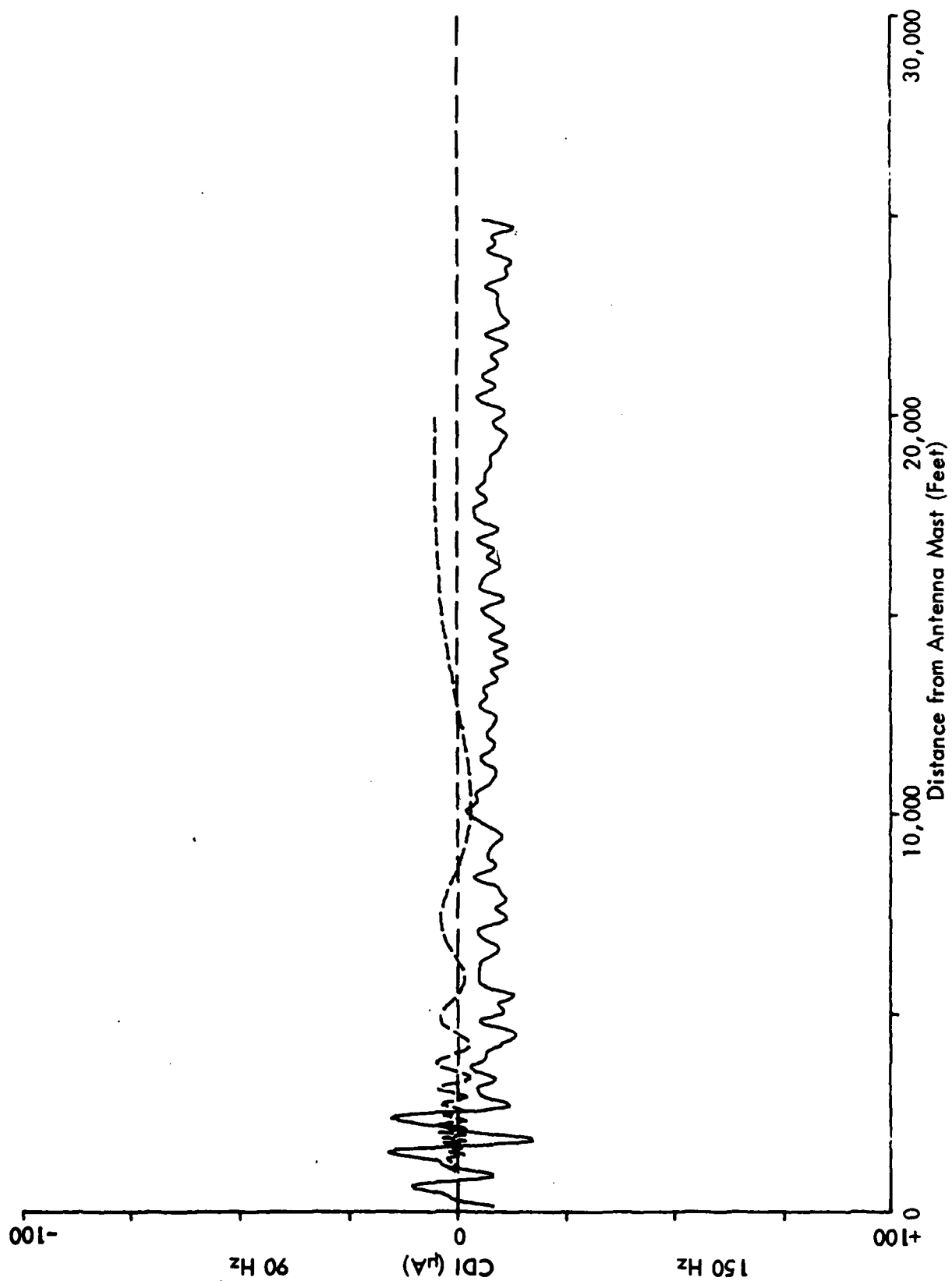
Figure 44. Calculated and measured on-course positions for the null-reference glide slope with a Piper Cherokee parked perpendicular to the runway 450 feet from the centerline and 1000 feet in front of the antennas.
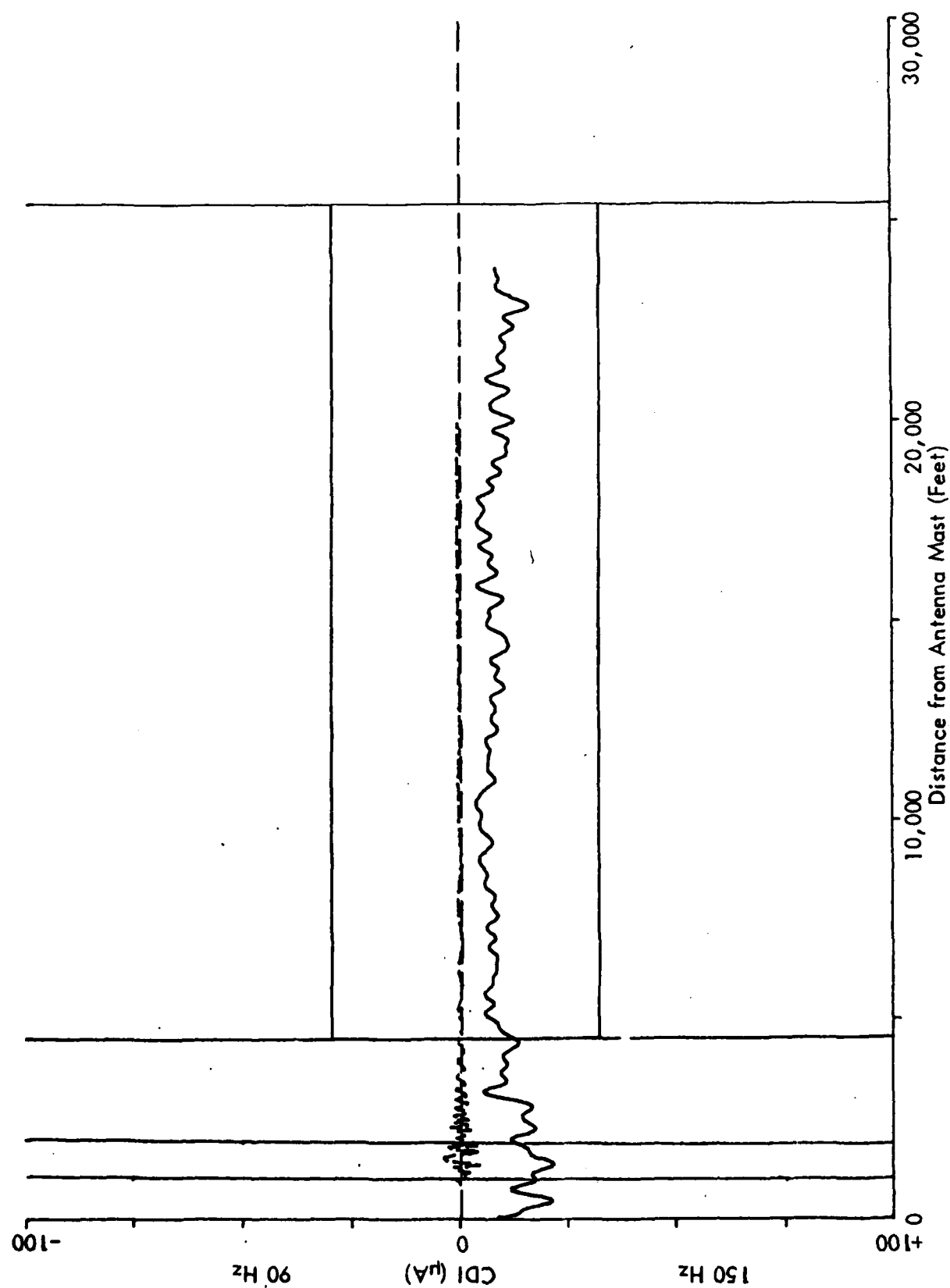
Figure 45. Calculated and measured on-course positions for the null-reference glide slope with a Convair 440 parked perpendicular to the runway 450 feet from the centerline and 250 feet in front of the antennas.

Figure 46. Calculated and measured on-course positions for the null-reference glide slope with a Convair 440 parked parallel to the runway 600 feet from the centerline and 0 feet in front of the antennas.
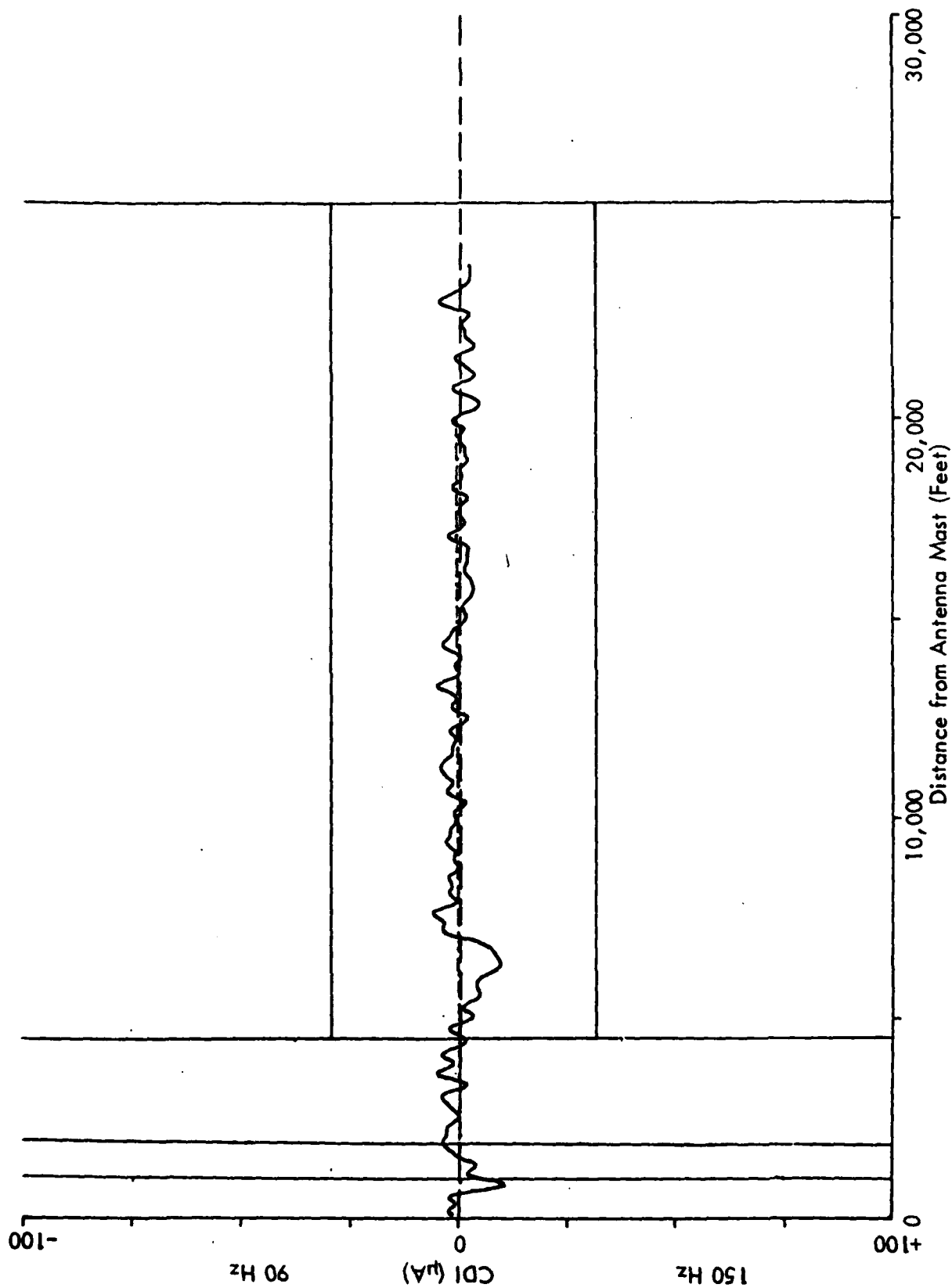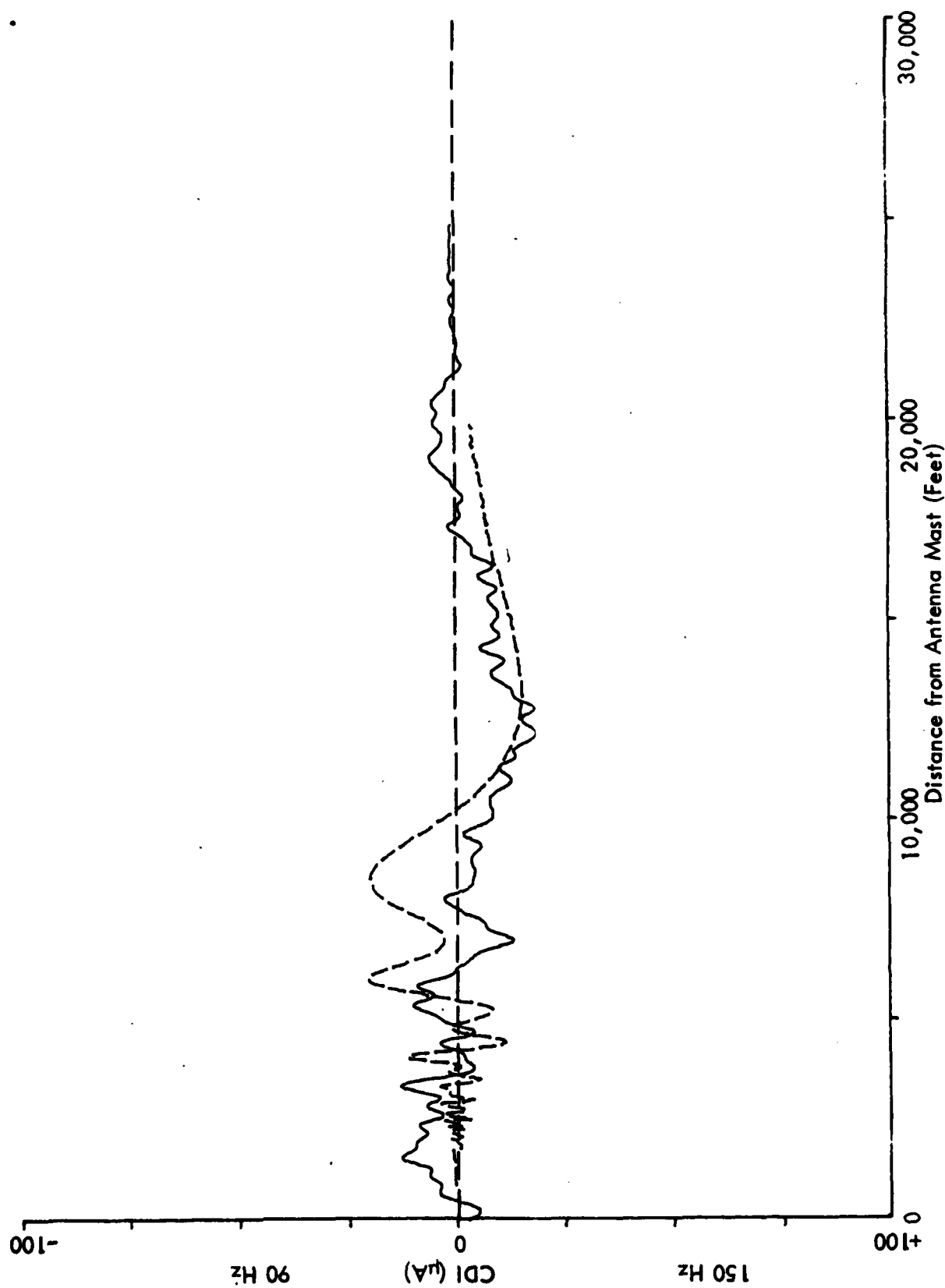
Figure 47. Calculated and measured on-course positions for the null-reference glide slope with a Convair 440 parked perpendicular to the runway 450 feet from the centerline and 1000 feet in front of the antennas.

-143-

Figure 48. Calculated and measured on-course positions for the null-reference glide slope with a Rockwell Commander parked perpendicular to the runway 450 feet from the centerline and 250 feet in front of the antennas.
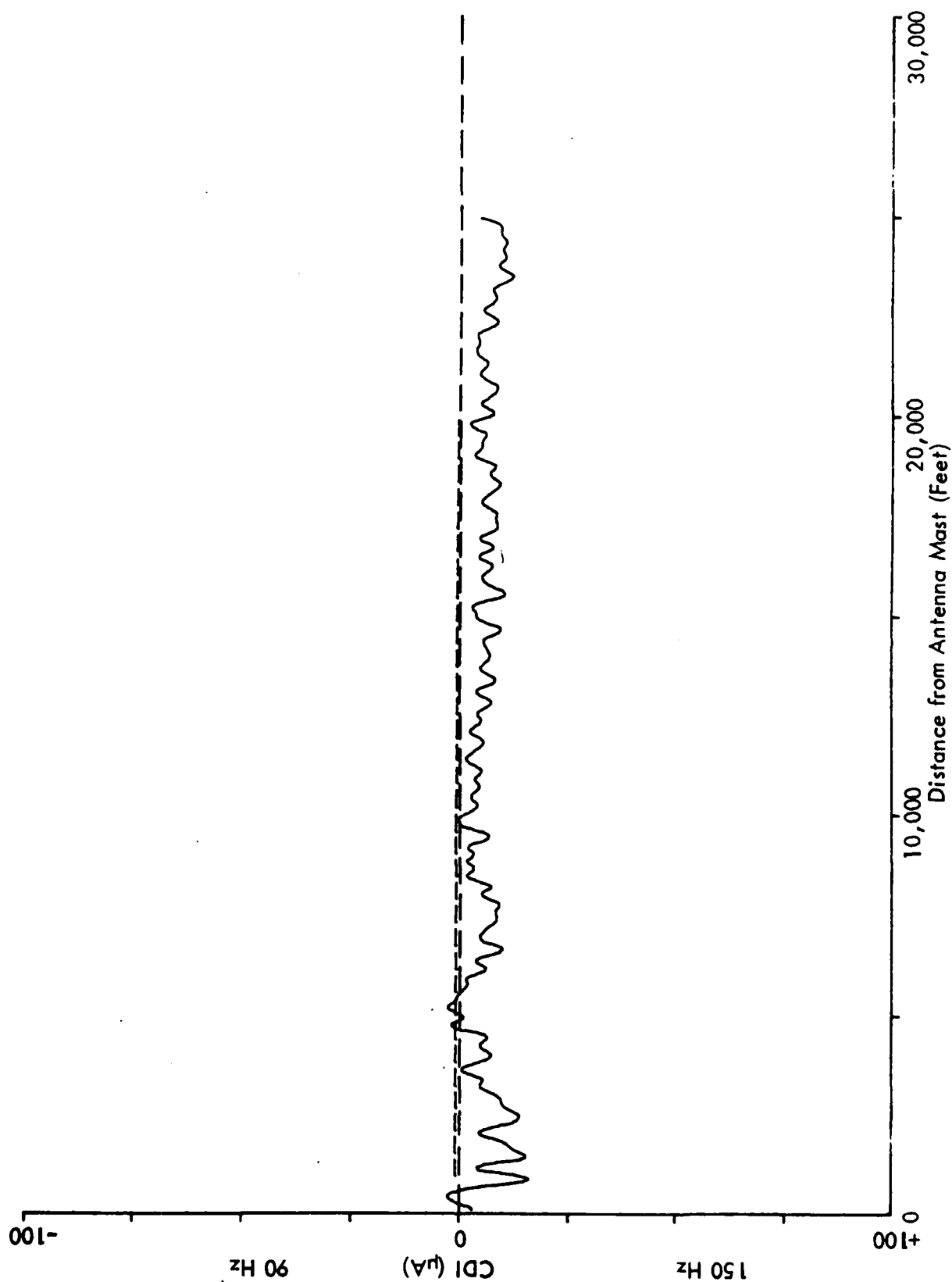
Figure 49. Calculated and measured on-course positions for the null-reference glide slope with a Rockwell Commander parked parallel to the runway 600 feet from the centerline and 1000 feet in front of the antennas.
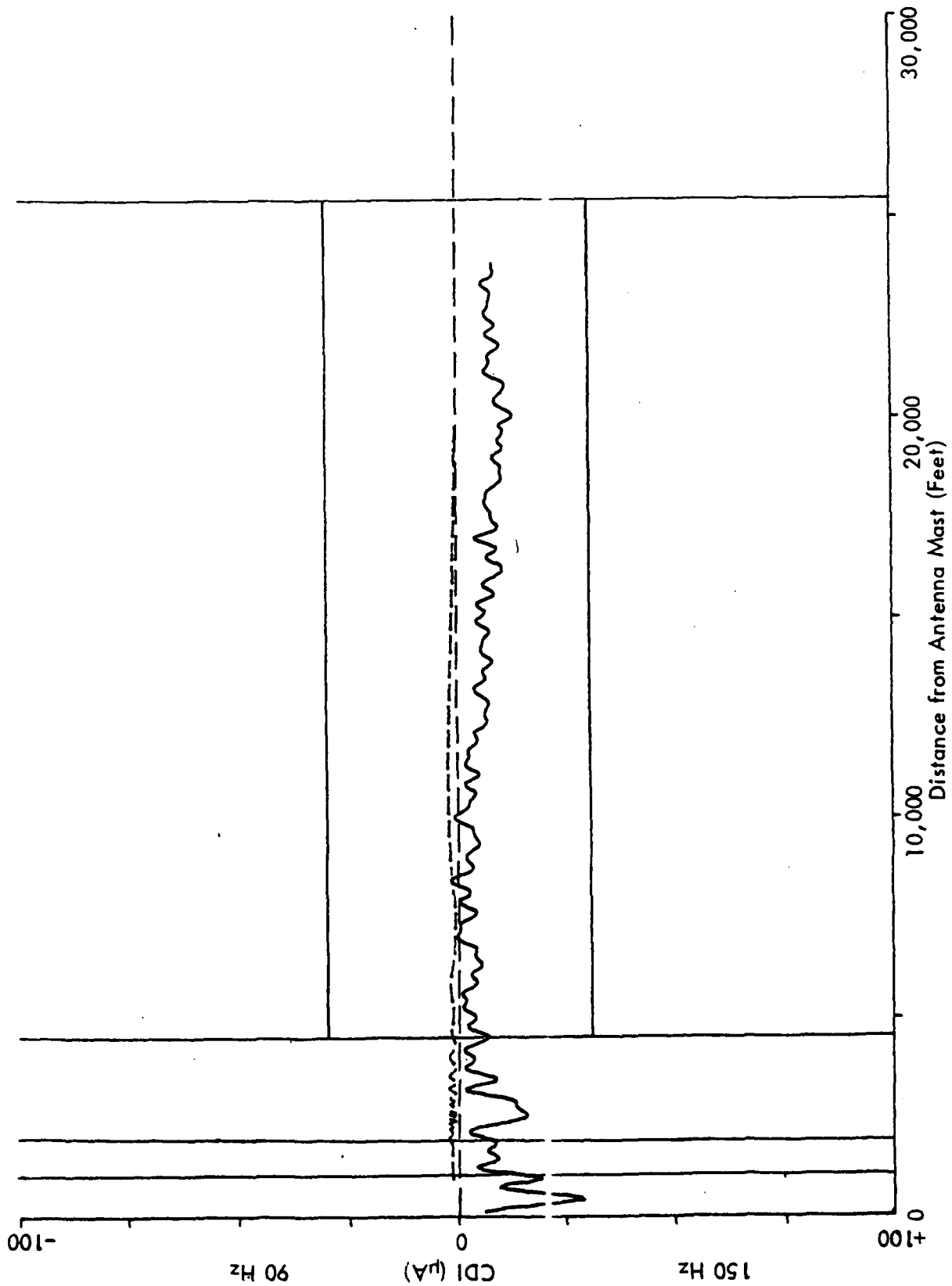
Figure 50. Calculated and measured on-course positions for the null-reference glide slope with a Rockwell Commander parked perpendicular to the runway 450 feet from the centerline and 1000 feet in front of the antennas.
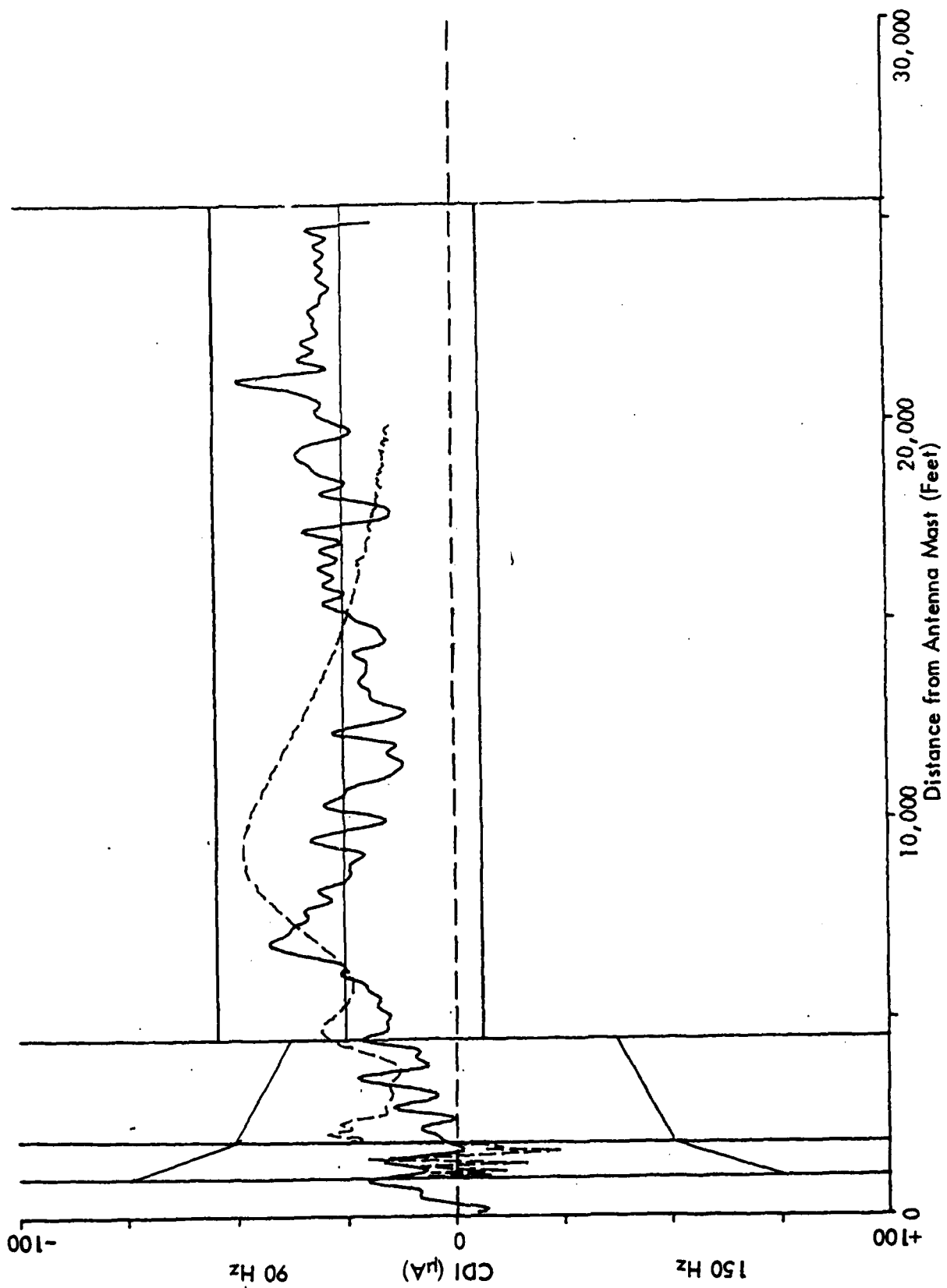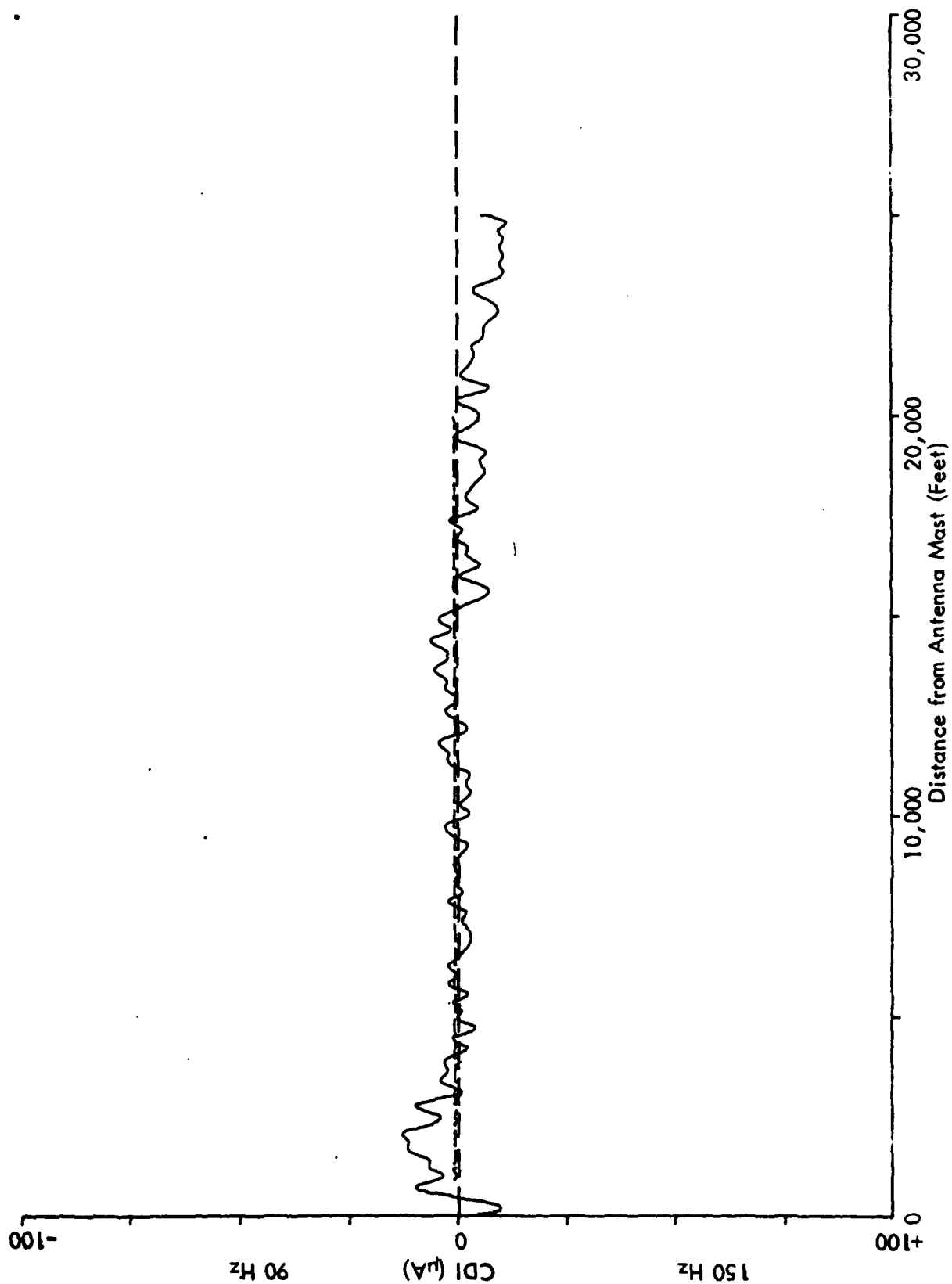
Figure 51. Calculated and measured on-course positions for the null-reference glide slope with a Rockwell Commander and a King Air parked perpendicular to the runway 450 feet from the centerline and 1000 feet in front of the antennas.

Figure 52. Calculated and measured on-course positions for the null-reference glide slope with a King Air and a Rockwell Commander parked perpendicular to the runway 450 feet from the centerline and 1000 feet in front of the antennas.

Figure 53. Calculated and measured on-course positions for the null-reference glide slope with a King Air, Rockwell Commander, and two Piper Cherokees parked perpendicular to the runway 450 feet from the centerline and 1000 feet in front of
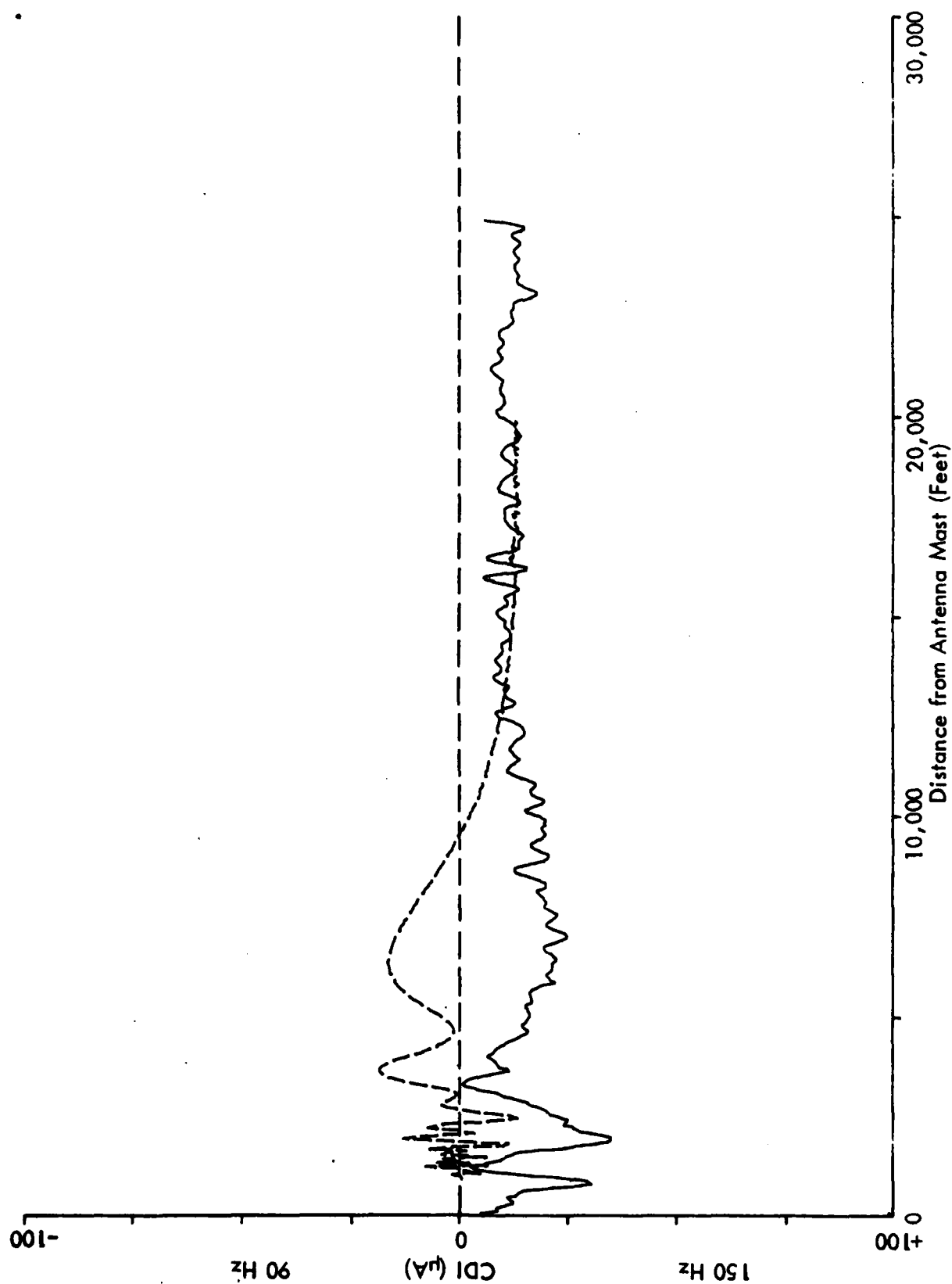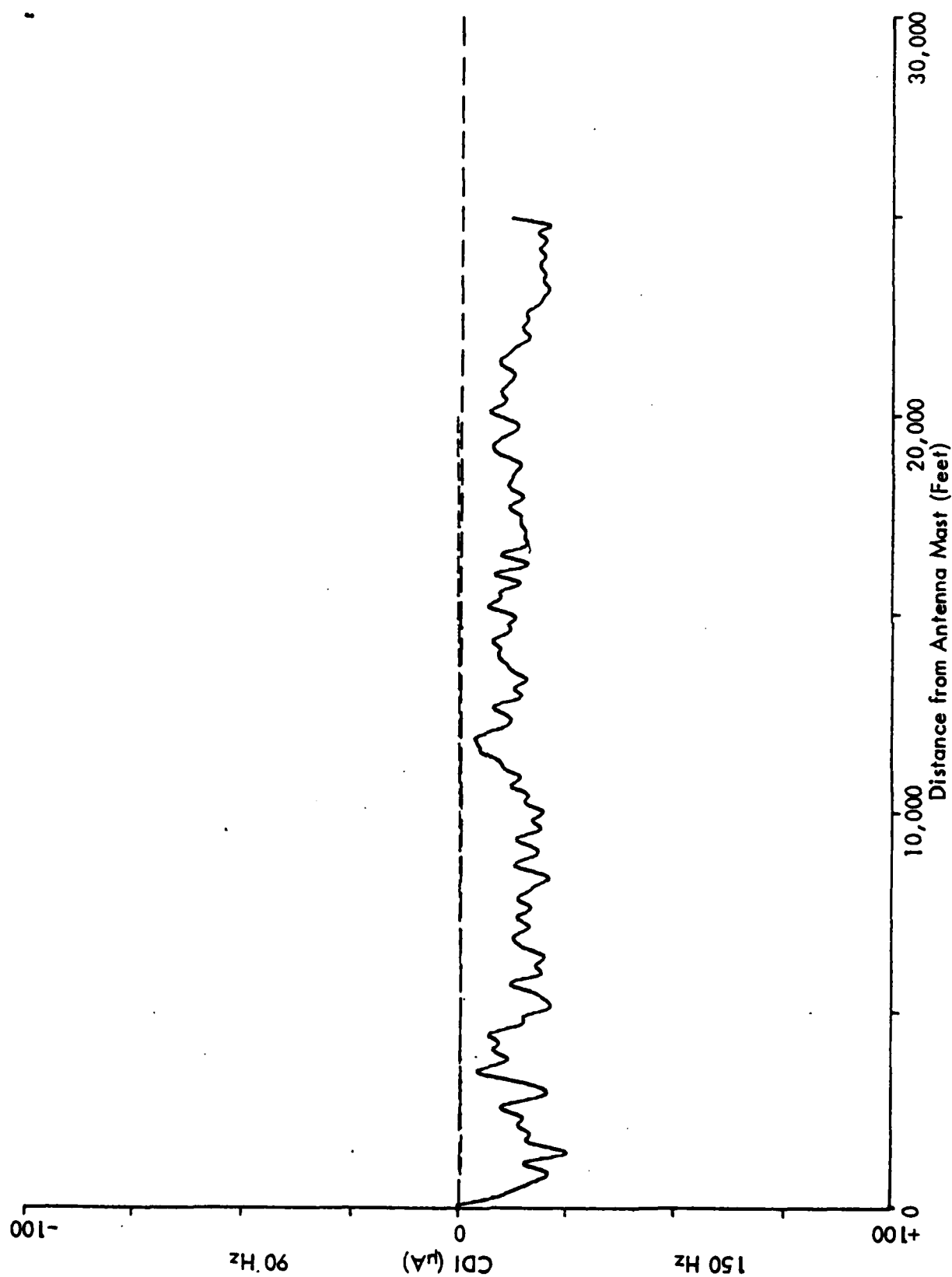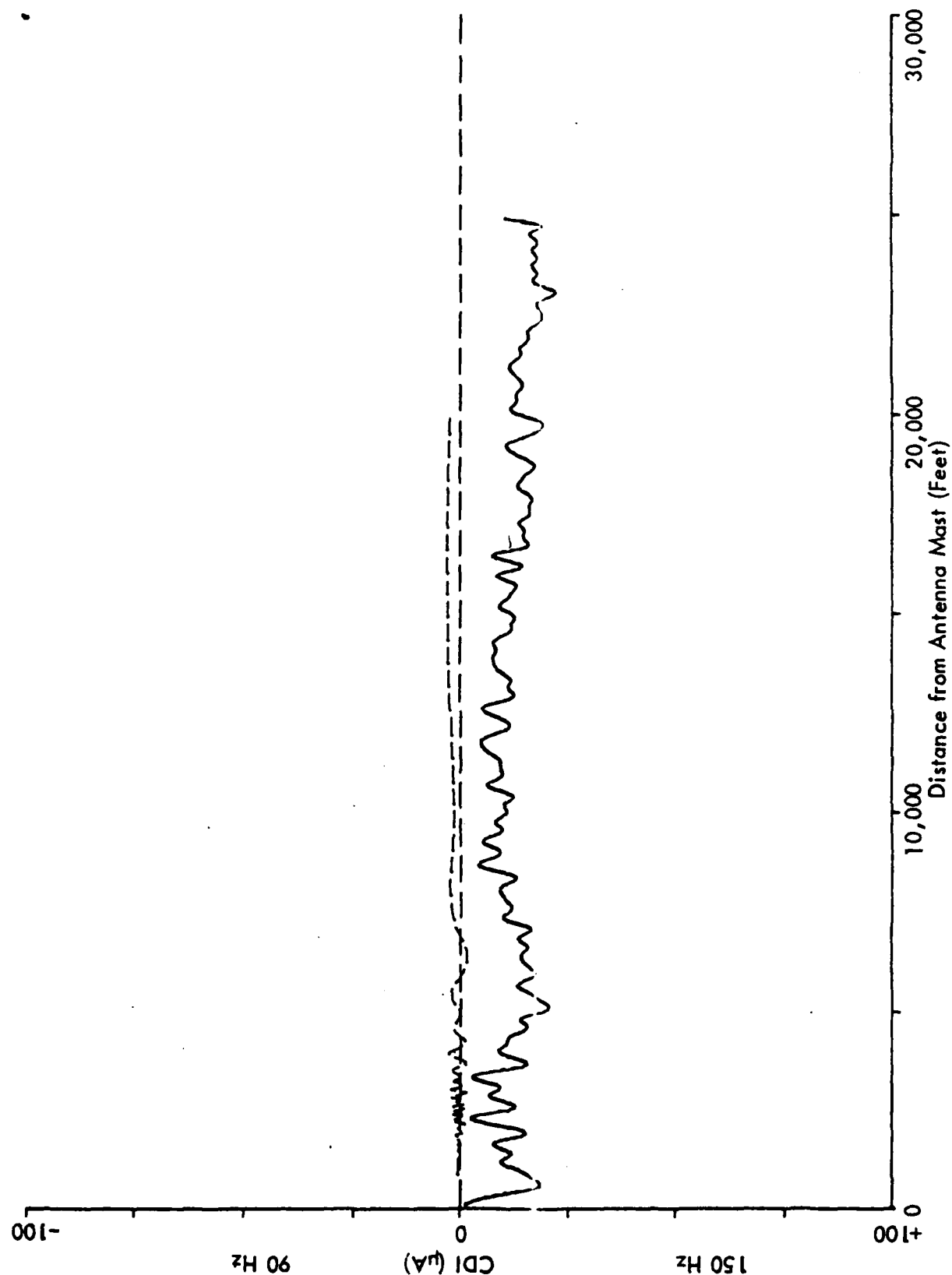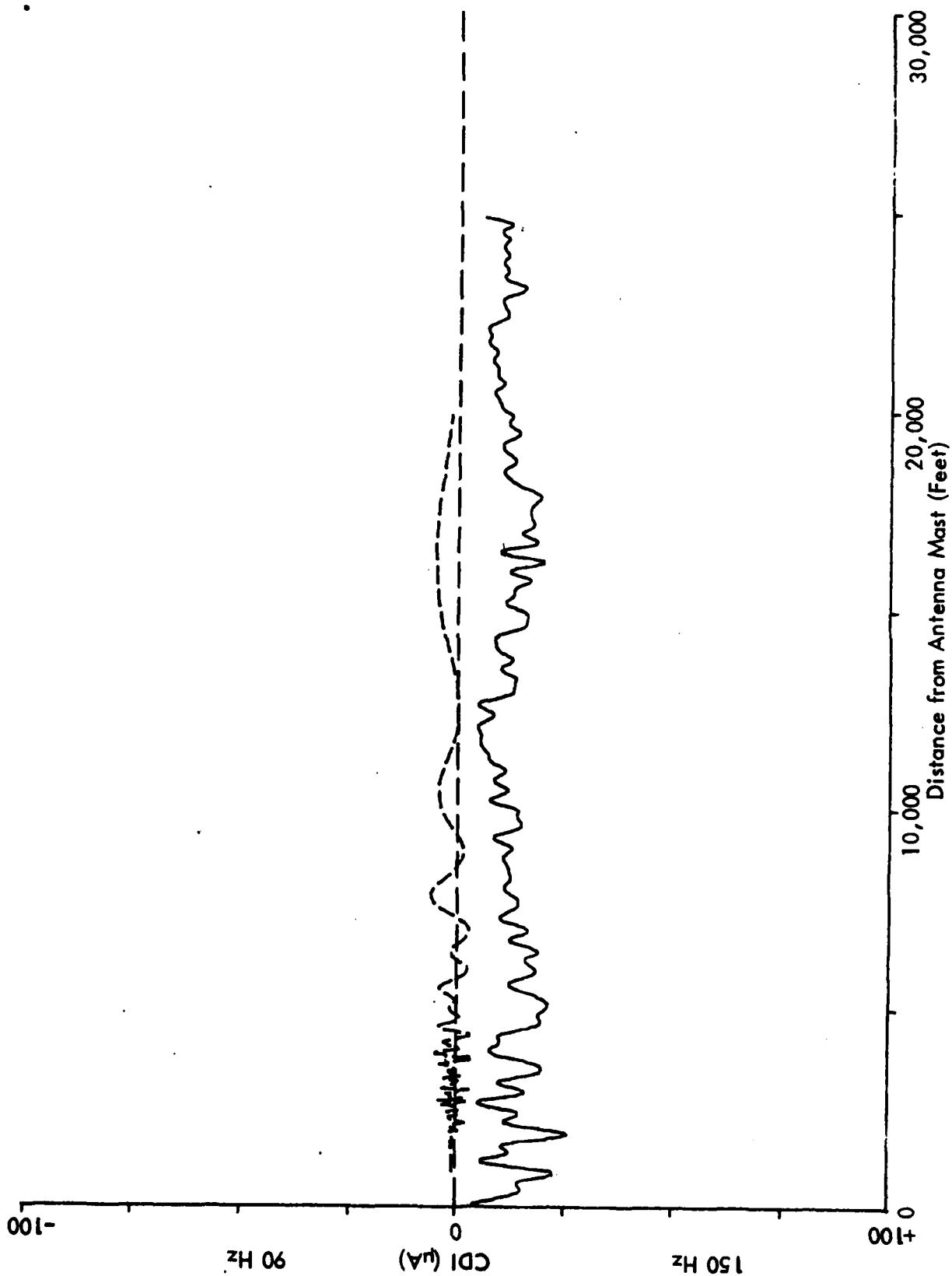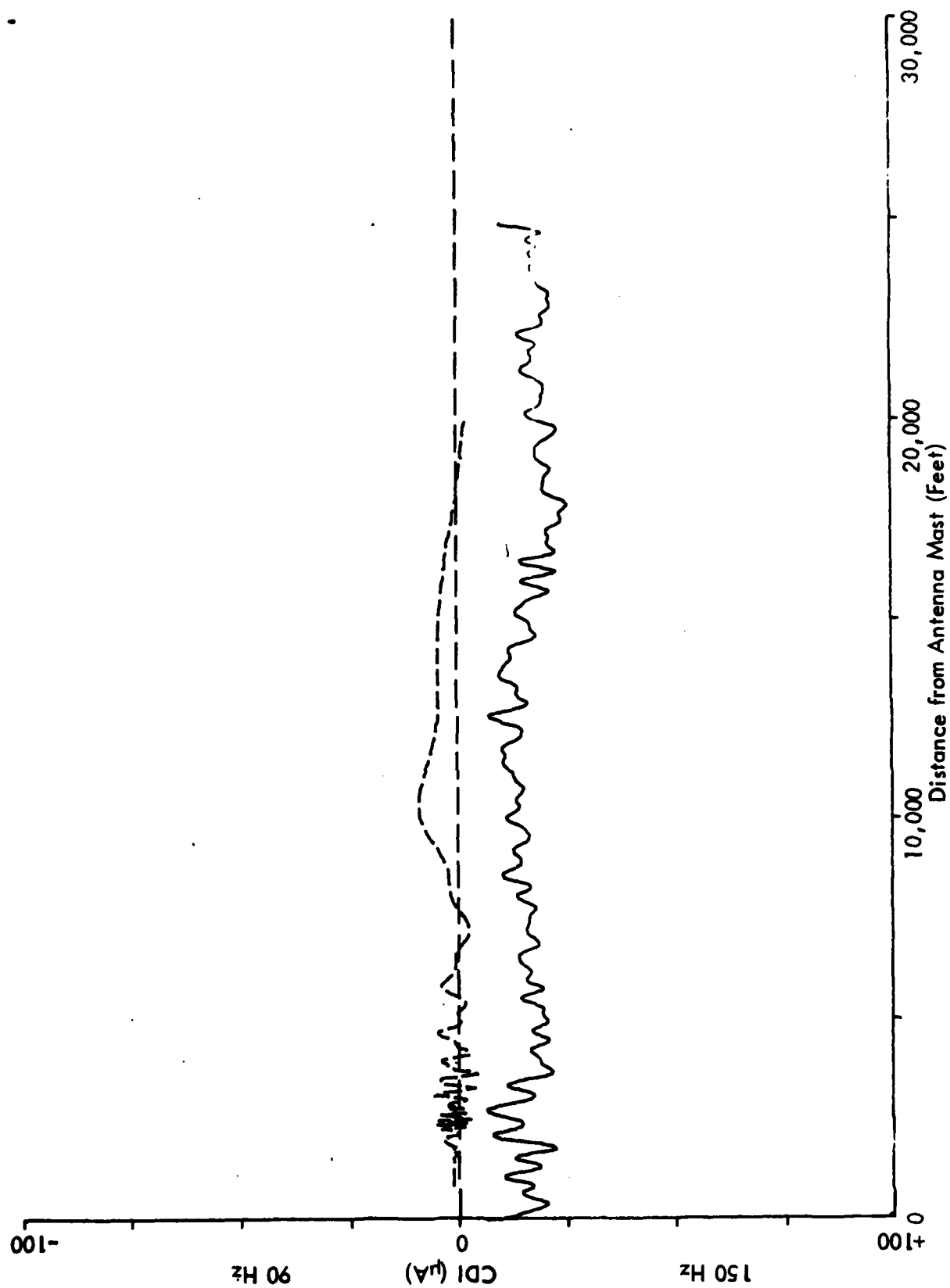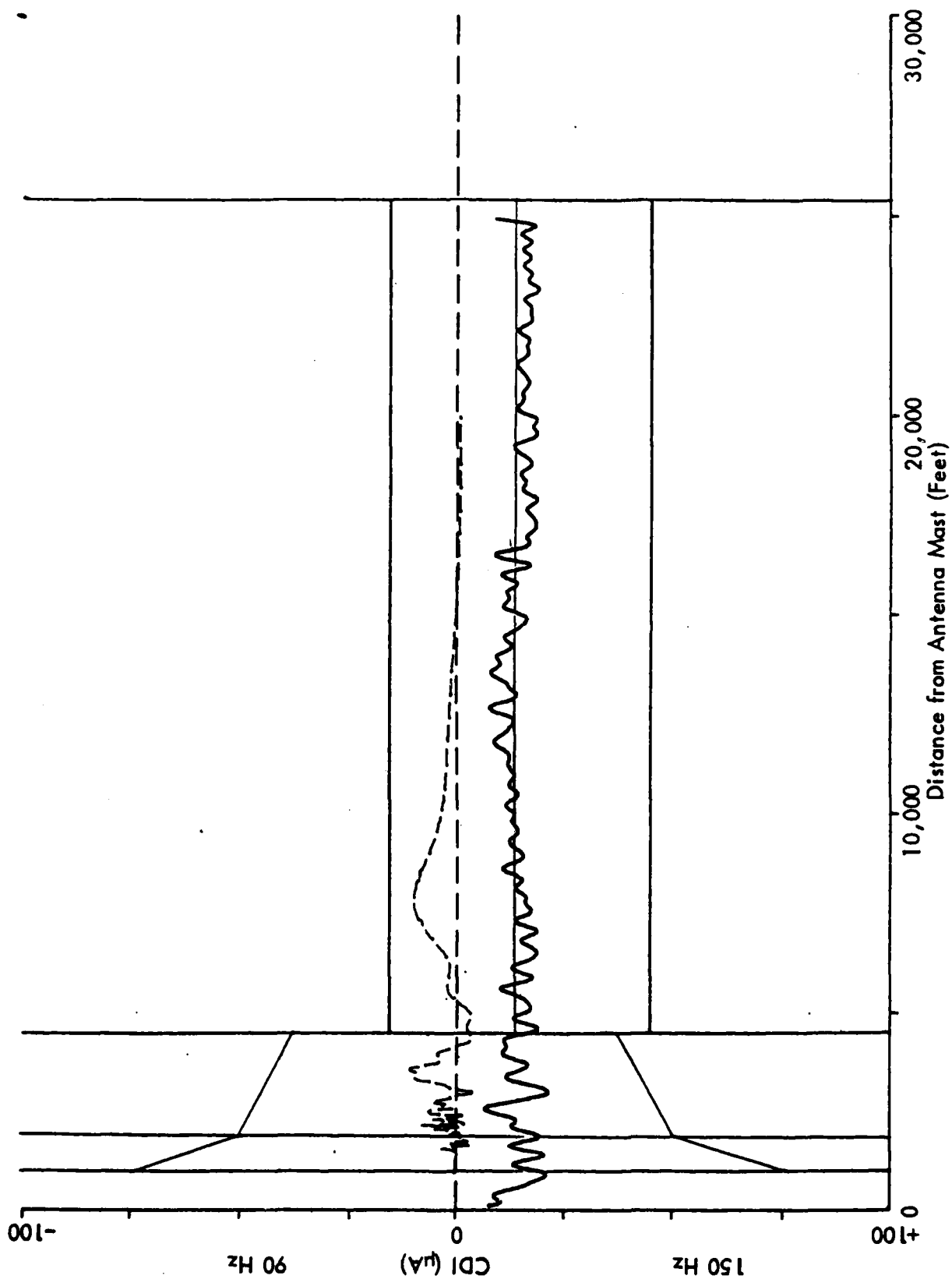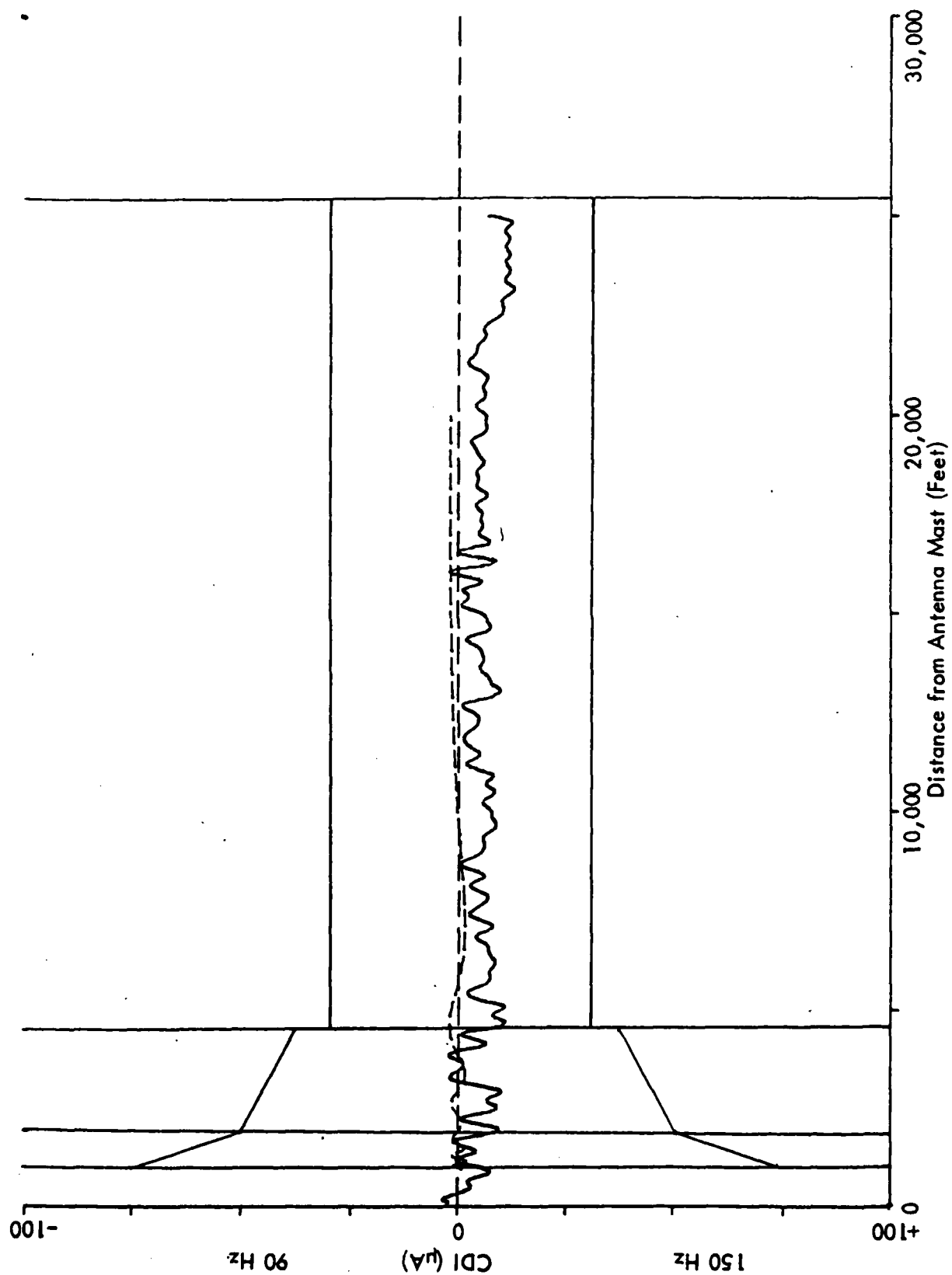
Figure 54. Calculated and measured on-course positions for the null-reference glide slope with a King Air, Rockwell Commander, and two Piper Cherokees parked parallel to the runway 600 feet from the centerline and 0 feet in front of the antennas.

IX.   INTERPOLATION AND EXTRAPOLATION FOR MULTIPLE REFLECTORS

Up until the time of this work there had been no known analytical study of the effects of multiple aircraft. Clearly the addition of more aircraft to the reflecting area adds significant complication. Whereas previously there were a large number of possibilities for location of the aircraft, now with multiple aircraft there is a linear increase in the possibilities. Additionally, there are the various permutations and combinations of aircraft orientations and organization.

When considering possible results, it is apparent that certain placements of n aircraft could produce additive effects due to simple superposition of the electromagnetic field in space. This would mean a worst case with n similar aircraft producing n times the effects of one. It should be apparent also that, given certain placements, an amount of cancellation could be produced given a specified receiving point in space. The end result for that region is less perturbation than that with a single aircraft.

The approach taken for this study was to look at worst case conditions because the aircraft on the ground could be expected to have a variety of positions that are reasonable and some of these could produce an additive effect. Calculations were made assuming superposition of the effects of one aircraft and therefore cannot be expected to be greater than n times the effect of one.

For example, comparing calculations for the Rockwell Commander located 1000 feet directly in front of the antennas one finds that the addition of a second aircraft of similar size (viz., a King Air C-90) doubles the amplitude of the displacement but now adds an interference pattern. This is essentially within the noise level of these particular measurements and does not provide significant roughness for an aircraft using the glide slope for an approach.

Figures 54 and 55 show the results of structure calculations and measurements when four aircraft are present. The measurement gives an indication that the calculation is indeed conservative. It is difficult to pick out the effects of the aircraft on the structure with the path noise of plus and minus 5 microamperes. The calculations point to the area where the path disturbance may be expected to take place; however, only in Zone 3 is there a hint of such a perturbation.

While a plethora of aircraft could in concept raise the effective ground level and thus lower the path angle, all indications are that this situation would not be approached in practice since the reflecting field cannot be expected to be a parking lot but rather it will only be invaded by aircraft queued for takeoff. This situation provides for a relatively small percentage of the reflecting area to be occupied with conducting aircraft surfaces. This is indeed fortuitous when considering the requirements for operation of the ILS.

While checks have been made for four aircraft located in the most critical positions considered practical and common, the addition of more aircraft will necessarily place them in less critical areas. This should minimize the effects of adding more aircraft simply because they cannot occupy the same physical areas and must be distributed linearly because of the very nature of a taxiway.

X.   RECOMMENDATIONS

The following recommendations are based principally on the technical work just completed which has identified areas which, if occupied by small, medium and large general aviation type aircraft, produce path perturbations which have been quantified through both theory and measurement.

1.   The user who seriously intends to use the data should determine the scale of his airport maps and convert the drawings of this report to that scale to facilitate the overlay process and determination of critical area boundaries.

2.   The airport operator, once critical area boundaries are identified, should install meaningful signs that clearly convey the message to stay out while instrument approaches are in progress. Signs which say merely "ILS" or "Cat I" are not satisfactory and should not be deployed.

3.   Users should identify the inherent noise of the ILS beams at the runways of interest. If the beam noise is high, then the critical area is going to be larger simply because a smaller perturbation will cause an out-of-tolerance condition to exist in the user's space.

4.   Contour maps should be used to identify that contour which, when added to the inherent noise, produces the tolerance limits set forth in the U.S. Flight Inspection Handbook, O AP 8200.1. The recommendation is that this be the boundary of the critical area.

5.   Because the size of the critical area is a function of the inherent noise produced by the site and it is desirable to keep this size to a minimum, efforts should be made to reduce the noise by fundamental site improvement.

6.   Consideration should be given to examining the effects of the smaller, commercial jet aircraft with respect to establishing critical areas. The completion of this present study now means that the effects of the various sizes of general aviation type aircraft along with the jumbo jet have been identified. A gap exists with respect to aircraft in the size range of the Douglas DC-9, Boeing 727, 767 and others. For completeness and a comprehensive understanding of path perturbational effects due to the mid-jet size aircraft, analyses and calculations should be made to cover these cases.

7.   A study should be performed similar to this one just completed to determine the effects of various aircraft placement when other configurations of glide slope are used, for example, the capture effect, sideband reference or endfire glide slope system.

XI. ACKNOWLEDGEMENT

)

XII. BIBLIOGRAPHY

[1] Lucas, J. G., "Study of ILS Multipath Effects by Microwave Model Techniques, Part IIA, Interference Effects Caused by Taxying Aircraft to Image Glidepath Systems," Air Navigation Group, School of Electrical Engineering, University of Sydney, Australia, July 1972.

[2] Reiffer, D. R., "Instrument Landing System for Cat III Operation, Multipath intereference effects due to ground movement of a Boeing 747 aircraft on Heathrow Airport, London," TELS 34/2/069, January,1971.

[3] Rondini, R. A. and R. H. McFarland, "Experimental Validation of Boeing 747 ILS Signal Scattering Calculations for Critical Area Determination," Final Report, FAA-RD-74-57 (EER 18-1), Avionics Engineering Center, Ohio University, Athens, Ohio, January 1974.

[4] Gorman, James T., "The Effects of Scattering from a 747 Aircraft Fuselage on the Operation of the Glide Path Portion of an Instrument Landing System," Master's thesis (supported by Federal Aviation Administration), Avionics Engineering Center, Ohio University, Athens, Ohio, March 20, 1971.

[5] Kwon, Young S., "The Effects of Reflection from Boeing 747 on Image Glide-Path Systems," Master's thesis (supported by Federal Aviation Administration), Avionics Engineering Center, Ohio University, Athens, Ohio, June 10, 1972.

[6] Rondini, Robert A., "A Study of Diffraction of Electromagnetic Waves Around Large Stationary Aircraft and Its Effects on Instrument Landing System Guidance Signals," Dissertation (supported by Federal Aviation Administration), Avionics Engineering Center, Ohio University, Athens, Ohio, June 1976.

[7] Chin, G., et. al., "User's Manual for ILSLOC: Simulation for Derogation Effects on the Localizer Portion of the Instrument Landing System," Report No. FAA-RD-73-76, Department of Transportation, Transportation Systems Center, Cambridge, MA, August 1973.

[8] Op cit., Rondini and McFarland.

[9] Siting Criteria for Instrument Landing Systems, Federal Aviation Administration, Order 6750.16A, August 18, 1973.

[10] U.S. Flight Inspection Handbook OAP 8200.1 217.2, Figure 217-1a (Change 32).

[11] Ibid.

[12] Op cit., Rondini.

[13] Op cit., Chin, et.al.

[14] Spohnheimer, N., "Report on Glide Slope Reflection from Taxiing
      Aircraft Outside the Critical Area at Portland, Oregon, Runway 10R,"
      December 28, 1978.

XIII. APPENDICES

Appendix A. Path Following Error and Control Motion Noise.

The Path Following Error (PFE) and Control Motion Noise (CMN) for the Path Structure can be determined by passing the time records through standardized filters, defined in figure A-1.

NOTE: The filter characteristics a·e based on a wide range of existing aircraft response properties and are believed to be adequate for foreseeable aircraft designs as well. Fo· CTOL aircraft the frequency response of the lateral or vertical/longi udinal channel is divided into three major spectral regions--a low, midd e and high frequency region, as follows:

(a) Low--Aircraft path following c mponents (less than 1.5 radians/ second - longitudinal channel) (less than .5 radian/second - lateral channel)

(b) Middle--Control surface motion;, wheel and column motion, aircraft attitude: (.5 to 10 radians/second - longitudinal channel) (.3 to 10 radians/second - lateral channel)

(c) High--Does not affect aircraft control and guidance.

While the term "path following error" suggests the difference between a desired flight path and the actual flight path taken by an aircraft following the guidance, in practice this error is estimated by instructing the test pilot to fly a desired ILS course and to measure the difference between the filtered guidance indication and the corresponding position measurement determined by a high-accuracy tracking instrument such as a theodolite with an appropriate ranging capability. The errors and spectral distribution thus obtained give an accurate estimate of the path following parameters. A similar technique is used to determine the control motion noise.

PFE test measurements are performed at the output of the standard filter. They provide an estimate of the aircraft's position error. In this formulation, the system bias (centering error) and path low frequency noise (which affects the aircraft position) are combined in a single measurement. The CMN (a measure of pilot acceptance factors) is also measured using a standard filter, which passes those frequencies that cause control activity during coupled flight.
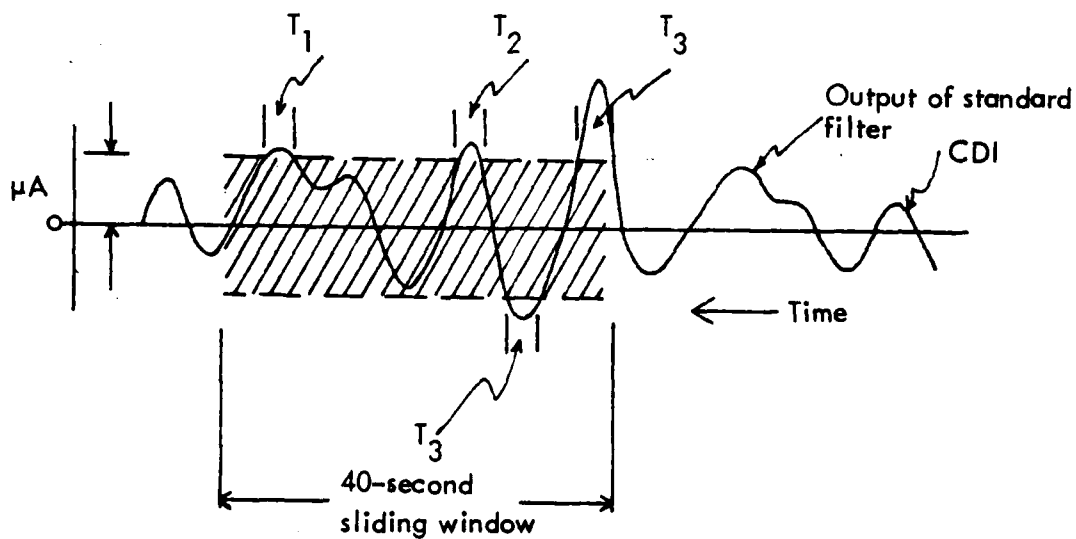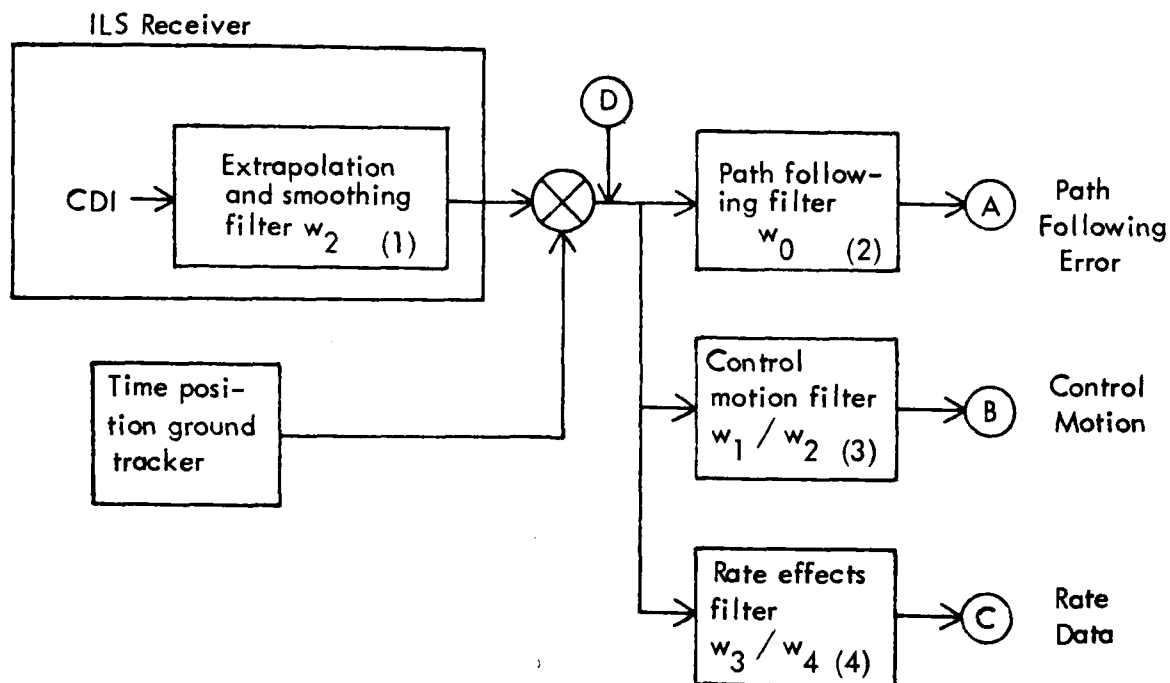
The PFE concept can simplify anaylsis by combining the bias and path following noise into a single measurement specification. Since there are enumerable combinations, the path following error concept greatly simplifies the calculations. It is an invariant specification in the sense that bias errors could be transformed into noise and vice versa without affecting the specification limits or their interpretation.

For multipath interference, the separation angle and differential phases are important considerations. However, for small, wide-bandwidth, random perturbations, the relation is accurate.

-157-

Signal quality is defined in terms of the Path Following Error (PFE) and Control Motion Noise (CMN) rather than the traditional bias and noise terminology. These parameters are preferable because: (1) they describe the interaction of the signal with the aircraft in terms which can be directly related to aircraft guidance and flight control systems responses; and (2) their measurement results in simplified interpretation of flight inspection records.

The angular error is the difference between the airborne receiver sampled data output and the true position angle at the sampling time. The ILS guidance signal is distorted by the ground/airborne equipment and by propagation—induced perturbations. To assess the suitability of signal—in—space for aircraft guidance, these perturbations are best viewed in the frequency domain (i.e., the error spectrum).[1] That is, the PFE occupies a frequency band which is essentially nonoverlapping with respect to the CMN frequency band. Thus, these quantities can be easily separated and measured using standard filters. More importantly, these components describe very different signal—in—space qualities.

)

_____

[1]It is the Fourier Transform of the flight test error trace.

ILS Receiver

CDI → Extrapolation and smoothing filter w_2 (1)

D

⊗

Time position ground tracker

Path following filter w_0 (2) → A Path Following Error

Control motion filter w_1 / w_2 (3) → B Control Motion

Rate effects filter w_3 / w_4 (4) → C Rate Data

T_1 T_2 T_3

µA

Output of standard filter

CDI

← Time

T_3

40-second sliding window

Notes: T = Region to be evaluated (60 seconds)
        C = Maximum error specification
        T_1 T_2 T_3... = Time intervals that noise exceeds allowable error
                         specifications for the facility to be acceptable in this region.

$$100 \frac{\left[T - (T_1 + T_2 + T_3 ...) \right]}{T} = 953$$

Figure A-1. Definition of standardized filters.
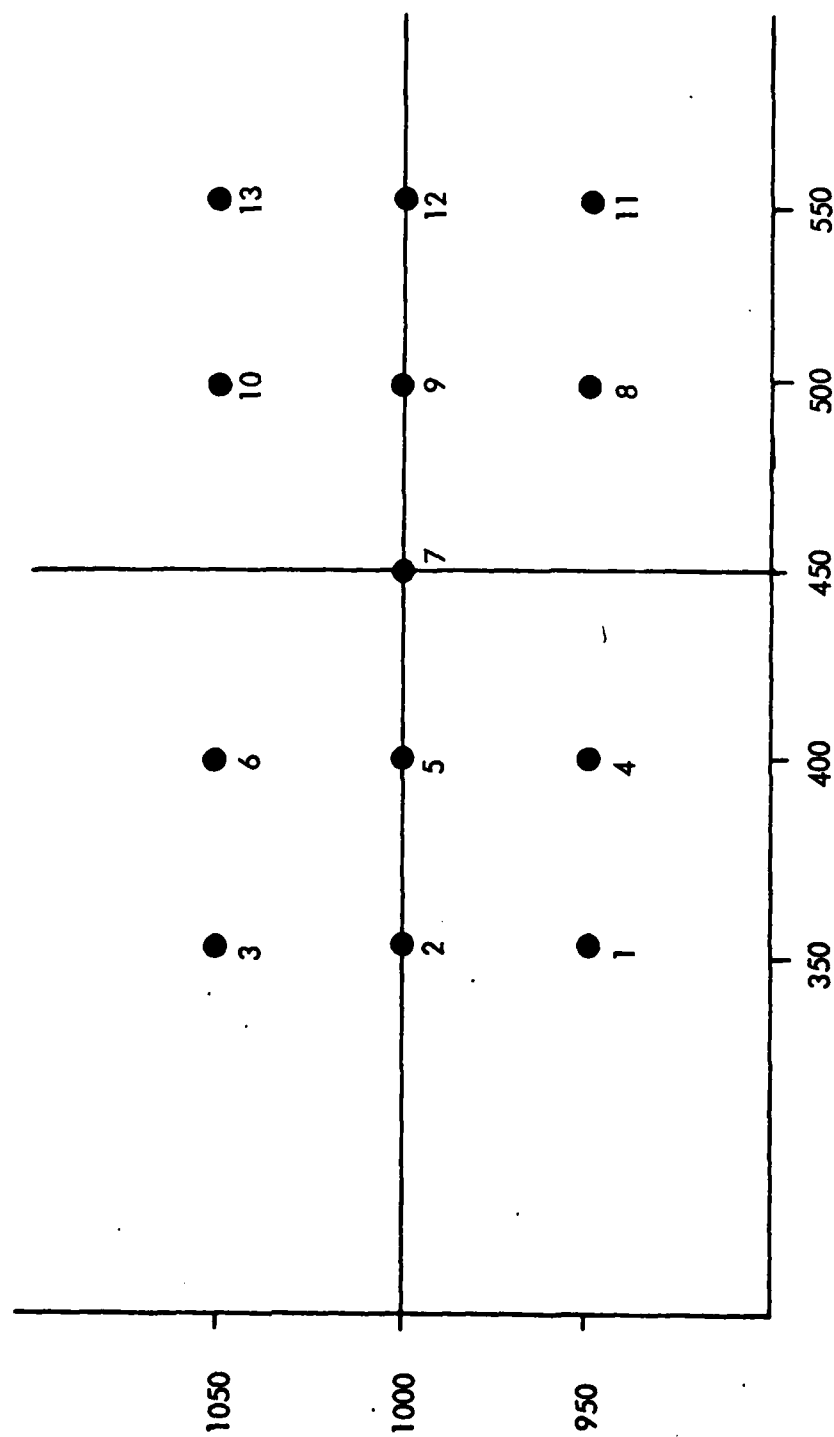
Figure B-1. Layout of points for examining the sensitivity of the glide slope structure to relatively small variations in positioning of the reflecting aircraft.
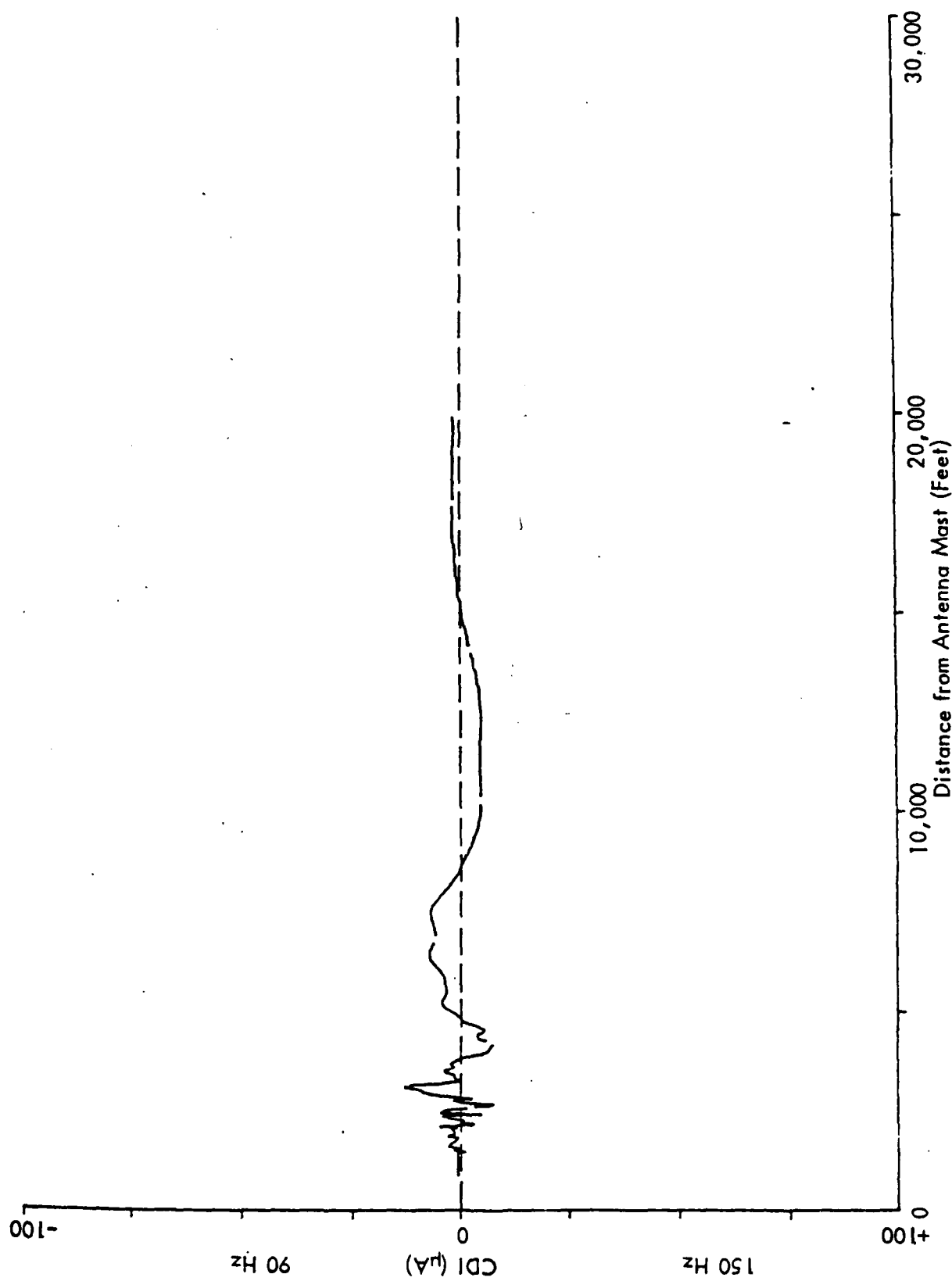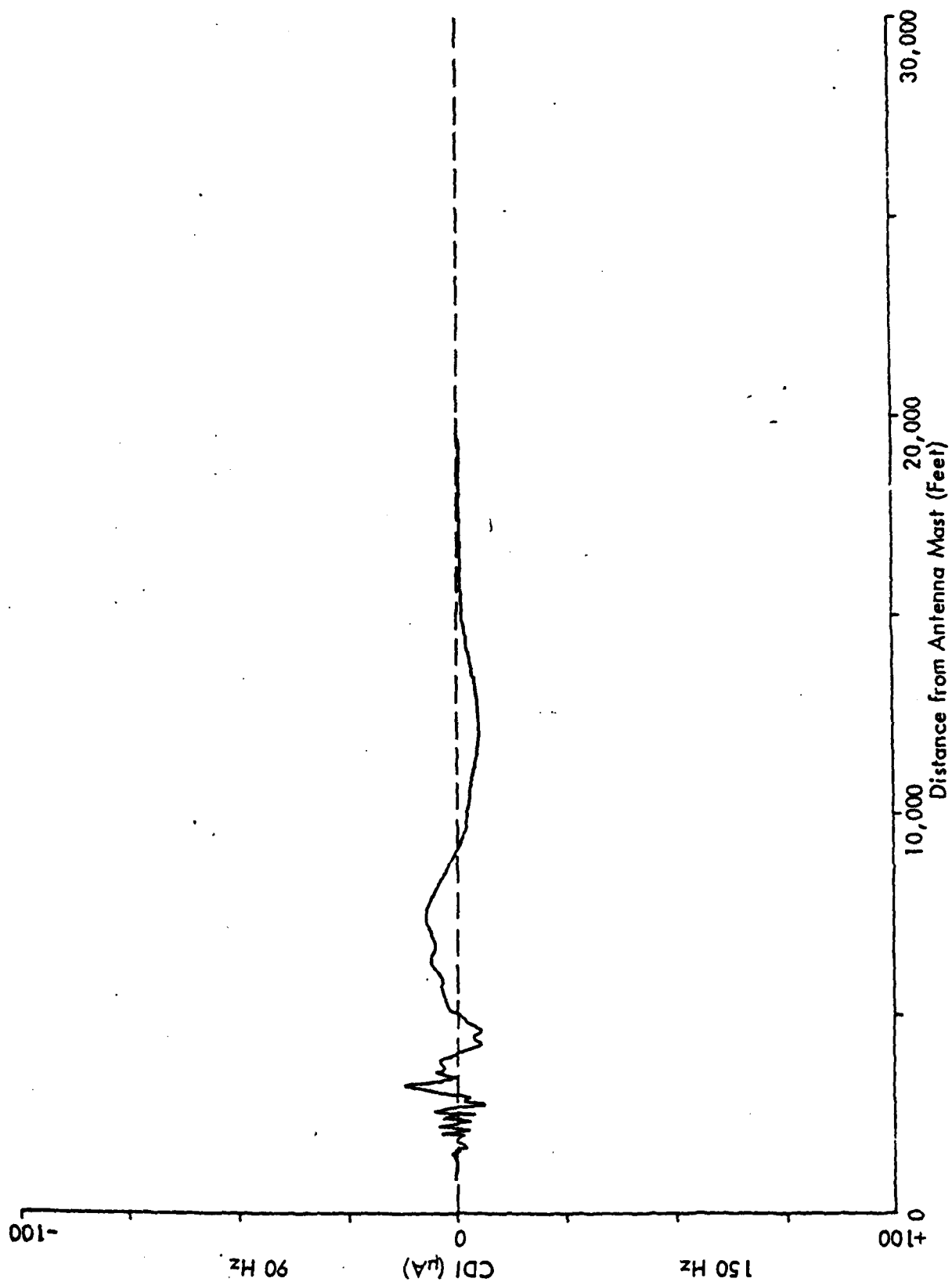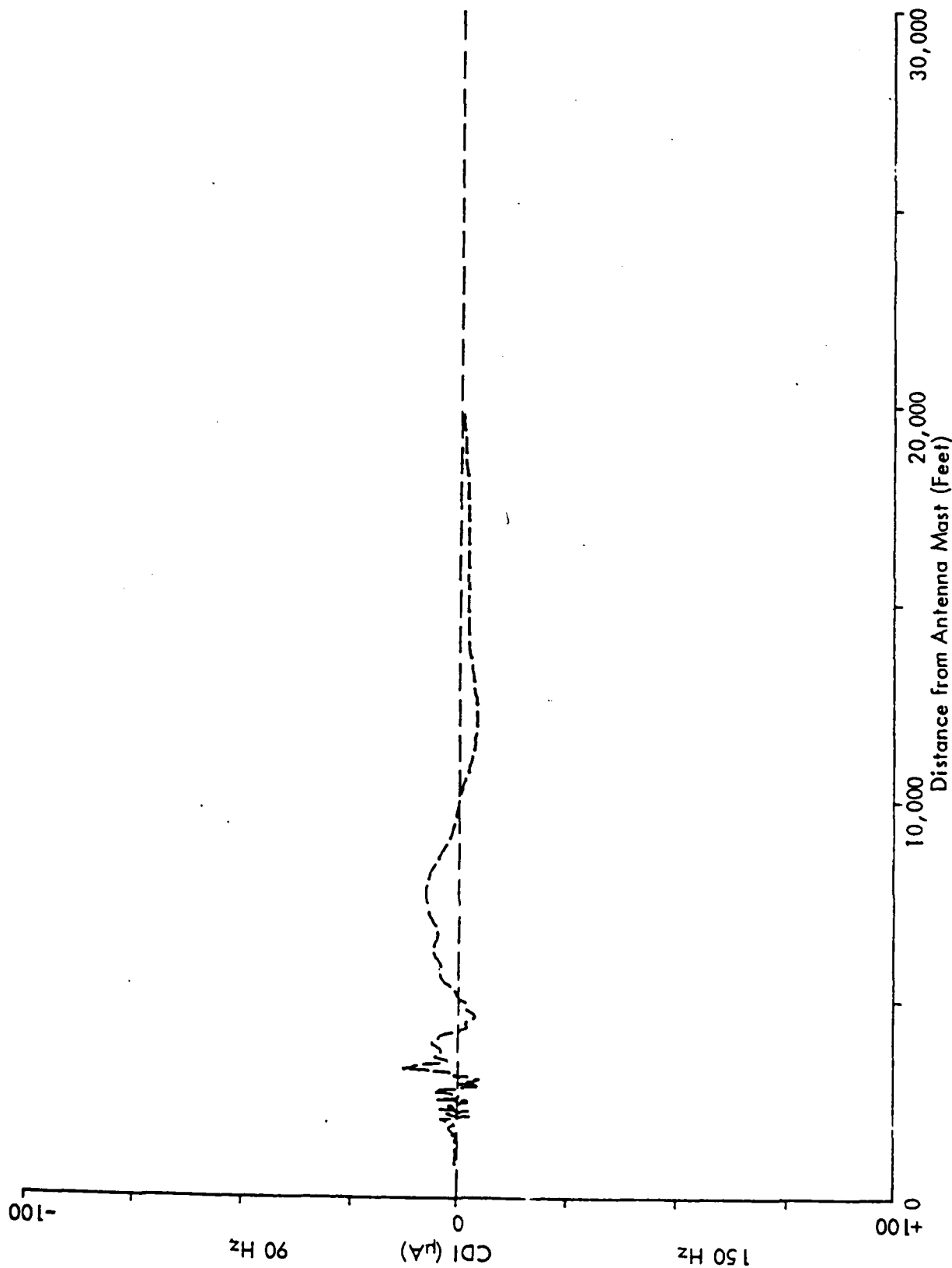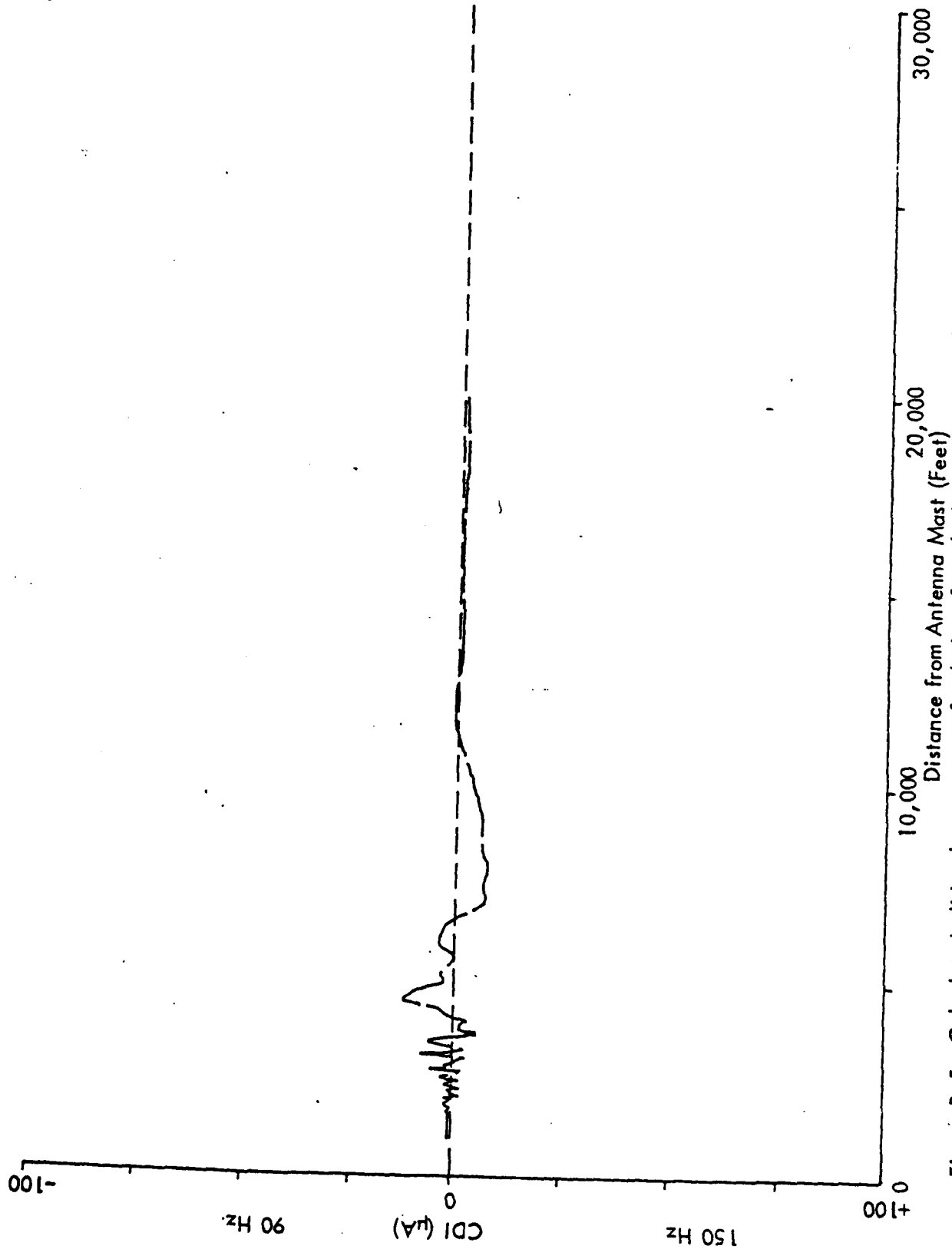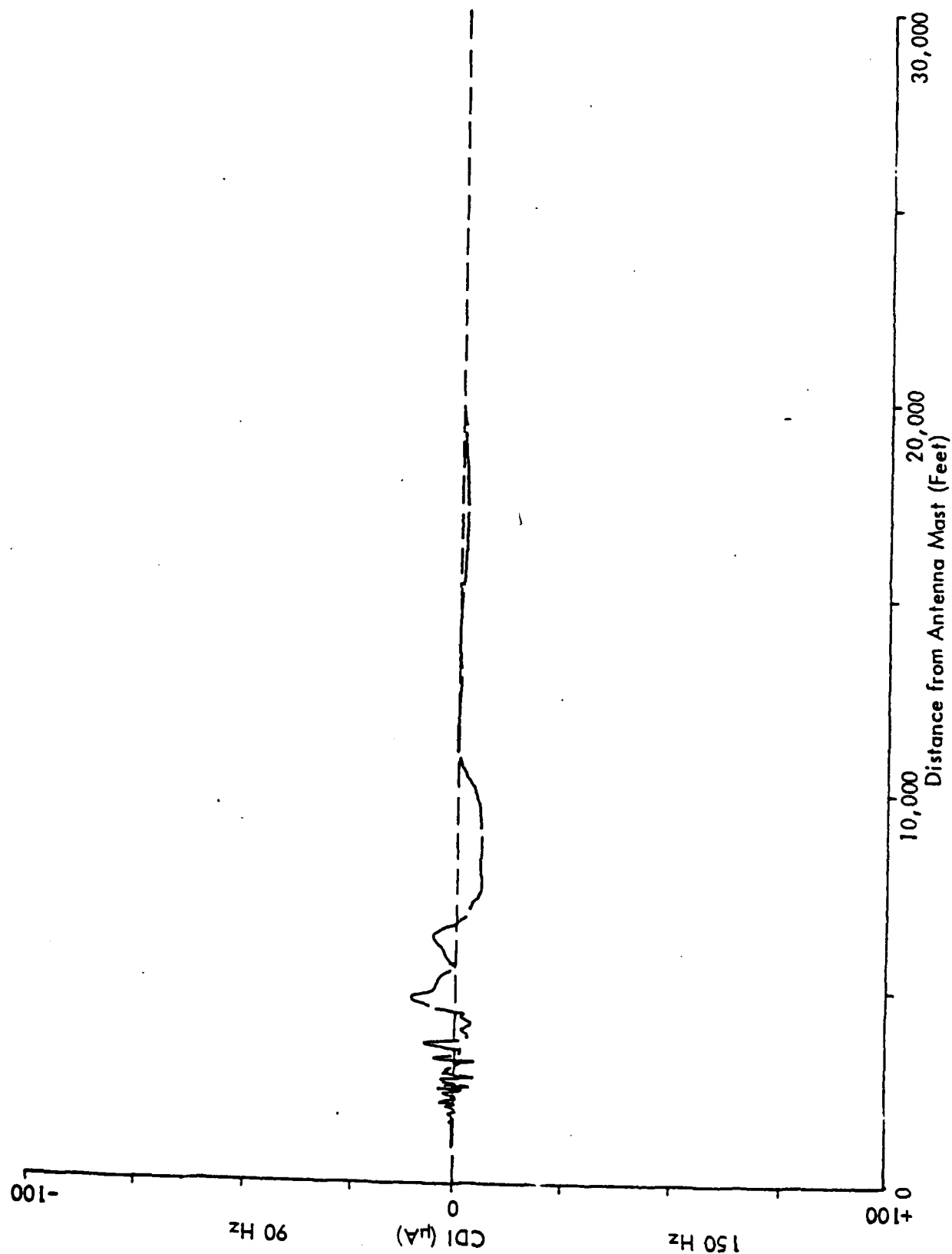
Figure B-2. Calculated glide slope response for 4 aircraft parked at position Number 1 given in Figure B-1. The orientations are perpendicular to runway centerline, tails away from runway with the King Air closest to the runway followed by a Rockwell Commander and 2 Piper Cherokees in that order. The coordinates are for the lead aircraft, a King Air.

Figure B-3. Calculated glide slope response for 4 aircraft parked at position Number 2 given in Figure B-1. Orientation and organization are the same as for Figure B-2.
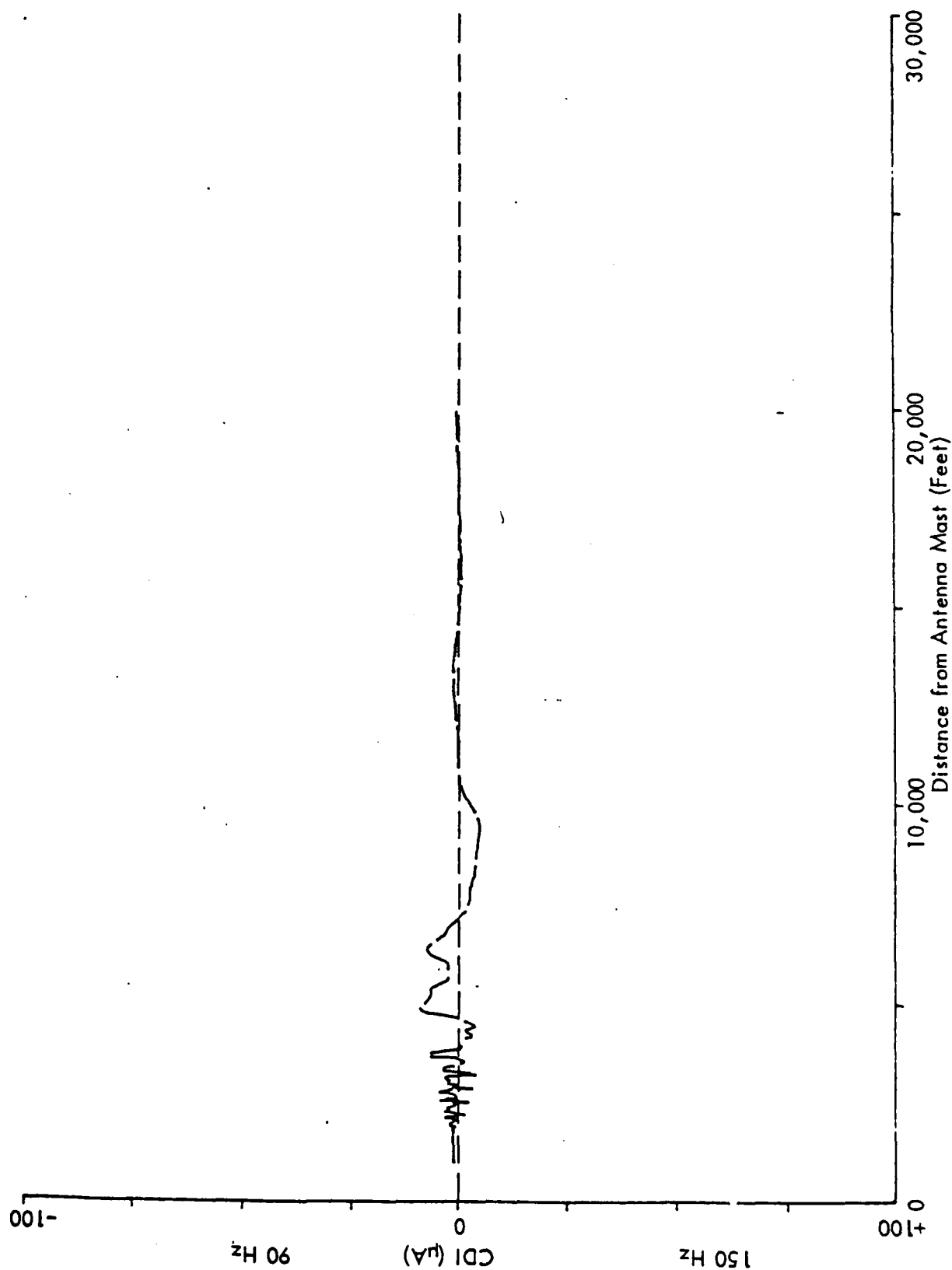
-162-

Figure B-4. Calculated glide slope response for 4 aircraft parked at position Number 3 given in Figure B-1. Orientation and organization are the same as for Figure B-2.
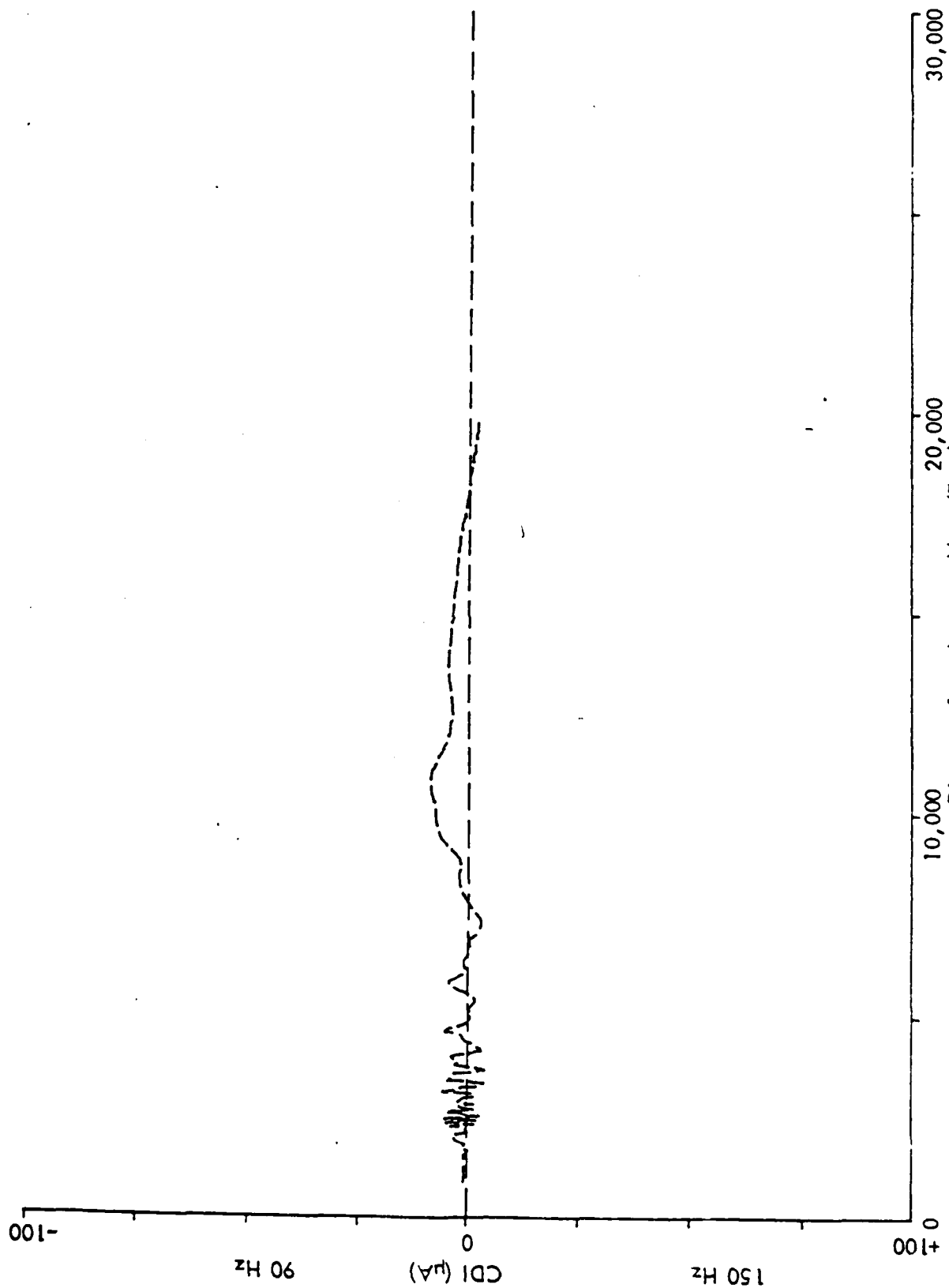
Figure B-5. Calculated glide slope response for 4 aircraft parked at position Number 4 given in Figure B-1. Orientation and organization are the same as for Figure B-2.
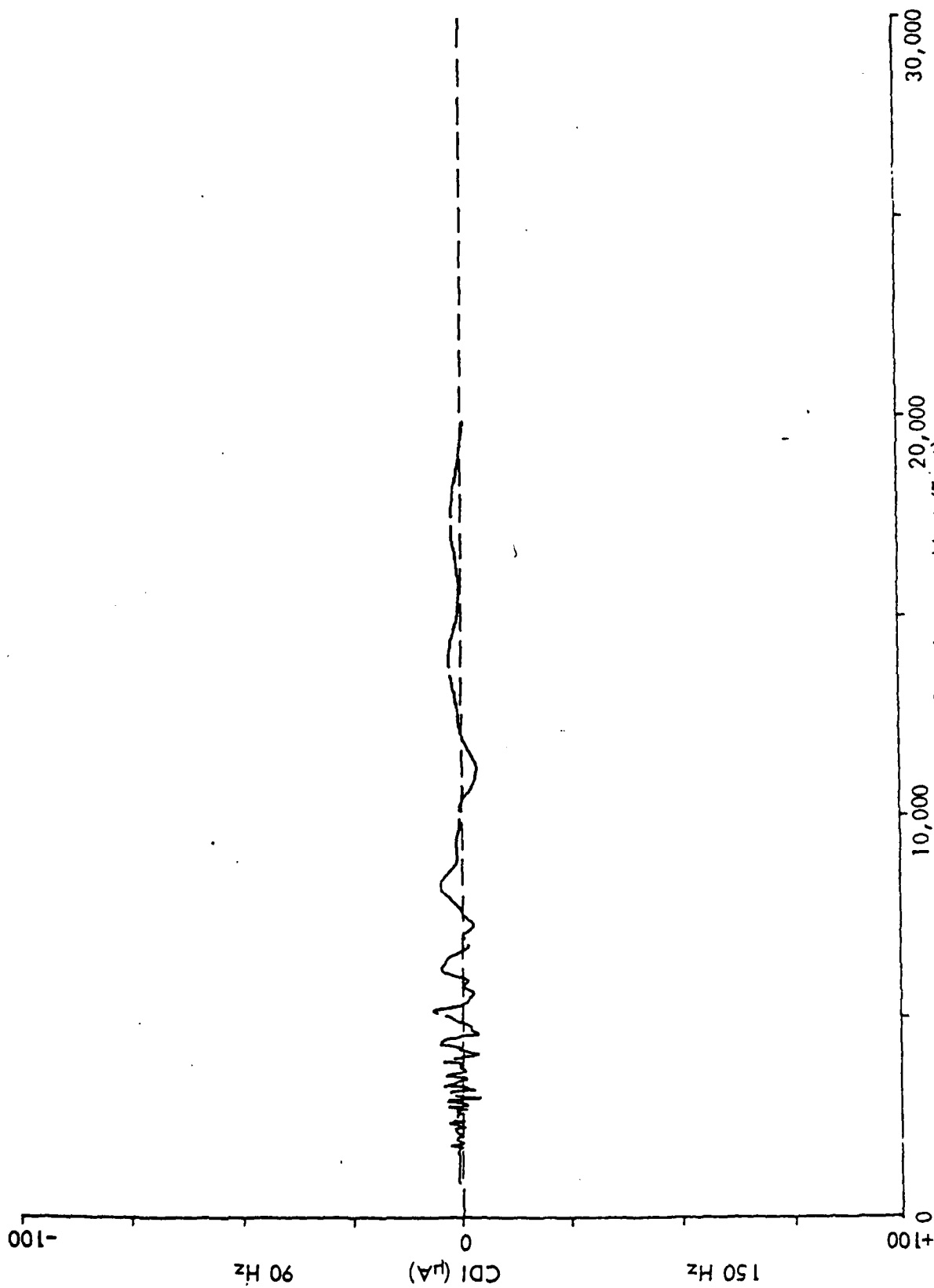
-164-

Figure B-6. Calculated glide slope response for 4 aircraft parked at position Number 5 given in Figure B-1. Orientation and organization are the same as for Figure B-2.

-165-

Figure B-7. Calculated glide-slope response for 4 aircraft parked at position Number 6 given in Figure B-1. Orientation and organization are the same as for Figure B-2.

Figure B-8. Calculated glide-slope response for aircraft parked at position Number 7 given in Figure B-1. Orientation and organization are the same as for Figure B-2.
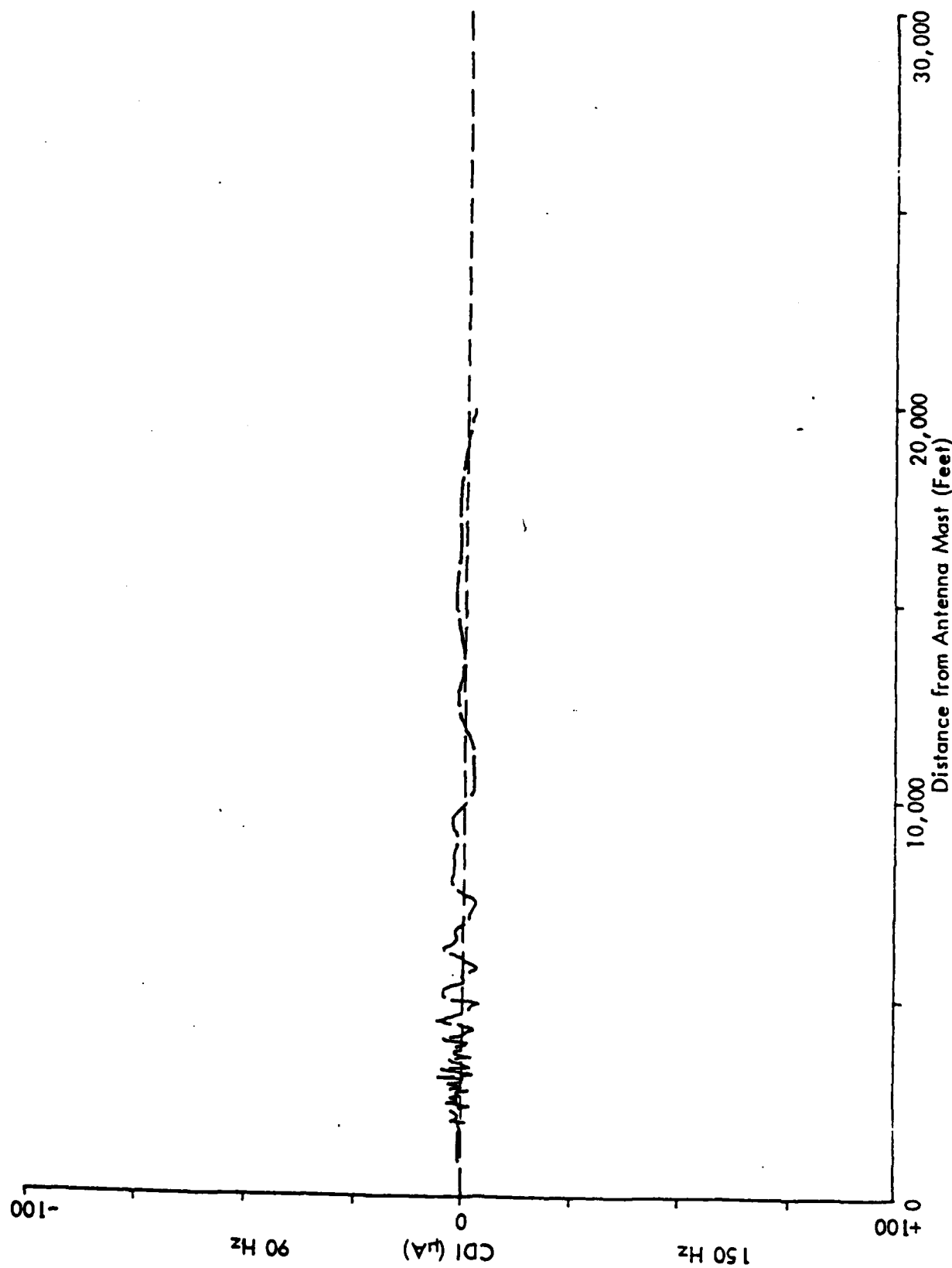
Figure B-9. Calculated glide-slope response for 4 aircraft parked at position Number 8 given in Figure B-1. Orientation and organization are the same as for Figure B-2.

END
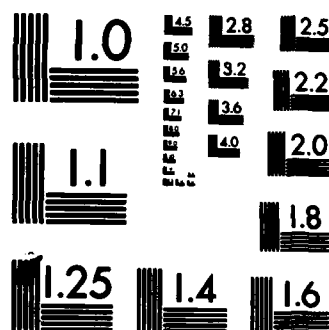
MICROCOPY RESOLUTION TEST CHART
NATIONAL BUREAU OF STANDARDS-1963-A

Figure B-10. Calculated glide-slope response for 4 aircraft parked at position Numb er 9 given in Figure B-1. Orientation and organization are the same as for Figure B-2.
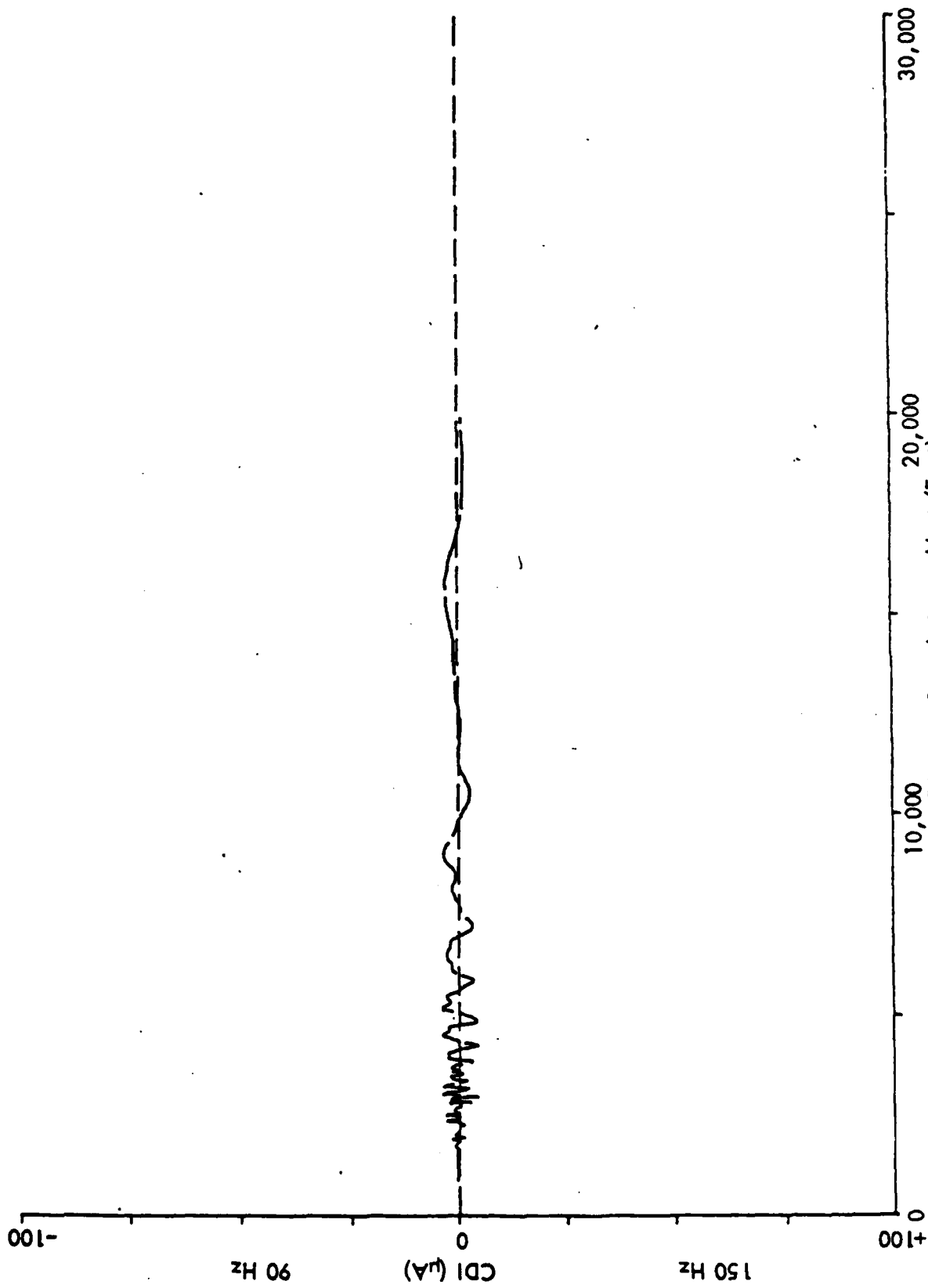
Figure B-11. Calculated glide-slope response for 4 aircraft parked at position Number 10 given in Figure B-1. Orientation and organization are the same as for Figure B-2.
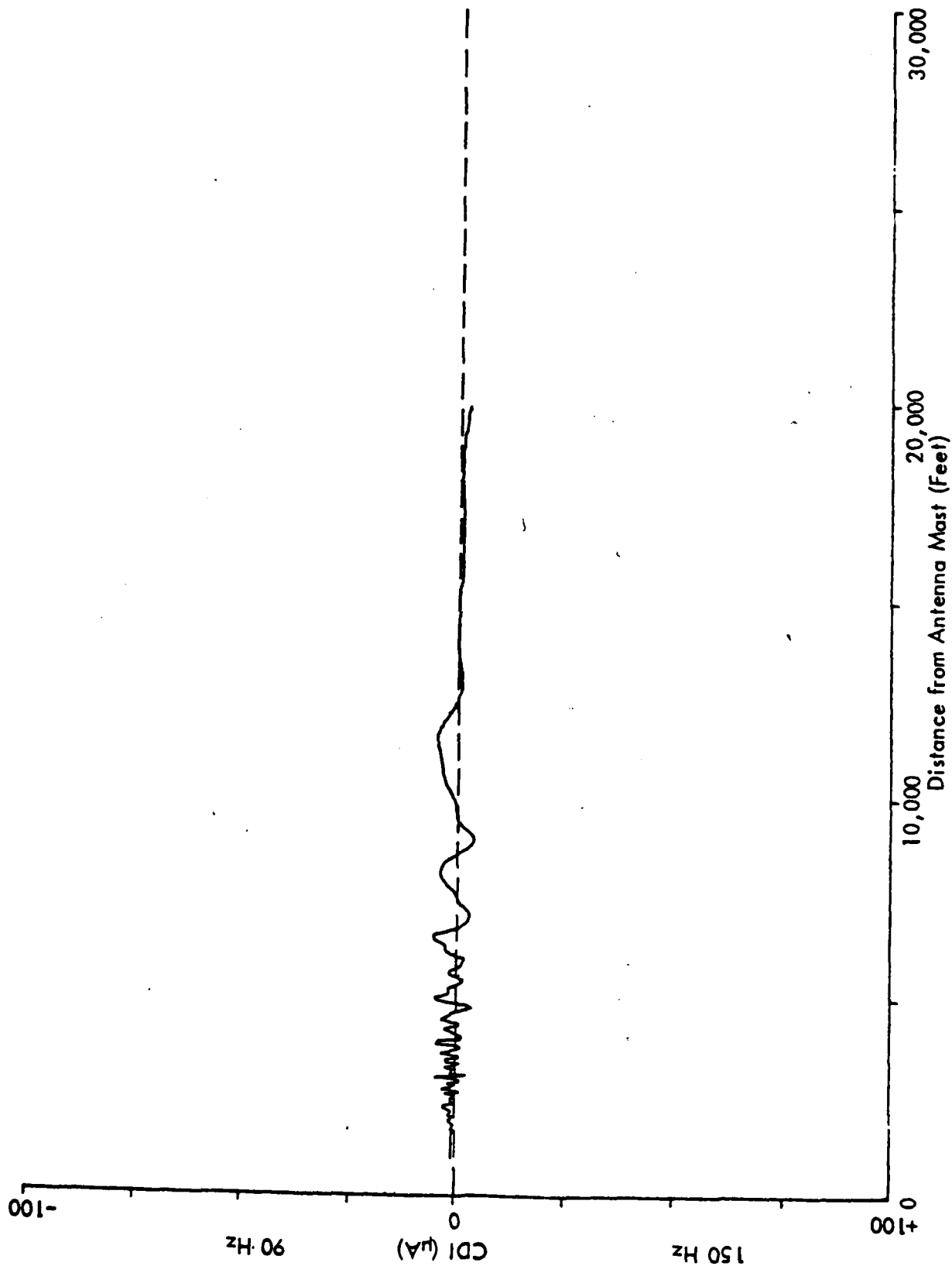
Figure B-12. Calculated glide-slope response for 4 aircraft parked at position Number 11 given in Figure B-1. Orientation and organization are the same as for Figure B-2.
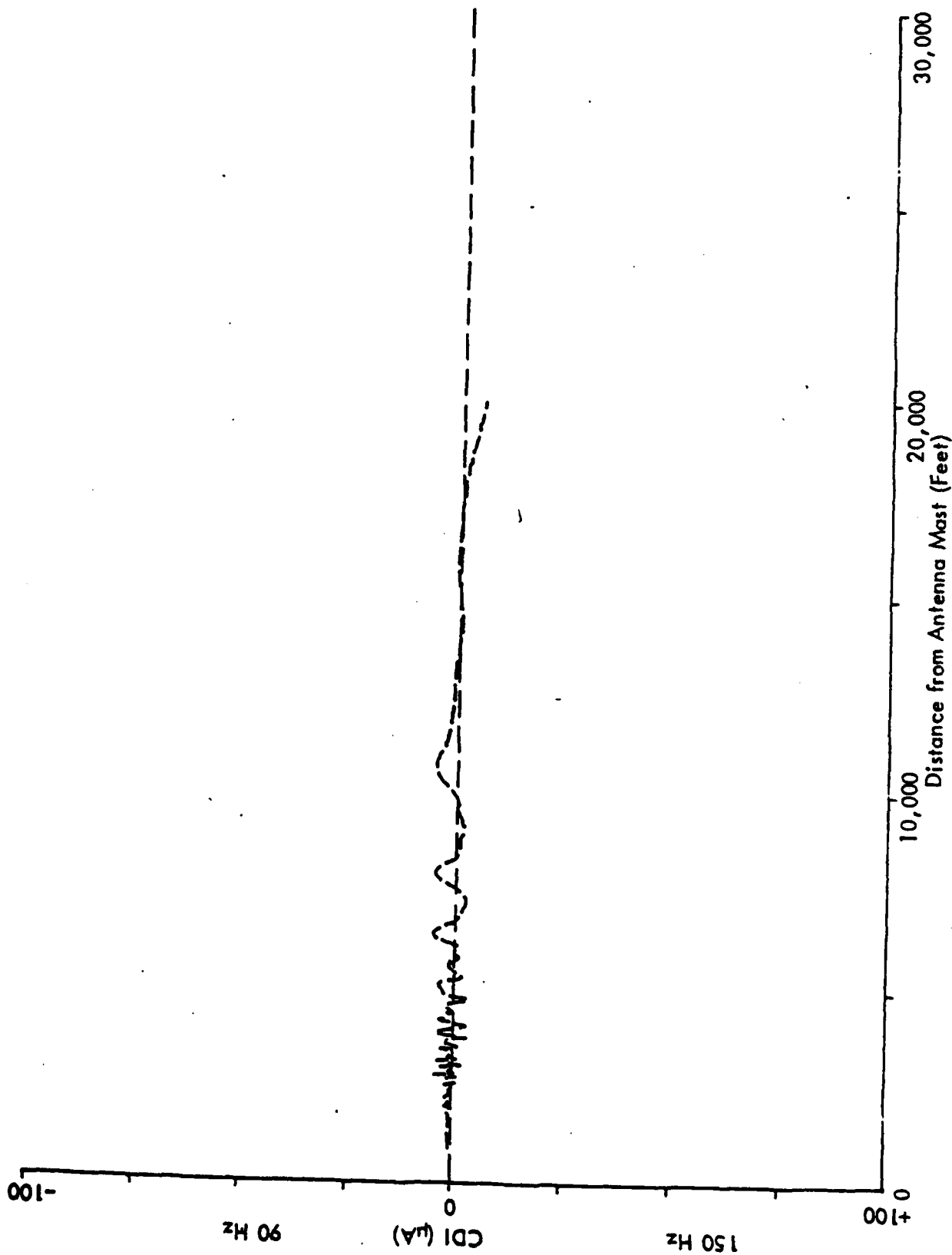
Figure B-13. Calculated glide-slope response for 4 aircraft parked at position Number 12 given in Figure B-1. Orientation and organization are the same as for Figure B-2.
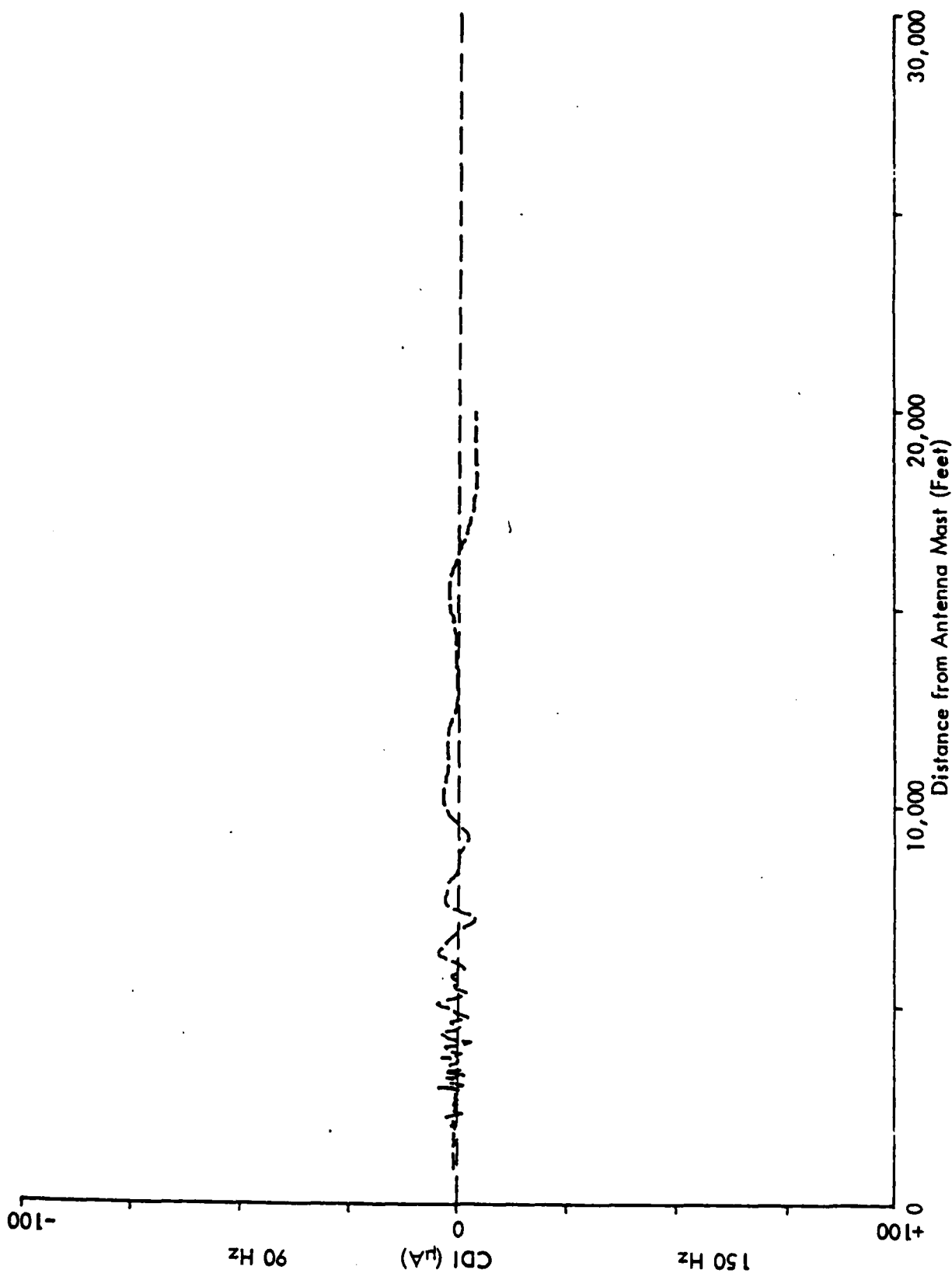
Figure B-14. Calculated glide-slope response for 4 aircraft parked at position Number 13 given in Figure B-1. Orientation and organization are the same as for Figure B-2.

END

FILMED

3-84

DTIC